Fluctuations and Criticality in Heavy-Ion Collisions

by

Xin An
B.S., Nankai University, 2012

THESIS

Submitted as partial fulfillment of the requirements
for the degree of Doctor of Philosophy in Physics
in the Graduate College of the
University of Illinois at Chicago, 2020

Chicago, Illinois

Defense Committee:

Mikhail Stephanov, Chair and Advisor
Olga Evdokimov
Wai-Yee Keung
Ho-Ung Yee
Gokce Basar, University of North Carolina at Chapel Hill

Fluctuations and Criticality in Heavy-Ion Collisions

Copyright 2020

by

Xin An

Abstract

Quantum Chromodynamics (QCD) predicts various extraordinary phases of matter whose underlying physics is described by the strong interaction. Identifying the QCD phase diagram, of which a critical point serves as the landmark, is one of the fundamental open subjects in modern physics. The properties of the QCD phase transitions and criticality can be studied by the relativistic heavy-ion collision experiments at various laboratory accelerator facilities, where a strongly interacting primordial matter is expected to form in extreme conditions on an event-by-event basis. Fluctuations are therefore indispensable for describing such stochastic process and become rather crucial for understanding the universal behavior when the system approaches the critical point. In this thesis, we will discuss the current methodology and challenge of discovering the QCD critical point, with an emphasis on the recent progress in quantifying the fluctuation-driven phenomena both in and out of equilibrium. The state-of-the-art formalism we developed constitutes an integral part of the theoretical framework for interpreting the experimental results from the ongoing RHIC Beam Energy Scan Program.

To my grandparents.

That's too simple to be true. It's an interesting idea, but Nature isn't that simple.

Niels Bohr, 1958

Contents

Contents vi

List of Figures ix

List of Tables xv

List of Abbreviations xvii

Acknowledgments xix

Summary xxi

1 Introduction 1
- 1.1 Overview 1
- 1.2 Fluctuations and Field Theory 9
  - 1.2.1 Classical Field Theory 9
  - 1.2.2 Renormalization Group Theory 11
  - 1.2.3 Effective Action 20
- 1.3 Critical Fluctuations 29
  - 1.3.1 Equilibrium Critical Fluctuations 29
  - 1.3.2 Non-Gaussian Fluctuations 32
  - 1.3.3 Non-equilibrium Dynamics of Critical Fluctuations 36
- 1.4 QCD Phase Diagram and Critical Point 39
  - 1.4.1 Review of QCD 39
  - 1.4.2 QCD Phase Diagram 42
  - 1.4.3 Mapping from Ising Theory to QCD 47
- 1.5 Heavy-Ion Collision Experiment 50
  - 1.5.1 Connection to Experimental Observables 50
  - 1.5.2 Heavy-Ion Collisions and Beam Energy Scan 55

2 Hydrodynamic Fluctuations 64
- 2.1 Hydrodynamics and Thermodynamics 67

2.2 Stochastic Fluctuating Hydrodynamics . . . 73
2.2.1 Hydrodynamic Fluctuations and Stochastic Noises . . . 73
2.2.2 Linearized Hydrodynamic Equations . . . 77
2.3 Deterministic Fluctuating Hydrodynamics . . . 82
2.3.1 Nonlinear Fluctuations . . . 82
2.3.2 Nonlinear Feedback . . . 85
2.3.3 A First Look of the Dynamics of Feedback . . . 87
2.4 Confluentization in Relativistic Flow . . . 89
2.4.1 Confluent Derivative of One-point Function . . . 90
2.4.2 Confluent Derivative of Equal-time Two-point Function . . . 92
2.4.3 Confluent Correlator and Wigner Function . . . 95
2.5 Relativistic Dynamics of Hydrodynamic Fluctuations . . . 98
2.5.1 Fluctuation Evolution Equations . . . 98
2.5.2 Hydro-kinetic Equations . . . 102
2.5.3 Hydro-kinetic Equations for Bjorken Flow . . . 108
2.6 Renormalization of Hydrodynamics . . . 111
2.6.1 Renormalization of Hydrodynamic Variables . . . 112
2.6.2 Long-time Tails . . . 122
2.7 Phonon Interpretation of the Hydro-kinetic Equation . . . 125
2.7.1 Phonon Kinetic Equation . . . 125
2.7.2 Phonon Contributions to Stress-Energy Tensor . . . 129
2.8 Discussion . . . 130

3 Dynamics of Critical Fluctuations **134**
3.1 Hydro+ . . . 136
3.2 Hydro++ . . . 140
3.2.1 Equations for Hydro++ . . . 140
3.2.2 Frequency Dependence of Transport Coefficients . . . 145
3.3 Discussion . . . 150

4 Fluctuations and Spinodal Points **153**
4.1 Non-perturbative Approach to Lee-Yang Edge Singularities . . . 153
4.1.1 Non-perturbative Functional Renormalization Group . . . 156
4.1.2 Critical Equation of State and Mean-field Scaling Prediction . . . 163
4.1.3 Solving the RG Flow Equations . . . 164
4.1.4 Critical Scaling Exponents and Hyperscaling Relations . . . 167
4.1.5 Relevance of Composite Operators and Quality of Finite Truncations 171
4.1.6 Residual Regulator Dependence and Principle of Minimal Sensitivity 173
4.2 Spinodal Points and Lee-Yang Edge Singularities . . . 176
4.2.1 Critical Equation of State and the Mean-field Approximation . . . 178
4.2.2 Beyond the Mean-field Approximation . . . 182

4.2.3 Singularities in the ε Expansion . . . 190
4.2.4 Singularities in the O(N)-symmetric ϕ^4 Theory . . . 199
4.3 Discussion . . . 203

5 Conclusion and Outlook **209**

Appendices **212**

A Reduction to Non-relativistic Hydrodynamics **212**

B Fundamental Thermodynamic Relations **215**

C Local Confluent Triad and Basis **217**
C.1 A Local Confluent Triad . . . 217
C.2 A Basis in the Space Orthogonal to $\hat{q}$ and u and Monopole Connection . . . 218

D Comparison to Known Results **220**

E Details of the Parametric Equation of State **224**
E.1 Parametric Equation of State at Order ε^2 . . . 224
E.2 Parametric Equation of State at Order ε^3 . . . 225

F Copyright Statements **229**

Bibliography **231**

List of Figures

1.1 (a) The chronology of early Universe (NASA/WMAP) and (b) the inner structure of the compact star (R. Schulze). 2
1.2 The basic stages of a heavy-ion (Pb-Pb) collision event in a nutshell (Wei Li). 5
1.3 Various potentials $U(\phi)$ for a ϕ^4 theory with $\lambda_4 > 0$ and different values of λ_2. By tuning the parameter $\lambda_2 \sim t \sim T - T_c$, one may arrive at the critical point of $U(\phi)$, see Sec. 1.3. The source term λ_1 (or magnetic field H in Ising model) is tuned or set to zero already. The red and green points are the local minimum and maximum of the potential respectively. 14
1.4 ϕ^3 potential at the Lee-Yang point obtained by tuning the parameter λ_1 (magnetic field) and keeping $\lambda_2 < 0$. Note there is only one independent relevant parameter for ϕ^3 theory. In another word, for any given λ_2, by tuning λ_1 one can always arrive at the Lee-Yang point which is described by the non-unitary ϕ^3 theory. An alternative and equivalent approach to arrive at a ϕ^3 theory is by shifting the field, as discussed in the context. Again, the red and green points are respectively the local minimum and maximum of the potential while the magenta point is the Lee-Yang (spinodal) point, which appears when the minimum and maximum point collides with each other. 17
1.5 The probability distribution for a given stochastic variable m. The dashed curve and solid curve describe the equilibrium and non-equilibrium distribution respectively. The non-equilibrium distribution is different from the equilibrium one due to the 2PI effective action (entropy). The width of the distribution $W_{mm}^{1/2}$ is broadened since more microscopic independent degree of freedoms are generated. However, the price to pay is that the peak of the distribution is shifted with an decreasing maximum entropy. This is because of the fact that the probability is summed to unity, $\int_m P(m) = 1$. 28
1.6 The diagrammatic representation of equilibrium non-Gaussian cumulants (cf. Eq. (1.98)), adapted from Ref. [64]. The solid circle stands for the field $\phi(x)$, and the open circle (vertex) for the coupling constant of ϕ^n attached by n legs. The waving line is the zero wavenumber ($q = 0$) propagator $m^{-1} = \xi^2$. 35

1.7 Illustration of the second (a), third (b) and fourth (c) moments of a distribution. In (a) curves of Gaussian distribution with different widths are presented. In (b) and (c), red curves are for negative values while the blue curves for the positive, both describe the deviation from a Gaussian distribution represented by the dashed curves. 35
1.8 The QCD phase diagram in $T-\mu$ plane [68]. 43
1.9 The QCD phase diagram in $T-\mu-m_{\rm ud}$ plane (Frithjof Karsch, University of Bielefeld). Here, T_c (red point) is the critical transition temperature in the chiral limit (do not confused by the critical temperature for the QCD critical point, which is also denoted by T_c in this thesis); T_{pc} (yellow point) is the pseudo critical transition temperature of QCD with massive (up and down) quarks; the dark-red point is the tri-critical point described by ϕ^6 theory; the blue point is the QCD critical end point that we mainly focus on in this thesis. The QCD phase diagram depicted in Fig. 1.8 is the slice partially bounded by the dashed lines, tuned by the physical quark masses. The dashed curves indicate the crossover transition, while the solid lines are lines of second-order phase transitions. The gray surface is a hyper-surface of first-order phase transition points. 44
1.10 A particular example of the non-universal map from Ising variables (t, H) to the QCD coordinate (μ, T). 49
1.11 Mapping kurtosis κ_4 from (t, H) coordinate to (μ, T) coordinate, adapted from Ref. [64]. The cumulant is negative (red) around the crossover side and positive along the first-order phase transition line. 50
1.12 Diagrammatic representation of $\kappa_3[Q]$ (left) and $\kappa_4[Q]$ (right) in Eq. (1.155), adapted from Ref. [63]. The wavy line represents the propagator of σ field, i.e., $1/m_\sigma^2 \sim \xi^2$, cross circle stands for the insertion of charges q_A, integrated by $\int_A$ of the loop with the blue points for the insertion $\partial/\partial\sigma$, the black points unattached with the loop are the vertices of the σ field (i.e., open circles in Fig. 1.6). 54
1.13 (a) The Relativistic Heavy Ion Collider (RHIC) in Brookhaven, New York, United States (Brookhaven National Laboratory) and (b) the High-Intensity Heavy Ion Accelerator Facility (HIAF) in Huizhou, Guangdong, China (Institute of Modern Physics, Chinese Academy of Sciences). 56
1.14 The relativistic nucleus-nucleus collisions and the production of QGP (adapted from Ref. [79]). 56

1.15 The collision energy dependence of the directed flow (v_1) slop parameter near mid-rapidity for protons, anti-protons and net-protons measured by the STAR collaboration, along with UrQMD calculations subject to the same cuts and fit conditions [80]. The produced particles such as anti-protons are supposed to behave monotonically. In contrast, protons and net protons are sensitive to the stopping effect, and the observed minimum for which resembles the predicted "softest point collapse" of flow. 58

1.16 Event-by-event net-particle multiplicity distributions for Au+Au collisions at $\sqrt{s_{NN}} = 14.5\,\mathrm{GeV}$ for net-charge ΔN_{Ch} (left), net-kaon ΔN_{K} (middle) and net-proton ΔN_{P} (right) for $0-5\%$ top central (black circles), $30-40\%$ central (red squares), and $70-80\%$ peripheral (blue stars) collisions [82]. 59

1.17 The collision energy dependence of the cumulant ratio $\kappa_4/\kappa_2 = \kappa\sigma^2$ (left) and $\kappa_3/\kappa_2 = S\sigma$ (right) for net-protons in Au-Au collisions at different centralities measured by the STAR collaboration. A non-monotonic behavior is seen in the most central collisions (filled-circles) [84]. 60

1.18 Theoretical prediction of equilibrium kurtosis $\kappa_4(\sqrt{s_{NN}})$ along the freezeout line (dashed green line). Figures are adapted from Ref. [86] and [64]. 61

1.19 Contour plot of equilibrium (a) and non-equilibrium kurtosis $K \equiv \kappa = \kappa_4/\kappa_2^2$ with different non-universal phenomenological inputs (b) and (c) adapted from Ref. [76]. The $K > 0$ region is colored in red and the $K < 0$ region in blue, in the opposite convention of Fig. 1.11. The white arrow represents the evolution trajectory of system while the green dashed line represents the freezeout surface. 62

2.1 The separation of hydrodynamic scales illustrated on top of the Japanese woodblock print, *The Great Wave off Kanagawa* (Katsushika Hokusai, 1830). The fluid is coarse grained such that each pixel represents a hydrodynamic cell of width b. The hydrodynamic variables, defined as local functions of the hydrodynamic cells, fluctuate at the scale of $y \geq b$, which is much less than the typical inhomogeneous scale (wavelength L) of the fluid background. . . 74

2.2 Schematic illustration of the confluent derivative for a Lorentz vector (one-point fluctuation ϕ_μ). In order to compare the "internal" difference of $\phi_\mu(x+\Delta x)$ and $\phi_\mu(x)$ at different spacetime points, we boost $\phi_\mu(x+\Delta x)$ (solid green arrow) from the local rest frame at $x + \Delta x$ to the local rest frame at x, the frame defines $\phi_\mu(x)$. 91

2.3 Schematic illustration of the Lorentz boost (represented here by an ordinary rotation) of point separation vector y needed to keep the point separation purely spatial in the local rest frame at a new point Δx, given $u(x + \Delta x) = \Lambda(\Delta x)^{-1}u(x)$. 93

2.4 Schematic illustration of the confluent correlator. 96

2.5 *Left:* Illustration of the surface orthogonal to the conservative flow u at each point. Boost is represented by ordinary rotation, preserving angles, for clarity. *Right:* The same is not possible for non-conservative flow, i.e., for nonzero vorticity. However, it is possible to make the normal vector to the surface (not shown) and the flow vector u (shown) at the same point be different by a purely vortical vector: $v^\mu = \partial^\mu \tau - u^\mu$, such that $\partial \cdot v = 0$. 111

2.6 A schematic curve of $W(x, q)$ (in red color) that manifests the decomposition given by Eq. (2.155). $W^{(0)}$ is the equilibrium value (blue dashed line) achieved at large q. The gradient expansion at small $k/\gamma q^2$ gives rise to the part linear in gradient, $W^{(1)}$. The remaining part $\widetilde{W}$, in large part from the contributions of wavenumber modes around q_*, is the long-time tails discussed in Sec. 2.6.2. The feedback contributions from the small-q modes are suppressed by the phase space integration. 117

3.1 A schematic plot of the vicinity of the critical end point (blue point) in the $T-\mu$ plane of the QCD phase diagram. The contours of the equilibrium correlation length ξ separate several distinct regimes characterized by frequency ω. See text for detailed illustration. 146

3.2 Frequency dependence of transport coefficients $\zeta(\omega)$ and $\lambda(\omega)$ in the vicinity of a critical point, where the divergence of ξ leads to several distinct regimes characterized by frequency ω (or corresponding wavenumber $k = \omega/c_s$). The crossover from ordinary hydrodynamics (Hydro) to Hydro+ is marked by the fall-off of $\zeta(\omega)$ at $\omega \sim \Gamma_\xi \sim \xi^{-3}$, while the Hydro+ itself breaks down at $\omega \sim \Gamma'_\xi \sim \xi^{-2}$ as signaled by the fall-off of $\lambda(\omega)$, when the crossover to Hydro++ regime occurs. Of course, in ordinary hydrodynamics both transport coefficients are constants independent of frequency (dashed line), while in Hydro+, which does describe the fall-off of $\zeta(\omega)$, the coefficient λ is still a constant. Hydro++ describes the fall-off of both $\zeta(\omega)$ and $\lambda(\omega)$. 148

4.1 Critical exponents $\sigma = 1/\delta$ and ν_c as a function of Euclidean dimension d for different truncations of the scale-dependent effective action Γ_k, as specified by the set of integers (n_U, n_Z, n_W) (cf. Sec. 4.1.3). The data for the truncation $(4, 2, 1)$ lies almost exactly on top of that for $(4, 2, 0)$. Shown in comparison are results from the one- and two-loop ε expansion [158, 132] as well as high-temperature series expansion data ($d = 3$) [132, 133]. We observe that the numerical accuracy of the functional RG results improves significantly as one goes to higher orders in the derivative and field expansion, respectively. . . . 165

4.2 Anomalous dimension η for different truncations of the scale-dependent effective action in $d = 3$, 4, and 5 dimensions. 168

4.3 Rescaled anomalous dimension $\eta(\alpha)/|\eta(\alpha_{\text{opt}})|$ shown as a function of α. Different curves correspond to data obtained in $d = 3$, 4, and 5 dimensions, respectively. The optimal value α_{opt} for which the critical exponent i s least sensitive to changes in the deformation parameter, i.e., $\eta'(\alpha = \alpha_{\text{opt}}) = 0$, shifts to larger values as the dimension d is lowered. The displayed values were obtained for a truncation of the scale-dependent effective action Γ_k of the type $(4, 2, 0)$. 175
4.4 (a) The mean-field Ising equation of state $M(H)$ and (b) the corresponding effective potential $V(M)$ at $H = 0$ in the low-temperature phase ($T < T_c$). The analytic continuation of the stable branch (dashed curve) is bounded by the spinodal points (red). The straight line connecting the two minima of the effective potential is determined by the Maxwell construction. 180
4.5 Analytic continuation $t \to -t$ from the principal, i.e., high-temperature sheet (left panel) to the low-temperature sheet (right panel) of the mean-field scaling function $z(w)$ in Eq. (4.52) with $w \sim Ht^{-3/2}$. Starting from $H > 0$ and $t > 0$, keeping $H > 0$ and $|t|$ fixed we rotate the phase $\arg t$ from 0 to $-\pi$ and trace the corresponding movement of the variable w along the shown circular path. The principal sheet features a pair of Lee-Yang branch cuts along the imaginary w axis, which terminate in the Lee-Yang edge singularities. Going through the cut we enter the metastable low-temperature branch ($H < 0$, $t < 0$). One reaches the stable branch ($H > 0$, $t < 0$) when $\arg t = -\pi$. From there one can also reach metastable branch $H < 0$ by rotating $\arg H$ from 0 to $\pm\pi$, which changes $\arg w$ by $\pm\pi$. 181
4.6 The Riemann sheet of $\operatorname{Im} z(w)$ in the complex w plane for the mean-field ϕ^4 theory subject to O(1) symmetry (a), and for the spherical model, i.e., the large-N limit of a O(N) theory (b). The red line stands for the Lee-Yang cut while the magenta line for the Goldstone cut. 183
4.7 Analytic continuation $t \to -t$ from the principal, i.e., high-temperature sheet (top left panel) to the low-temperature sheet (top right panel) and the following successive processes (from bottom right panel to left) of the scaling function $z(w)$ of the Ising theory as conjectured by Fonseca and Zamolodchikov, where $w \sim Ht^{-\beta\delta}$, while keeping the magnetic field $H > 0$ fixed at $d = 4 - \varepsilon$. After analytic continuation the metastable branch $H < 0$ can be accessed by rotating H clockwise in the complex plane, while keeping $t < 0$ fixed. The line representing the Langer cut is rotated away from imaginary axis by an angle $\Delta\phi$, cf. Eq. (4.56). 186
4.8 The Fonseca-Zamolodchikov conjecture for $t < 0$, illustrated in the complex H plane. The line along the negative real H axis represents the Langer cut. The second cut on the ancillary sheet is the Lee-Yang cut, which is associated with the Lee-Yang edge singularity. The latter is expected to be the nearest singularity under the Langer cut. 187

4.9 We show the position of the two zeros w_1 and w_2 (solid points) and single pole w_0 (open circle) of the parametrically represented inverse isothermal susceptibility $F'(z)$ at order $\mathcal{O}(\varepsilon^2)$ in the complex w plane ($b_1 \neq 0$). Note, only the singularities in the upper half of the complex w plane are shown. . 197

4.10 (a) Equation of state $M(H)$ of the three-dimensional $\mathrm{O}(N)$ model in the $N \to \infty$ limit and (b) the corresponding effective potential $V(M)$ at $H = 0$ in the low-temperature phase ($T < T_\mathrm{c}$). The dashed curve illustrates the analytic continuation of the stable branch (solid curve). In addition to the spinodal singularities at nonvanishing H, the presence of massless Goldstone modes induces singularities on the coexistence line ($T < T_\mathrm{c}$ and $H \to 0$). . . 201

4.11 The phase diagram of the ferromagnetic system in the $T - n$ plane. The left panel is phase diagram for a mean-field theory where there are distinct boundaries of the stable, metastable and unstable phase, separated by the coexistence curve (solid) and spinodal curve (dashed) respectively. However, such boundaries are dimmed beyond mean-field approximation when fluctuations are taken into account. 207

E.1 The parameters c_n, $n = 1, 2, 3$ as a function of b_1. We observe a critical value $b_1 \approx 0.552$ above which all solutions θ_n^2, $n = 1, 2, 3$, are real. 226

E.2 We show the distribution of the zeros w_1, w_2, and w_3 (solid points) and pole w_0 (open circle) of the parametrized inverse isothermal susceptibility $F'(z)$ up to $\mathcal{O}(\varepsilon^3)$. Here, $b_1 \gtrsim 0.552$, such that all singular points align either along the Lee-Yang cut (situated on the imaginary w axis) or the Langer cut (along the dashed line). Note, only the singularities in the upper half of the complex w plane are shown. 227

List of Tables

1.1 Analogous quantities in statistic mechanics and scaler quantum field theory, the ± sign and β factors are neglected. 24
1.2 Critical scaling of thermodynamic quantities. 31
1.3 Summary of several dynamical universality class models discussed in this thesis. $c \approx 0.7(1 - 1.7\varepsilon)$, $x_\lambda \approx \varepsilon$. 39

4.1 Diagrammatic representation of the functional RG flow equations for the scale-dependent effective action Γ_k and the n-point 1PI vertices $\Gamma_k^{(n)}$ generated from the n-th order functional derivatives of Γ_k. The double line represents the regularized propagator $G^{(2)}$ defined in Eq. (4.10). The cross vertex stands for the insertion of $\partial_s R_k$, while the black verticies with n legs for $\Gamma^{(n)}$. . . . 160
4.2 Operators and canonical dimension of associated parameters and couplings that appear in the expansion of Γ_k (cf. Eq. (4.16)). Note that we drop the RG scale index k, since the canonical dimensions are defined at the Gaussian fixed point of the RG β functions. 161
4.3 Numerical values for the anomalous dimension η and critical exponents σ, ν_c in $d = 3$, 4, and 5 dimensions. Here, we show our best estimates with errors to account for possible systematic effects (see Sec. 4.1.6). These values were obtained with an exponential regulator ($\alpha = 1$) (cf. Eq. (4.36)) and the truncation of the type $(7, 5, 0)$. 170
4.4 Different estimates for the critical exponent σ (as compiled in Ref. [139]) including results from the constrained three- and four-loop ε' expansion [139], strong-coupling expansion [140], Monte Carlo methods [141, 142], and conformal bootstrap [143]. The values obtained from the functional RG, with an exponential regulator ($\alpha = 1$) and truncation of the type $(7, 5, 0)$, lie within error bars of Refs. [140, 141, 142], and are slightly larger the values provided by constrained Padé approximants of three- and four-loop ε' expansion results [139], but are smaller than those obtained by conformal bootstrap methods [143]. 171

4.5 Anomalous dimension $\eta = \eta(\alpha)$ at the Lee-Yang point in d dimensions, evaluated for the (deformed) exponential regulator $R^{\exp}_{\alpha,k}(q) = \alpha \bar{Z}_k q^2 \left[\exp(q^2/k^2) - 1\right]^{-1}$ with $\alpha > 0$. The optimal value of α depends on the dimension, i.e., $\alpha_{\mathrm{opt}} = \alpha_{\mathrm{opt}}(d)$ (cf. Fig. 4.3). The shown values were obtained using a truncation of the scale-dependent effective action Γ_k defined by the index set $(4, 2, 0)$. 174

D.1 The behavior of thermodynamic coefficients used in the paper in different limits. For non-relativistic ideal gas $\gamma = c_p/c_v > 1$ denotes adiabatic constant and M the molecule mass. 223

List of Abbreviations

BES Beam Energy Scan

BEST Beam Energy Scan Theory

BNL Brookhaven National Laboratory

CFT Conformal Field Theory

CGC Color-Glass Condensate

CMB Cosmic Microwave Background

EOM Equation of Motion

EOS Equation of State

FAIR Facility for Antiproton and Ion Research

FRG Functional Renormalization Group

HADES High Acceptance Di-Electron Spectrometer

HIAF High-Intensity Heavy Ion Accelerator Facility

HIC Heavy-Ion Collisions

IR Infrared

LF Laboratory Frame

LHC Large Hadron Collider

LHS Left Hand Side

LRF Local Rest Frame

MPD Multi Purpose Detector

nPI *n*-particle-irreducible

QCD Quantum Chromodynamics

QFT Quantum Field Theory

RG Renormalization Group

RHIC Relativistic Heavy Ion Collider

RHS Right Hand Side

SPS Super Proton Synchrotron

UV Ultraviolet

Acknowledgments

First and foremost, I would like to thank my advisor, Professor Mikhail Stephanov, for his patient guidance and continuous supports throughout my PhD career. His insightful perception, illuminating advices and persistent encouragement not only prompt me to tackle the hard problems, but also influence the way I think about physics. Without his dedicated efforts, this dissertation thesis would never have been formulated.

In my first few years in Chicago, I had learned the advanced physics with a broad range of subjects at UIC and UChicago, in large part from Prof. Snezhana Abarzhi, Tom Imbo, Wai-Yee Keung, Arthur Licht, Dirk Morr, Lian-Tao Wang and my advisor Mikhail Stephanov. Their passionate and heuristic instructions beaconed the path of my journey to a marvelous destination. In the Department of Physics at UIC, I have communicated to many extraordinary physicists. I would like to thank Prof. Olga Evdokimov, David Hofman and Dirk Morr for joining the committee of my preliminary exam and dissertation defense, as well as our graduate advisor, James Nell, for his professional advices as always.

I have had the good fortune to work in the UIC nuclear theory group with Gokce Basar, Masaru Hongo, Amadeo Jimenez-Alba, Tigran Kalaydzhyan, Wai-Yee Keung, Shiyong Li, Bo Ling, Kiminad Mamo, David Mesterhazy, Dragana Pilipovic, Maneesha Pradeep, Todd Springer, Mikhail Stephanov, Yuya Tanizaki, Ho-Ung Yee and Yi Yin. It's been my great honor for having chances to collaborate and discuss with our brilliant and friendly group members, individually or collectively in the group meeting. The first time when I attended the group meeting was as fresh as though it had happened yesterday, at that time I could not do more than just listen. Benefited from the unspectacular learning process, I became one of the discussants and presenters years later and began to enjoy the informal discussions. Those productive times have been an unforgettable memory in my mind. I would like to express my special thanks to Prof. Ho-Ung Yee, for his meticulous guidance and stimulating discussions throughout my PhD study; Prof. Wai-Yee Keung, for his genial conversations and impressive instructions; Prof. Gokce Basar and Dr. David Mesterhazy, for their fruitful collaboration and versatile assistance; Prof. Yi Yin and Dr. Bo Ling, for their enlightening suggestions and help in my early stage of PhD study, and particularly for Yi's invitation and discussions in many academic events; Ms. Maneesha Pradeep and Dr. Dragana Pilipovic, for having numerous discussions in our sharing office.

I would also like to thank my colleagues Jingyi Chao, Lipei Du, Ulrich Heinz, Joseph Kapusta, Dmitri Kharzeev, Volker Koch, Shuai Liu, Xiaofeng Luo, Mauricio Martinez, Swagato Mukherjee, Jorge Noronha, Jacquelyn Noronha-Hostler, Paolo Parotto, Scott Pratt, Thomas Schaefer, Chun Shen, Shuzhe Shi, Edward Shuryak, Dam Thanh Son, Huichao Song, Derek Teaney, Shanjin Wu, Nu Xu, Yi Zhang, and many others I had met and talked with in the community. I apologize for not listing all of them here individually. Special thanks to my undergraduate thesis advisor, Prof. Xiaobing Zhang, who drew my attention to the physics I'm currently working on when I was at Nankai.

Last but not least, I thank my families in particular my parents for their long-standing care and support in my life, especially in the tough time of the COVID-19 pandemic. Fortunately my roommates and friends in Chicago help me a lot with the passing years. They make me feel like I had never been far away from home. It is very difficult to list each of them here but nevertheless I would like to express my sincere appreciation to them all.

Parts of this dissertation are based on my previous publications [1, 2, 3, 4, 5, 6]. These work are supported by the European Research Council under the European Union's Seventh Framework Programme (FP7); the Swiss National Science Foundation; the U.S. Department of Energy, Office of Science, Office of Nuclear Physics, within the framework of the Beam Energy Scan Theory (BEST) Topical Collaboration.

Summary

In this dissertation thesis, we review and formulate the theory of fluctuations which is expected to be employed in the ongoing relativistic heavy-ion collision experiments. We begin with a review of the path integral formalism of classical field theory and its alternative approach, the effective action, where all fluctuations are incorporated via the renormalization group analysis. Provided the basic concepts, we analyze the fluctuations in a dichotomous description, i.e., fluctuations which are in equilibrium and out of equilibrium, static and dynamic, critical and non-critical, Gaussian and non-Gaussian, perturbative and non-perturbative, local and non-local, etc. In this thesis, special attention is paid to the hydrodynamic fluctuations and critical fluctuations, both of which are crucial for describing the evolution of the strongly interacting fluid droplet transiting the QCD critical point. We establish the general hydro-kinetic framework for the non-equilibrium hydrodynamic (thermal) fluctuations, and accommodate it in the vicinity of the critical point. Besides the QCD critical point, we also analyze the equilibrium fluctuations that is non-perturbative near the Lee-Yang critical point. Based on the universality argument our conclusions and their phenomenological consequences could be connected and identified in the realistic scenarios.

Chapter 1

Introduction

1.1 Overview

It has been known for about half century that our nature is governed by four fundamental forces: gravitational, electromagnetic, weak and strong interaction. After a persistent development in the half century since the milestone work by Gross, Wilczek, Pilitzer [7, 8] and Fritzsch, Gell-Mann, Leutwyler [9], physicists nowadays believe that Quantum Chromodynamics (QCD), as an essential ingredient of the Standard Model, has been a fundamental theory for strong interactions (see Sec. 1.4.1 for review). QCD is managed to provide a framework consisting of two aspects: first, how the majority of the visible matters is made of in our Universe, and second, how those matters interact themselves. Although QCD successfully describes the building blocks of matters and their dynamic interactions at the applicable scale the theory itself claims, not too much is well understood about the equilibrium and non-equilibrium properties of hot and dense matters whose underlying physics is described by strong interaction. Such matters are expected to occur in the early age of Universe, the core of compact star and in recent decades in ground-based laboratory facilities (Fig. 1.1). Nevertheless, there are two basic properties charactering the strong interaction: asymptotic freedom and confinement. The former predicts the existence of the most primordial state of

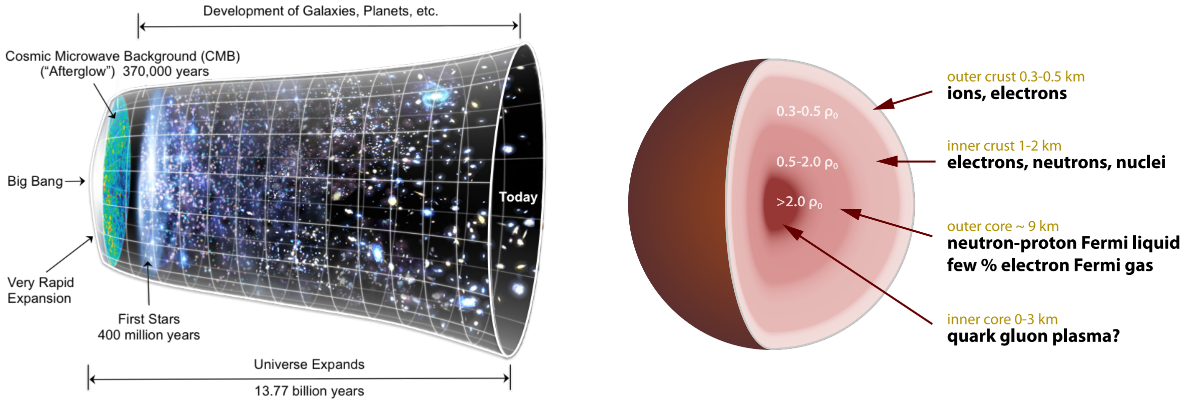
Development of Galaxies, Planets, etc.
Cosmic Microwave Background (CMB)
("Afterglow") 370,000 years
Big Bang
Very Rapid Expansion
First Stars
400 million years
Today
Universe Expands
13.77 billion years
0.3-0.5 ρ_0
0.5-2.0 ρ_0
>2.0 ρ_0
outer crust 0.3-0.5 km
ions, electrons
inner crust 1-2 km
electrons, neutrons, nuclei
outer core ~ 9 km
neutron-proton Fermi liquid
few % electron Fermi gas
inner core 0-3 km
quark gluon plasma?

(a) (b)

Figure 1.1: (a) The chronology of early Universe (NASA/WMAP) and (b) the inner structure of the compact star (R. Schulze).

matter – Quark-gluon plasma (QGP), and the latter indicates a world of confining hadrons that is familiar to our daily life. It was then recognized that various models based on QCD predict a transition from the hadronic phase to the QGP phase [10, 11, 12].

Understanding the phases of matters and the ubiquitous transition phenomena between them have always been a fundamental scientific question the human beings quested in the history. The phase transition of liquids and gases, had been an underlying principle to promote the First Industrial Revolution and affects our daily experience. Why is this phases of QCD matter also important? Of course, the answer is more than simply "because it was there" (Leigh Mallory), it, to some extent, also provides us a universal description of phases of strongly interacting system, the lesson we learned and the method we developed from which, shall be very likely to shed light for us to understand many other puzzling phenomena from condensed matter physics [13, 14, 15, 16] to string theory [17, 18, 19, 20], and some of which might even play an important role for our future lifestyles.

Steven Weinberg once said in an interview, that "by knowing the story behind our theories, we, as physicists, can feel part of a great historical progression. That sense of motion keeps us at our desks and in our laboratories" [21]. In fact, it might be surprising that the scientific languages we are using in our studies are not something the human beings knew very well even several decades earlier. The journey of the exploration on phase transitions is such an example, it really began not too long ago in the history of science. The earliest known pursuit was probably performed in 1822 by Cagniard de la Tour, who discovered continuous transition from liquid to vapor and observed the critical temperature by heating and compressing certain liquids in his cannon barrel experiments [22]. Similar phenomena was also discovered for carbon dioxide by Thomas Andrews in 1869, who introduced the term "critical point". Four years later (1873), in the thesis for doctoral degree Van der Waals wrote an equation of state (EOS) with a critical point of the liquid-gas phase transition [23]. At the beginning of the twentieth century, Marian Smoluchowski discovered the density fluctuations in the gas phase (1904) and soon realized the relation between density fluctuations and criticality in the study of critical opalescence (1908). Inspired by Smoluchowski's explanation, Albert Einstein provided a quantitative formula for the light scattering due to the density fluctuations in 1910. In the first half of twentieth century, a mathematical model of ferromagnetism was studied by Ising (1925) and Onsager (1944) and turned out to be a widely-used important model in modern physics [24, 25]. In 1937, Landau developed the mean-field theory of phase transitions and critical phenomena [26]. The theory beyond mean-field approximation, as a part of the renormalization group theory, is developed by Kandanoff, Wilson, Fisher, et al., during the second half of the twentieth century [27, 28, 29, 30] (see also Sec. 2.6).

As a consequence of renormalization, it is quite natural to realize that different critical phenomena can be categorized into various universality classes. The universality of critical phenomena makes the knowledge of the well-studied theory, for instance, the Ising model or, more broadly, ϕ^4 field theory, important to the study of a wide range of phenomena [31] from Curie points in magnets and liquid-gas transitions, to the cosmologically relevant phase transition in the gauge-Higgs sector of the Standard model [32], and the phase diagram of QCD at finite density studied in heavy-ion collisions [10, 11, 12]. Nowadays, although very much is known about the phases of liquid and gas, yet still very little about the phases of strongly interacting matter, especially at finite temperatures and densities, in contrast to those of hot plasma for high temperature (early Universe) and the cold quark matter for high density (core of superdense stars), of which we have a better understanding. Fortunately, the matters at various temperatures and densities can be produced in laboratory facilities by the experiments of the ultra-relativistic nucleus-nucleus collisions, i.e., heavy-ion collisions (HIC) [33]. A basic stages of HIC is illustrated in Fig. 1.2. The particle accelerators are ideal incubators of copies of our "early Universe", "superdense stars" and most remarkably, the smallest, most vortical primordial fluid created on earth. Since the record of its first head-on collisions, Relativistic Heavy Ion Collider (RHIC) in Brookhaven National Laboratory (BNL) achieved fruitful experimental results and significantly promoted our understanding of quark matters. By tuning the beam energies, the created matters would experience the strong interacting phases at different temperatures and densities, leaving its footprint in the QCD phase diagram. Therefore, the accelerator facilities provide us a versatile approach to study the strongly interacting matters and their phase transitions (see Sec. 1.5.2 for review). However, the price we have to pay is that, unlike Cagniard de la Tour who could "seat down" and manipulate his apparatus patiently, the droplets created in heavy-ion collisions survive in a extremely short lifetime (about 10 fm/c), during which the non-equilibrium and non-homogeneous media expand and freeze out dramatically fast. Thus, the non-equilibrium dynamics are essential to understand the phases of matter created in heavy-ion collisions. The dynamics for critical phenomena is reviewed in Chap. 3.

The main results presented in this thesis are parts of the theoretical framework for interpreting the experimental results from the RHIC Beam Energy Scan (BES) program. In particular, we will focus on the QGP evolution which is well described by the perfect hydrodynamics, whose theoretical prediction is consistent with the BES-I results (e.g., the elliptic flow discussed in Sec. 1.5.2). In heavy-ion collisions, the relativistic evolution of the strongly interacting matter can be described by the hydrodynamics reasonably and unreasonably well. Besides, the typical system size is large enough to be treated hydrodynamically but small enough for hydrodynamic fluctuations to be important and directly observable via

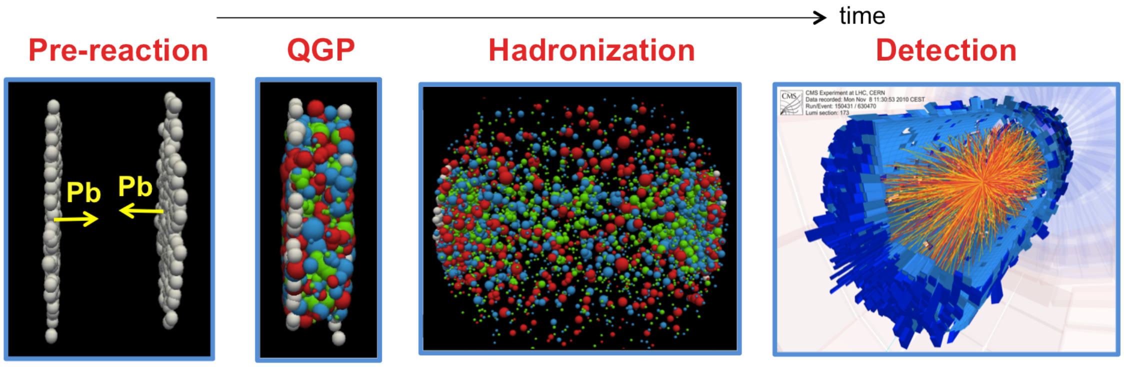

Figure 1.2: The basic stages of a heavy-ion (Pb-Pb) collision event in a nutshell (Wei Li).

event-by-event measurements. Thus, a hydrodynamic framework with fluctuations is in demand. Moreover, the fluctuations near the critical point are likely to explain the relevant BES-I results by comparing with their theoretical prediction based on static equilibrium assumption (Sec. 1.5.2). However, it is an intriguing hint rather than the smoking gun for the triumph of discovering a critical point, because the non-equilibrium hydrodynamic evolution with memory effect (e.g., Fig. 1.19), which could potentially change the prediction based on equilibrium theory even qualitatively, hasn't yet been taken into account. Furthermore, it is still not clear how one could treat the non-perturbative and non-equilibrium process occurred along with the first-order phase transition in heavy-ion collisions. Thus, as an integral part of the solution to answer those questions, this thesis consists of two major ingredients: first, a general systematic framework of hydrodynamics with non-equilibrium fluctuations and critical slowing down, which is essential for the comparison to experiment (Chap. 2 and 3); and second, a better understanding of the analyticity of the critical equation of state based on universality, which is not only indispensable for the system of hydrodynamic equations to be closed, but also conducive to the understanding of first-order phase transitions from a profound perspective (Chap. 4).

Motivated by the heavy-ion collision experiments, the dynamics of charge fluctuations was recently studied by Ref. [34, 35, 36, 37]. However, in a hydrodynamic flow charge fluctuations are not independent of other hydrodynamic modes (such as energy and momentum density fluctuations). A well-known example is that, due to the convection of hydrodynamic fluid, the dynamical universality class of QCD critical point is ascribed to Model H instead of Model B [38]. Moreover, as this thesis will discuss, these fluctuation modes couple with each other and all play important roles as long as the system approaches the critical point. Hydro+ [39], a hydrodynamic framework incorporate only one such mode, is thus significantly extended. Based on a few simplifications and approximations which is convenient for numerical implementation, we would be able to understand how the framework of Hydro+ (and possibly its extension) is visualized in realistic scenarios such as heavy-ion collisions [40, 41, 42].

A systematic treatment of hydrodynamic fluctuations can be dated back to 1950s by Landau and Lifshitz, based on the stochastic Langevin dynamics. The stochastic formalism of hydrodynamic fluctuations was studied for a relativistic fluid since last decades [43, 44, 45, 46], again, largely motivated by the progressive heavy-ion collision experiments. In the stochastic sector, dealing with the divergences from the noise is inevitable and troublesome. On the other hand, a complimentary formalism was pioneered by Andreev in 1970s in a non-relativistic context [47]. Unlike the Landau-Lifshitz formalism, the variables this formalism dealt with are all deterministic. By performing a renormalization procedure, all divergences coming from the noise are absorbed into the bare hydrodynamic variables, and the resulting deterministic equations are cutoff independent and therefore simulation friendly. In recent years, the deterministic (also referred to as hydro-kinetic) approach was studied for a relativistic fluid subject to the symmetry of boost-invariance [48, 49, 50], and was partially generalized to a neutral fluid with arbitrary background in Ref. [1]. In Chap. 2, we present such a general systematic formalism describing dynamics of fluctuations in an arbitrary relativistic hydrodynamic fluid. To be more specific, we derive a deterministic evolution equation for the fluctuation modes which nontrivially matches the kinetic equation for phonons propagating on an arbitrary background including relativistic inertial and Coriolis forces due to acceleration and vorticity of the flow. We introduce a concept of confluent connection which takes into account the relativity of "equal time" in the definition of the equal-time correlator of fluctuations. Feedback of fluctuations modifies hydrodynamic coefficients including viscosities and conductivity. We then perform necessary renormalization of short-distance singularities to obtain cutoff independent deterministic equations suitable for efficient numerical implementation. Notwithstanding, the formalism presented in Ref. [1] is yet still inadequate for its implementation near the critical point, since the conserved charges play an important role due to the critical slowing down. In a following work, Ref. [2], we accommodate a U(1) charge in the hydro-kinetic theory and implement it in the vicinity of a critical point. In Chap. 3, we discuss this implementation with the critical dynamics. Focusing on the critical mode we show how this general formalism matches existing Hydro+ description of fluctuations near the QCD critical point [39] and nontrivially extends it inside and outside of the critical region. The last part of the thesis, Chap. 4, focuses on the equilibrium properties of the QCD critical point. In this chapter, we address a number of outstanding questions associated with the analytic properties of the universal equation of state of the ϕ^4 theory, which describes the ubiquitous critical behavior in the same universality class of Ising model and QCD. We discuss the relation between the spinodal points and Lee-Yang edge singularities in and beyond the mean-field approximation. The non-perturbative nature of Lee-Yang points is described by ϕ^3 interaction, which can be analyzed by the functional renormalization process for the equilibrium fluctuations.

Before we discuss these topics in detail, in the remaining part of Chap. 1, we will review the relevant theoretical fundamentals and selected experimental results related to the fluctuations and criticality in heavy-ion collisions. Form the modern point of view, we are living in an "effective" world, where all our descriptions of the world rely on the scales we have reached, and the information from the underlying physics characterized by the microscopically short-distance fluctuations, are encoded in the low energy observables already. The bridge of the microscopic quantum theory and macroscopic effective theory, is known as renormalization. We will discuss Wilson's basic idea of renormalization group in Sec. 2.6. The renormalization procedure could be performed by integrating out fluctuations in the momentum-shell slides successively, or do it once analytically if feasible, relying on the validity of perturbation analysis. By introducing an infrared (IR) regulator, it is plausible to identify a scale-dependent Wilsonian effective action, such that all fluctuations beyond the scale parameter are already integrated out. Such formalism does not rely on the perturbative scheme and is therefore very convenient for studying the non-perturbative fluctuations (Sec. 4.1.1). In Sec. 1.2.3, we introduce the concept of the one-particle-irreducible (1PI) effective action, whose minimum directly provides the expectation value of the quantum field. Moreover, it serves as a connection from the Euclidean field theory to the statistic mechanics, a puzzling duality that helps us to study the phase transitions in a field-theoretic language. Following this we extend the concept to n-particle-irreducible (nPI) effective action and limit our discussion to the 2PI case, which will be used in Sec. 3.1 to understand how the two-point fluctuations correlators drive the system out of equilibrium (decrease the entropy from its maximum). We will also briefly discuss the critical fluctuations, both in equilibrium and out of equilibrium, in Gaussian approximation and beyond Gaussian approximation (Sec. 1.3). In particular, we illustrate the basic idea that how to connect the fluctuations of the critical modes to the measurable observables, and finally present the relevant intriguing results from RHIC BES program, being a part of the motivation to perform the research this thesis will discuss. It is nevertheless worthwhile to emphasize that the most important concept introduced in Chap. 1, the effective action. We will soon see how it plays its crucial role in each topic of this thesis.

In this thesis, we adopt the natural unit $k_B = c = \hbar = 0$ if not specified. We are trying to keep the notation convention and minimize their conflicts. However, when such a conflict occurs, we believe it shall be understood in the context where it appears unambiguously.

1.2 Fluctuations and Field Theory

1.2.1 Classical Field Theory

The equilibrium physics of a system is completely determined by the partition function (Wick-rotated generating function) for one or a few fluctuating fields, say, $\phi(x)$, considered as the deviation from the background field $\bar{\phi}$. In response to an external source $J(x)$ the partition function is written as

$$\mathcal{Z}[J] = e^{\mathcal{W}[J]} = \int \mathcal{D}\phi \exp\left\{-\mathcal{S}[\phi(x)] + \int d^d x J(x) \cdot \phi(x)\right\}, \tag{1.1}$$

where an unimportant prefactor $\mathcal{Z}_0 = e^{-\mathcal{S}[\bar{\phi}]}$ is phased out by normalization and

$$\mathcal{S}[\phi(x)] = \int d^d x \, \mathcal{L}(\phi(x), \partial_\mu \phi(x)) = \int d^d x \left[\frac{1}{2} Z(\partial_\mu \phi)^2 + U(\phi(x)) + \dots\right] \tag{1.2}$$

is the Euclidean d-dimensional *classical action* defined by the spacetime integration of the classical Lagrangian (density) $\mathcal{L}$, which is assumed to be *local* and translation invariant in spacetime. It could be expanded in powers of ϕ and its gradients to arbitrary high orders. In particular, the classical potential is formulated in a series

$$U(\phi(x)) = \lambda_1 \phi + \frac{1}{2}\lambda_2 \phi^2 + \frac{1}{3!}\lambda_3 \phi^3 + \frac{1}{4!}\lambda_4 \phi^4 + \dots \tag{1.3}$$

where only the first few terms, which will be primarily discussed in this thesis, are presented. From the viewpoint of renormalization group (RG) theory (Sec. 2.6), it is sufficient to keep finite amount of terms that are infrared relevant. Note that ϕ itself could have components ϕ_i satisfying an internal $O(N)$ symmetry where $i = 1, \dots, N$. It is of particular interest to consider two special limits when $N = 1$ and $N \to \infty$, in which cases ϕ^N model reduces to the Ising model and the spherical model respectively. These two models will be analyzed later in Chap. 4.

The expectation value of an operator $\mathcal{O}(\phi)$ is defined by a average with all microscopic (quantum) configuration

$$\langle \mathcal{O} \rangle = \frac{\int \mathcal{D}\phi \, \mathcal{O}(\phi) e^{-\mathcal{S}[\phi]}}{\int \mathcal{D}\phi \, e^{-\mathcal{S}[\phi]}} \tag{1.4}$$

where $e^{-\mathcal{S}[\phi]} = e^{-\int d^d x \mathcal{L}(\phi)}$ is analogous to the probability for a given field configuration $\phi(x)$, i.e., the partition function of a microscopic canonical ensemble in statistic mechanics. We will come back to this in Sec. 1.2.3.

Let's take a closer look of each terms in the classical action. First, we should notice that the overall prefactor of the effective action is redundant and could be chosen freely. A common way to fix this degree of freedom is to rescale ϕ by absorbing the factor Z in the kinetic term, in another word, one usually chooses the normalization $Z = 1$, thus the effective action is left with less parameters. Among those parameters, the linear parameter λ_1 vanishes by definition if the classical potential is expanded around an extreme; the quadratic parameter $\lambda_2 \equiv m^2$ defines the mass of the field and is interpreted as the curvature of the potential at the extreme; λ_n with $n \geq 3$ are non-Gaussian interaction terms, a theory in the absence of which is called *free field theory*. The free field theory can be readily handled by performing the Gaussian-like path integration. However, a general analytic evaluation of the path integral with interactions usually relies on the cumulant expansion of small parameters (formulated by Feynman diagrams).

The equation of motion (EOM) is given by

$$\frac{\delta \mathcal{S}[\phi(x)]}{\delta \phi(x)} = \frac{\partial \mathcal{L}(x)}{\partial \phi(x)} - \partial_\mu \frac{\partial \mathcal{L}(x)}{\partial(\partial_\mu \phi(x))} = J(x). \tag{1.5}$$

Substitute Eq. (1.2) and (1.3) (setting $Z = 1$ and neglecting higher order terms) into the above equation we obtain

$$\partial^2 \phi(x) = \frac{\delta U(\phi(x))}{\delta \phi(x)} - J(x). \tag{1.6}$$

If the Lagrangian $\mathcal{L}$ is invariant up to a four-divergence $\mathcal{K}^\mu$ under an infinitesimal deformation of the field configuration

$$\phi(x) \to \phi(x) + \alpha \delta\phi(x), \quad \mathcal{L}(x) \to \mathcal{L}(x) + \alpha \partial_\mu \mathcal{K}^\mu(x), \tag{1.7}$$

where α is an infinitesimal parameter, the *Noether's Theorem* states that there exists a conserved current

$$\mathcal{J}^\mu(x) = \frac{\partial \mathcal{L}(x)}{\partial(\partial_\mu \phi(x))} \delta\phi(x) - \mathcal{K}^\mu(x), \tag{1.8}$$

also referred to as the Noether current, associated with this continuous symmetry and satisfying the conservation law

$$\partial_\mu \mathcal{J}^\mu = 0\,. \tag{1.9}$$

The Noether's Theorem can also be generalized to an infinitesimal spacetime transformation $x^\mu \to x^\mu - a^\mu$, such that

$$\phi(x) \to \phi(x+a) = \phi(x) + a^\mu \partial_\mu \delta\phi(x), \quad \mathcal{L}(x) \to \mathcal{L}(x+a) = \mathcal{L}(x) + a^\mu \partial_\mu \mathcal{L}(x), \tag{1.10}$$

compare to Eq. (1.8) the conserved current in this case is

$$\mathcal{J}^\mu(x) = a_\nu T^{\mu\nu}(x), \tag{1.11}$$

where

$$T^{\mu\nu} = \frac{\partial \mathcal{L}(x)}{\partial(\partial_\mu \phi(x))} \partial^\nu \phi(x) - g^{\mu\nu} \mathcal{L}(x) \tag{1.12}$$

is the *stress-energy tensor*, also referred to as the energy-momentum tensor since it is associated with the symmetry of spacetime translation. Provided the Lagrangian in Eq. (1.2) the stress energy tensor is

$$T^{\mu\nu}(x) = \partial^\mu \phi \partial^\nu \phi - g^{\mu\nu} \left[\frac{1}{2} (\partial_\lambda \phi)^2 + U(\phi) \right]. \tag{1.13}$$

The well-known stress-energy tensor for ideal hydrodynamics reads

$$T^{\mu\nu} = (\varepsilon + p) u^\mu u^\nu + p g^{\mu\nu}. \tag{1.14}$$

1.2.2 Renormalization Group Theory

In Sec. 1.1, what do we mean by "effective" when we refer to an effective field theory? From the modern point of view, an effective field theory is a low-energy and long-distance proxy of a bare theory defined at an ultraviolet (UV) scale with respect to certain symmetries. The connection of the two theories describing physics at different scales are *renormalization*. It is a coarse-graining procedure managed to integrate out the ultraviolet degree of freedoms, namely, the large-momentum fluctuations. The ultraviolet contributions are usually divergent, and a sensible low-energy effective theory relies on the cancellation of all such ultraviolet divergence and the physical observables must be independent of the fake ultraviolet scales. There are several different renormalization procedures, let's firstly review the momentum-shell method that is initially developed by Kadanoff and Wilson [27, 28, 29].

ϕ^4 Theory

Wilson's approach is based on the path integral representation of the generating functional $\mathcal{W}[J]$, originally defined at an ultraviolet scale Λ which is much larger than any energy scales of practical interest, i.e.,

$$\mathcal{Z}[J] = e^{\mathcal{W}[J]} = \int [\mathcal{D}\phi]_{|k|<\Lambda} \exp\left\{ -\mathcal{S}[\phi(x),\Lambda] + \int d^d x J(x)\cdot\phi(x) \right\}, \tag{1.15}$$

where

$$e^{-\mathcal{S}[\phi(x),\Lambda]} = \int [\mathcal{D}\phi]_{|k|>\Lambda} e^{-\mathcal{S}[\phi(x)]}. \tag{1.16}$$

Let's for simplicity consider a massive ϕ^4 theory subject to a $Z(2)$ symmetry, defined at scale Λ as

$$\mathcal{S}[\phi(x)] = \int d^d x\, \mathcal{L} = \int d^d x \left[\frac{1}{2}(\partial_\mu \phi)^2 + \frac{1}{2}\lambda_2 \Lambda^2 \phi^2 + \frac{1}{4!}\lambda_4 \Lambda^{4-d}\phi^4 + \dots \right], \tag{1.17}$$

where all the coefficients are rescaled by Λ such that they are dimensionless. A typical shape of the potential $U(\phi)$ is plotted in Fig. 1.3. Treating terms other than the first (kinetic) term as perturbation, the action upon a single momentum-shell integration over $k \in [b\Lambda, \Lambda]$ reads

$$\begin{aligned} \mathcal{S}[\phi(x)] &= \int d^d x\, \mathcal{L} \\ &= \int d^d x \left[\frac{1}{2}(1+\Delta Z)(\partial_\mu \phi)^2 + \frac{1}{2}(\lambda_2 + \Delta\lambda_2)\Lambda^2 \phi^2 + \frac{1}{4!}(\lambda_4 + \Delta\lambda_4)\Lambda^{4-d}\phi^4 + \dots \right] \\ &= \int d^d x' \left[\frac{1}{2}(\partial'_\mu \phi')^2 + \frac{1}{2}\lambda'_2 \Lambda^2 \phi'^2 + \frac{1}{4!}\lambda'_4 \Lambda^{4-d}\phi'^4 + \dots \right], \end{aligned} \tag{1.18}$$

where in the last line we have introduced

$$\begin{gathered} x' = xb\,, \quad k' = k/b\,, \quad \phi' = [b^{2-d}(1+\Delta Z)]^{1/2}\phi\,, \\ \lambda'_2 = (\lambda_2 + \Delta\lambda_2)(1+\Delta Z)^{-1} b^{-1}, \quad \lambda'_4 = (\lambda_4 + \Delta\lambda_4)(1+\Delta Z)^{-2} b^{d-4}. \end{gathered} \tag{1.19}$$

The rescaled action $\mathcal{S}$, defined with a lower energy cutoff ($b\Lambda$) beyond which all high-energy fluctuations are integrated out, is referred to as the *Wilsonian effective action*[1]. In such coarse graining process, all coupling constants in the above expressions alter as a consequence of both rescaling and higher-order corrections. Successive integrations could be performed all the way down to a typical infrared scale (e.g., mass or external momentum), as long as the shifted effective coupling λ' remains small in order for perturbation theory to work. The transformation of Lagrangian becomes continuous when $b \to 1$, and such process is referred to as the *renormalization group* (RG). All the large-momentum fluctuations (including loop corrections) are absorbed into the effective couplings at tree level. The consequence of which is that the coupling is running, described by the RG equations (β functions). Note, however, the momentum-shell integration performed iteratively could be instead performed all at once if one sends $b \to 0$, which is technically simple. The price one needs to pay is that the integration might have ultraviolet divergences but one gets rid of the awkward slice integration with artificial parameter b. The two approaches should nevertheless be equivalent.

If we start with a massless free-field Lagrangian where all coupling constants vanish, i.e.,

$$\mathcal{L}_0 = \frac{1}{2}(\partial_\mu \phi)^2, \tag{1.20}$$

the Lagrangian will remain the same upon rescaling since there is no contribution from the interactions. This corresponds to a *Gaussian fixed point* (free-field fixed point) of the renormalization group flow. If we turn on the λ_4 coupling constant for the ϕ^4 interaction and take into account the leading loop contribution, after one iteration we find at $d < 4$ that

$$\lambda_4' = b^{d-4}\lambda_4 \left(1 - \frac{3\lambda_4}{2}\int_{b\Lambda \le |k| < \Lambda} \frac{K_d k^{d-1} dk}{(k^2)^2}\right) = b^{d-4}\lambda_4 \left(1 - \frac{3K_d(b^{d-4}-1)\Lambda^{d-4}}{2(4-d)}\lambda_4\right), \tag{1.21}$$

where

$$K_d = \frac{S_d}{(2\pi)^d} = \frac{2}{(4\pi)^{d/2}\Gamma(d/2)} \tag{1.22}$$

---

[1] Note that the Wilsonian effective action is different from the 1PI effective action introduced in Sec. 1.2.3, see discussion thereby.

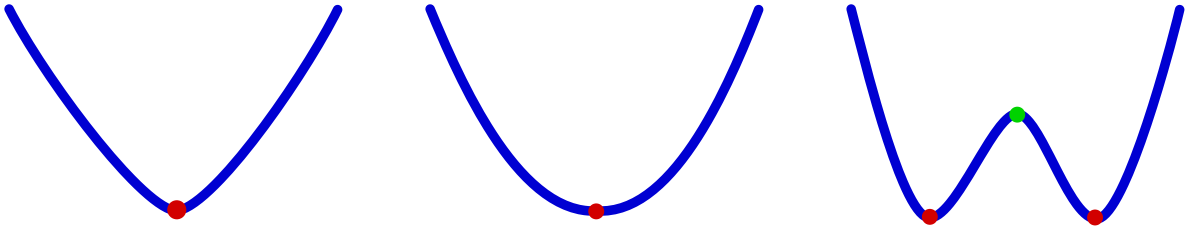
(a) $\lambda_2 > 0$ (b) $\lambda_2 = 0$ (c) $\lambda_2 < 0$

Figure 1.3: Various potentials $U(\phi)$ for a ϕ^4 theory with $\lambda_4 > 0$ and different values of λ_2. By tuning the parameter $\lambda_2 \sim t \sim T - T_c$, one may arrive at the critical point of $U(\phi)$, see Sec. 1.3. The source term λ_1 (or magnetic field H in Ising model) is tuned or set to zero already. The red and green points are the local minimum and maximum of the potential respectively.

is the loop factor and S_d is the surface area of the unit sphere in d dimensions, in particular, $K_{d=4} = 1/(8\pi)^2$. The effects of rescaling and higher-order corrections compensate each other, implying that there exists another fixed point of the renormalization group flow, referred to as the *Wilson-Fisher fixed point* [30]. Like all other quantum field theories (QFT) of physical interests, this fixed point approaches to the Gaussian fixed point at a specific limit, in this case $d \to 4$. In this limit the theory is weakly coupled and free-field like, thus the perturbation theory based on Feynman diagram analysis shall works.

Expand Eq. (1.21) in double series of $\varepsilon = 4 - d$ and λ_4, one finds the corresponding renormalization group equation (β function defined in Eq. (1.29)) for λ_4 up to second order to be

$$\beta(\lambda_4) = \frac{\partial \lambda_4}{\partial \log b} = -\varepsilon\lambda_4 + \frac{3}{2}\lambda_4^2\,, \tag{1.23}$$

where we have absorbed the loop factor K_d into the coupling constant λ_4, by taking the substitution $\lambda_4 \to \lambda_4/K_d$ effectively. Such absorption makes the RG equations more succinct. When $d \geq 4$ ($\varepsilon \leq 0$) the β function is positive, predicting the coupling flows to zero at infrared scales. On the other hand, when $d < 4$ ($\varepsilon > 0$), the β function has a nontrivial zero, the

Wilson-Fisher fixed point, which is given by the solution of $\beta(\lambda_4^*) = 0$, i.e.,

$$\lambda_4^* = \frac{2}{3}\varepsilon\,. \tag{1.24}$$

It is more tricky to deal with renormalized correlation functions, where the cutoff is sent to infinity and thus the renormalization conditions are in demand to define the theory at certain (arbitrary) renormalization scale μ. Let's consider the renormalized n-point functions of the form

$$G^{(n)}(x_1, x_2, \ldots, x_n; \mu, \{\lambda_i\}) \equiv \langle \phi(x_1)\phi(x_2)\ldots\phi(x_n)\rangle, \tag{1.25}$$

where $\lambda_i = \lambda_2, \lambda_4, \ldots$ represents a set of coupling constants. The computation of $G^{(n)}$ originating from the fixed bare action relies on the renormalization scale μ. If we perform a shift

$$\mu \to \mu + \delta\mu, \tag{1.26}$$

correspondingly we need the following adjustment

$$\lambda_i \to \lambda_i + \delta\lambda_i\,, \quad \phi \to (1+\delta\eta)\phi\,, \quad dG^{(n)} \to (1+n\delta\eta)dG^{(n)}, \tag{1.27}$$

giving rise to the *Callan-Symanzik equation*

$$\left[\mu\frac{\partial}{\partial\mu} + \beta(\lambda_i)\frac{\partial}{\partial\lambda_i} + n\gamma(\{\lambda_i\})\right] G^{(n)}(\mu, \lambda) = 0\,, \tag{1.28}$$

where $\beta(\lambda_i)$ and $\gamma(\{\lambda_i\})$ are functions describing the RG evolution rate of coupling λ and field strength normalization $Z^{1/2}$ respectively. They are defined by

$$\beta(\lambda_i) = \mu\frac{\partial}{\partial\mu}\lambda_i\,, \quad \gamma(\{\lambda_i\}) = \frac{\mu}{2}\frac{\partial}{\partial\mu}\log Z\,, \tag{1.29}$$

where $\mu\frac{\partial}{\partial\mu}$ is precisely $\frac{\partial}{\partial \log b}$ with $b = \mu/\Lambda$. The β function for $d \to 4$ can be generically written as

$$\beta(\lambda_i) = (-[\lambda_i] + \gamma_{\lambda_i})\lambda_i\,, \tag{1.30}$$

where $[\lambda_i]$ and $\gamma_{\lambda_i} \equiv \gamma_{\lambda_i}$ are respectively the mass dimension and γ function associated with $\{\lambda_i\}$, the former comes from the dimensionless rescaling and the latter describes the RG evolution rate. For $\lambda_i = \lambda_4$ this equation turns out to be the β function given by Eq. (1.23). In the absence of fluctuations ($d > d_c = 4$), $\gamma_{\lambda_4} = 0$, the only solution is the trivial Gaussian fixed point $\lambda_4 = 0$, the relevance against which classifies the operators $\mathcal{O}_{\lambda_i}$ associated with λ_i into three categories:

$$\begin{aligned} [\lambda_i] > 0\,, &\qquad \mathcal{O}_{\lambda_i} \text{ is relevant (super-renormalizable)}\,; \\ [\lambda_i] = 0\,, &\qquad \mathcal{O}_{\lambda_i} \text{ is marginal (renormalizable)}\,; \\ [\lambda_i] < 0\,, &\qquad \mathcal{O}_{\lambda_i} \text{ is irrelevant (non-renormalizable)}\,. \end{aligned} \tag{1.31}$$

We shall emphasize the relevance of an operator has its meaning when a particular fixed point is specified, otherwise it is by default referred to the Gaussian fixed point, for example, at $d < 4$ we say the ϕ^4 operator is relevant (against Gaussian fixed point) but it is however irrelevant against the Lee-Yang fixed point (see Chap. 4). In the presence of fluctuations ($d < d_c = 4$), as we discussed before, the competition of $[\lambda_4]$ and γ_{λ_4} gives rise to the Wilson-Fisher fixed point λ_4^*. For $\lambda_i = \lambda_2$, we have

$$\beta(\lambda_2) = \mu\frac{\partial}{\partial\mu}\lambda_2 = (-2 + \gamma_{\lambda_2})\lambda_2\,, \tag{1.32}$$

with the solution

$$\lambda_2(\mu) = \lambda_2(\Lambda)\left(\frac{\Lambda}{\mu}\right)^{2-\gamma_{\lambda_2}}\,. \tag{1.33}$$

At long distances Λ/μ increase and the mass term becomes more and more important in the Lagrangian. The criterion for mass term to be important is given by

$$\lambda_2(\mu \sim \xi^{-1}) \sim 1\,, \tag{1.34}$$

which defines the correlation length at the Wilson-Fisher fixed point,

$$\xi \sim \lambda_2^{-\nu} \sim m^{-2\nu} \tag{1.35}$$

where we have used $\lambda_2(\Lambda) = m^2/\Lambda^2$ and

$$\nu^{-1} = 2 - \gamma_{\lambda_2}(\lambda_4^*)\,. \tag{1.36}$$

We will discuss more about the massless limit $\lambda_2 \to 0$ in Sec. 1.3, where the fluctuations that ϕ^4 theory describes becomes critical.

ϕ^3 Theory

The extreme of an action (or the potential in the homogeneous case) is usually referred as to the *saddle point*. For a given field configuration there might be more than one saddle point around which we can perform a perturbative series expansion. Different perturbation series are typically associated with different sectors (excitations) of the field theory. We have analyzed in a nutshell the renormalization of ϕ^4 theory satisfying a $Z(2)$ symmetry ($\lambda_1 = \lambda_3 = 0$). The framework can be generally applied to other field theories, among those a particular interest will be given to the ϕ^3 theory. It is somewhat related to the ϕ^4 theory being discussed. As we shall see in Sec. 4, when we consider the ϕ^4 theory in the presence of an external field (Fig. (1.4)), or analytically continue the ϕ^4 theory into the complex plane, where there are saddle points or critical points around which the ϕ^3 theory becomes more relevant. In other words, such saddle points can be reached by tuning relevant parameters or shifting the field configuration from the original saddle point (e.g., the minimum of a ϕ^4 potential, see Fig. 1.4).

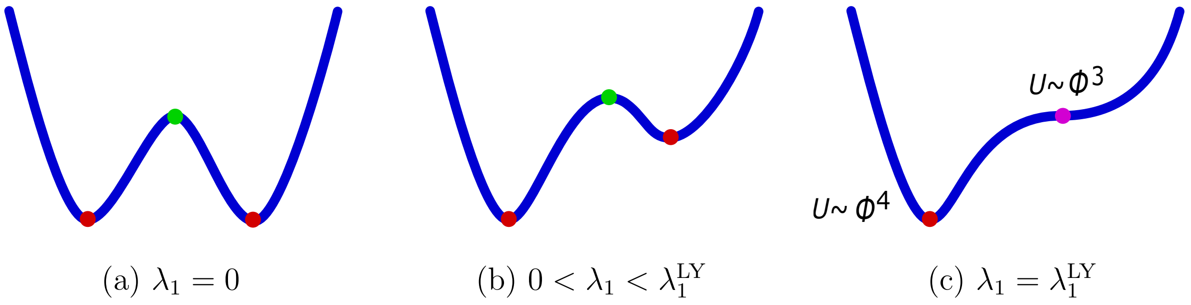

(a) $\lambda_1 = 0$ (b) $0 < \lambda_1 < \lambda_1^{\mathrm{LY}}$ (c) $\lambda_1 = \lambda_1^{\mathrm{LY}}$

Figure 1.4: ϕ^3 potential at the Lee-Yang point obtained by tuning the parameter λ_1 (magnetic field) and keeping $\lambda_2 < 0$. Note there is only one independent relevant parameter for ϕ^3 theory. In another word, for any given λ_2, by tuning λ_1 one can always arrive at the Lee-Yang point which is described by the non-unitary ϕ^3 theory. An alternative and equivalent approach to arrive at a ϕ^3 theory is by shifting the field, as discussed in the context. Again, the red and green points are respectively the local minimum and maximum of the potential while the magenta point is the Lee-Yang (spinodal) point, which appears when the minimum and maximum point collides with each other.

Let's begin with the classical Lagrangian defined in d-dimensional Euclidean space, i.e.,

$$\mathcal{L}(\phi(x)) = \int d^dx \left[\frac{1}{2}(\partial_\mu\phi)^2 + U(\phi)\right] = \int d^dx \left[\frac{1}{2}(\partial_\mu\phi)^2 + \lambda_1\phi + \frac{1}{2}\lambda_2\phi^2 + \frac{1}{4!}\lambda_4\phi^4\right], \quad (1.37)$$

where we absorbed the dimension scale factor Λ of each term for simplicity. The classical field ϕ is already considered as a fluctuation field on top of a background which is irrelevant here. The critical points are defined by the following two conditions

$$U'(\phi) = \lambda_1 + \lambda_2\phi + \frac{1}{3!}\lambda_4\phi^3 = 0\,, \quad (1.38)$$

$$U''(\phi) = \lambda_2 + \frac{1}{2}\lambda_4\phi^2, \quad (1.39)$$

which gives

$$\phi_{\text{LY}} = \left(-\frac{2\lambda_2}{\lambda_4}\right)^{1/2}, \quad \lambda_1^{\text{LY}} \equiv \lambda_1(\phi_{\text{LY}}) = -\frac{2\lambda_2}{3}\phi_{\text{LY}} = -\frac{2\lambda_2}{3}\left(-\frac{2\lambda_2}{\lambda_4}\right)^{1/2}. \quad (1.40)$$

This critical point is referred to as the Lee-Yang point associated with the Lee-Yang edge singularity. For both $\lambda_2 > 0$ and $\lambda_4 > 0$ (corresponding to high temperature phase of ϕ^4 theory), λ_1^{LY} is purely imaginary, in accordance with the Lee-Yang theorem [51, 52]. If we consider a field shift $\phi \to \phi + \Delta\phi$ where $\Delta\phi$ is space independent, we obtain

$$\begin{aligned}\mathcal{L}(\phi(x)) = \int d^dx \Bigg[&\frac{1}{2}(\partial_\mu\phi)^2 + \frac{1}{2}\left(\lambda_2 + \frac{1}{2}\lambda_4(\Delta\phi)^2\right)\phi^2 + \frac{1}{3!}(\lambda_4\Delta\phi)\phi^3 + \frac{1}{4!}\lambda_4\phi^4 \\ &+ \left(\lambda_1 + \lambda_2\Delta\phi + \frac{1}{3!}\lambda_4(\Delta\phi)^3\right)\phi\Bigg], \end{aligned} \quad (1.41)$$

where the field ϕ is the shifted one. When $\Delta\phi = \phi_{\text{LY}}$, the linear and quadratic term vanishes. We then can expand the Lagrangian around the Lee-Yang point, it can be obtained by applying the substitution $\Delta\phi \to \Delta\phi + \phi_{\text{LY}}$ in Eq. (1.41) and expand in $\phi - \phi_{\text{LY}}$:

$$\begin{aligned}\mathcal{L}(\phi(x)) = \int d^dx \Bigg[&\frac{1}{2}(\partial_\mu\phi)^2 + \frac{1}{2}g\left(\phi - \phi_{\text{LY}}\right)\phi^2 + \frac{1}{3!}\left(g + \lambda_4(\phi - \phi_{\text{LY}})\right)\phi^3 + \frac{1}{4!}\lambda_4\phi^4 \\ &+ \left(\lambda_1 - \lambda_1^{\text{LY}}\right)\phi + \mathcal{O}\left((\phi - \phi_{\text{LY}})^2\right)\Bigg], \end{aligned} \quad (1.42)$$

where a cubic coupling g breaking the $Z(2)$ symmetry emerges and is defined by

$$g = \lambda_4\phi_{\text{LY}} = (-2\lambda_2\lambda_4)^{1/2}. \quad (1.43)$$

Alternatively, one can expand the Lagrangian in the vicinity of the local minimum where the linear term in Eq. (1.41) vanishes, one obtain

$$\mathcal{L}(\phi(x)) = \int d^dx \left[\frac{1}{2}(\partial_\mu\phi)^2 + \left(\frac{g(\lambda_1 - \lambda_1^{\mathrm{LY}})}{2}\right)^{1/2}\phi^2 + \frac{1}{3!}\left(g + \lambda_4\left(\frac{2(\lambda_1 - \lambda_1^{\mathrm{LY}})}{g}\right)^{1/2}\right)\phi^3 \right.$$
$$\left. + \frac{1}{4!}\lambda_4\phi^4 + \mathcal{O}(\lambda_1 - \lambda_1^{\mathrm{LY}})\right]. \tag{1.44}$$

Eq. (1.42) and (1.44) are related by the mean-field equation of state for the Lee-Yang points:

$$\lambda_1 - \lambda_1^{\mathrm{LY}} = \frac{1}{2}g(\phi - \phi_{\mathrm{LY}})^2. \tag{1.45}$$

Effectively, one can define the mass term

$$m^2 = g(\phi - \phi_{\mathrm{LY}}) = \left(2g(\lambda_1 - \lambda_1^{\mathrm{LY}})\right)^{1/2}. \tag{1.46}$$

Unlike the ϕ^4 theory, mass is not an independent relevant variable. Given that λ_4 is irrelevant [53], a missive ϕ^3 theory would be sufficient to describe the Lee-Yang edge singularities. Below we shall sketch the main feature of the ϕ^3 theory, based on the terse expression

$$\mathcal{L}(\phi(x)) = \int d^dx \left[\frac{1}{2}(\partial_\mu\phi)^2 + \lambda_1\Lambda^{\frac{d+2}{2}}\phi + \frac{1}{2}\lambda_2\Lambda^2\phi^2 + \frac{1}{3!}\lambda_3\Lambda^{\frac{6-d}{2}}\phi^3\right]. \tag{1.47}$$

Similar to what we have done for ϕ^4 theory, we need to take into account the contribution of cubic fluctuations to the free-field theory. Indeed, all the tricks we played with ϕ^4 theory shall be straightforwardly applied to ϕ^3 theory. However, unlike the ϕ^4 theory to which the perturbative renormalization theory applies when $\varepsilon = 4 - d$ is small, for ϕ^3 theory the perturbative calculation can be handled only if $\varepsilon' = 6-d$ is small. In this limit, the β function (Eq. (1.30)) for cubic coupling λ_3 is obtained by taking into account the contribution from its lowest-order (triangle) loop diagram:

$$\beta(\lambda_3) = -\frac{\varepsilon'}{2}\lambda_3 - \frac{3}{4}\lambda_3^3, \tag{1.48}$$

where we have once again absorbed the loop factor K_d into the coupling constant λ_3, i.e., $\lambda_3^2 \to \lambda_3^2/K_d$. The solution of this equation gives rise to another nontrivial fixed point, the

Lee-Yang fixed point:

$$\lambda_3^* = \left(-\frac{2\varepsilon'}{3}\right)^{1/2}, \tag{1.49}$$

which is imaginary as long as ε' is real. Clearly, the results obtained from perturbative RG can not be trusted at $d = 3$ ($\varepsilon' = 3$), thus a non-perturbative approach, which will be discussed in Sec. 4.1.1, is in demand.

1.2.3 Effective Action

We have discussed the basic idea of renormalization group theory in two naive examples, ϕ^3 and ϕ^4 scaler theory. From these examples we see how the fluctuations of microscopic degrees of freedom can be handled systematically in order to get into a macroscopic effective description in the formulation of Wilsonian effective action. As the field strength and coupling constants are renormalized by these fluctuations, the expectation value of the field, $\langle\phi\rangle$, is altered as well. The evaluation of the path integral of QFT is in general not that easy. Thus it is convenient to introduce an *effective action* [54, 55], that can provide us the exact value of $\langle\phi\rangle$ at its stationary point. In another words, we are seeking an alternative, classical approach to solve the quantum problem. The effective action is different from the classical action by the corrections from quantum and thermal fluctuation. It is also distinguished from the Wilsonian effective action introduced in Sec. 2.6, since it incorporates fluctuations from all energy scales and thus is scale independent[2]. To some extent, the renormalization is managed to obtain a well-defined, finite effective action by adjusting a finite set of parameters and counter terms in the classical action. The effective action, as we will see soon, plays an essential role in connecting the quantum field theory and statistic mechanics.

---

[2] However, it is still possible to introduce a scale-dependent effective action, combining the spirit of the 1PI effective action and Wilsonian effective action, see Sec. 4.1.1 for details.

Equilibrium (1PI) Effective Action

The effective action is mathematically defined by the Legendre transform of the generating functional $\mathcal{W}[J]$ (cf. Eq. (1.1))

$$\Gamma[\varphi] \equiv \sup_J \int d^4x J(x)\varphi(x) - \mathcal{W}[J] \tag{1.50}$$

where

$$\varphi(x) = \langle\phi(x)\rangle_J = \frac{\delta\mathcal{W}[J]}{\delta J(x)} = \frac{\delta\log\mathcal{Z}[J]}{\delta J(x)} = \frac{\int\mathcal{D}\phi\, e^{-\int\mathcal{L}-J\phi}\phi(x)}{\int\mathcal{D}\phi\, e^{-\int\mathcal{L}-J\phi}} \tag{1.51}$$

is the expectation value (order parameter) of ϕ in the presence of the source J. The field ϕ could be vectors or spinors but we consider scalers here as it's sufficient for the scope of this thesis. The effective action satisfies the equation of motion

$$\left.\frac{\delta\Gamma[\varphi]}{\delta\varphi(x)}\right|_{\varphi=\langle\phi\rangle_J} = J(x). \tag{1.52}$$

Like Eq. (1.5), this equation tells us that in the absence of the source current J, the expectation value of the classical field, $\langle\phi\rangle$, is given by the stationary point of Γ. In this sense, the effective action $\Gamma[\varphi]$ is analogous to the classical action $\mathcal{S}[\phi]$. However, $\Gamma[\varphi]$ is designed to incorporate both thermal and quantum fluctuations already by performing the path integral calculation, and hence more convenient and straightforward for practical purpose. Similar to what we have done on $\mathcal{S}[\phi]$, we can alternatively expand the effective action in powers of momentum, read off in the position space as

$$\Gamma[\varphi(x)] = \int d^dx\, \mathcal{L}_{\text{eff}}(\varphi(x), \partial_\mu\varphi(x)) = \int d^dx \left[\frac{1}{2}(\partial_\mu\varphi(x))^2 - U_{\text{eff}}(\varphi(x)) + \dots\right], \tag{1.53}$$

where $\mathcal{L}_{\text{eff}}$ is the (1PI) effective Lagrangian and U_{eff} is the effective potential[3]. The solution of Eq. (1.52) will be independent on x if we consider Lorentz-invariant vacuum state, therefore the kinetic terms vanish in such case and the effective action, as an extensive quantity, should be proportional to the effective potential, i.e., $\Gamma(\varphi) \propto -U_{\text{eff}}(\varphi)$. Eq. (1.52) then reduces to

---

[3] At tree level the effective potential coincides with the classical potential. Thus he subscript "eff" may be dropped later in this thesis if there is no risk to cause confusion.

$$\frac{\partial U_{\text{eff}}(\varphi)}{\partial \varphi}\Big|_{\varphi=\langle\phi\rangle_J} = -J. \tag{1.54}$$

This is the condition to determine the expectation value of ϕ in the presence of external source J. The relation between J and φ (and other possible relevant variables) is known as the equation of state (EOS) in condensed matter physics.

Indeed, introducing $\Gamma[\varphi]$ has its advantage in the sense the generating function $\mathcal{W}[J]$ may be calculated as a sum of tree (0PI, i.e., diagrams are disconnected by cutting any internal lines) diagrams as if the action were $\Gamma[\varphi]$ instead of $\mathcal{S}[\phi]$, since all 1PI diagrams are already collected in $\Gamma[\varphi]$ as sub-diagrams. In terms of the effective action $\Gamma[\varphi]$ we can rewrite Eq. (1.1) as

$$\mathcal{Z}[J] = e^{\mathcal{W}[J]} = \int_{\text{tree}} \mathcal{D}\varphi \exp\left\{-\Gamma[\varphi(x)] + \int d^dx J(x)\cdot\varphi(x)\right\}, \tag{1.55}$$

where φ is considered as an external field and only connected tree diagrams are involved in the calculation of $\mathcal{W}[J]$. At the stationary point $\varphi = \langle\phi\rangle_J$, we obtain exactly

$$\mathcal{Z}[J] = e^{\mathcal{W}[J]} = \exp\left\{-\Gamma[\varphi(x)] + \int d^dx J(x)\cdot\varphi(x)\right\}_{\varphi=\langle\phi\rangle_J}, \tag{1.56}$$

Similar to $\mathcal{W}[J]$ serves as the the generating function of the connected correlation functions,

$$\frac{\delta^n \mathcal{W}[J]}{\delta J(x_1)\ldots\delta J(x_n)} = \langle\phi(x_1)\ldots\phi(x_n)\rangle_{\text{c}} = G^{(n)}, \tag{1.57}$$

the effective action also serves as the generating function of the one-particle-irreducible (1PI) amputated correlation functions (proper vertices),

$$\frac{\delta^n \Gamma[\varphi]}{\delta\varphi(x_1)\ldots\delta\varphi(x_n)} = \langle\phi(x_1)\ldots\phi(x_n)\rangle_{\text{1PI}} = \Gamma^{(n)}. \tag{1.58}$$

Note $G^{(n)}$ and $\Gamma^{(n)}$ are related, in the case of two-point function as an example,

$$G^{(2)}(J) = \left(\Gamma^{(2)}[\varphi]\right)^{-1}. \tag{1.59}$$

Provided Eq. (1.58) the effective action could be written in a Taylor series

$$\Gamma[\varphi] = \sum_{n=2}^{\infty} \frac{1}{n!} \int d^d x_1 \dots d^d x_n \, \varphi(x_1) \dots \varphi(x_n) \, \Gamma^{(n)}(x_1, \dots, x_n). \tag{1.60}$$

Assume φ to be homogeneous for simplicity, the Callan-Symanzik equation for $\Gamma(\varphi) \propto -U_{\text{eff}}(\varphi)$ reads[4]

$$\left[\mu \frac{\partial}{\partial \mu} + \beta(\lambda_i) \frac{\partial}{\partial \lambda_i} - \gamma(\{\lambda_i\}) \varphi \frac{\partial}{\partial \varphi}\right] \Gamma(\mu, \{\lambda_i\}) = 0\,, \tag{1.61}$$

where $\varphi \frac{\partial}{\partial \varphi}$ counts the number of powers of φ in $\Gamma[\varphi]$ or $U_{\text{eff}}(\varphi)$. The solution of Eq. (1.61) will be discussed in Sec. 1.3.

For a miraculously deep reason, the classical statistic physics in d-dimensional space is dual to the Euclidean quantum field theory defined in d-dimensional spacetime ($(d-1)$-dimensional space). If we consider the Ising theory where magnetization is linearly coupled to the external magnetic field H, the partition function is given by

$$\mathcal{Z}(H) = e^{-\beta G(H)} = \int \mathcal{D}[\phi] e^{-\beta \int_x (\mathcal{H}[\phi] - H\phi)} \tag{1.62}$$

where the Hamiltonian density $\mathcal{H}[\phi]$ multiplied by $\beta = 1/T$ is dual to the classical action $\mathcal{S}$ and the field ϕ is linearly coupled to the external magnetic field H dual to the source term J. The Gibbs free energy[5]

$$G(H) = -\beta^{-1} \log \mathcal{Z}(H) \tag{1.63}$$

multiplied by β plays the role of the generating function $\mathcal{W}[J]$, and the Helmholtz free energy is obtained by the Legendre transform

$$F(M) = \sup_H \left(G(H) + HM\right) = \sum_n \frac{F^{(n)}}{n!} M^n, \tag{1.64}$$

where

$$M = \langle \phi \rangle_H = -\frac{\partial G(H)}{\partial H} = \beta^{-1} \frac{\partial \log \mathcal{Z}(H)}{\partial H} = \frac{\int_x \mathcal{D}[\phi] \, e^{-\beta \int (\mathcal{H} - H\phi)} \phi(x)}{\int_x \mathcal{D}[\phi] \, e^{-\beta \int (\mathcal{H} - H\phi)}} \tag{1.65}$$

---

[4] Notice the sign change in front of $\gamma(\lambda)$ compared to the Callan-Symanzik equation for $G^{(n)}$.

[5] The terminology might be different in different context. Sometimes Gibbs free energy is also termed grand (canonical) potential or even Helmholtz free energy. Although each of these terminologies has clear definition in condensed matter physics, the use of their names seems to be not rigorous in field theory.

is the magnetization analogous to the classical field φ. Thus $F(M)$ is analogous to the effective action $\Gamma[\varphi]$ and one can introduce the probability charactering the configuration of M,

$$P(M) \sim (\mathcal{Z}(H))^N = \exp\left[-N\beta(F(M) - HM)\right], \tag{1.66}$$

where N is an extensive quantities (e.g., total degrees of freedom or the volume of the system) that goes to infinity at thermodynamic limit. The most stable thermodynamical state is reached when P is maximized, in the thermodynamic limit, it is realized at the saddle point satisfying

$$\frac{\partial F(M)}{\partial M} = H\,. \tag{1.67}$$

In a stochastic system, the general configuration could deviate the mostly probable state and the fluctuation analysis is discussed in Sec.1.4.3. The dual relations of statistic mechanics and (scaler) quantum field theory are summarized in Tab. 1.1.

Statistic Mechanics	Quantum Field Theory
M	φ
H	J
$F(M)$	$\Gamma[\varphi]$
$G(H)$	$\mathcal{W}[J]$

Table 1.1: Analogous quantities in statistic mechanics and scaler quantum field theory, the ± sign and β factors are neglected.

Before conclude this subsection, we shall discuss a bit on the evaluation of $\mathcal{W}[J]$ or $\Gamma[\varphi]$, a challenging problem as one needs to sum over infinitely many Feynman diagrams. In most cases, one can only evaluate the path integral by using the steepest-descent method (saddle-point approximation) around the stationary point ϕ_s, which is the solution of the equation of motion, Eq. (1.5). Treat ϕ_s as a background field and expand the action up to quadratic order in fluctuation $\delta\phi = \phi - \phi_s$, one obtains, by performing the Gaussian integration, that

$$\mathcal{W}[J] = \mathcal{S}[\phi_s] + J\phi_s - \frac{1}{2}\operatorname{Tr}\log\left[\partial^2 - U''(\phi_s)\right] + \dots \tag{1.68}$$

from which one finds the Coleman-Weinberg effective action (and potential) (using $\varphi \approx \phi_s$ at leading order and φ is space independent)

$$\begin{aligned}\Gamma[\varphi] &= \mathcal{S}[\varphi] - \frac{1}{2}\operatorname{Tr}\log\left[\partial^2 - U''(\varphi)\right] + \ldots \\ &= \mathcal{S}[\varphi] + \frac{1}{2}\int d^dx \int \frac{d^dk}{(2\pi)^4}\log\left[k^2 + U''(\varphi)\right] + \ldots \\ &= V\left[U^{(0)} + U^{(1)} + \ldots\right] \end{aligned} \tag{1.69}$$

where $U^{(0)} = \mathcal{S}[\varphi]/V$ and

$$U^{(1)} = \frac{1}{2}\int \frac{d^dk}{(2\pi)^4}\log\left[\frac{k^2 + U''(\varphi)}{k^2}\right] \approx \frac{U''(\varphi)^2}{64\pi^2}\log[U''(\varphi)] + \ldots \tag{1.70}$$

is the one-loop correction and the all divergent terms are canceled by renormalization counter terms. The effective potential is understood as the expectation value of energy density (per unite volume) for a state in which the expectation value of the field is $\varphi = \langle\phi\rangle$. It shall be a convex function, i.e., $U''(\varphi) \geq 0$, in order to have a one-to-one map between conjugate variables of the Legendre transform. However, this condition is not always satisfied. Notice that $U^{(1)}$ vanishes if $U''(\varphi) = 0$. Furthermore, if $U''(\varphi) < 0$, $U(\varphi)$ develops imaginary parts [56], associated with the Lee-Yang cut which will be discussed formally in Chap. 4. The imaginary part of the effective potential is interpreted as half of the probability of decay per unit volume and time [57].

Non-equilibrium (nPI) Effective Action

In equilibrium, the effective action $\Gamma = \Gamma_{1\mathrm{PI}}[\varphi]$ only depends on the average of the field, $\varphi = \langle\phi\rangle_J$, as a consequence of the single Legendre transform given by Eq. (1.50). This is no longer true in the non-equilibrium situation, in which case the properties of the system also rely on multi-point functions $G^{(n)} = \langle\phi(x_1)\ldots\phi(x_n)\rangle_{\mathrm{c}}$ that is *independent* of φ. Thus the effective action shall become a functional of all independent variables, i.e.,[6]

$$\Gamma_{\mathrm{nPI}}[\varphi, G_n] = \sup_{J,\{K_n\}} \left(\int_x J\varphi + \int_{x_1,\ldots x_n} \sum_{n=2}^{\infty} \frac{1}{n!} K_n G^{(n)} - \mathcal{W}_{\mathrm{nPI}}[J,\{K_n\}] \right), \tag{1.71}$$

obtained from infinitely many Legendre transforms of the extended n-particle-irreducible (nPI) generating function $\mathcal{W}_{\mathrm{nPI}}[J,\{K_n\}]$, subject to the condition

$$\frac{\delta \mathcal{W}_{\mathrm{nPI}}[J,\{K_n\}]}{\delta J} = \varphi\,, \tag{1.72a}$$

$$\frac{\delta \mathcal{W}_{\mathrm{nPI}}[J,\{K_n\}]}{\delta K_n} = \frac{1}{n!} G^{(n)}. \tag{1.72b}$$

The equations of motion for the effective action is thus

$$\frac{\delta \Gamma_{\mathrm{nPI}}[\varphi, G^{(n)}]}{\delta \varphi} = J\,, \tag{1.73a}$$

$$\frac{\delta \Gamma_{\mathrm{nPI}}[\varphi, G^{(n)}]}{\delta G_n} = \frac{1}{n!} K_n\,, \tag{1.73b}$$

where J and K_n are the sources conjugate to φ and $G^{(n)}$ respectively. Let's consider the simplest case, the 2PI effective action (2PI entropy functional) $\Gamma_{\mathrm{2PI}} = S_2$ following Ref. [39]:

$$S_2[\varphi, G^{(2)}] = \Gamma_{\mathrm{2PI}}[\varphi, G^{(2)}] = \sup_{J,K_2} \left(J\varphi + \frac{1}{2}\langle \phi K_2 \phi \rangle - \mathcal{W}_{\mathrm{2PI}}[J, K_2] \right). \tag{1.74}$$

Unfortunately, the exact $\mathcal{W}_{\mathrm{2PI}}$ and therefore Γ_{2PI} is not known, however, one can evaluate it using the saddle-point approximation as we did to obtain Eq. (1.68). Thus

$$\mathcal{W}_{\mathrm{2PI}}[J, K_2] \approx S_0[\varphi] + J\varphi + \frac{1}{2}\varphi K_2 \varphi + \frac{1}{2}\log\det G^{(2)}, \tag{1.75}$$

where $S_0[\varphi]$ is the classical equilibrium entropy. Substituting this expression into Eq. (1.74) and use $\langle \phi K_2 \phi \rangle = \mathrm{Tr}\, K_2 G^{(2)} + \varphi K_2 \varphi$, we obtain

$$S_2[\varphi, G^{(2)}] \approx S_0[\varphi] + \frac{1}{2}\,\mathrm{Tr}\left(\log G^{(2)} + S_0'' G^{(2)} + 1 \right), \tag{1.76}$$

---

[6] Here we consider the single scaler field, an extension to multi-field theory shall be straightforward.

where $-G^{(2)} = (S_0'' + K_2)^{-1}$. In the absence of K_2, this expression reduces to Eq. (1.69), i.e.,

$$S_1[\varphi] \approx S_0[\varphi] + \frac{1}{2}\,\mathrm{Tr}\log(-S_0''). \tag{1.77}$$

Thus we can express S_2 in terms of S_1 as

$$S_2[\varphi, G^{(2)}] = S_1[\varphi] + \frac{1}{2}\,\mathrm{Tr}\left(\log(-S_0''G^{(2)}) + S_0''G^{(2)} + 1\right). \tag{1.78}$$

One can check $S_2 \leq S_1$ and S_2 is maximized at $S_2|_{K_2=0} = S_1$.

The expression of S_2 can be understood as following: the logarithmic term describe the uncertainty of the system as the Boltzmann entropy does, since $\sqrt{G^{(2)}}$ is the width of distribution $P(\phi)$ accounting the number of all microscopic states; the remaining terms vanish when $K_2 = 0$, and therefore describes the "force" K_2 driving the system away from equilibrium state characterized by S_0, i.e., $\langle S\rangle = S_0 - K_2G^{(2)} < S_0$ where $K_2 = -\frac{\partial S_2}{\partial G^{(2)}}$. See Fig. 1.5 for an illustration of its formulation in hydrodynamics with a slow mode (Hydro+), where $G^{(2)} \sim W_{mm} \sim N_{mm}$ (see Chap. 2).

Note, when φ and $G^{(2)}$ has space dependence, the trace becomes an integration of the continuous variable x. Furthermore, one can decompose the two-point function as a sum of all the wavenumber components, i.e., $G^{(2)}(x) \sim \int_q N^{(2)}(x,q)$, thus in terms of $N^{(2)}(x,q)$ Eq. (1.78) is modified to

$$\begin{aligned} S_2[\varphi, N^{(2)}] &= S_1[\varphi] + \frac{1}{2}\int \frac{d^3x d^3q}{(2\pi)^3}\left(\log(-S_0''(x,q)N^{(2)}(x,q)) + S_0''(x,q)N^{(2)}(x,q) + 1\right) \\ &= S_1[\varphi] + \frac{1}{2}\int \frac{d^3x d^3q}{(2\pi)^3}\left(\log\frac{N^{(2)}(x,q)}{N^{(2)}_{(\mathrm{eq})}(x,q)} - \frac{N^{(2)}(x,q)}{N^{(2)}_{(\mathrm{eq})}(x,q)} + 1\right), \end{aligned} \tag{1.79}$$

where we have introduced the equilibrium two-point function in phase space, i.e., $N^{(2)}_{(\mathrm{eq})}(x,q) = -S_0''(x,q)^{-1}$. Eq. (1.79) does not depend on the normalization of the two point function $G^{(2)}$ or $N^{(2)}$. It serves as a bridge for us to establish the connection between the hydro-kinetic theory and Hydro+ formalism in Sec. 3.1 (cf. Eq. (3.9)).

We shall keep in mind that path integral formulation in QFT describes spacetime dynamics at zero temperature while partition function in statistic mechanics describes finite

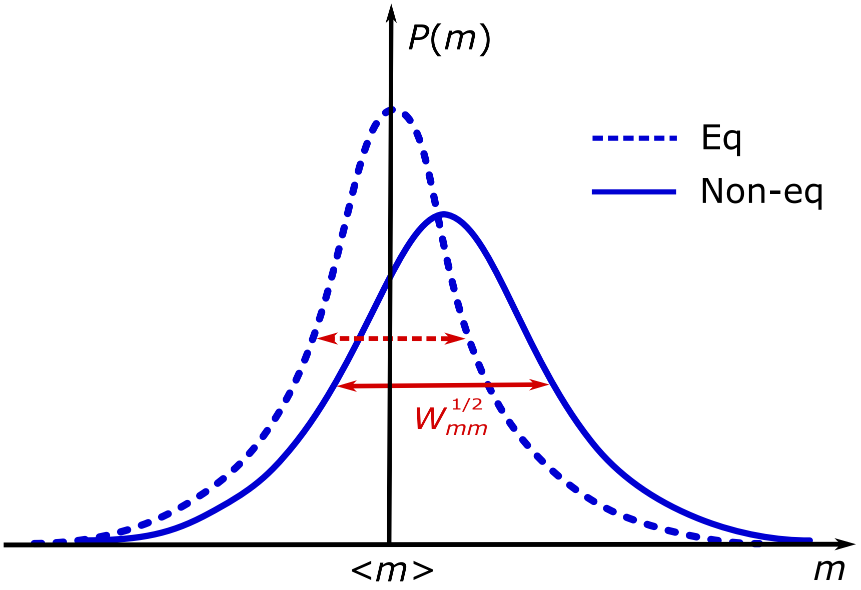

Figure 1.5: The probability distribution for a given stochastic variable m. The dashed curve and solid curve describe the equilibrium and non-equilibrium distribution respectively. The non-equilibrium distribution is different from the equilibrium one due to the 2PI effective action (entropy). The width of the distribution $W_{mm}^{1/2}$ is broadened since more microscopic independent degree of freedoms are generated. However, the price to pay is that the peak of the distribution is shifted with an decreasing maximum entropy. This is because of the fact that the probability is summed to unity, $\int_m P(m) = 1$.

temperature equilibrium thermodynamics which is time-independent. To combine both aspects and establish a time-dependent finite temperature non-equilibrium field theory, one needs to evoke the Schwinger-Keldysh (SK) formalism [58]. Formulating our theory discussed in Chap. 2 in SK formalism shall be an exciting task, however it is beyond the scope of this thesis. Related developments can be found in Ref. [59, 60, 61].

1.3 Critical Fluctuations

1.3.1 Equilibrium Critical Fluctuations

It has long been known that the various critical phenomena could be categorized into certain universality classes, both statically and dynamically. This classification only depends on the a few properties of the system, such as symmetry (number of field components N), dimension d, and the presence or absence of the conservation law, regardless of the disparity of the microscopic physics which might be complicated. This long-standing miracle in history is turned out to be nothing but a natural consequence of the renormalization group theory.

Let's firstly focus on the equilibrium fluctuations discussed generically in Sec. 1.2. In statistic mechanical interpretation, the bare mass parameter is related to the reduced temperature t by

$$\lambda_2(\Lambda) \sim t \equiv \frac{T - T_c}{T_c}, \tag{1.80}$$

where T_c is the critical temperature that is model dependent. According to Eq. (1.35), we have, however, the universal scaling relation which is model independent:

$$\xi \sim t^{-\nu}. \tag{1.81}$$

We say the equilibrium fluctuation becomes *critical* when we tune $\lambda_2 \to 0$ ($T \to T_c$), as illustrated in Fig. 1.3. This is a particularly simple example since the only relevant parameter (to the fixed point of physical interests) is the mass parameter λ_2, in the absence of other possible relevant parameters such as the magnetic field parameter λ_1 for all d or cubic coupling constant λ_3 at $d < 6$. Those relevant parameters, if present, must also be tuned together with λ_2 in order for the RG flow approaching the fixed point. During such running of flow, all irrelevant parameters gradually approach their fixed-point values. It is possible that there exists a region in which the relevant parameters remain small but all irrelevant parameters die out or approach their fixed-point values. This region is called the *scaling region*, where the correlation function can be expressed generically in its scaling form. For example solving Eq. (1.28) for $G^{(2)}$ one finds in the scaling region that

$$G^{(2)}(x;\mu,\lambda_2) \sim \frac{1}{|x|^{d-2+\eta}} f(\lambda_2(|x|\mu)^{1/\nu}), \tag{1.82}$$

where

$$\eta = 2\gamma_{\lambda_4}(\lambda_4^*), \tag{1.83}$$

ν is given by Eq. (1.36), $f(x)$ is a scaling function which falls exponentially at large distances:

$$f(\lambda_2(|x|\mu)^{1/\nu}) \sim e^{-\lambda_2^\nu \mu |x|} = e^{-m|x|}, \tag{1.84}$$

where we have identified $\lambda_2^\nu \mu = m = \xi^{-1}$.

In the critical region where the RG flow passes around the Wilson-Fisher fixed point but all relevant parameters are still small, the solution of Eq. (1.61) can be generically written in terms of certain universal scaling functions

$$U_{\text{eff}} = \varphi^{2d/(d-2)} f(\varphi\mu^{-(d-2)/2}, \lambda_4 = \lambda_4^*) = \varphi^{1+\delta} g(\lambda_2 \varphi^{-1/\beta}). \tag{1.85}$$

According to the correspondence of statistic mechanics (Ising theory) and scaler quantum field theory (Tab. 1.1), the analogous expression of Eq. (1.85) in Ising theory is

$$F(M,t) = M^{1+\delta} g(tM^{-1/\beta}) = t^{\beta(1+\delta)} h(Mt^{-\beta}), \tag{1.86}$$

and

$$H = \frac{\partial F(M,t)}{\partial M} = t^{\beta\delta} h'(Mt^{-\beta}). \tag{1.87}$$

Similar expressions are summarized in Tab. 1.2.

The critical exponents satisfy a set of useful scaling laws:

$$\text{Fisher scaling law :} \quad \gamma = (2-\eta)\nu \tag{1.88a}$$

$$\text{Josephson scaling law :} \quad \nu d = 2 - \alpha \tag{1.88b}$$

$$\text{Rushbrooke scaling law :} \quad \alpha + 2\beta + \gamma = 2 \tag{1.88c}$$

$$\text{Widom scaling law :} \quad \gamma = \beta(\delta - 1) \tag{1.88d}$$

Thermodynamic Quantities	Notation	Scaling
Free energy	F or G	$\lvert t\rvert^{\beta(1+\delta)}$
Specific heat	C_V	$\lvert t\rvert^{\alpha}$
Magnetization	M	$\lvert t\rvert^{\beta}$
Magnetic field	H	$\lvert t\rvert^{\beta\delta}$
Correlation length	ξ	$\lvert t\rvert^{-\nu}$
Susceptibility	χ_T	$\lvert t\rvert^{-\gamma}$

Table 1.2: Critical scaling of thermodynamic quantities.

which can be readily derived from thermodynamic relations. Among those critical exponents ν and η are more fundamental since they are directly related to $\gamma_{\lambda_2}(\lambda_4^*)$ and $\gamma_{\lambda_4}(\lambda_4^*)$ by Eq. (1.36) and (1.83) respectively. A field-theoretic calculation for $O(N)$ model gives

$$\eta = \frac{(N+2)}{2(N+8)^2}\varepsilon^2 + \mathcal{O}(\varepsilon^3), \quad \nu^{-1} = 2 - \frac{N+2}{N+8}\varepsilon - \frac{(N+2)(13N+44)}{2(N+8)^3}\varepsilon^2 + \mathcal{O}(\varepsilon^3). \tag{1.89}$$

The other critical exponents could be obtained by using the scaling laws given by Eq. (1.88), the results are

$$\alpha = \frac{(4-N)}{2(N+8)}\varepsilon - \frac{(N+2)^2(N+28)}{4(N+8)^3}\varepsilon^2 + \mathcal{O}(\varepsilon^3), \tag{1.90a}$$

$$\beta = \frac{1}{2} - \frac{3}{2(N+8)}\varepsilon + \frac{(2N^2+5N+2)}{2(N+8)^3}\varepsilon^2 + \mathcal{O}(\varepsilon^3), \tag{1.90b}$$

$$\delta = 3 + \varepsilon + \frac{(N^2+14N+60)}{2(N+8)^2}\varepsilon^2 + \mathcal{O}(\varepsilon^3), \tag{1.90c}$$

$$\gamma = 1 + \frac{(N+2)}{2(N+8)}\varepsilon + \frac{(N+2)(N^2+22N+52)}{4(N+8)^3}\varepsilon^2 + O(\varepsilon^3). \tag{1.90d}$$

When $d \geq 4$, these results reduces to their mean-field values predicted by Landau's theory, simply by setting $\varepsilon = 0$.

The equilibrium thermodynamic fluctuations are important to describe the phase transition phenomena in statistic system. Given a Gibbs free energy $G(\{H_i\})$ (or generating action $\mathcal{W}$) where $\{H_i\}$ is a set of relevant parameters including external sources as well as relevant coupling constants, the order of phase transition is determined by the analyticity of $M_i = -\partial G/\partial H_i$ where M_i is conjugate to H_i. If M_i is discontinuous (continuous), the phase transition is first (second) order[7]. First order phase transition can be also identified if two local minima of the effective potential are degenerate while the curvatures at the minima are still positive, the degenerate ground states are separated by a potential barrier. In contrast, second order phase transition is identified if the global minimum just develops two or more degenerate minima and the curvature remains zero, corresponding to the infinitely large correlation length associated with a fixed point. The fixed point is lying in the multi-dimensional critical hyper-surface expanded only by all irrelevant parameters (coefficients of irrelevant operators against fixed point). The RG flow in the full multi-dimensional space expanded by all parameters will terminate ultimately at such fixed point, if it starts from certain initial value of the relevant parameters at ultraviolet scale which define the critical point.

So far we are working with Euclidean space at $d = 4 - \varepsilon$ by dimension continuation. We shall still emphasize that our results rely on the perturbative analysis where the relevant quartic coupling constant at long distances are still small (of order ε). Although there might be no qualitatively differences, the perturbative renormalization theory fails in our real world where $d = 3$ ($\varepsilon = 1$). We will discuss the non-perturbative renormalization approach in Sec. 4.1.1.

1.3.2 Non-Gaussian Fluctuations

The Gaussian fluctuations are characterized by evaluating the two point functions in the saddle-point (mean-field) approximation in the thermodynamic limit:

$$G^{(2)}(x_1, x_2) = \langle \phi(x_1)\phi(x_2) \rangle = \frac{T}{4\pi |x_1 - x_2|} \exp\left[-\frac{|x_1 - x_2|}{\xi} \right], \tag{1.91}$$

---

[7] In Ising theory M_i is the magnetization, whose analyticity is shown in Fig. 1.10.

where T is restored by absorbing β in the Hamiltonian $\mathcal{H}$. This result is consistent with that given by Eq. (1.82) and (1.84) in the Gaussian limit ($\eta = 0$) and $d = 3$. Upon the Fourier transform it corresponds to the free-field propagator

$$W^{(2)}(q) = \frac{T}{m^2 + q^2} = \frac{T\xi^2}{1 + (q\xi)^2}, \tag{1.92}$$

where $m = \xi^{-1} = U''(\langle\phi\rangle)^{1/2}$ and q is the wavenumber conjugate to $x_1 - x_2$. The second-order phase transitions occur when $U''(\langle\phi\rangle) = 0$ tuned by the critical value of relevant parameters, indicating that the correlation length ξ is divergent in thermodynamic limit. Notice that when talking about the divergence of fluctuations near the critical point, one means a collective phenomenon involving the correlated fluctuations of infinitely many degree of freedom in the correlated volume ξ^3 which is infinitely large, rather than a common misunderstanding that the magnitude of fluctuations is divergent. In fact, one can introduce the extensive quantity

$$\phi_V \equiv \int d^3x \phi(x), \tag{1.93}$$

and the (square) magnitude of fluctuations could be measured by the second moment of which as

$$\kappa_2[\phi_V] = \langle\phi_V^2\rangle = V \int d^3x \langle\phi(x)\phi(0)\rangle \approx VT\xi^2, \tag{1.94}$$

where in the last step we present the mean-field results by substitute Eq. (1.91) into the above expression. It can be thought as the $q = 0$ wavenumber mode of $W^{(2)}$, i.e.,

$$\kappa_2[\phi_V] = \langle\phi_V^2\rangle = VW^{(2)}(q = 0) \approx VT\xi^2, \tag{1.95}$$

obtained straightforwardly from Eq. (1.92). In the case the correlation length ξ is much smaller compare to the inhomogeneity scale of the system (such as the hydro-kinetic theory discussed in Chap. 2), Eq. (1.91) could be approximated as a delta function, i.e.,

$$G^{(2)}(x_1, x_2) = \lim_{\xi \to 0} \frac{T}{4\pi|x_1 - x_2|} \exp\left[-\frac{|x_1 - x_2|}{\xi}\right] \approx T\xi^2 \delta^{(3)}(x_1 - x_2), \tag{1.96}$$

such that the space integration of which is normalized to the same result of Eq. (1.94). A more systematic analysis for the non-equilibrium two-point functions for multi-variables are discussed in Chap. 2.

As we mentioned in Sec. 2.6, from our RG analysis we realize for $d = 3$ non-Gaussian fluctuations are also relevant. Thus, non-Gaussian fluctuations that vanish in the free-field theory has to be taken into account in two aspects. First, the expressions for two-point functions need to be modified accordingly, e.g., the critical exponent η (cf. Eq. (1.82)), albeit very small, has to be restored in Eq. (1.91) and Eq. (1.92):

$$G^{(2)}(x_1 - x_2) \sim \frac{1}{|x_1 - x_2|^{d-2+\eta}} \exp\left[-\frac{|x_1 - x_2|}{\xi}\right], \quad W^{(2)}(q) \sim \frac{\xi^{2-\eta}}{1 + (q\xi)^{2-\eta}}, \tag{1.97}$$

where the expression $W^{(2)}(q)$ is approximated in its asymptotic form at large $q\xi$ [62]. This modification is negligible if one considers a system where the correlation length is not to large (such as the case of heavy-ion collisions). Second, what matters more is the non-Gaussian fluctuations themselves, to which the above analysis are extended as [63]

$$\kappa_2[\phi_V] = \langle \phi_V^2 \rangle = VT\xi^2, \tag{1.98a}$$

$$\kappa_3[\phi_V] = \langle \phi_V^3 \rangle = \lambda_3 VT^2\xi^6 = \tilde{\lambda}_3 VT^{3/2}\xi^{9/2}, \tag{1.98b}$$

$$\kappa_4[\phi_V] = \langle \phi_V^4 \rangle_{\rm c} = \langle \phi_V^4 \rangle - 3\langle \phi_V^2 \rangle^2 = VT^3(3(\lambda_3\xi)^2 - \lambda_4)\xi^8 = VT^2(3\tilde{\lambda}_3^2 - \tilde{\lambda}_4)\xi^7, \tag{1.98c}$$

where the subscript "c" means connected, since the disconnected diagrams $\langle \phi_V^2 \rangle^2$ are subtracted. We also used $\lambda_3 = \tilde{\lambda}_3 T (T\xi)^{-3/2}$ and $\lambda_4 = \tilde{\lambda}_4 (T\xi)^{-1}$ from RG scaling analysis where $\tilde{\lambda}_3$ and $\tilde{\lambda}_4$ are rescaled dimensionless coupling constants[8]. κ_n are the connected cumulants of the distribution $\mathcal{Z} = \exp[-\beta\mathcal{H}[\phi]]$. The corresponding diagrammatic representation is illustrated in Fig. 1.6. The message Eq. (1.98) convey to us is that the higher-order cumulants are more sensitive to the correlation length and thus the critical point.

Sometimes it is more convenient to introduce a set of normalized intensive quantities (cumulants), following the conventional notation:

$$\sigma^2 = \kappa_2, \quad S\sigma = \frac{\kappa_3}{\kappa_2}, \quad \kappa\sigma^2 = \frac{\kappa_4}{\kappa_2}. \tag{1.99}$$

---

[8] Note here we follow the convention of Ref. [63] that only $\mathcal{H}[\phi]$ instead of $\beta\mathcal{H}[\phi]$ are expanded in ϕ, i.e., $\mathcal{H}[\phi] = \frac{1}{2}(\nabla\phi)^2 + \frac{1}{2}m^2\phi^2 + \frac{1}{3!}\lambda_3\phi^3 + \frac{1}{4!}\lambda_4\phi^4$, thus the mass dimension counting for the coupling constants is different from those for $\beta\mathcal{H}[\phi]$.

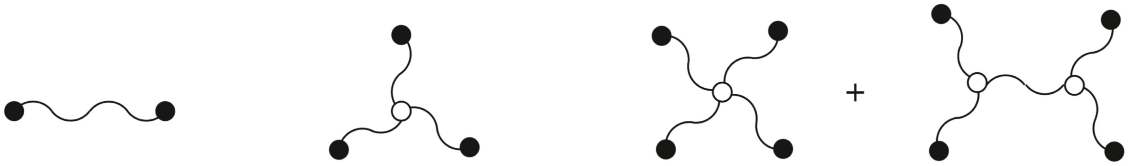

Figure 1.6: The diagrammatic representation of equilibrium non-Gaussian cumulants (cf. Eq. (1.98)), adapted from Ref. [64]. The solid circle stands for the field $\phi(x)$, and the open circle (vertex) for the coupling constant of ϕ^n attached by n legs. The waving line is the zero wavenumber ($q = 0$) propagator $m^{-1} = \xi^2$.

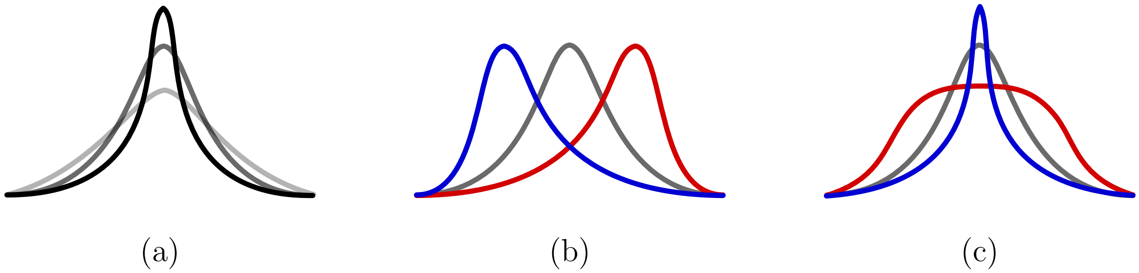

Figure 1.7: Illustration of the second (a), third (b) and fourth (c) moments of a distribution. In (a) curves of Gaussian distribution with different widths are presented. In (b) and (c), red curves are for negative values while the blue curves for the positive, both describe the deviation from a Gaussian distribution represented by the dashed curves.

Here σ^2, S and κ are referred to as the variance, skewness and kurtosis, which measures the width, asymmetry and tailedness (flatness) of a distribution respectively (Fig. 1.7). This normalization (ratio of extensive quantities) eliminates the dependence of extensive quantities such as participant numbers and volumes. Thus the normalized intensive quantities are independent of the particle number or volume fluctuations.

The field ϕ is understood as one or a set of order parameters near the critical point. The fluctuations of ϕ are not directly measurable by the heavy-ion collision experiments. In Sec. 1.5.2 we will discuss its connection to experimental observables. In the case of QCD critical point which is believed to reside at high baryon density regime, in large part the order parameters are characterized by the conserved baryon charges. The above analysis also applies if one identifies $\phi \sim \delta n/n$, the ratio of baryon density fluctuation to its background. For a systematic and general treatment of non-Gaussian fluctuations for conserved charges, see Ref. [65].

1.3.3 Non-equilibrium Dynamics of Critical Fluctuations

Now let's turn to the dynamic critical fluctuations. The central ideas of the modern theory of dynamic critical phenomena was systematically summarized by Hohenberg and Halperin in their insightful introductory review [66].

Following the Hamiltonian field theory, we introduce the momentum density conjugate to ϕ as

$$\pi(x) \equiv \frac{\partial \mathcal{L}}{\partial \dot{\phi}(x)}. \tag{1.100}$$

The Hamiltonian density is nothing but the Legendre transform of the Lagrangian density, i.e.,

$$\mathcal{H}(\pi, \phi) \equiv \pi(x)\dot{\phi}(x) - \mathcal{L} = \frac{1}{2}\pi^2 + \frac{1}{2}(\boldsymbol{\nabla}\phi)^2 + U(\phi) \tag{1.101}$$

where in the second equality we have used Eq. (1.2) and therefore $\pi = \dot{\phi}$. It is subject to the Hamiltonian equations

$$\dot{\phi} = \frac{\delta \mathcal{H}(\pi, \phi)}{\delta \pi} = \{\phi, \mathcal{H}\}, \quad \dot{\pi} = -\frac{\delta \mathcal{H}(\pi, \phi)}{\delta \phi} = \{\pi, \mathcal{H}\}, \tag{1.102}$$

where we have introduced the Poisson bracket

$$\{\mathcal{O}, \mathcal{H}\} = \frac{\partial \mathcal{O}}{\partial \phi}\frac{\partial \mathcal{H}}{\partial \pi} - \frac{\partial \mathcal{O}}{\partial \pi}\frac{\partial \mathcal{H}}{\partial \phi}. \tag{1.103}$$

Similarly we can define ($\mathcal{W}[J] \to -\beta G[J]$, $\Gamma[\varphi] \to \beta\mathcal{F}[\varphi]$, $\mathcal{S}[\phi] \to \beta\mathcal{H}[\phi]$)

$$\mathcal{Z}[J] = e^{-\beta\mathcal{F}[\varphi] + \int d^dxJ\cdot\varphi} = \int \mathcal{D}\phi \exp\left\{-\beta\mathcal{H}[\phi(x)] + \int d^dx J(x)\cdot\phi(x)\right\}. \tag{1.104}$$

Let's interpret $\varphi \equiv \{\varphi_i\}$ as a set of real macroscopic variables describing the system at long distances and times, separated from other variables whose typical scales are fast in times or short in distances. In other words, φ is a subset of a complete microscopic variables whose time evolution is described by the deterministic equations. Examples of variables φ could be the long-wavelength components of the conserved quantities or the long-wavelength fluctuations of the order parameters for a phase transition. At the macroscopic scales, the time evolution of φ is instead described phenomenologically by a first-order stochastic differential equation:

$$\partial_t \breve{\varphi}_a = \{\breve{\varphi}_a, \beta\mathcal{F}[\breve{\varphi}]\} = -M_{ab}\frac{\delta(\beta\mathcal{F}[\breve{\varphi}])}{\delta\breve{\varphi}_b} + \xi_a\,, \tag{1.105}$$

where $M_{ab} = D_{ab} + \Omega_{ab}$ is the kinetic coefficient and is decomposed into the symmetric part $D_{ab} = D_{ba}$ and anti-symmetric part $\Omega_{ab} = -\Omega_{ba}$. ξ_a is the fluctuating force that ensures the equilibration of the system. Its two-point correlation is assumed to be a Gaussian distribution:

$$\langle \xi_a(x)\xi_b(x')\rangle = 2D_{ab}\delta^{(d)}(x - x'). \tag{1.106}$$

The fact that the amplitude of the noise correlator is precisely set by D_{ab} is not a coincidence. It is determined by the fluctuation-dissipation theorem which will be detailed later. All fast degrees of freedom (the microscopic forces) are subsumed in random noise, thus $\varphi(t+\Delta t)$ is not completely determined by $\varphi(t)$, at each time slice, the noise gives rise to a random kick and the value of φ is characterized by the probability distribution $P(\varphi, t)$, whose dynamic evolution is described by Fokker-Plank equations.

In the case of single variable φ, Ω_{ab} vanishes and we have

$$\partial_t \breve{\varphi} = -D\frac{\delta(\beta\mathcal{F}[\breve{\varphi}])}{\delta\breve{\varphi}} + \xi\,, \tag{1.107}$$

where we have used the breve accent ˘ to distinguish a stochastic quantity from its ensemble average. We shall emphasize that Eq. (1.105) or (1.107) is a phenomenological equation manifested near equilibrium. Nonetheless, it captures the universal long-wavelength physics which can be classified into several dynamic universality classes. If $D \sim \gamma$ where γ is a relaxation coefficients, Eq. (1.107) describes the dynamics of a non-conservative variable, which is referred to as *Model A*. While if $D \sim \boldsymbol{\nabla}\cdot(\gamma\boldsymbol{\nabla})$, Eq. (1.107) becomes a conservation equation describing the diffusion dynamics of a conserved variable, referred to as *Model B*. If D_{ab} is a matrix coupling multiple conserved variables, as the case of hydrodynamics where transverse momenta couple to a conserved critical mode, the model is known as *Model H*.

It describes the dynamical universality of systems from liquid-gas phase transition to QCD critical point [38]. For other dynamical models see Ref. [67].

Similar to the way we dealt with effective action in Eq (1.53), we can expand the free energy as

$$\beta\mathcal{F}[\varphi(x)] = \int d^dx \left[\frac{1}{2}(\boldsymbol{\nabla}\varphi(x))^2 + \frac{1}{2}m^2\varphi(x)^2 + \dots\right], \tag{1.108}$$

where we neglect the non-Gaussian parts for a moment and the integration on x is purely spatial (as a consequence that the d-dimensional space in classical statistic mechanics is dual to the d-dimensional Euclidean spacetime in quantum field theory). Substituting the above expression into the single variable equation, Eq. (1.107), and linearizing it near $\delta\varphi = \breve{\varphi} - \varphi$, one finds

$$\partial_t\delta\varphi(x) = -D\left(m^2 - \boldsymbol{\nabla}^2\right)\delta\varphi(x) + \xi(x), \tag{1.109}$$

and its expression upon the Fourier transforms

$$\tilde{\varphi}(q) = \int d^3xe^{-iq\cdot x}\varphi(x), \quad \tilde{\xi}(q) = \int d^3xe^{-iq\cdot x}\xi(x) \tag{1.110}$$

reads

$$\partial_t\delta\tilde{\varphi}(q) = -\frac{\delta\tilde{\varphi}(q)}{\tau_q} + \tilde{\xi}, \tag{1.111}$$

where

$$\tau_q^{-1} = D(q)(m^2 + q^2). \tag{1.112}$$

In Model A, $D(q) \sim \gamma$ which is independent of q, thus one can introduce a relaxation time $\tau_0 \sim (m^2\gamma)^{-1}$ for the homogeneous (zero-wavenumber) component of φ, which diverges as $m^2 \sim t \sim T - T_c \to 0$. The effect that the relaxation time diverges near the critical point is called the *critical slowing down*. The q-dependent relaxation time τ_q is smeared when $t \to 0$ due to $q \neq 0$. However, as we shall see in Chap. 3, for typical $q \sim \xi^{-1}$ where ξ is the correlation length, Eq. (1.112) indicates $\tau_{q\sim\xi^{-1}} \sim \xi^2$, thus the effect of critical slowing down remains and plays an important role in the dynamical description of critical fluctuations. In model B, the effect of critical slowing down is even more significant, since in this case

$D(q) \sim \gamma q^2$, thus $\tau_{q\sim\xi^{-1}} \sim \xi^4$. In Model H for $d = 3$, the conductivity $\lambda \sim \xi^{x_\lambda} \approx \xi^1$ is divergent due to the convection of the fluid, therefore $\gamma \sim \lambda/\chi_T \sim \xi^{-1}$ and hence $\tau_{q\sim\xi^{-1}} \sim \xi^3$.

If we take into account the non-Gaussian fluctuations in Eq. (1.53), we have to adopt the dynamical renormalization group theory. Similar to the idea of static renormalization group discussed in Sec. 2.6, the exponents of ξ in relaxation time shall be modified beyond free-field approximation. In general, the relaxation time can be put into the scaling form

$$\tau_q = t^{-y} F_\tau\left(q\xi(t)\right) = t^{-z\nu} F_\tau(q t^{-\nu}). \tag{1.113}$$

where where y and z are the dynamic critical exponents to be determined and $F_\tau(x)$ satisfies the conditions

$$\begin{aligned} &F_\tau(x) \to \text{constant}, \quad x \to 0, \\ &F_\tau(x) \to x^{-y/\nu}, \quad x \to \infty. \end{aligned} \tag{1.114}$$

The large-x behavior is determined such that $F_\tau(x \to \infty)$ does not depend on t in the scaling region, which would also implies $z = y/\nu$. When we take the mean-field value $y = 1$ and $z = 2$, the scaling is consistent with Eq. (1.112) where $D \sim \gamma$.

Dynamical Model	Description	z
Model A	non-conserved fields	$2 + c\eta$
Model B	conserved fields	$4 - \eta$
Model H	conserved field with fluid	$4 - \eta - x_\lambda$

Table 1.3: Summary of several dynamical universality class models discussed in this thesis. $c \approx 0.7(1 - 1.7\varepsilon)$, $x_\lambda \approx \varepsilon$.

1.4 QCD Phase Diagram and Critical Point

1.4.1 Review of QCD

The classical Lagrangian density of QCD can be written as

$$\mathcal{L}_{\text{QCD}} = \bar{\psi}_f^\alpha \left(i \not{D}_{\alpha\beta} - m_f \delta_{\alpha\beta}\right) \psi_f^\beta - \frac{1}{4} F_{\mu\nu}^a F_a^{\mu\nu}, \tag{1.115}$$

where ψ_f^α $(\alpha = 1, ..., N_c)$ with flavor indexed by $f = (u, d, s, c, t, b)$ is the quark field in the fundamental representation of $\mathrm{SU_c}(N_c)$, while

$$F^a_{\mu\nu} = \partial_\mu A^a_\nu - \partial_\nu A^a_\mu - g f_{abc} A^b_\mu A^c_\nu \tag{1.116}$$

is the field strength tensor of Yang-Mills (gluon) field A^a_μ $(a = 1, ..., N_c^2 - 1)$ in the adjoint representation of $\mathrm{SU_c}(N_c)$, where g is the dimensionless coupling constant of QCD and f_{abc} is the totally anti-symmetric structure constant. In the case of QCD $N_c = 3$ however we still keep N_c here without loss of generality. The kinetic term for quarks is defined by

$$\not{D} \equiv \gamma^\mu D_\mu, \quad D_\mu \equiv \partial_\mu + ig\mathcal{T}^a A^a_\mu. \tag{1.117}$$

where γ^μ is the Dirac matrix, $\mathcal{T}^a$ $(a = 1, ..., N_c^2 - 1)$ is the Hermitian generator of the $\mathrm{SU_c}(N_c)$ group satisfying the Lie algebra

$$\left[\mathcal{T}^a, \mathcal{T}^b\right] = i f_{abc} \mathcal{T}^c, \tag{1.118}$$

In the fundamental representation, $\mathcal{T}^a$ is written by the $N_c \times N_c$ matrices t^a, which reduces to the Pauli matrices for $N_c = 2$ and to the Gell-Mann matrices for $N_c = 3$ respectively (up to a factor of 1/2). The generator t^a satisfies

$$\mathrm{Tr}(t^a t^b) = \frac{1}{2}\delta_{ab}, \quad (t^a t^a)_{ij} = C_\mathrm{F}\delta_{ij} \quad \text{with} \quad C_\mathrm{F} = \frac{N^2 - 1}{2N}. \tag{1.119}$$

In the adjoint representation, $\mathcal{T}^a$ is instead written by the $(N_c^2 - 1) \times (N_c^2 - 1)$ matrices $(T^a)_{bc} = -i f_{abc}$ satisfying

$$\mathrm{Tr}(T^a T^b) = N\delta_{ab}, \quad (T^a T^a)_{bc} = C_\mathrm{A}\delta_{bc} \quad \text{with} \quad C_\mathrm{A} = N_c. \tag{1.120}$$

Introducing $A_\mu \equiv t^a A^a_\mu$ and $F_{\mu\nu} \equiv t^a F^a_{\mu\nu}$, the field strength tensor can be written more compactly as

$$F_{\mu\nu} = \partial_\mu A_\nu - \partial_\nu A_\mu + ig\left[A_\mu, A_\nu\right] = -\frac{i}{g}\left[D_\mu, D_\nu\right]. \tag{1.121}$$

The classical equation of motions are obtained from Eq. (1.115):

$$\begin{aligned} &\text{Dirac equation:} \quad \left(i\not{D} - m\right)\psi_f = 0, \\ &\text{Yang-Mills equation:} \quad \left[D_\mu, F^{\mu\nu}\right] = g j^\nu, \end{aligned} \tag{1.122}$$

here $j^\mu = t^a j^\mu_a$ and $j^\mu_a = \bar{\psi}_f \gamma^\mu t^a \psi_f$.

In the spirit of Wilson's renormalization group discussed in Sec. 2.6, one can compute the β function for the coupling constant g in the perturbative regime:

$$\beta(g) = \mu \frac{\partial}{\partial \mu} g = -\frac{1}{(4\pi)^2}\left(11 - \frac{2}{3}N_f\right) g^3 + \ldots, \tag{1.123}$$

the corresponding solution of which in terms of the fine structure constant $\alpha_s(\mu)$ is

$$\alpha_s(\mu) = \frac{g^2}{4\pi} = \frac{4\pi}{\left(11 - \frac{2}{3}N_f\right)\log\left(\frac{\mu^2}{\Lambda^2_{\mathrm{QCD}}}\right)} + \ldots \tag{1.124}$$

where $\Lambda_{\mathrm{QCD}} \approx 200\,\mathrm{MeV}$ is the QCD scale parameter determined from experiments. Clearly, the β function is negative for $N_f \leq 16$. Thus, α_s decreases as μ increases, known as the *ultraviolet asymptotic freedom*. In this regime perturbative calculation is reliable and can be used in the hard process such as deep-inelastic scattering. In contrast, α_s increases as μ decreases, a behavior known as the *infrared slavery*. This means at low-energy, the underlying QCD action is non-perturbative and the QCD vacuum is confined, thus alternative effective approaches are in demand. Indeed, due to the strong coupling, nonlinearity of gluon interaction, color confinement and many-body effect, it is difficult to describe the QCD matters directly from the deceptively simple-looking first principle QCD Lagrangian. The alternative effective approaches include the bag model, chiral perturbation theory, lattice QCD, Nambu-Jona-Lasinio (NJL) model, etc. In particular, in the vicinity of QCD critical point, we could construct an effective model based on NJL model and the Ginzburg-Landau-Wilson paradigm to describe the critical phenomena.

Before we conclude this subsection let's take a second look of Eq. (1.115) from the viewpoint of symmetry. First, the terms constructed in Eq. (1.115) are such that they are invariant under the $\mathrm{SU_c}(N_c)$ gauge transformation, in other words all terms violating the gauge invariance are prohibited[9]. Second, in the massless limit ($m = 0$), Eq. (1.115) is also invariant under the $\mathrm{SU_L}(N_f) \times \mathrm{SU_R}(N_f)$ chiral transformation. Although the chiral symmetry is not exact since quark is massive, it remains a good approximation as long as the running mass $m \ll \Lambda_{\mathrm{QCD}}$ manifested in the short-distance scales. The spontaneous breaking and restoration of chiral symmetry in vacuum distinct two different phases in the QCD phase diagram, as discussed in the next subsection.

---

[9] Nevertheless, the famous QCD θ term, albeit gauge-invariant, violets the CP-symmetry and causes the strong CP problem, and hence is not presented here. Furthermore, the auxiliary fields fixing the gauge are also not taken into account.

1.4.2 QCD Phase Diagram

A phase diagram characterizes and distinguishes the equilibrium states of a thermodynamic system provided certain independent thermodynamic variables. The choice of independent variables is arbitrary but tricky. In the most well-known example, the two-dimensional phase diagram of liquid and gas, if temperature T and pressure p is provided at fixed total particle numbers $N = nV$, the corresponding thermodynamic equilibrium state (phase) are uniquely determined, thus T and p are convenient variables to distinct the phases of water. This is due to the fact that given temperature T and pressure p at fixed N, the thermodynamic equilibrium state is such that it minimizes the Gibbs free energy $G = G(T, p) = E - TS + PV = \mu N$, whose natural variables are T and p, reflected by the fundamental thermodynamic equations $dG = Vdp - SdT$ at fixed N. By natural variables it means by taking derivative of a thermodynamic quantity as a function of which determines all the thermodynamic properties of the system. The phase boundaries where phase transition occurs are one-dimensional lines corresponding to the coexistence of two phases (say phase A and phase B with density n_A and n_B respectively). As a consequence, if one instead chooses n and T as the phase diagram variables, given T and p fixed, there might be infinitely many coexistence states, with density a linear combination of n_A and n_B, occurs in the phase diagram expanded by n and T (see, for example, Fig. 4.11). Therefore, in the case we are interested in the coexistence region and beyond, n and p shall be more convenient variables, although we need to pay the price that the one-to-one correspondence between the thermodynamic variables and equilibrium states is lost. More generally speaking, we could consider the extended generating functional $\mathcal{W}[\{J_i\}]$, where $\{J_i\}$ is a set of source-like external fields, such as temperature, chemical potential, (quark) mass, coupling constant and so on. Consequently, the dimensionality of the phase diagram increases as we consider more and more relevant parameters.

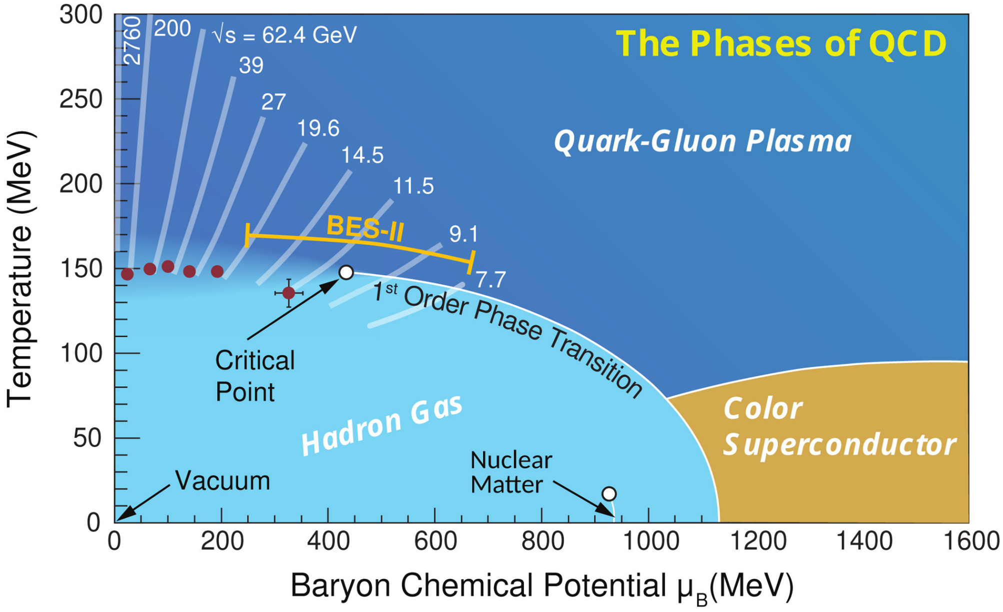

Figure 1.8: The QCD phase diagram in $T-\mu$ plane [68].

In the case of QCD phase diagram in two dimensions, the two phase diagram variables are commonly chosen to be temperature T and baryon chemical potential $\mu = \mu_{\mathrm{B}}$, the natural variables of grand potential (Landau free energy) $\Omega = \Omega(T,\mu) = E - TS - \mu N = -pV$ which is minimized in thermal and chemical equilibrium, since $d\Omega = -SdT - Nd\mu$ at fixed volume V. The partition function is read off as

$$\mathcal{Z} = \int \mathcal{D}[A,\psi,\bar{\psi}] e^{-\mathcal{S}_{\mathrm{QCD}}[A,\psi,\bar{\psi}]} = \mathrm{Tr}\, e^{-\beta(\hat{H}_{\mathrm{QCD}}-\mu\hat{N})} = e^{-\beta\Omega(T,\mu,V)} = e^{\beta P(T,\mu)V}, \qquad (1.125)$$

where

$$\begin{aligned}\mathcal{S}_{\mathrm{QCD}}[A,\psi,\bar{\psi}] &= \int d^d x \left(\mathcal{L}_{\mathrm{YM}} + \bar{\psi}_f^{\alpha}\left(i\not{D}_{\alpha\beta} - (m_f - \mu_f\gamma_0)\delta_{\alpha\beta}\right)\psi_f^{\beta}\right) \\ &= \int d^d x \left(\mathcal{L}_{\mathrm{QCD}}(m_f = 0) - m_f\bar{\psi}_f\psi_f + \mu_f\bar{\psi}_f\gamma_0\psi_f\right), \qquad (1.126)\end{aligned}$$

and $\mu_f = \mu_{\mathrm{B}}/3$ is the chemical potential of each quark flavor, conjugate to the baryon density $n = \langle \bar{\psi}\gamma_0\psi \rangle$. From this expression it is clear that m_f serves as a relevant parameters that could extend the dimensionality of the QCD phase diagram. Indeed, the nature of phase transition is sensitive to the quark masses (as indicated by Columbia plot [69]), and our real world chooses the typical values of quark mass for which we are living in a particular "slice" of the multi-dimensional space of the QCD phase diagram (Fig. 1.9).

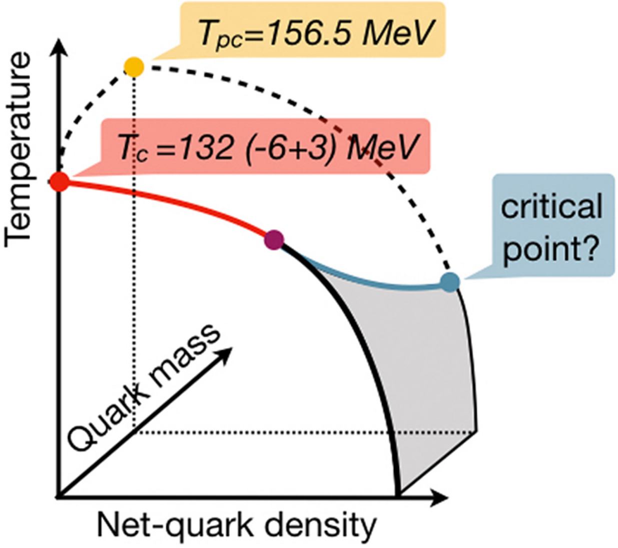

Figure 1.9: The QCD phase diagram in $T-\mu-m_{\mathrm{ud}}$ plane (Frithjof Karsch, University of Bielefeld). Here, T_c (red point) is the critical transition temperature in the chiral limit (do not confused by the critical temperature for the QCD critical point, which is also denoted by T_c in this thesis); T_{pc} (yellow point) is the pseudo critical transition temperature of QCD with massive (up and down) quarks; the dark-red point is the tri-critical point described by ϕ^6 theory; the blue point is the QCD critical end point that we mainly focus on in this thesis. The QCD phase diagram depicted in Fig. 1.8 is the slice partially bounded by the dashed lines, tuned by the physical quark masses. The dashed curves indicate the crossover transition, while the solid lines are lines of second-order phase transitions. The gray surface is a hyper-surface of first-order phase transition points.

As we mentioned, it is difficult to study the critical point from the the classical QCD action. Alternatively, an elaborate effective action is provided by Pisarski and Wilczek [70].

The classical QCD Lagrangian could have the following broad symmetry:

$$\mathrm{SU_c}(N_c) \times \mathrm{U_B}(1) \times \mathrm{U_A}(1) \times \mathrm{SU_L}(N_f) \times \mathrm{SU_R}(N_f), \tag{1.127}$$

where $\mathrm{SU_c}(N_c) \times \mathrm{U_B}(1)$ is intact but $\mathrm{U_A}(1) \times \mathrm{SU_L}(N_f) \times \mathrm{SU_R}(N_f)$ could be broken for the chiral symmetry breaking. Pisarski and Wilczek then constructed their effective action based on the symmetry and stability by keeping the lowest dimensional relevant operators:

$$\begin{aligned}\mathcal{L}_{\mathrm{PW}} = & \frac{1}{2}\,\mathrm{Tr}\,\partial\Phi^\dagger\partial\Phi + \frac{m^2}{2}\,\mathrm{Tr}\,\Phi^\dagger\Phi + \frac{g_1}{4!}(\mathrm{Tr}\,\Phi^\dagger\Phi)^2 + \frac{g_2}{4!}\,\mathrm{Tr}(\Phi^\dagger\Phi)^2 \\ & - \frac{c}{2}(\det\Phi + \det\Phi^\dagger) - \frac{1}{2}\,\mathrm{Tr}\,h(\Phi + \Phi^\dagger),\end{aligned} \tag{1.128}$$

where the last two terms are for axial anomaly and quark mass respectively,

$$\Phi_{ij} = \frac{1}{2}\bar{\psi}_i(1+\gamma_5)\psi_j \sim \sum_{f=0}^{N_f^2-1} \Phi^a t^a \tag{1.129}$$

is a color-singlet complex, $N_f \times N_f$ matrix. In the presence of axial anomaly and $N_f = 2$ (up and down quarks), one can show that the effective Lagrangian turns to a $\boldsymbol{\phi}^4$ model subject to O(4) symmetry:

$$\mathcal{L}_{\mathrm{PW}} = \frac{1}{2}(\partial\boldsymbol{\phi})^2 + \frac{m^2 - c}{2}\boldsymbol{\phi}^2 + \frac{g_1 + g_2/2}{4!}(\boldsymbol{\phi}^2)^2, \tag{1.130}$$

where $\boldsymbol{\phi} = (\langle\bar{\psi}\psi\rangle, \langle\bar{\psi}i\gamma_5\boldsymbol{\tau}\psi\rangle)$ is a four-component vector field made up of the quark condensate singlet $\langle\bar{\psi}\psi\rangle$ and pion triplet $\langle\bar{\psi}i\gamma_5\boldsymbol{\tau}\psi\rangle$. $\boldsymbol{\tau}$ denotes the Pauli matrices.

As we have mentioned in the previous subsection, the QCD phase diagram shall reflect the fundamental properties of QCD: the spontaneous chiral symmetry breaking (restoration) and confinement (deconfinement). Once quarks acquire their current masses by the electroweak symmetry breaking, both of them are valid only in an approximate level, therefore strictly speaking there is no good order parameter to distinguish the two phases quantitatively. However, assuming the two properties are exact, it is possible to choose the thermal expectation value of quark condensate[10]

$$\langle\bar{\psi}\psi\rangle \begin{cases} = 0 & \text{restoration phase subject to } \mathrm{SU_L}(N_f)\times\mathrm{SU_R}(N_f); \\ \neq 0 & \text{breaking phase subject to } \mathrm{SU_V}(N_f) \end{cases} \tag{1.131}$$

as one sector of the order parameters to measure the phase transition[11]. For $N_f = 2$, the vacuum symmetry is approximately broken to $\mathrm{SU_V}(2)$, the Goldstone bosons associated with such symmetry breaking are loosely portrayed as pions assigned to an isospin triplet, $\langle\bar{\psi}i\gamma_5\boldsymbol{\tau}\psi\rangle$). Since the symmetry breaks only approximately, pions, unlike ordinary Goldstone bosons, acquire finite masses. Thus the O(4) symmetry is broken to O(1) or Z(2) near the critical point. Moreover, regardless of whether the symmetry is exact or not, we shall emphasize that the order parameter could be one or a set of long-wavelength fluctuations near the critical point associated to the second-order phase transitions. Unlike other systems (e.g., ferromagnet system where the order parameter is magnetization M), the order parameter of QCD critical point is hard to determine, it is a combination of

- chiral condensate fluctuations: $\bar{\psi}\psi - \langle\bar{\psi}\psi\rangle$;
- baryon density fluctuations: $\bar{\psi}\gamma_0\psi - \langle\bar{\psi}\gamma_0\psi\rangle$;
- hydrodynamic fluctuations: $T^{\mu\nu} - \langle T^{\mu\nu}\rangle$;

and so on. All of which have the correlation lengths diverging in the same order of magnitude near the critical point. Following the convention, we shall call the mixed order parameters σ field in this thesis.

---

[10] Although the chiral condensate $\langle\bar{\psi}\psi\rangle$ formed near the Dirac sea is analogous to the cooper pair $\langle\psi\psi\rangle$ formed near the Fermi surface. However, the quark and anti-quark only condensate at strong coupling, while a cooper pair of quarks is preferred at large density of states in the weak coupling, the latter is known as the color superconducting phase highlighted in Fig. 1.8.

[11] The choices of order parameter are not unique, other possible choices are for example Wilson/Polyakov loop for the confinement and deconfinement.

We are now in the right position to construct the effective model for describing the phase transition in terms of the order parameter σ. The partition function is (cf. Eq. (1.56))

$$\mathcal{Z} = \exp[-\beta G[J]] = \exp[-\beta \mathcal{H}[\sigma] + \int_x H\sigma] \tag{1.132}$$

where the Hamiltonian (Landau functional) are expanded around the expectation value in thermal average $\langle\sigma\rangle$

$$\mathcal{H}[\sigma] = \int d^d x \sum_n \lambda_n (\sigma - \langle\sigma\rangle)^n. \tag{1.133}$$

The Z(2) symmetry require that odd-order terms vanishes and the minimum order required for capturing the second-order phase transition is $n = 4$, thus we shall employ a ϕ^4 theory and all corresponding discussion and results in Sec. 1.2 shall be straightforwardly applied here. Since both the QCD critical point and Ising critical point are described by the universality class of ϕ^4 theory, it is therefore feasible to map the critical equation of state of Ising theory, which is well known, to the case of QCD where the critical equation of state is much more difficult to construct.

1.4.3 Mapping from Ising Theory to QCD

The fluctuation of magnetizations in Ising theory is described by the probability introduced in Eq. (1.66), where the free energy is described by the ϕ^4 theory

$$F(M) = \frac{1}{2} t M^2 + \frac{1}{4!} u M^4. \tag{1.134}$$

If we simply identify $\phi = M$ and therefore $\phi_V = N\delta M$ (cf. Eq. (1.93)), then the Gibbs free energy

$$G(H) = \sup_M F(M) - HM = \sum_{n=2}^{\infty} \frac{\kappa_n}{n!} H^n \tag{1.135}$$

serves as a generating function of the cumulant

$$\kappa_n = \langle \phi_V^n \rangle = -NT \left(\frac{\partial^n G(H)}{\partial H^n} \right)_T = -NT \left(\frac{\partial^{n-1} M(H)}{\partial H^{n-1}} \right)_T. \tag{1.136}$$

For example,

$$\kappa_2 = \langle \phi_V^2 \rangle = N^2 \langle (\delta M)^2 \rangle = TN\chi_T^{-1} \tag{1.137}$$

where $\chi_T^{-1} = \left(\frac{\partial^2 F}{\partial M^2}\right)_T = \left(\frac{\partial H}{\partial M}\right)_T$ is the isothermal susceptibility, which vanishes when $F''(M) = 0$. Thus, the equilibrium cumulants could be completely determined by the equation of state $M = M(H)$.

The analytic expression for $M(H)$ is already cumbersome in the mean-field approximation, and becomes unmanageable when fluctuations are taken into account. In certain limit, the equation of state manifests itself in a scaling form, where the contribution of fluctuations are resumed into the critical exponents, however, such scaling function can not be applied uniformly to the whole critical region but only a particle regime (see Sec. 4.2.3 for instance). This problem is controllably solved by introduce the *Josephson-Schofield (JS) Parametric Representation* in the small $\varepsilon = 4-d$ limit. In this representation one introduces two parameters, R and θ, which mimic role of radial distance and polar angle near the critical point (as a origin). Then, any thermodynamic quantity Φ can be parametrized in terms of two parameters R and θ in the general form near the critical point [71, 72, 73],

$$\Phi(R, \theta) = \bar{\Phi}_0 R^x \phi(\theta), \tag{1.138}$$

where $\bar{\Phi}$ is the normalization constant, x is a appropriate critical exponent, and $\phi(\theta)$ is a scaling function to be determined by the thermodynamic relations. We leave the detail discussion to Sec. 4.2.3 and Appendix 4.2.3 when exploring the analyticity of the Ising equation of state.

Since, as we mentioned in the previous subsection, the critical points of Ising theory and QCD can be described the same universality class of $Z(2)$ symmetry. Thus, it is possible to map the critical mode as well as critical equation of state of Ising model to that of QCD:

$$M \longmapsto \sigma\,, \quad G_{\text{Ising}}(t, H) \longmapsto P_{\text{QCD}}(T, \mu). \tag{1.139}$$

The map is assumed to be a linear coordinate variables transform

$$(R, \theta) \longmapsto (t, H) \longmapsto (T, \mu) \tag{1.140}$$

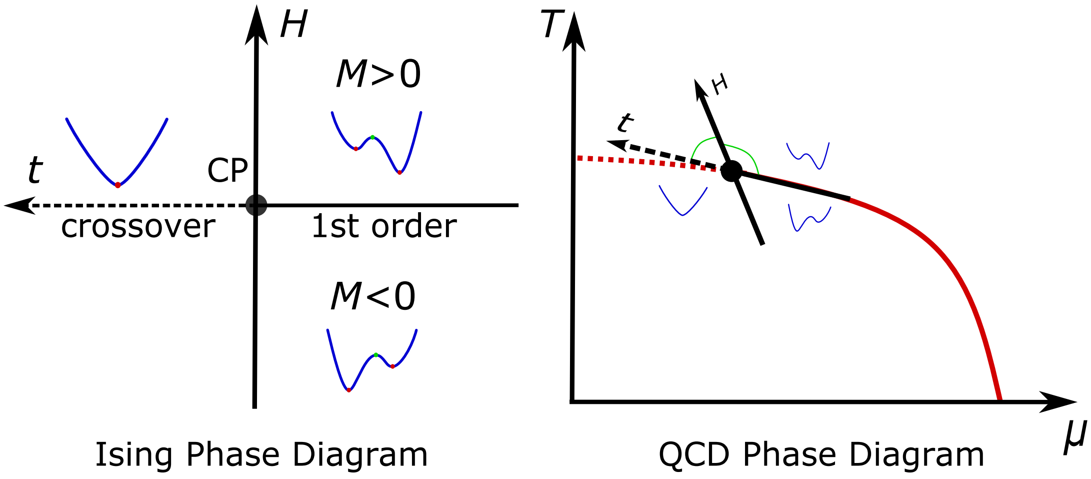

Figure 1.10: A particular example of the non-universal map from Ising variables (t, H) to the QCD coordinate (μ, T).

and depend on a set of non-universal parameters, such as the location of critical point, the size of the critical region and the mapping angles. A particular map is depicted in Fig. 1.10. Recently, a family of lattice-QCD based equations of state with a Ising critical point is constructed and some of the non-universal parameters are able to be constrained. We refer the readers to Ref. [74, 75].

Once all the non-universal input is fixed, the map is uniquely determined. The equilibrium cumulants as a function of the relevant coordinate variables are also determined. Fig. 1.11 shows an example how the kurtosis κ_4 are mapped from the Ising coordinate to the QCD coordinate.

We shall keep in mind that the map presented in Fig. 1.11 is between the equilibirum cumulants, which can be completely determined by the equilibrium partition function of the thermodynamic system. In a non-equilibrium process like heavy-ion collisions, the thermodynamic variables do not equilibrate fast enough compared to the typical fireball expansion or quenching rate, thus the static map such like Fig. 1.11 does not suffice to provide all the information needed to match the experimental results. In other words, the dynamic

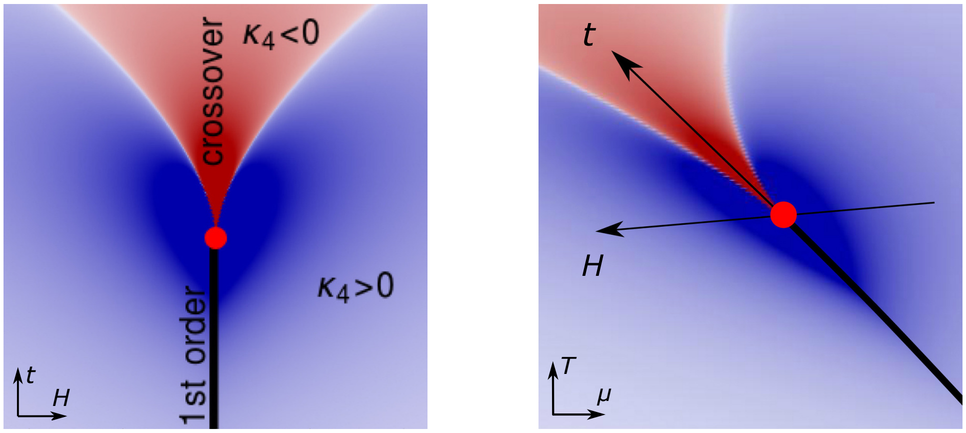

Figure 1.11: Mapping kurtosis κ_4 from (t, H) coordinate to (μ, T) coordinate, adapted from Ref. [64]. The cumulant is negative (red) around the crossover side and positive along the first-order phase transition line.

evolution of cumulants incorporate the correct dynamic universal behavior of QCD critical point [38], has to be studied. Remember, the cumulants are basically the moments of partition (probability distribution) and thus can be directly calculated from the generating function. Unlike the stationary case where the distribution is determined by its thermodynamic equilibrium when entropy is maximized, the distribution function would acquire a time dependence described by the Fokker-Planck equations out of equilibrium. A simple model for a non-conserved zero-momentum critical mode is studied in Ref. [76] and the results presented in Fig. 1.19 indicate a significant memory effect of the cumulant evolution. Without a more realistic and systematic study of the non-equilibrium contribution to the final fluctuations measures, any sound conclusion would be considered unauthentic.

1.5 Heavy-Ion Collision Experiment

1.5.1 Connection to Experimental Observables

As we point out in Sec. 1.3, heavy-ion collision experiments do not directly measure the critical mode and its fluctuations. What the experiment do measure, however, are the momenta and other quantum numbers (charge, baryon number, strangeness, spin, etc.) of detected particles (protons, pions, etc.), on an event-by-event basis. Notwithstanding, the critical mode does couple to the detected particles, through the coupling the critical mode would influence the experimental observables of the measurable particles.

Since the experiments do not measure the spatial correlations of fluctuations, we have to translate the spatial correlation to the momentum space. The range of correlation in momentum space is determined by the momentum distribution (momentum width) of particles within the correlated spatial volume ξ^3. In the Bjorken-like expansion of heavy-ion collisions, the typical correlation range in spatial rapidity is $\Delta\eta_{\text{corr}} \approx \xi/\tau_{\text{f}} \sim 0.1 - 0.3$ where $\tau_{\text{f}} \sim 10$ fm is the freezeout time and $\xi \sim 1 - 3$ fm is the freezeout correlation length near the critical point. Provided the Boltzmann distributions in momentum space of a non-relativistic particle with mass m,

$$f(\boldsymbol{p}) \sim \exp\left[-\frac{\boldsymbol{p}^2}{2mT}\right], \tag{1.141}$$

the momentum thermal spread width is read off as $\Delta p = \sqrt{mT}$, corresponding to a typical correlation range in kinematic rapidity $\Delta y_{\text{corr}} = \mathcal{O}(1)$ for protons, which is much larger than the correlation range in spatial rapidity, i.e., $\Delta y_{\text{corr}} \gg \Delta\eta_{\text{corr}}$. Therefore, Δy_{corr} is in contrast not sensitive to the correlation length ξ as the cumulants do. Nevertheless, the magnitude of momentum correlations is directly related to the correlation length.

At freezeout, the particles are described by the phase-space distribution function, say $f_A(\boldsymbol{x})$ where the subscript A labels the momentum $\boldsymbol{p}$ and a set of conserved quantum numbers distinguishing the species of the particles. The spatial distribution is blind to the experimental apparatus and thus it's more convenient to introduce the one-particle momentum distribution function[12]

$$n_A = \int d^3\boldsymbol{x} f_A(\boldsymbol{x}), \tag{1.142}$$

---

[12] The one-particle momentum distribution at *freezeout* is given by the Cooper-Frye formula. The spatial integration is over a particlization hypersurface Σ^μ, i.e., $\int d^3x \sim \int_\Sigma d\Sigma_\mu p^\mu$. For simplicity we would bypass this delicate freezeout prescription.

whose event average is defined by

$$\rho_A \equiv \frac{dN}{d^3\boldsymbol{p}_A} = \langle n_A \rangle \tag{1.143}$$

and thus the average of the fluctuation $\delta n_A = n_A - \langle n_A \rangle$ vanishes by definition, i.e., $\langle \delta n_A \rangle = 0$. What we are interested in are of course the multi-particle correlations. The event average of two-particle distribution function is similarly defined by

$$\rho_{AB} \equiv \frac{dN}{d^3\boldsymbol{p}_A d^3\boldsymbol{p}_B} = \langle n_A n_B \rangle - \delta_{AB} \langle n_A \rangle, \tag{1.144}$$

where the second term in the last equality eliminates the double counting of pair particles with exactly the same momentum and quantum numbers. Introducing

$$\langle \delta n_A \delta n_B \rangle = \langle n_A n_B \rangle - \langle n_A \rangle \langle n_B \rangle = \int d^3\boldsymbol{x}_A d^3\boldsymbol{x}_B \langle \delta f_A(\boldsymbol{x}_A) \delta f_B(\boldsymbol{x}_B) \rangle, \tag{1.145}$$

the two-particle correlation function are convenient to expressed by

$$C_{AB} = \rho_{AB} - \rho_A \rho_B = \langle \delta n_A \delta n_B \rangle - \delta_{AB} \langle n_A \rangle. \tag{1.146}$$

The inclusive conserved quantities (multiplicity number), such as the total charge[13]

$$Q = \int_A q_A \, n_A, \tag{1.147}$$

are simply the integration over all relevant quantum numbers A which is experimental visible within certain acceptance ranges. The multiplicity in each event Q fluctuates around its average measured by

$$\delta Q = Q - \langle Q \rangle, \quad \langle Q \rangle = \int_A q_A \, \langle n_A \rangle. \tag{1.148}$$

Thus the multiplicity distribution can be characterized by the cumulants. For example, the second-order cumulant is

$$\kappa_2[Q] = \langle (\delta Q)^2 \rangle = \int_A \int_B q_A q_B \langle \delta n_A \delta n_B \rangle. \tag{1.149}$$

---

[13] The results for total particle numbers N are obtained by setting the quantum number q_A to unity. The results for particular conserved quantities are obtained by specifying the integration acceptance A.

In realistic case, the measurable multi-particle correlation functions such as C_{AB} are contributed from many sources, such as the initial fluctuations, flow-induced correlations, jets, etc. However, among the various sources the critical fluctuations are particularly extractable, in a sense it only relies on the critical region affecting a small beam energy scan interval. For this reason we will only consider how the critical fluctuations step in and change the scenario.

The critical mode σ is consider as a classical field serving as a slowly varying background of the free measurable particles such as pions π [77], whose one-particle phase-space distribution reads

$$f_A = \frac{1}{e^{\beta E_A} \mp 1} \tag{1.150}$$

where $+$ and $-$ sign are for fermions and bosons respectively and $E_A = E_A(\boldsymbol{p}; \sigma)$ now also depends on the critical mode σ. Thus, expanding the above expression to linear order in $\delta\sigma$, one obtains the fluctuation of the one-particle phase-space distribution incorporating the contribution from the critical mode:

$$\delta f_A(\boldsymbol{x}) = \delta f_A^{(\text{free})}(\boldsymbol{x}) + \frac{\partial f_A}{\partial \sigma}\delta\sigma(\boldsymbol{x}) = \delta f_A^{(\text{free})}(\boldsymbol{x}) - \frac{\beta g_A}{\gamma_A} f_A(1 \pm f_A)\delta\sigma(\boldsymbol{x}), \tag{1.151}$$

where $g_A = \frac{\partial m_A(\sigma)}{\partial \sigma}$ is a coupling constant of the $\sigma\pi\pi$ interaction (which gives rise to the σ-dependence of pion mass, i.e., $m_A = m + g_A\sigma$), $\gamma_A = \frac{\partial m_A}{\partial E_A}$ is the Lorentz factor of the particle, and we have used

$$\frac{\partial f_A}{\partial \sigma} = -\beta \frac{\partial E_A(\sigma)}{\partial \sigma} f_A(1 \pm f_A). \tag{1.152}$$

The two-particle phase-space correlation at freezeout is obtain by using Eq. (1.151) and (1.96), with the help of $\langle \delta f_A \delta f_B \rangle = \langle f_A \rangle \delta_{AB}$ according to the Poisson distribution manifested for the uncorrelated gas:

$$\langle \delta f_A \delta f_B \rangle = \left(\delta_{AB} \langle f_A \rangle + T\xi^2 \frac{\partial f_A}{\partial \sigma} \frac{\partial f_B}{\partial \sigma} \right) \delta^{(3)}(\boldsymbol{x}_A - \boldsymbol{x}_B). \tag{1.153}$$

Accordingly Eq. (1.145),

$$\langle \delta n_A \delta n_B \rangle = \delta_{AB} \langle n_A \rangle + \int d^3x T\xi^2 \frac{\partial n_A}{\partial \sigma} \frac{\partial n_B}{\partial \sigma}, \tag{1.154}$$

where the first terms is the trivial Poisson distribution. Using Eq. (1.149), one can obtain the second-order cumulant which is presented below together with its generalization to the non-Gaussian cases:

$$\kappa_2[Q] = \langle(\delta Q)^2\rangle = \int_A q_A^2\langle n_A\rangle + \int d^3x T\xi^2 \left(\int_A q_A \frac{\partial f_A}{\partial\sigma}\right)^2 , \tag{1.155a}$$

$$\kappa_3[Q] = \langle(\delta Q)^3\rangle = \int_A q_A^3\langle n_A\rangle + \int d^3x \tilde{\lambda}_3 T^{3/2}\xi^{9/2} \left(\int_A q_A \frac{\partial f_A}{\partial\sigma}\right)^3 , \tag{1.155b}$$

$$\kappa_4[Q] = \langle(\delta Q)^4\rangle_c = \int_A q_A^4\langle n_A\rangle + \int d^3x\tilde{(}3\tilde{\lambda}_3^2 - \tilde{\lambda}_4)T^2\xi^7 \left(\int_A q_A \frac{\partial f_A}{\partial\sigma}\right)^4 . \tag{1.155c}$$

A diagrammatic interpretation is given in Fig. 1.12. Eq. (1.155) says the non-Gaussian cumulants of fluctuations are more sensitive to the critical point in a sense they depend on the correlation length ξ with a larger power, i.e., $\kappa_n[Q] \sim \xi^{\frac{5n-6}{2}}$.

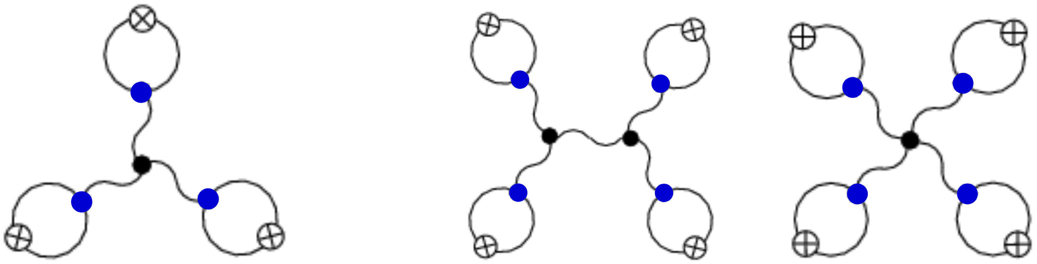

Figure 1.12: Diagrammatic representation of $\kappa_3[Q]$ (left) and $\kappa_4[Q]$ (right) in Eq. (1.155), adapted from Ref. [63]. The wavy line represents the propagator of σ field, i.e., $1/m_\sigma^2 \sim \xi^2$, cross circle stands for the insertion of charges q_A, integrated by $\int_A$ of the loop with the blue points for the insertion $\partial/\partial\sigma$, the black points unattached with the loop are the vertices of the σ field (i.e., open circles in Fig. 1.6).

In order to enhance the contribution from the critical mode, a few remarks are attached here: first, since it is usually assumed that $g_A \propto m_A$ as in the sigma model, the contribution of the critical mode is much significant for heavier particles, therefore, compare to pions, the strength of the critical signal is less significant than protons, for which the above analysis shall also apply; second, remember the measurable quantities are sensitive to the acceptance window, including the momentum rapidity ranges and selected quantum numbers of particles.

It has been show in Ref. [78] that the extension of rapidity accpetance coverage would significantly increase the magnitude of the critical fluctuation signatures; third, since the positive and negative charges cancel the critical contribution from each other, the critical contribution to cumulants of positive-definite quantities are typically larger than that of such quantities as net charges.

1.5.2 Heavy-Ion Collisions and Beam Energy Scan

Unlike the early Universe or the core of compact stars, which we can only analyze based on the remnant information from the Big Bang or the astronomic observation of the remote stars, the Earth-based accelerator facilities provide an ideal incubator for controllable events of nucleus-nucleus collisions. The ongoing and upcoming experiments are performed at facilities include: Relativistic Heavy Ion Collider (RHIC) at BNL in New York, USA; the Super Proton Synchrotron (SPS) and Large Hadron Collider (LHC) at CERN in Geneva, Switzerland; the High Acceptance Di-Electron Spectrometer (HADES) and Facility for Antiproton and Ion Research (FAIR) at GSI in Darmstadt, Germany; the Multi Purpose Detector (MPD) at NICA in Dubna, Russia; the High Intensity Heavy-Ion Accelerator Facility (HIAF) at IMP in Huizhou, China. The study in this thesis are tightly related to the RHIC Beam Energy Scan (BES) Program. Before we arrive there, let's take a brief review of the experimental results from RHIC and LHC.

In heavy-ion experiment, the bulk properties of the created matters are characterized by the particle yields at given acceptance ranges in momentum and other quantum numbers. From the spectra and yields one can extract the system properties at its freezeout moment. For instance, the temperature and collective flow velocity at kinetic freezeout can be extracted by the so-called blast-wave model, in which a blue-shifted radial flow velocity profile is provided. Furthermore, the temperature and chemical potential at chemical freezeout can be identified based on the thermal analysis of particle yields and the Hadron Resonance Gas (HRG) model. Both work remarkably well in comparing to the experimental results.

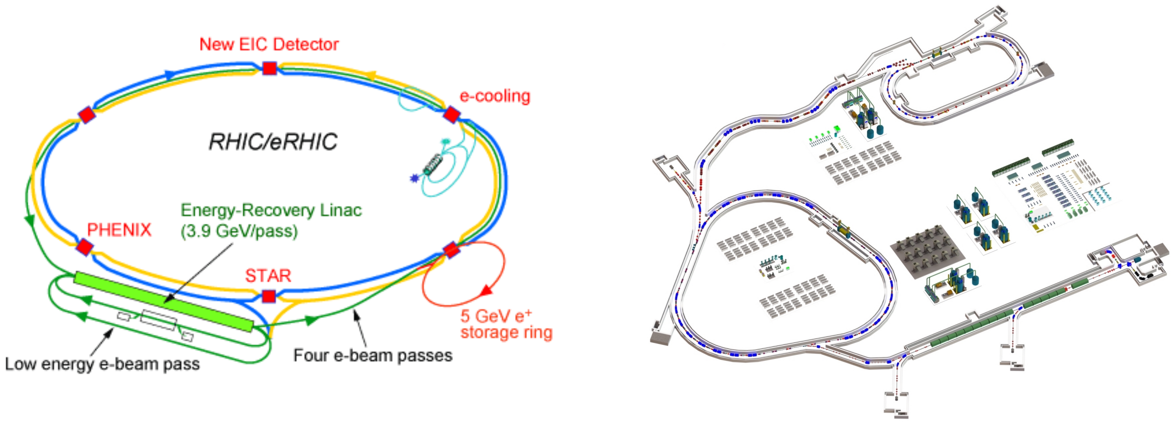
New EIC Detector
e-cooling
RHIC/eRHIC
Energy-Recovery Linac
(3.9 GeV/pass)
PHENIX
STAR
5 GeV e+
storage ring
Low energy e-beam pass
Four e-beam passes

(a) (b)

Figure 1.13: (a) The Relativistic Heavy Ion Collider (RHIC) in Brookhaven, New York, United States (Brookhaven National Laboratory) and (b) the High-Intensity Heavy Ion Accelerator Facility (HIAF) in Huizhou, Guangdong, China (Institute of Modern Physics, Chinese Academy of Sciences).

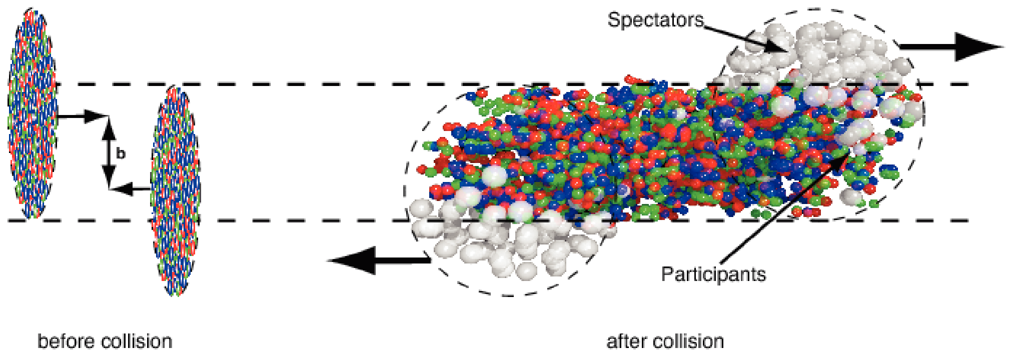
Spectators
b
Participants
before collision
after collision

Figure 1.14: The relativistic nucleus-nucleus collisions and the production of QGP (adapted from Ref. [79]).

Although the beam energy and direction is well controlled by the accelerator in the fixed laboratory frame (LF), the collision event happens in a random location with different orientation of the reaction plane, Ψ_R, which is spanned by the beam direction and impact parameter of the incoming nuclei. The beam direction is naturally identified as the azimuthal axis of the reaction plane. Since the collision is not initially in a symmetric patten in real space geometry, we would expect an azimuthal asymmetry of the particles yields in the final momentum distribution. Such azimuthal asymmetry could be analyzed by the Fourier series decomposition in the azimuthal angle ϕ relative to the reaction plane Ψ_R:

$$\frac{dN}{d\phi} = \frac{N}{2\pi}\left(1 + \sum_{i=1}^{\infty} 2v_n \cos\left(n(\phi - \Psi_R)\right)\right), \quad v_n = \frac{1}{N}\int d\phi \frac{\partial N}{\partial \phi} \cos\left(n(\phi - \Psi_R)\right) \tag{1.156}$$

where the Fourier coefficients of nth harmonics, v_n, describe the bulk and deformation of the azimuthal momentum distribution and are also referred as the *collective flow* parameters. One can further introduce the multi-particle correlation function, e.g., $v_n^2 = \langle \cos\left(n(\phi_1 - \phi_2)\right)\rangle$, independent of the reaction plane Ψ_R which is not known a priori. The first harmonic, v_1, represents a dipole deformation describing the preferred emission direction of particles. The slope of v_1 in rapidity is referred to as the directed flow[14], which vanishes in the mid-rapidity region due to the geometric symmetry. Moreover, the energy dependence of the directed flow near mid-rapidity exhibits a non-monotonic behavior (see Fig. 1.15 and Ref. [80, 81]), where there exists a minimum is referred to as the softest point collapse of the flow and serves as a possible signature of a first-order phase phase transitions. The second harmonics, v_2, referred to as the elliptic flow, is the quadrupole deformation and describes how the system responds to the initial geometric asymmetry in momentum space. More specifically, the anisotropy of pressure gradients gives rise to the significant elliptic flow in off-central collisions. Such observation serves as a smoking gun of the formation of a strongly coupled quark-gluon plasma.

From the experimental results of bulk properties and collectivity, one already observes non-monotonic behavior and possible hints for a phase transition. To have a sound conclusion one needs to consider a better observables more sensitive to the phase transition, the fluctuations. As we discussed in Sec. 1.3 and Sec. 1.5.1, one of the ideal observables sensitive the critical point is the cumulants of the multiplicity distribution of measurable particles.

---

[14] Note here v_n could also have momentum and rapidity dependence, in which case it only describes the azimuthal momentum distribution at given momentum and rapidity bin.

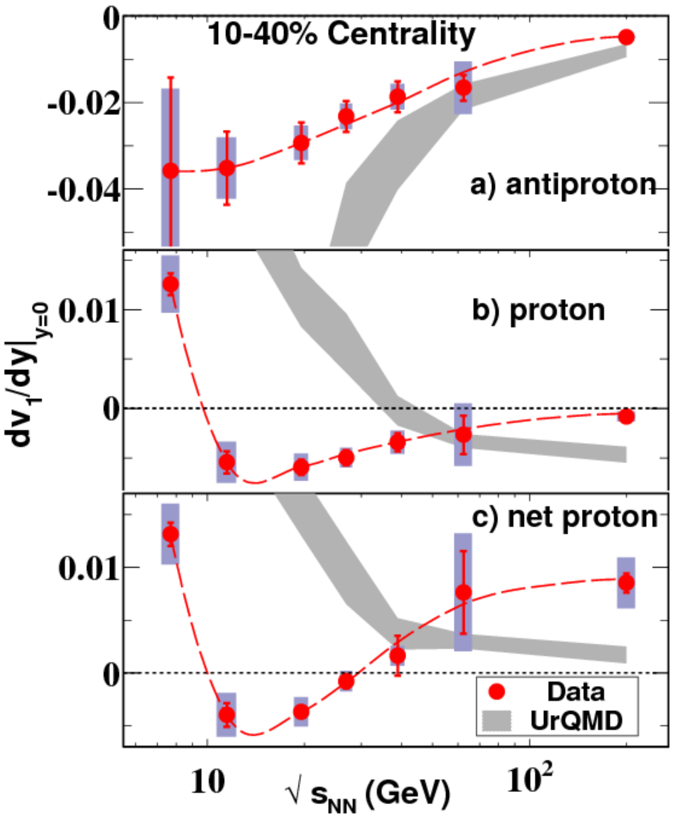

Figure 1.15: The collision energy dependence of the directed flow (v_1) slop parameter near mid-rapidity for protons, anti-protons and net-protons measured by the STAR collaboration, along with UrQMD calculations subject to the same cuts and fit conditions [80]. The produced particles such as anti-protons are supposed to behave monotonically. In contrast, protons and net protons are sensitive to the stopping effect, and the observed minimum for which resembles the predicted "softest point collapse" of flow.

In the context of the RHIC BES phase I, these particles (quantum numbers) are net protons, net charges and net kaons, approximating the conservation of baryon numbers, charge numbers and strangeness numbers. The charge numbers can be characterized by the pion numbers since pion is the most abundant charged particles. The proxies of baryon numbers and strangeness numbers, although not conserved, are net-proton and net-kaon numbers respectively. All these proxies of conserved quantum numbers exhibit qualitatively similar results (Fig. 1.16) [82, 83], however, among which the net-proton numbers shall give rise to more significant critical contribution since the proton has larger mass compared to kaons and pions, see Sec. 1.5.1 for detailed discussion. Fig 1.17 shows the energy dependence of the fourth-order cumulant ratio $\kappa_4/\kappa_2 = \kappa\sigma^2$ and third-order cumulant ratio $\kappa_3/\kappa_2 = S\sigma$ for net-protons in Au-Au collisions at different centralities [84]. This is an “intriguing hint” for the existence of the QCD critical point.

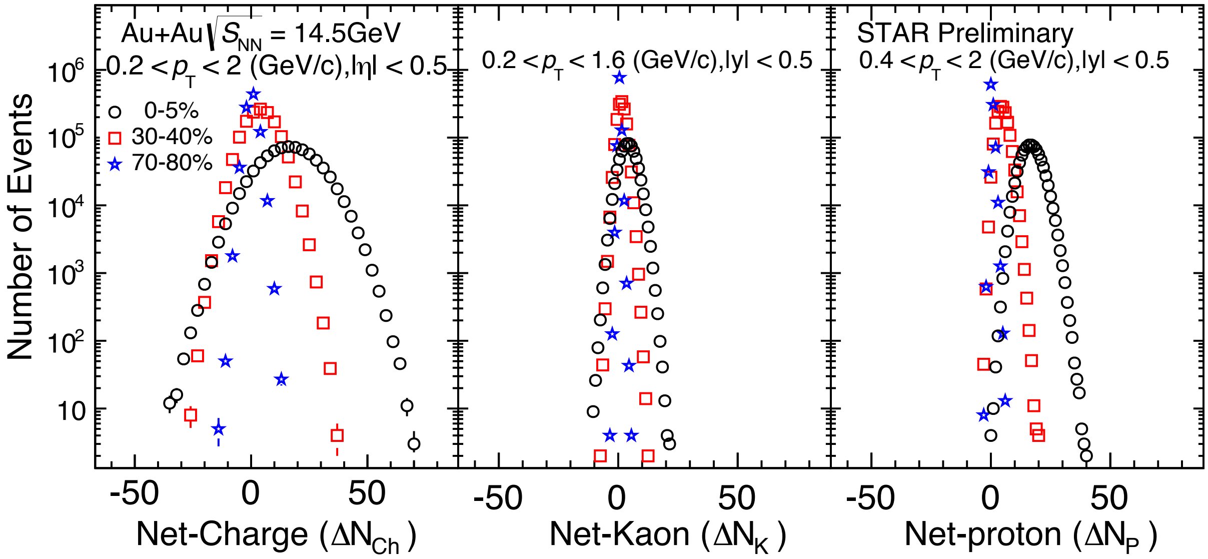

Figure 1.16: Event-by-event net-particle multiplicity distributions for Au+Au collisions at $\sqrt{s_{NN}} = 14.5\,\text{GeV}$ for net-charge ΔN_{Ch} (left), net-kaon ΔN_{K} (middle) and net-proton ΔN_{P} (right) for $0-5\%$ top central (black circles), $30-40\%$ central (red squares), and $70-80\%$ peripheral (blue stars) collisions [82].

The approach to obtain the above experiment results is called beam energy scan. By tuning the beam energy $\sqrt{s_{NN}}$, the evolution of the created matters could be mapped to a particular trajectory in various regions of the QCD phase diagram, terminated at the freezeout curve parametrized by [85]

$$T(\mu) = a - b\mu^2 - c\mu^4, \tag{1.157}$$

where $a \approx 0.166\,\text{GeV}$, $b \approx 0.139\,\text{GeV}^{-1}$ and $c \approx 0.053\,\text{GeV}^{-3}$, and the energy dependence of

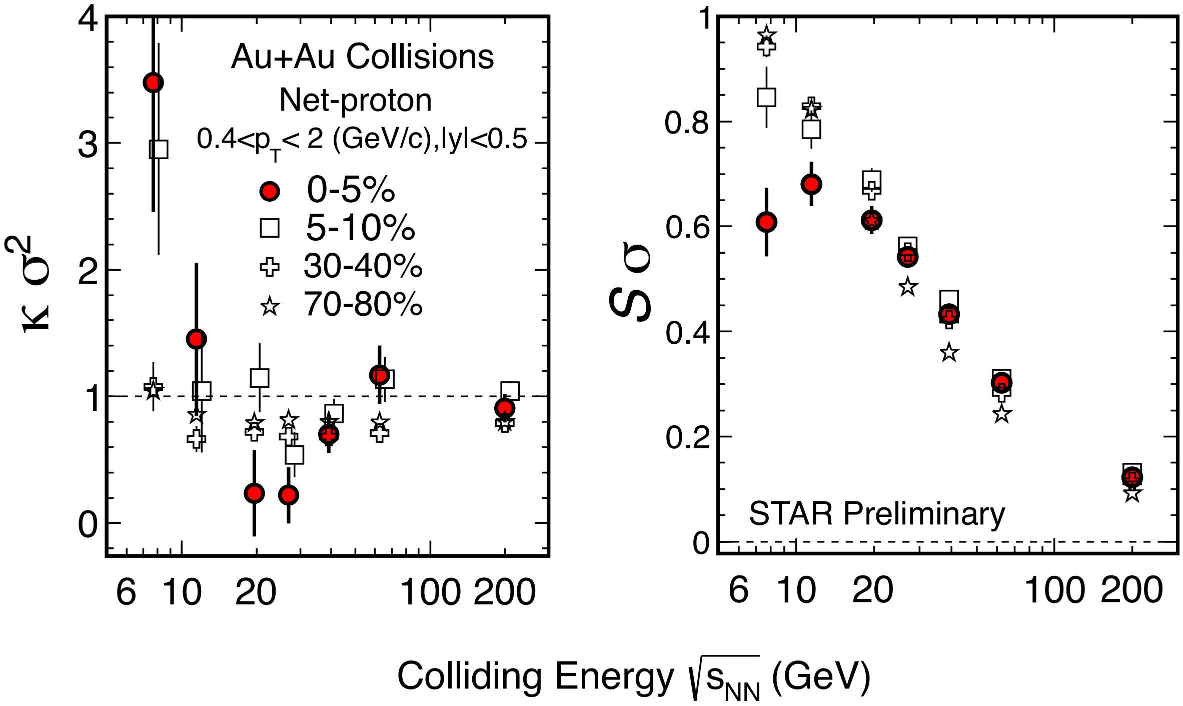

Figure 1.17: The collision energy dependence of the cumulant ratio $\kappa_4/\kappa_2 = \kappa\sigma^2$ (left) and $\kappa_3/\kappa_2 = S\sigma$ (right) for net-protons in Au-Au collisions at different centralities measured by the STAR collaboration. A non-monotonic behavior is seen in the most central collisions (filled-circles) [84].

the baryon chemical potential can be parameterized as

$$\mu(\sqrt{s_{NN}}) = \frac{d}{1 + e\sqrt{s_{NN}}} \tag{1.158}$$

where $d \approx 1.308\,\text{GeV}$ and $e \approx 0.273\,\text{GeV}^{-1}$. The coefficients a, b, c, d, e are phenomenological parameters determined by the thermal model of particle yields. The amount of entropy increase as $\sqrt{s_{NN}}$ but the net baryon numbers are fixed by the initial nuclei.

If the beam energy $\sqrt{s_{NN}}$ is in the LHC ranges (above 2.76 TeV), after the incoming nuclei collides with each other, very few baryon charges are doped in the central rapidity region in a hot medium with high temperature, thus the chemical potential, which is locally defined in this region, are quite small and becomes even smaller when the collisions is peripheral

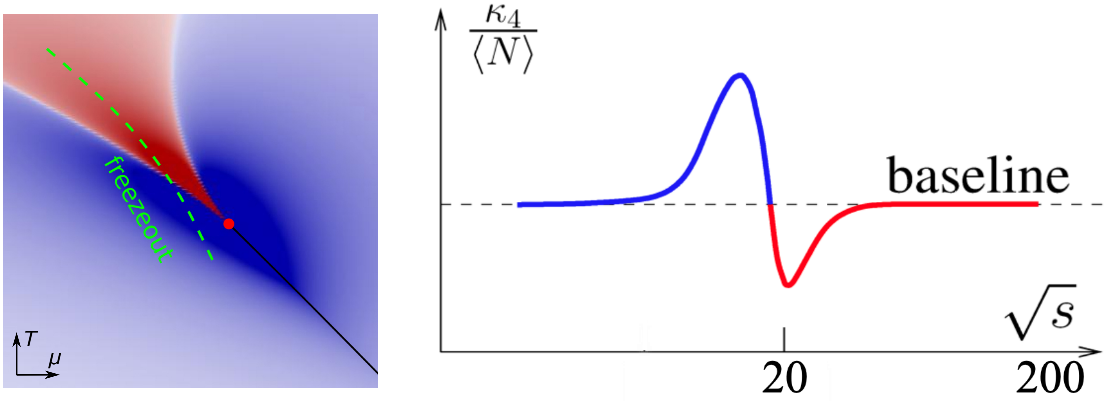

Figure 1.18: Theoretical prediction of equilibrium kurtosis $\kappa_4(\sqrt{s_{NN}})$ along the freezeout line (dashed green line). Figures are adapted from Ref. [86] and [64].

(with fewer baryon numbers at mid-rapidity). On the other hand, when $\sqrt{s_{NN}}$ falls into the RHIC ranges (200-27 GeV for BES phase I and 19.6-7.7 GeV for BES phase II) and the collision is more central-like, more baryon charges are doped at mid-rapidity (known as the baryon stopping) and the local chemical potential is larger but the temperature drops. A few representative trajectory for the system evolution with various beam energies are drawn in Fig. 1.8. By varying the beam energies, the representative trajectory may possibly pass the QCD critical point and the associated first-order phase transition line. Thus, one would expect that the basic thermodynamic properties of the created matters should change nontrivially, such as possible non-monotonic behavior of the observables (presented in Fig. 1.15 and 1.17) as function of $\sqrt{s_{NN}}$ emerges at freezeout. Fig. 1.18 shows a theoretic prediction of the kurtosis $\kappa_4(\sqrt{s_{NN}})$ provided a freezeout line.

As we discussed in the previous subsection, the non-equilibrium dynamics would change the equilibrium cumulant distribution in the phase diagram. In a simplified model discussed in Ref. [76], the authors demonstrate that, depending on non-universal parameters (e.g., the relaxation rate of critical fluctuations), the cumulants can differ significantly from their equilibrium expectations. Fig. 1.19 shows that memory effects persist even for trajectories that skirt the edge of the critical regime. One can imagine that, with a more realistic and delicate setup, the beam energy or chemical potential dependence of the experimental

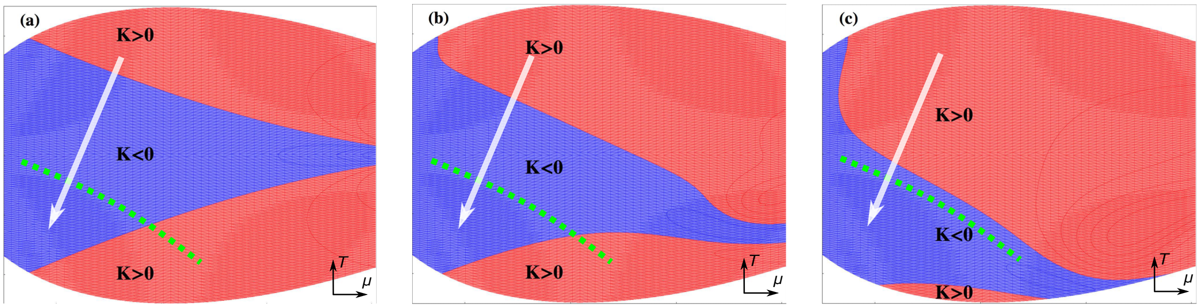

(a) (b) (c)

Figure 1.19: Contour plot of equilibrium (a) and non-equilibrium kurtosis $K \equiv \kappa = \kappa_4/\kappa_2^2$ with different non-universal phenomenological inputs (b) and (c) adapted from Ref. [76]. The $K > 0$ region is colored in red and the $K < 0$ region in blue, in the opposite convention of Fig. 1.11. The white arrow represents the evolution trajectory of system while the green dashed line represents the freezeout surface.

measures discussed in this subsection would also receive a qualitative change. Attempts are made on this subject in order to provide the quantitative prediction for the upcoming BES phase II results [65].

Before we conclude this section, we address several remarks. First, it is noteworthy that the cumulant of multiplicity distribution of conserved quantity is not the unique proposed experimental measures of the critical point. Other suggestions can be found in, for example, Ref. [87, 88, 89, 90, 91]. Second, it is important to keep in mind that there are many other sources that do contribute to the fluctuation measures in heavy ion collisions. In the event-by-event collisions, we have to take into account all of those stochastic fluctuations emerging at each stage of each event. In this thesis, we focus more on the fluctuation in the fireball evolution process that can be described hydrodynamically and argue that they are more sensitive to the critical point. However, in order to establish a quantitative framework for interpreting the experiment results, it is insufficient to neglect the beam-energy-scan dependence of other fluctuation sources. For instance, before the onset of hydrodynamic fluctuations, initial fluctuations already emerge. At each collision event, the impact parameter and hence the size of the created fireball varies. In other words, the volume of the system fluctuates on a event-by-event basis. The volume fluctuations can be characterized by the participant number $N_{\rm part}$ subject to the baryon number conservation. Besides that, the initial geometry also fluctuates and can be characterized by the Fourier component of the azimuthal asymmetry [92]. Furthermore, the partonic distribution of initial sources (Color-Glass Condensate, CGC) in the wounded nucleons fluctuates in the transverse plane [93]. The initial fluctuations will propagate in the process of the QGP evolution and the hadronization stages. After the freezeout, the hadronic phases (jets) still evolve stochastically, in the propagating process of fluctuations, the existing fluctuations could be washed out and additional sources of fluctuations could be created. Finally, the fluctuations are encoded in the observables collected by the detector. The detection efficiency, acceptance and data analysis gives rise to further fluctuations and statistic uncertainties. Although we argue that these fluctuations are not as sensitive as the hydrodynamic (thermal) fluctuations to the critical point, they nevertheless provide the background that can be used to extract the critical signature *quantitatively*. For example, the initial fluctuations have larger correlation range in rapidity than the thermal fluctuations (similar to the primordial fluctuations of CMB); the geometry fluctuations may be more significant in the collective flow measurement than in the multiplicity cumulant; etc. Nevertheless, we will focus on the hydrodynamic fluctuations in this thesis. In the following chapters, we will provide a systematic formalism for describing the hydrodynamic fluctuation, and discuss its implementation in the vicinity of the (QCD) critical point.

Chapter 2

Hydrodynamic Fluctuations

This chapter contains materials published in

- X. An, G. Basar, M. Stephanov and H.-U. Yee, *Relativistic Hydrodynamic Fluctuations*, Phys. Rev. C **100** no. 2, (2019) 024910, arXiv:1902.09517 [hep-th] [1]. Copyright (2019) by the American Physical Society (APS).
- X. An, G. Basar, M. Stephanov and H.-U. Yee, *Fluctuation dynamics in a relativistic fluid with a critical point*, accepted by Phys. Rev. C, arXiv:1912.13456 [hep-th] [2]. Copyright (2020) by the American Physical Society (APS).
- X. An, *Fluctuation dynamics in a relativistic fluid with a critical point*, accepted by Nucl. Phys. A, arXiv:2003.02828 [hep-th] [3]. Copyright (2020) by authors.

The subject of hydrodynamic fluctuations is particularly relevant to heavy-ion collisions. The system size L is not astronomically large compared to the typical microscopic scale, ℓ_{mic}, (factor 10 at most is a typical scale separation).[1] As a result, fluctuations are large enough to be easily observable in experiments. In addition, since the leading corrections to hydrodynamics are due to the nonlinear feedback of fluctuations, we cannot afford to neglect them – a luxury one is used to in ordinary fluid dynamics. Fluctuations are even more important when enhanced by critical phenomena.

---

[1] In the context of heavy-ion collisions, $\ell_{\text{mic}} \sim 1/T \sim 1$ fm, while the typical hydrodynamic gradient scale is set by the (transverse) size of the nucleus $L \sim R \sim 10$ fm.

From the modern point of view, hydrodynamics is a systematic expansion in spatial gradients. More precisely, it is the expansion of constitutive equations for stress tensor (and conserved current). The expansion parameter is the ratio of a typical hydrodynamic wavenumber $k = 1/L$ to a microscopic scale, say temperature T, or inverse scattering length, or, generically, $1/\ell_{\text{mic}}$. In this view, the ideal, non-dissipative (i.e., reversible) hydrodynamics is the truncation of this expansion at lowest (zeroth) order. At first order in gradients (i.e., at order k^1 or, more precisely, $(k\ell_{\text{mic}})^1$) one recovers standard Landau-Lifshitz or Navier-Stokes hydrodynamics. It is the following order in this expansion that concerns us here. That order is not k^2, but rather is $k^{3/2}$ (or $k^{d/2}$ in d-dimensions). Such non-analytic behavior in k and, therefore, nonlocal contributions come from fluctuations in hydrodynamics. Thus it is essential to understand the physics of hydrodynamic fluctuations to faithfully describe physics of heavy-ion collisions.[2]

Furthermore, in addition to modifying hydrodynamic equations by effectively nonlocal contributions, the fluctuations themselves are measured in heavy-ion collision experiments. In particular, one of the most fundamental questions these experiments aim to answer is the existence and location of the critical point on the QCD phase diagram [94, 64]. The signature of this phenomenon is a certain non-monotonic behavior of event-by-event fluctuation measures when the parameters of the collision (such as $\sqrt{s_{NN}}$) is varied in order to “scan” QCD phase diagram [10, 95] (Sec. 1.5.2). This non-monotonic behavior presented in Fig. 1.17 is driven by critical phenomena and thus predictable without being able to determine QCD equation of state at finite density (still an unsolved theoretical problem).

---

[2] Second order (k^2) corrections could be dominant instead of fluctuations in special cases, where fluctuations are suppressed, as in some large-N theories. Also for dimensions greater than 4, fluctuations are parametrically smaller than k^2 terms. This work shall be concerned with the generic hydrodynamics in three spatial dimensions, relevant for QCD fireball evolution in heavy-ion collisions, among other applications.

The existing predictions for critical behavior rely significantly on the assumption of local thermal equilibrium. However, near the critical point, the equilibrium is increasingly difficult to achieve due to critical slowing down and a finiteness of expansion time. Essentially, this limitation determines the magnitude of the observable signatures of the critical point [95, 96]. Therefore the ability to describe the dynamical evolution of fluctuations during the fireball evolution, in particular, in the proximity the critical point is crucial. The goal of this chapter is to provide such a description.

One of the recent advances towards this goal has been the introduction of Hydro+ in Ref. [39], with a recent numerical implementation in a simplified setup reported in Ref. [41, 42]. Focusing on the mode responsible for the critical slowing down, identifying it with the fluctuation correlator of the slowest hydrodynamic mode, the authors of Ref. [39] proposed the evolution equation which describes the relaxation of this non-hydrodynamic mode to equilibrium. Extending hydrodynamics by addition of such a mode one is then able to broaden the range of applicability of hydrodynamics near the critical point and describe the dominant mode of critical fluctuations at the same time. The crucial ingredient of this formalism is a non-equilibrium entropy of fluctuations derived in Ref. [39].

We approach this problem from a different direction. We start with the general formalism of relativistic hydrodynamic fluctuations introduced earlier in Ref. [1] for neutral (chargeless) fluids and extend it to include a crucial ingredient – baryon charge density. QCD critical point, if it exists, is located at finite baryon density. The approach we pursue, in which the two-point correlators of hydrodynamic variables play the role of additional non-hydrodynamic variables, has been introduced and developed recently in the context of heavy-ion collisions, but limited to special types of flow such as longitudinal boost-invariant expansion in Refs. [48, 49, 50]. In a more general but non-relativistic case this approach was pioneered by Andreev in the 1970's [47]. The approach is often referred to as 'hydro-kinetic' to acknowledge the similarity between the two-point correlators and the distribution functions in kinetic theory. In particular, the dynamics of the correlators of the pressure fluctuations is essentially equivalent to the kinetics of the phonon gas. This physically intuitive picture was the original source of this formalism [97, 48] and was rigorously derived in general relativistic context in Ref. [1].

The hydro-kinetic approach should be also contrasted with the traditional stochastic hydrodynamics where the noise is introduced into hydrodynamic equations as in Refs. [98, 43]. From this point of view, the 'hydro-kinetic' approach could also be called 'deterministic', as it replaces stochastic equations with deterministic equations for the evolution of correlation functions. Of course, the two approaches solve the same system of stochastic equations, but in complementary ways. The advantage of the deterministic approach is that it allows one to deal with the problem of the "infinite noise": the noise amplitude needs to become infinitely large as the hydrodynamic cell size is sent to zero, even though the physical effect of the noise is finite due to its averaging out in a medium whose properties vary slowly in space and time. The effect of the infinite (or more precisely cutoff dependent) noise can be absorbed into renormalization of hydrodynamic equations – a procedure which can be performed analytically in the deterministic approach. This avoids having to deal with numerical cancellations which would otherwise be necessary in a direct implementation of stochastic equations.

Near the critical point the deterministic approach we develop here, although different from Hydro+ in Ref. [39], nevertheless leads to the description of fluctuations in terms of two-point correlators as in Hydro+. In this thesis we verify that in the limit of large correlation length the two approaches exactly match. This is a nontrivial check of the validity of both approaches. Furthermore, since the deterministic approach is more general it allows us to extend the Hydro+ approach both closer to the critical point and further away from the critical point to describe also ordinary, noncritical fluctuations.

2.1 Hydrodynamics and Thermodynamics

Hydrodynamics [99], or more broadly, the fluid mechanics [100, 101], a classical subject studied by human beings since ancient times, is rejuvenated in recent years [100, 101]. A major impetus of this renaissance comes from the rapid progress of the study on physics of heavy-ion collisions, both in theory and experiment. The increasing body of experimental evidence that relativistic hydrodynamics is describing the evolution of the expanding fireball created in these collisions motivates technical developments as well as a closer look at many fundamental theoretical concepts in hydrodynamics.

Indeed, hydrodynamics is a long wavelength effective theory providing the framework to describe dynamic system across difference scales, from the large-scale structure of the Universe, to the small system created by colliding high-energy particles. Its broad application is rooted in the widely-accepted assumption that, hydrodynamics concerns itself with the motion of a *continuous* medium, where the element of the fluid is referred to as the hydrodynamic cell. In other words, hydrodynamics does not concern the ultraviolet degrees of freedom in specific scenarios beyond the scale of the hydrodynamic cell. Thus, regardless of whatever scenario one is considering, the fundamental equations of hydrodynamics can be always written generically as one or a set of conservation equations in the following form:

$$\frac{\partial}{\partial t}\psi + \boldsymbol{\nabla}\cdot\mathbf{flux}[\psi] = 0\,. \tag{2.1}$$

It says that the amount of the conserved quantity, $\psi = \psi(t, \boldsymbol{x})$, can only change by the flux flowing into or out of a given volume. The way how the flux depend on the conserved quantity, $\mathbf{flux} = \mathbf{flux}[\psi]$, is called the constitutive relations. Example of such conserved quantities and flux could be energy, momentum and charge. In this thesis, we will focus on the system subject to the conservation of energy, momentum and U(1) charge, and the extension of which to a broader system of conservation laws shall be straightforward.

In relativistic hydrodynamics, the conservation equations for energy, momentum and U(1) charge could be written in a covariant form

$$\partial_\mu T^{\mu\nu} = 0\,, \tag{2.2a}$$

$$\partial_\mu J^{\mu} = 0\,, \tag{2.2b}$$

where $T^{\mu\nu}$ and J^μ are the energy-momentum tensor and charge current vector respectively. Since there are three conservation laws (respect to energy, momentum and charge) taken into account, there are five independent fundamental hydrodynamic variables (two scalers and one vector with three components), served as conserved quantities in hydrodynamic equations. The choice of the five hydrodynamic variables are not unique, however. A natural choice would be the two natural variables of local equilibrium entropy density, i.e., energy density ε, charge density n, as well as the fluid velocity u_μ. Thus

$$T^{\mu\nu} = T^{\mu\nu}(\varepsilon, n, u), \quad J^\mu = J^\mu(\varepsilon, n, u). \tag{2.3}$$

Eq. (2.2b) is a scaler equation describing the conservation of charge density, while Eq. (2.2b) is a vector equation, which can be contracted by the longitudinal and transverse projection. The longitudinal equation

$$u_\nu \partial_\mu T^{\mu\nu} = 0 \tag{2.4}$$

describes the conservation of energy density while the transverse equation (also referred to as the Euler equation)

$$\Delta_{\mu\nu} \partial_\lambda T^{\lambda\nu} = 0 \tag{2.5}$$

describes the conservation of momentum density, where $\Delta_{\mu\nu} \equiv g_{\mu\nu} + u_\mu u_\nu$ is the standard spatial projection operator to the spatial hypersurface orthogonal to u, i.e., $\Delta_{\mu\nu} u^\mu = 0$.

The constitutive relations in Eq. (2.3) are organized as an expansion in powers of spatial gradients, and are decomposed into the ideal part (zeroth order in gradients) and gradient part. The ideal part could be obtained by applying Lorentz transformation

$$u^\mu = \Lambda^\mu{}_\lambda u^\lambda \,, \quad g^{\mu\nu} = \Lambda^\mu{}_\lambda \Lambda^\nu{}_\kappa g^{\lambda\kappa} \tag{2.6}$$

from the local rest frame (LRF) where $u = (1, \mathbf{0})$, i.e.,

$$T^{\mu\nu}_{\text{LRF}}(\varepsilon, n) = \text{diag}(\varepsilon, p(\varepsilon, n), p(\varepsilon, n), p(\varepsilon, n)) \,, \quad J^\mu_{\text{LRF}}(n) = (n, \mathbf{0}) \tag{2.7}$$

are defined in thermodynamic equilibrium and $p(\varepsilon, n)$ is the pressure given by the equation of state and satisfying Pascal's Law. Namely,

$$T^{\mu\nu}_{\text{ideal}} = \Lambda^\mu{}_\lambda \Lambda^\nu{}_\kappa T^{\lambda\kappa}_{\text{LRF}} = \varepsilon\, u^\mu u^\nu + p(\varepsilon, n) \Delta^{\mu\nu} \,, \quad J^\mu_{\text{ideal}} = \Lambda^\mu{}_\lambda J^\lambda_{\text{LRF}} = n u^\mu \,. \tag{2.8}$$

Since in the local rest frame the system is in equilibrium, the hydrodynamic variables defined in such frame shall know about the thermodynamic laws. What information can we extract from thermodynamics? Remember, one of the reasons we choose ε and n as hydrodynamic variables is that they are natural variables of entropy density (entropy per volume)

$$s = \beta w - \alpha n\,, \tag{2.9}$$

i.e., the first law of thermodynamics:

$$ds = \beta d\varepsilon - \alpha dn\,. \tag{2.10}$$

The pressure can be obtained by the Legendre transformation of entropy density with respect to ε and n,

$$\beta p = s - \beta\varepsilon + \alpha n\,, \tag{2.11}$$

and accordingly Eq. (2.10) becomes the Gibbs-Duhem relation

$$dp = -\frac{w}{\beta}d\beta + \frac{n}{\beta}d\alpha = sdT + nd\mu\,, \tag{2.12}$$

where w is the enthalpy density defined by

$$w \equiv \varepsilon + p = Ts + \mu n\,, \tag{2.13}$$

and temperature T as well as chemical potential μ are defined via derivatives of entropy density s

$$\beta \equiv \left(\frac{\partial s}{\partial \varepsilon}\right)_n = \frac{1}{T}\,, \quad \alpha \equiv -\left(\frac{\partial s}{\partial n}\right)_\varepsilon = \frac{\mu}{T}\,. \tag{2.14}$$

Substitute Eq. (2.8) into Eq. (2.4), (2.5) and (2.2b), one obtains the conservation equations for ideal hydrodynamics:

$$u\cdot\partial\varepsilon = -w\theta\,, \quad u\cdot\partial u_\mu \equiv a_\mu = -\frac{1}{w}\partial_{\perp\mu}p\,, \quad u\cdot\partial n = -n\theta\,. \tag{2.15}$$

Eq. (2.9), (2.10) together with (2.15) imply that the entropy is conserved:

$$u\cdot\partial s = -s\theta\,. \tag{2.16}$$

If we introduce the entropy per charge

$$m \equiv \frac{s}{n}\,, \tag{2.17}$$

Eq. (2.15) and (2.16) give

$$u \cdot \partial m = 0\,. \tag{2.18}$$

The conservation of entropy is not an independent conservation laws in ideal hydrodynamics, and it breaks down when the system dissipate energy in the presence of gradients. Note, once the equilibrium thermodynamics are given in the local rest frame, the thermodynamics in any frame is established as well, and the terms zeroth order in gradients are unambiguously determined. The terms first-order in gradients, however, are subject to the convention of frame choice. In fact, there is no unambiguous definition of thermodynamic variables out of equilibrium in the presence of gradients. Assume the system is not far from equilibrium, then the non-equilibrium corrections could be expressed approximately in terms of the gradients of the equilibrium thermodynamic variables defined in the local rest frame. Therefore, a frame transformation would not only result in a change of the local equilibrium state, but also the gradient corrections. Among various choices, there are two widely-used frames, the Landau frame and the Eckart frame, that are local rest frames defined such that the energy flow and charge flow vanish in which respectively. Once the frame is chosen, the velocity u^μ is also unambiguously defined. Landau frame is more appropriate for application to the central rapidity region where the baryon density is small. Hydrodynamics, of course, does not rely on the frame choice. In this thesis, without specification we will use Landau frame.

Without loss of generality, we write

$$\begin{aligned} T^{\mu\nu}(\varepsilon, n, u) &= T^{\mu\nu}_{\text{ideal}}(\varepsilon, n, u) + \Pi^{\mu\nu}(\varepsilon, n, u), \\ J^{\mu}(\varepsilon, n, u) &= J^{\mu}_{\text{ideal}}(\varepsilon, n, u) + \nu^{\mu}(\varepsilon, n, u), \end{aligned} \tag{2.19}$$

where the ideal part is given by Eq. (2.8), and

$$s^{\mu}(\varepsilon, n, u) = s^{\mu}_{\text{ideal}}(\varepsilon, n, u) + \sigma^{\mu}(\varepsilon, n, u), \tag{2.20}$$

where

$$s^{\mu}_{\text{ideal}}(\varepsilon, n, u) = \Lambda^{\mu}{}_{\lambda} s^{\lambda}_{\text{LRF}} = s(\varepsilon, n) u^{\mu}\,, \quad s^{\mu}_{\text{LRF}}(\varepsilon, n) = (s(\varepsilon, n), \mathbf{0}). \tag{2.21}$$

The dissipative terms are completely vanish in the local rest frame by definition, i.e.,

$$T^{\mu\nu} u_{\mu} = \varepsilon u^{\nu}\,, \quad J^{\mu} u_{\mu} = -n\,, \quad s^{\mu} u_{\mu} = -s\,. \tag{2.22}$$

The so-called Landau's matching conditions given by Eqs. (2.22) *define* three Lorentz invariants, i.e., ε, n and s, and imply the following constraints,

$$\Pi^{\mu\nu} u_{\mu} = 0\,, \quad \nu^{\mu} u_{\mu} = 0\,, \quad \sigma^{\mu} u_{\mu} = 0\,, \tag{2.23}$$

hold in any frame. It states that the dissipative terms must be transverse (spatial).

The local entropy is no longer conserved in the presence of the dissipation induced by external perturbations. The second law of thermodynamics require

$$\partial_{\mu} s^{\mu} \geq 0\,. \tag{2.24}$$

Using Eq. (2.19), (2.20), (2.22), (2.23) we find from Eq. (2.4) that

$$\partial_{\mu} s^{\mu} \equiv \partial_{\mu}(s u^{\mu} - \alpha \nu^{\mu}) = -\nu^{\mu} \partial_{\mu} \alpha - \beta \Pi^{\mu\nu} \partial_{\mu} u_{\nu} = -\nu^{\mu} \partial_{\mu} \alpha - \frac{1}{2} \beta \Pi^{\mu\nu} \left(\partial_{\mu} u_{\nu} + \partial_{\nu} u_{\mu} \right), \tag{2.25}$$

where in the second equality we have used the symmetric property $\Pi^{\mu\nu} = \Pi^{\nu\mu}$. Eq. (2.25) together with Eq. (2.23) uniquely determines the dissipative terms of first-order hydrodynamics in Landau frame:

$$\Pi^{\mu\nu}(\varepsilon, n, u) = -2\eta(\varepsilon, n) \left(\theta^{\mu\nu} - \frac{1}{d} \Delta^{\mu\nu} \theta \right) - \zeta(\varepsilon, n) \Delta^{\mu\nu} \theta\,, \tag{2.26a}$$

$$\nu^{\mu}(\varepsilon, n, u) = -\lambda(\varepsilon, n) \partial^{\mu}_{\perp} \alpha(\varepsilon, n)\,, \tag{2.26b}$$

$$\sigma^{\mu}(\varepsilon, n, u) = -\alpha(\varepsilon, n) \nu^{\mu}(\varepsilon, n, u)\,, \tag{2.26c}$$

where

$$\theta^{\mu\nu} \equiv \frac{1}{2} \left(\partial^{\mu}_{\perp} u^{\nu} + \partial^{\nu}_{\perp} u^{\mu} \right), \quad \theta \equiv \theta^{\mu}_{\mu} \equiv \partial \cdot u\,, \quad \partial^{\mu}_{\perp} \equiv \Delta^{\mu\nu} \partial_{\nu}\,, \tag{2.27}$$

and the coefficients of the gradient terms, (η, ζ, λ), known as the transport coefficients, are shear viscosity, bulk viscosity and charge conductivity respectively. They are assumed be functions of (equilibrium) thermodynamic variables, ε and n in our choice. According to Eq. (2.24), (2.26) and (2.27), they must be positive semidefinite:

$$\eta \geq 0\,, \quad \zeta \geq 0\,, \quad \lambda \geq 0\,. \tag{2.28}$$

In this thesis, we only truncate the hydrodynamical expansion to first order in spatial gradients of hydrodynamic variables. However, one should keep in mind that the first-order hydrodynamics fails to satisfying the requirement of causality and stability. To solve this problem, one needs to go beyond the first order and consider theories developed by Israel and Stewart [102].

2.2 Stochastic Fluctuating Hydrodynamics

2.2.1 Hydrodynamic Fluctuations and Stochastic Noises

Since we are describing a thermal system, the hydrodynamic variables (operators) are stochastic – fluctuating between members of the statistical ensemble describing our system (in heavy-ion collisions – between collision events). However, due to macroscopic averaging (coarse graining) involved in their construction they behave as classical (commuting) stochastic variables. In other words, fluctuations at scales shorter than b are averaged out, i.e., the ultraviolet degrees of freedom are suppressed. In this sense, $\Lambda = 1/b$ plays the role of the ultraviolet (wave-vector) cutoff. The suppressed fluctuations involve the thermal (classical) and quantum parts, whereas the quantum fluctuations are negligible compared to classical fluctuations. The precise condition for that is that the quantum uncertainty of the energy due to finite characteristic time of the evolution of these variables is much smaller than their typical thermal energy, T. The fastest evolving degrees of freedom after coarse graining are sound modes with wave-length b. Their frequency c_s/b must therefore be much

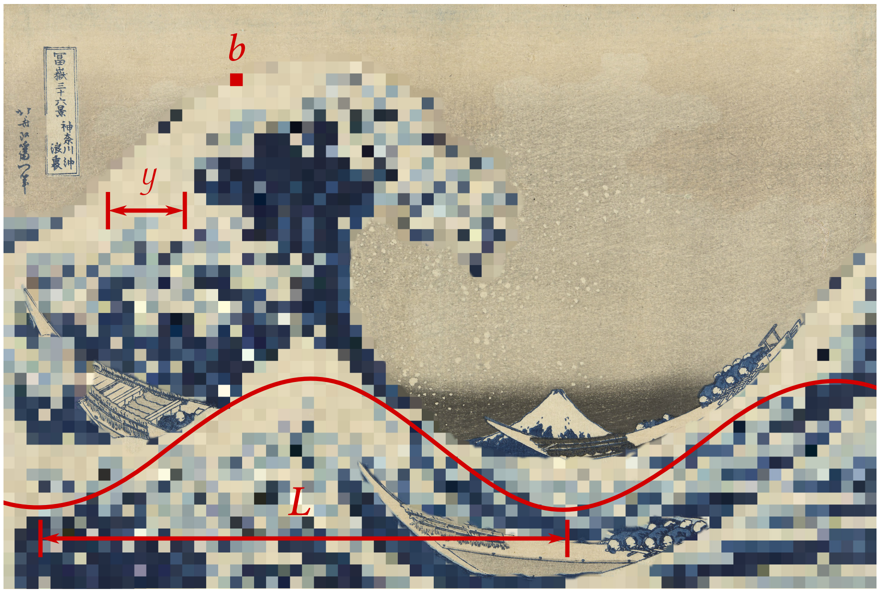

Figure 2.1: The separation of hydrodynamic scales illustrated on top of the Japanese woodblock print, *The Great Wave off Kanagawa* (Katsushika Hokusai, 1830). The fluid is coarse grained such that each pixel represents a hydrodynamic cell of width b. The hydrodynamic variables, defined as local functions of the hydrodynamic cells, fluctuate at the scale of $y \geq b$, which is much less than the typical inhomogeneous scale (wavelength L) of the fluid background.

smaller than T, i.e., $b \gg c_s/T$. In framework of hydro-kinetic theory, the scale hierarchy would be[3]

$$k, \gamma q^2/c_s \ll q < \Lambda \ll T \quad \text{or} \quad L \gg y > b \gg \ell_{\text{mic}}. \tag{2.29}$$

For illustration purpose we depict the scale separation in Fig. 2.1.

Throughout the thesis we will use the breve accent ˘ to distinguish a stochastic quantity from its ensemble average, following the conventions in Ref. [1]. Let us refer to the stochastic hydrodynamic variables defined via coarse-graining as $\breve{\psi}(t, \boldsymbol{x})$. The ensemble average of the variable $\psi \equiv \langle \breve{\psi} \rangle$ obeys Eq. (2.1) which is deterministic, while the fluctuating variable $\breve{\psi}$ itself obey a equation which has to be stochastic:

---

[3] In heavy-ion collisions these scales are not perfectly separated, and “much greater” would typically mean “greater by a factor of $2-3$”. The window of scales underlying hydrodynamic description is between the microscopic time scale set by temperature, $1/T \sim 1$ fm$/c$, and the typical evolution time scale set by the typical (transverse) size of the system (e.g., gold nucleus), $L \sim 5$ fm: $\tau_{\text{ev}} = L/c_s \sim 10$ fm$/c$, where we took $c_s \sim 0.5c$. The local equilibration (diffusion) scale can be estimated as $\ell_{\text{eq}} \sim \sqrt{\tau_{\text{ev}}/T} \sim 3$ fm. A reasonable hydrodynamic cell size (cutoff) could be chosen to be between c_s/T and ℓ_{eq}, i.e., $b \sim 1-2$ fm.

$$\frac{\partial}{\partial t}\breve{\psi} + \boldsymbol{\nabla} \cdot (\mathbf{flux}[\breve{\psi}] + \mathbf{noise}) = 0\,, \tag{2.30}$$

where the stochastic constitutive relations are given by $\mathbf{flux}[\breve{\psi}] + \mathbf{noise}$, with a noise term involved. In relativistic hydrodynamics, this relations read

$$\breve{T}^{\mu\nu} = T^{\mu\nu}(\breve{\varepsilon}, \breve{n}, \breve{u}) + \breve{S}^{\mu\nu}, \quad \breve{J}^{\mu} = J^{\mu}(\breve{\varepsilon}, \breve{n}, \breve{u}) + \breve{I}^{\mu}, \tag{2.31}$$

where $T^{\mu\nu}(\breve{\varepsilon}, \breve{n}, \breve{u})$ and $J^{\mu}(\breve{\varepsilon}, \breve{n}, \breve{u})$ are the same functions given by Eq. (2.19), but evaluated by the stochastic hydrodynamic variables. As a matter of fact, all expressions discussed in Sec. 2.1 shall hold in fluctuating hydrodynamics except that the constitutive relations Eq. (2.3) are replaced by the stochastic ones given by Eq. (2.31), and at the same time the hydrodynamic variables, $\breve{\varepsilon}$, $\breve{n}$ and $\breve{u}$ (instead of ε, n and u), are fluctuating. This is due to the fact that, the fluctuations between different members of the macrocanonical ensemble of the given thermal system, are sourced (driven) by random noises ($\breve{S}^{\mu\nu}$, $\breve{I}^{\mu}$). The spatial scale of UV degrees of freedom resulting in the noise are much smaller than the hydrodynamic cells, therefore the noise are assumed to be white, sampled over a Gaussian distribution with an amplitude determined by the fluctuation-dissipation theorem,

$$\begin{gathered}
\langle \breve{S}^{\mu\nu}(x) \rangle = \langle \breve{I}^{\lambda}(x) \rangle = 0\,, \quad \langle \breve{S}^{\mu\nu}(x) \breve{I}^{\lambda}(x') \rangle = 0\,, \quad \langle \breve{I}^{\mu}(x) \breve{I}^{\nu}(x') \rangle = 2\lambda \Delta^{\mu\nu} \delta^{(4)}(x - x')\,, \\
\langle \breve{S}^{\mu\nu}(x) \breve{S}^{\lambda\kappa}(x') \rangle = 2T \left[\eta \left(\Delta^{\mu\kappa}\Delta^{\nu\lambda} + \Delta^{\mu\lambda}\Delta^{\nu\kappa} \right) + \left(\zeta - \frac{2}{3}\eta \right) \Delta^{\mu\nu}\Delta^{\lambda\kappa} \right] \delta^{(4)}(x - x')\,,
\end{gathered} \tag{2.32}$$

where λ, T, η and ζ here assumed be functions of *averaged* thermodynamic variables. Generically speaking, the noise amplitude also depends on the fluctuating hydrodynamic variables, however, the feedback of the fluctuations to the noise amplitude is in higher order of gradients and thus are neglected here. The fluctuation-dissipation theorem relates systematic and random part of microscopic forces. It quantifies the general relation between the response of a given system to an external perturbation and the internal fluctuation of the system in the absence of that perturbation [103]. We will show later how our formalism reproduces this relations.

The stochastic hydrodynamic equation (cf. Eq. (2.2))

$$\partial_\mu \breve{T}^{\mu\nu} = 0\,, \quad \partial_\mu \breve{J}^\mu = 0\,, \tag{2.33}$$

together with constitutive relations Eq. (2.31), determine the evolution of the system. In principle, it is possible to numerically solve the stochastic equation with some coarse-graining, or wave vector cutoff Λ, which regularizes the infinite amplitude of the noise arising from the $\delta^{(4)}(x - x')$ term. However, as we already mentioned in the introduction, the results would depend sensitively on the cutoff Λ due to nonlinearities of hydrodynamic equations. We will come back to this problem later.

Since we have the freedom to choose an independent pair of scalar variables arbitrarily, we use this freedom to keep our calculations and resulting equations relatively simple. We find the following set of variables particularly convenient:

$$\breve{m} \equiv m(\breve{\varepsilon}, \breve{n}) \quad \text{and} \quad \breve{p} \equiv p(\breve{\varepsilon}, \breve{n})\,, \tag{2.34}$$

where the entropy per charge $m(\varepsilon, n)$ and pressure $p(\varepsilon, n)$ are defined by Eq. (2.17) and (2.11). This choice simplifies our calculations because the fluctuations of m and p are statistically independent in equilibrium and correspond to two eigenmodes of linearized ideal hydrodynamic equations. We shall denote the ensemble averages of these variables by simply removing the accent, i.e.,

$$m \equiv \langle \breve{m} \rangle\,, \quad p \equiv \langle \breve{p} \rangle\,, \quad u \equiv \langle \breve{u} \rangle\,. \tag{2.35}$$

Having defined variables m and p as average values (one-point functions) of primary variables in Eqs. (2.35) we shall now define other deterministic variables, which appear in our equations, such as ε and n as *functions* of m and p obtained via equation of state:

$$\varepsilon \equiv \varepsilon(m, p)\,, \quad n \equiv n(m, p)\,. \tag{2.36}$$

Note that, due to nonlinearities in these relationships, $\varepsilon \neq \langle \breve{\varepsilon} \rangle$ and $n \neq \langle \breve{n} \rangle$.

In order to describe the evolution of these deterministic quantities we shall perform the ensemble average on the stochastic equations. Although this eliminates the noise terms, because of the nonlinearities in the constitutive equations the averaged equations cannot be simply obtained by substituting stochastic variables by their averages. We shall describe the effect of these nonlinearities on the evolution of average values (i.e., one-point functions in Eq. (2.35)) in Sec. 2.6. These effects, to lowest order in the magnitude of the fluctuations, are given in terms of the two-point functions. Our goal in Sec. 2.5 will be to derive evolution equation for these correlators. We should also keep in mind that these two-point functions are of interest in their own right, since they describe the magnitude of the fluctuations and correlations which, in heavy-ion collisions, are measurable.

2.2.2 Linearized Hydrodynamic Equations

In this section we derive the stochastic hydrodynamic equations linearized in deviations of the stochastic variables from their average values in Eq. (2.35):

$$\breve{m} = \langle \breve{m} \rangle + \delta m \,, \quad \breve{p} = \langle \breve{p} \rangle + \delta p \,, \quad \breve{u}^\mu = \langle \breve{u}^\mu \rangle + \delta u^\mu \,. \tag{2.37}$$

To linear order, the fluctuations of $\breve{m}$ and $\breve{p}$ are simply related to fluctuations of $\breve{\varepsilon} = \varepsilon(\breve{m}, \breve{p})$ and $\breve{n} = n(\breve{m}, \breve{p})$ by a linear transformation with coefficients given by thermodynamic derivatives. We shall use the following intuitive short-hand notations for these derivatives:

$$d\varepsilon = \varepsilon_m dm + \varepsilon_p dp \,, \quad dn = n_m dm + n_p dp \tag{2.38}$$

whose exact definitions are given in Appendix B. Similarly, we find it useful to express the fluctuations of the thermodynamic function $\breve{\alpha} = \alpha(\breve{\varepsilon}, \breve{n})$ defined in Eq. (2.10) in terms of δm and δp and define corresponding coefficients:

$$d\alpha = \alpha_m dm + \alpha_p dp \,. \tag{2.39}$$

Of course, due to nonlinearities in the equation of state the relationship between fluctuations of $(\breve{\varepsilon}, \breve{n}, \breve{\alpha})$ and $(\breve{m}, \breve{p})$ is nonlinear, and we shall deal with this in Section 2.6 where we consider the second order terms in the fluctuation expansion.

Now we are ready to expand the constitutive equations to linear order in fluctuations:

$$\begin{aligned}
\breve{T}^{\mu\nu} &\approx T^{\mu\nu}(\varepsilon, n, u) + \varepsilon_m u^\mu u^\nu \delta m + (\, g^{\mu\nu} + (1+\varepsilon_p) u^\mu u^\nu)\, \delta p + w\, (u^\mu \delta u^\nu + u^\nu \delta u^\mu) \\
&\quad - \eta(\partial_\perp^\mu \delta u^\nu + \partial_\perp^\nu \delta u^\mu) - \left(\zeta - \frac{2}{3}\eta\right) \Delta^{\mu\nu} \partial \cdot \delta u + \breve{S}^{\mu\nu}, \\
\breve{J}^\mu &\approx J^\mu(\varepsilon, n, u) + n_m u^\mu \delta m + n_p u^\mu \delta p + n \delta u^\mu - \lambda \alpha_m \partial_\perp^\mu \delta m - \lambda \alpha_p \partial_\perp^\mu \delta p + \breve{I}^\mu. \qquad (2.40)
\end{aligned}$$

The equations of motion for both the background and the fluctuations are obtained by substituting Eq. (2.40) into Eq. (2.33). By definition, Eq. (2.37), one-point averages of fluctuations vanish, $\langle \delta m \rangle = \langle \delta p \rangle = \langle \delta u \rangle = 0$. Therefore, upon averaging the equations of motion, $\langle \partial_\mu \breve{T}^{\mu\nu} \rangle = \langle \partial_\mu \breve{J}^\mu \rangle = 0$, we obtain

$$\partial_\mu T^{\mu\nu}(\varepsilon, n, u) = 0\,, \quad \partial_\mu J^\mu(\varepsilon, n, u) = 0\,, \qquad (2.41)$$

At leading order in gradients, this gives us equations of ideal hydrodynamics, Eq. (2.15), which we shall use in the following calculations below. Here $a_\mu \equiv u \cdot \partial u_\mu$ is the fluid acceleration. Inserting Eqs. (2.41) back into the original stochastic equations, Eqs. (2.33), we obtain the linearized equations of motion for the fluctuations. To present these equations compactly we introduce the relaxation/diffusion coefficients

$$\gamma_\eta \equiv \frac{\eta}{w}\,, \quad \gamma_\zeta \equiv \frac{\zeta}{w}\,, \quad \gamma_\lambda = -\lambda \frac{\alpha_m w}{T n^2}\,, \quad \gamma_p = \lambda c_s^2 \alpha_p^2 T w\,. \qquad (2.42)$$

We also use the thermodynamic relation,

$$\frac{w}{n} d\left(\frac{n}{w}\right) = -\frac{1}{w}\left(1 - \frac{\alpha_p}{\alpha_m} T n\right) dp - \frac{T n}{\alpha_m w} d\alpha\,, \qquad (2.43)$$

and express our equations in terms of gradients of p and α. With the help of above expressions, we find, after some amount of algebra, the following equations of motion for our fluctuating variables:

$$\begin{aligned}
u\cdot\partial\delta m =& -\frac{1}{\alpha_m}\left(\alpha_p w a_\nu+\partial_{\perp\nu}\alpha\right)\delta u^\nu+\gamma_\lambda{\partial_\perp}^2\delta m+\frac{\alpha_p}{\alpha_m}\gamma_\lambda{\partial_\perp}^2\delta p-\frac{1}{Tn}\partial_\mu u_\nu\breve{S}^{\mu\nu}+\frac{w}{Tn^2}\partial_\mu\breve{I}^\mu,\\
u\cdot\partial\delta p =& -c_s^2\varepsilon_m\theta(1-\dot{\varepsilon_m})\delta m-\left(1+c_s^2+2\dot{c_s}\right)\theta\delta p-w\left[c_s^2\partial_{\perp\nu}-(1-c_s^2)a_\nu\right]\delta u^\nu\\
&+\frac{\alpha_m}{\alpha_p}\gamma_p{\partial_\perp}^2\delta m+\gamma_p{\partial_\perp}^2\delta p-\dot{T}\partial_\mu u_\nu\breve{S}^{\mu\nu}-c_s^2\alpha_p Tw\,\partial_\mu\breve{I}^\mu,\\
u\cdot\partial\delta u_\mu =& -\frac{\varepsilon_m a_\mu}{w}\delta m-\frac{1}{w}\left(\partial_{\perp\mu}+\frac{1+c_s^2}{c_s^2}a_\mu\right)\delta p-(-u_\mu a_\nu+\partial_{\perp\nu}u_\mu-c_s^2\Delta_{\mu\nu}\theta)\delta u^\nu\\
&+\left[\gamma_\eta\Delta_{\mu\nu}{\partial_\perp}^2+\left(\gamma_\zeta+\frac{1}{3}\gamma_\eta\right)\partial_{\perp\mu}\partial_{\perp\nu}\right]\delta u^\nu-\frac{1}{w}\Delta_{\mu\nu}\partial_\lambda\breve{S}^{\lambda\nu}.
\end{aligned}\tag{2.44}$$

We also introduced a useful notation "dot" for the operation defined as:

$$\dot{X}=\left(\frac{\partial\log X}{\partial\log s}\right)_m=\frac{s}{X}\left(\frac{\partial X}{\partial s}\right)_m\tag{2.45}$$

for a given thermodynamic quantity X. Note that since this operation is a logarithmic derivative it satisfies

$$(XY)^{\dot{}}=\dot{X}+\dot{Y}.\tag{2.46}$$

This operator appears in our equations because, to leading order (ideal hydrodynamics), $(u\cdot\partial)\,m=0$ and $(u\cdot\partial)(\log X)=-\dot{X}\theta$.

The quantity $\dot{T}$, similarly to coefficients defined in Eqs. (2.38) and (2.39), involves second order thermodynamic derivatives, i.e., second derivatives of the entropy $s(\varepsilon,n)$. Since there are only three independent second-order thermodynamic derivatives, all such quantities can be expressed in terms of three independent ones. We find that a convenient choice, making equations most transparent, at this stage of the calculation, is α_m, α_p defined in Eq. (2.39) and

$$c_s^2\equiv\left(\frac{\partial p}{\partial\varepsilon}\right)_m.\tag{2.47}$$

In the intermediate steps of the following calculations, we shall sometimes use other second derivatives also, if necessary, in order to keep our expressions as simple as we can. At the end, to express our final results, we shall switch to another set, c_s, c_p and $\dot{T}$, which contains more commonly used second-order derivatives. The quantity $\dot{T}$ is not common, but it appears naturally and makes equations more transparent and concise. It also has a reasonably simple meaning, in particular, in a neutral fluid and also in a conformal fluid, where $\dot{T} = c_s^2$ (see Tab. D.1 in Appendix D). If desired, it can be traded for a more common quantity, such as c_v, using Eq. (D.8). Converting second-order derivatives defined in Eqs. (2.38) and (2.39) into different independent sets is easily accomplished via the relations below (see also Appendix B):

$$\begin{gathered} \varepsilon_m = (Tn)^2\alpha_p = Tn\left(1-\frac{\dot{T}}{c_s^2}\right), \quad n_m = \frac{(\alpha_p Tn - 1)Tn^2}{w} = -\frac{\dot{T}Tn^2}{c_s^2 w}, \\ \varepsilon_p = c_s^{-2}, \quad n_p = \frac{n}{c_s^2 w}, \quad \alpha_m = -\frac{w}{c_p T}. \end{gathered} \tag{2.48}$$

The quantities $\dot{c}_s$ and $\dot{\varepsilon}_m$ involve third-order thermodynamic derivatives (i.e., third derivatives of a $s(\varepsilon, n)$).

Another commonly known quantity we shall find useful in what follows is the heat conductivity coefficient

$$\kappa \equiv \left(\frac{w}{Tn}\right)^2 \lambda \tag{2.49}$$

in terms of which the diffusion coefficient is simply

$$\gamma_\lambda = \frac{\kappa}{c_p}. \tag{2.50}$$

We introduce a collective notation for the fluctuating modes,

$$\phi_A \equiv (Tn\delta m, \delta p/c_s, w\delta u_\mu), \tag{2.51}$$

where normalization of the modes is chosen to make resulting matrix equations simpler and more symmetric. Indeed, one can introduce the heat energy density defined as [104]

$$\breve{q}_h = \breve{\varepsilon} - \frac{w}{n}\breve{n} \tag{2.52}$$

such that

$$\delta q_h = \breve{q}_h - q_h = Tn\delta m \tag{2.53}$$

where $q_h \equiv \langle \breve{q}_h \rangle = -p$ (but $\breve{q}_h \neq \breve{p} = \breve{\varepsilon} - \breve{w}$ unless $\delta(w/n) = 0$). Eq. (2.52) and (2.52) provide the physical meaning of the fluctuating mode ϕ_m, which is less obvious than those of ϕ_p and ϕ_μ. With Eq. (2.51) we can now write the above equations for the linearized fluctuations (Eq. (2.44)) in a compact matrix form,

$$u \cdot \partial \phi_A = -\big(\mathbb{L} + \mathbb{D} + \mathbb{K}\big)_{AB} \phi^B - \xi_A \,, \tag{2.54}$$

where $\mathbb{L}$, $\mathbb{D}$, and $\mathbb{K}$ are 6×6 matrix operators. The operators $\mathbb{L}$ and $\mathbb{D}$ are the ideal and dissipative terms, respectively, $\mathbb{K}$ contains the corrections due to the first-order gradients of background flow, and six-vector ξ_A denotes the random noise. Explicitly

$$\begin{aligned}
\mathbb{L} &\equiv \begin{pmatrix} 0 & 0 & 0 \\ 0 & 0 & c_s \partial_{\perp\nu} \\ 0 & c_s \partial_{\perp\mu} & 0 \end{pmatrix}, \\
\mathbb{D} &\equiv \begin{pmatrix} -\gamma_\lambda {\partial_\perp}^2 & (c_s \alpha_p T n)^{-1} \gamma_p {\partial_\perp}^2 & 0 \\ c_s \alpha_p T n \gamma_\lambda {\partial_\perp}^2 & -\gamma_p {\partial_\perp}^2 & 0 \\ 0 & 0 & -\gamma_\eta \Delta_{\mu\nu} {\partial_\perp}^2 - (\gamma_\zeta + \tfrac{1}{3}\gamma_\eta) \partial_{\perp\mu} \partial_{\perp\nu} \end{pmatrix}, \\
\mathbb{K} &\equiv \begin{pmatrix} (1 + \dot{T})\theta & 0 & \frac{Tn}{\alpha_m} \left(\alpha_p a_\nu + \frac{1}{w} \partial_{\perp\nu} \alpha \right) \\ c_s \alpha_p (1 - \dot{\varepsilon_m}) T n \theta & (1 + c_s^2 + \dot{c_s})\theta & \left(2 - \frac{(\alpha_p T n)^2}{\alpha_m} \right) c_s a_\nu - \frac{c_s \alpha_p T^2 n^2}{\alpha_m w} \partial_{\perp\nu} \alpha \\ \alpha_p T n a_\mu & \frac{1 + c_s^2}{c_s} a_\mu + \partial_{\perp\mu} c_s & -u_\mu a_\nu + \partial_{\perp\nu} u_\mu + \Delta_{\mu\nu} \theta \end{pmatrix}, \\
\xi &\equiv \left(-\frac{w}{n} \partial_\lambda \breve{I}^\lambda ,\, c_s \alpha_p T w \partial_\lambda \breve{I}^\lambda ,\, \Delta_{\mu\kappa} \partial_\lambda \breve{S}^{\lambda\kappa} \right).
\end{aligned} \tag{2.55}$$

Equation (2.54) for linearized fluctuations provides the foundation for the fluctuation evolution equations for the two-point correlation functions, derived in the next section. This is the building block for the evolution equation of the higher-point functions.

2.3 Deterministic Fluctuating Hydrodynamics

2.3.1 Nonlinear Fluctuations

The physical effects of fluctuations on hydrodynamic flow manifest themselves through two-point functions and also high-point functions. This is because, by definition, the first order fluctuations average to zero (i.e. $\langle \phi_A(x) \rangle = 0$ via Eq. (2.37)) and the leading order corrections to $\langle \breve{T}^{\mu\nu} \rangle$ and $\langle \breve{J}^{\mu} \rangle$ come from the second order terms in the fluctuation expansion (i.e. the two-point functions) whose time evolution equation we derive in this section. Our strategy is to use equations of motion for linearized fluctuations, Eq. (2.54), to derive an evolution equation for the "equal-time" two-point correlation function of fluctuations, obtained by averaging over the statistical ensemble generated by the stochastic noises. How these two-point functions modify the hydrodynamic flow, in other words the feedback of fluctuations on background flow, will be discussed in Section 2.6.

In addition to the one-point functions of fluctuations, $\phi_A = \breve{\psi}_A - \psi_A$, the two-point correlation functions (correlators) are defined by

$$G_{AB}(x, y) \equiv \langle \phi_A(x^+) \phi_B(x^-) \rangle \,, \tag{2.56}$$

which are ensemble averaged products at two spacetime points

$$x^{\pm} = x \pm y/2 \,, \tag{2.57}$$

where $x = (x^+ + x^-)/2$ is the midpoint position and $y = x^+ - x^-$ is the separation. In general, the correlator G_{AB} could be evaluated with fluctuations not only at different space points, but also different times. However, solving equations with such non-equal-time correlator is more challenging due to the causality issue. Thus it is more convenient to study the equal-time correlator first. The definition of equal-time correlator, e.g., $G_{AB}(x, y)$, depends on the frame of reference. In the laboratory frame, all observers agree with a unique time t, which is globally defined, and the correlator read off as

$$G_{AB}(x, \boldsymbol{y}) \equiv \langle \phi_A(t, \boldsymbol{x}^+) \phi_B(t, \boldsymbol{x}^-) \rangle \,, \tag{2.58}$$

with two three-dimensional space points

$$\boldsymbol{x}^{\pm} = \boldsymbol{x} \pm \boldsymbol{y}/2\,. \tag{2.59}$$

However, in the case of a generic *relativistic* hydrodynamic flow, the concept of "equal time" is no longer obvious. In such relativistic flow, the most natural choice of the frame of reference, is the comoving frame, i.e., the rest frame of the fluid that is locally different in different spacetime points. There is no well-defined global unique time as in the laboratory frame. We will discuss this issue in more detail later.

However, The concepts of "equal-time" and "spatial" y coordinates we invoke when defining $G_{AB}(x, y)$ and its Wigner transformation in the above discussion become nontrivial in a general background of relativistic flow. Both concepts require choosing a frame of reference. The most natural choice – the local rest frame (i.e., comoving frame) of the fluid, characterized by the (average) fluid velocity $u^{\mu}(x)$ – varies point to point with x. The change of the frame from point to point is responsible for changing the values of various vector components of hydrodynamic fluctuations ϕ_A, such as δu_{μ}, entering in the definition of G_{AB} in Eq. (2.56). This variation is purely kinematic (Lorentz boost) and has nothing to do with the local dynamics of fluctuations that we are interested in. In Sec. 2.4 we will define a measure of fluctuations and a measure of its changes with space and time to be independent of such mundane kinematic effects, by introducing the notions of "confluent correlator" and "confluent derivative".

In a static homogeneous equilibrium state of the fluid, the correlator is translationally invariant, i.e., depends only on the separation y and not on the midpoint position x. Furthermore, because equilibrium correlation length is shorter than the coarse grained resolution of hydrodynamics, the equilibrium equal-time correlation function is essentially a delta function of the separation vector y with the magnitude determined by the the well-known functions of average thermodynamic variables (e.g., ε and n).

Furthermore, not only the local thermodynamic conditions, and thus *equilibrium* magnitude of fluctuations, slowly vary in spacetime, but also the fluctuations themselves are driven *out* of equilibrium. Therefore, not only the fluctuation correlator depends slowly on x, but it also acquires nontrivial y dependence, beyond the equilibrium delta function. It is crucial that the scale of that y dependence is short compared to the scale of the dependence on x.

The estimate of the y-dependence scale can be made by observing that the equilibration of fluctuations of hydrodynamic variables is a diffusive process (since the variables obey conservation equations). This means that the scale of equilibration ℓ_* is the diffusion length during time interval characteristic of the evolution. For the reciprocal quantities such as fluctuation wavenumber $q_* \equiv 1/\ell_*$ and the frequency $c_s k$ of the sound, one obtains $\gamma q_*^2 \sim c_s k$ and thus $q_* = \sqrt{c_s k/\gamma} \gg k$. In other words, $\ell_* \ll L \equiv 1/k$. This separation of scales of y and x dependence of the correlation function, or between characteristic wavenumbers q of the fluctuations and k of the background will be used to systematically organize our calculations and results in the form of an expansion in $k/q \ll 1$ as well as $k\ell_{\text{mic}} \ll 1$. Note that, for the characteristic wavenumbers of the fluctuations and the background, the ratio $k/q \sim (k\ell_{\text{mic}})^{1/2}$. In other words, this expansion is controlled by a power of the same small parameter as the hydrodynamic gradient expansion itself.

With this separation of scales in mind, it is convenient to work with the Wigner transform of $G_{AB}(x, y)$, that is essentially the Fourier transform with respect to (spatial components of) y, which we shall label as $W_{AB}(x, q)$. Since q corresponds to the wave vector of fluctuating modes that contribute to G_{AB}, it is similar in concept to the momentum of a particle in quantum mechanics. In this quantum mechanical analogy, the Wigner transform would be the (matrix valued) phase-space distribution of the fluctuation modes or a density matrix in phase space, (x, q), in an effective kinetic theory of fluctuation quanta. The evolution equation of $W_{AB}(x, q)$, which is derived in this section, closely resembles a Boltzmann-type kinetic equation for the fluctuation degrees of freedom that are, in the case of hydrodynamics, phonons. In this thesis we present a set of equations for relativistic hydrodynamics *with a conserved charge*, which contains additional nontrivial features compared to the results for a neutral fluid presented in Ref. [1]. Some of these features, such as the existence of the slow scalar mode, play an important role in the critical dynamics near the QCD critical point which we discuss in Section 3.2.

2.3.2 Nonlinear Feedback

Hydrodynamics describes the evolution of the average values, or one-point functions, of hydrodynamic variables, such as ε, n, u, or more precisely, by our choice, m, p, u. The equations governing this evolution are obtained by averaging conservation equations (2.33). However, the evolution of the one-point functions is affected by the feedback from the higher-point functions. This is because energy momentum-tensor and charge current are *nonlinear* functions of the fluctuating variables, $\breve{m}$, $\breve{p}$ and $\breve{u}$, as follows from the constitutive relations, Eq. (2.3), as well as the equation of state. In order to calculate the contribution of the two-point functions, we begin by expanding the energy-momentum tensor $\langle T^{\mu\nu}\rangle$ and the charge current $\langle J^{\mu}\rangle$ given in Eq. (2.3), up to quadratic order in the fluctuating variables ϕ_A. Upon averaging over the ensemble, the linear terms in ϕ_A vanish by definition, $\langle\phi_A\rangle = 0$, and only the two-point function contributions, expressed in terms of

$$\langle\phi_A(x)\phi_B(x)\rangle = G_{AB}(x, y=0) \equiv G_{AB}(x)\,, \tag{2.60}$$

remain. Here $A \in (m, p, 0, 1, 2, 3)$. The mixed index $A \in (m, p, 0, 1, 2, 3)$ is raised and lowered by the "metric", $\mathrm{diag}(1, 1, -1, 1, 1, 1)$. However the object u_A is not a vector, rather an array that conveniently combines scalar and vector modes, expressed in the collective notation as

$$u_A \equiv (0, 0, u_\mu)\,. \tag{2.61}$$

Expanding the (bare) equation of state up to second order in fluctuations leads to

$$\begin{aligned}\varepsilon(\breve{m},\breve{p}) &= \varepsilon(m,p) + \varepsilon_m\delta m + \varepsilon_p\delta p + \frac{1}{2}\varepsilon_{mm}(\delta m)^2 + \varepsilon_{mp}\delta m\delta p + \frac{1}{2}\varepsilon_{pp}(\delta p)^2 + \dots\,,\\ n(\breve{m},\breve{p}) &= n(m,p) + n_m\delta m + n_p\delta p + \frac{1}{2}n_{mm}(\delta m)^2 + n_{mp}\delta m\delta p + \frac{1}{2}n_{pp}(\delta p)^2 + \dots\,,\end{aligned} \tag{2.62}$$

where the coefficients of linear terms were already defined in Eq. (2.38). The coefficients of bilinear terms are third order thermodynamic derivatives and are defined similarly (see Appendix B, Eqs. (B.10)). Similarly to expressions for second-order thermodynamic derivatives in terms of three independent ones c_s, c_p and $\dot{T}$ in Eq. (2.48), the third order thermodynamic derivatives can be also expressed in terms of two independent third order derivatives $\dot{c}_p$ and $\dot{c}_s$ as[4]

$$\begin{aligned} \varepsilon_{mm} &= -\frac{Tn^2}{c_s^2 c_p}\left(1-\dot{c}_p+\dot{T}-c_s^2+\frac{2c_pT\dot{T}}{w}\left(1-\frac{\dot{T}}{c_s^2}\right)\right), \quad \varepsilon_{pp}=-\frac{2\dot{c}_s}{c_s^4 w}, \\ n_{mm} &= -\frac{Tn^3}{c_s^2 c_p w}\left(1-\dot{c}_p+\dot{T}-\frac{2c_pT\dot{T}}{c_s^2 w}\right), \quad n_{pp}=-\frac{\left(c_s^2+2\dot{c}_s\right)n}{c_s^4 w^2}. \end{aligned} \tag{2.63}$$

As a result, we obtain the following expansion for $\langle T^{\mu\nu}\rangle$ and $\langle J^\mu\rangle$:

$$\begin{aligned} \langle \breve{T}^{\mu\nu}(x)\rangle = {}& T^{\mu\nu}(\varepsilon,n,u)+\frac{\varepsilon_{mm}}{2T^2n^2}u^\mu u^\nu G_{mm}(x)+\frac{\varepsilon_{pp}c_s^2}{2}u^\mu u^\nu G_{pp}(x)+\frac{1}{w}G^{\mu\nu}(x) \\ &+\frac{\varepsilon_m}{wTn}\left(G^{m\mu}(x)u^\nu+G^{m\nu}(x)u^\mu\right)+\frac{c_s(1+\varepsilon_p)}{w}\left(G^{p\mu}(x)u^\nu+G^{p\nu}(x)u^\mu\right), \end{aligned} \tag{2.64a}$$

$$\langle \breve{J}^{\mu}(x)\rangle = J^\mu(\varepsilon,n,u)+\frac{n_{mm}u^\mu}{2T^2n^2}G_{mm}(x)+\frac{c_s^2 n_{pp}u^\mu}{2}G_{pp}(x)+\frac{n_m}{wTn}G^{m\mu}(x)+\frac{c_s n_p}{w}G^{p\mu}. \tag{2.64b}$$

where we neglected the fluctuations of the viscous part $\Pi^{\mu\nu}$ and ν^μ, which are parametrically smaller than the terms kept in the above expansion[5]. It should be noted that not all six variables ϕ_A are independent since, due to normalization $\breve{u}\cdot\breve{u}=-1$, we have a constraint $u^A\phi_A=0$. Correspondingly,

$$u^A(x^+)G_{AB}(x,y)=G_{AB}(x,y)u^B(x^-)=0\,. \tag{2.65}$$

These constraints follow from the orthogonality $u^\mu(x^\pm)\delta u_\mu(x^\pm)=0$ and relate different vector components of $G_{AB}(x,y)$ in a y-dependent way.

The mixed term, $G_{mp}(x)\sim\langle\delta m\delta p\rangle$, is dropped because it is a rapidly oscillating component of G whose contribution vanishes after time averaging, as explained in Sec. 2.5.2.

---

[4] Note that there are four independent third order derivatives (four independent third order derivatives of entropy), but only two are needed in Eqs. (2.63). We do not need expressions for ε_{mp} and n_{mp} because they will drop out upon time averaging, as described below.

[5] We rely on $\gamma q\sim q/T\ll 1$, according to Eq. (2.29), where q is the typical wave vector of the fluctuations.

Furthermore, we neglect the fluctuations of the viscous part $\Pi^{\mu\nu}$ relying on the scale hierarchy $\gamma q \sim q/T \ll 1$. The two point functions $G_{AB}(x)$ given by solutions of fluctuation kinetic equations are nontrivial functionals of the background gradients and contain both local and nonlocal terms which are associated with renormalization and long-time tails respectively.

2.3.3 A First Look of the Dynamics of Feedback

We start with the evolution equation for the two-point function $G_{AB}(x,y)$ defined in Eq. (2.56), and choose y to be spatial in the frame $u(x)$. The time evolution of $G_{AB}(x,y)$ is obtained by

$$\begin{aligned}
&u(x)\cdot\partial\, G_{AB}(x,y) \equiv \partial_t\langle\phi_A(x^+)\phi_B(x^-)\rangle\\
=&\lim_{\delta t\to 0}\frac{1}{\delta t}\langle\phi_A(x^+ + \delta t)\phi_B(x^- + \delta t) - \phi_A(x^+)\phi_B(x^-)\rangle\\
=&\lim_{\delta t\to 0}\frac{1}{\delta t}\langle(\partial_t\phi_A(x^+))\phi_B(x^-)\delta t + \phi_A(x^+)(\partial_t\phi_B(x^-))\delta t + (\partial_t\phi_A(x^+))(\partial_t\phi_B(x^-))\delta t^2\rangle\\
=&\langle(\partial_t\phi_A(x^+))\phi_B(x^-)\rangle + \langle\phi_A(x^+)(\partial_t\phi_B(x^-))\rangle\\
&+\lim_{\delta t\to 0}\frac{1}{\delta t}\int_{u\cdot x^+}^{u\cdot x^+ + \delta t} u\cdot dx' \int_{u\cdot x^-}^{u\cdot x^- + \delta t} u\cdot dx''\langle\xi_A(x')\xi_B(x'')\rangle,
\end{aligned}\tag{2.66}$$

where we introduce $\delta t \equiv u(x)\cdot\delta x$ and $\partial_t \equiv u(x)\cdot\frac{\partial}{\partial x}$ for a moment to shorten the expression. We also adopt a rule that the derivative operator, ∂, always acts on the *first* argument of the function, such as x in $G(x,y)$, or $x^\pm$ in $\phi(x^\pm)$. Derivative with respect to the second argument, if there is any, will be labeled explicitly. We have used $\langle\xi(x')\phi(x'')\rangle = 0$ since the noise and fluctuation are uncorrelated at the same time. Next, we convert the time derivatives in the RHS of (2.66) into spatial derivatives. In order to do so we have to expand $u(x) = u(x^\pm) \mp \frac{1}{2}y\cdot\partial u(x)$ and use the evolution equation for the one point function, Eq. (2.54). To perform the resulting averaging in the RHS of Eq. (2.66) we need to know the average of the two-point function of the noise, which can be calculated using the definition in Eq. (2.55) and Eq. (2.32):

$$\langle\xi_A(x')\xi_B(x'')\rangle = 2\mathbb{Q}_{AB}\delta^{(4)}(x'-x'')\,,\tag{2.67}$$

where

$$\mathbb{Q}=Tw\begin{pmatrix}\alpha_m^{-1}\gamma_\lambda{\partial_\perp}^2 & (c_s\alpha_pTn)^{-1}\gamma_p{\partial_\perp}^2 & 0\\ (c_s\alpha_pTn)^{-1}\gamma_p{\partial_\perp}^2 & -\gamma_p{\partial_\perp}^2 & 0\\ 0 & 0 & -\left(\gamma_\eta\Delta_{\mu\nu}{\partial_\perp}^2+\left(\gamma_\zeta+\frac{1}{3}\gamma_\eta\right)\partial_{\perp\mu}\partial_{\perp\nu}\right)\end{pmatrix}. \tag{2.68}$$

Proceeding from Eq. (2.66) along these steps we arrive at

$$\begin{aligned}u\cdot\partial G_{AB}(x,y)=&-(\mathbb{L}^{(y)}+\frac{1}{2}\mathbb{L}+\mathbb{D}^{(y)}+\mathbb{K}+\mathbb{Y})_{AC}\,G^C{}_B(x,y)\\&-(-\mathbb{L}^{(y)}+\frac{1}{2}\mathbb{L}+\mathbb{D}^{(y)}+\mathbb{K}+\mathbb{Y})_{BC}G_A{}^C(x,y)\\&+2\mathbb{Q}^{(y)}_{AB}\delta^3(y_\perp)\,,\end{aligned} \tag{2.69}$$

where the superscript (y) on an operator indicates that the derivatives within that operator act on y, the second argument of $G_{AB}(x,y)$. For example,

$$\mathbb{L}^{(y)}\equiv\begin{pmatrix}0&0&0\\0&0&c_s(x)\partial^{(y)}_{\perp\nu}\\0&c_s(x)\partial^{(y)}_{\perp\mu}&0\end{pmatrix}. \tag{2.70}$$

The matrix $\mathbb{Y}$,

$$\mathbb{Y}\equiv\begin{pmatrix}\Delta_{\lambda\kappa}&0&0\\0&(1-c_s^2)\Delta_{\lambda\kappa}&c_su_\nu\Delta_{\lambda\kappa}\\0&c_su_\mu\Delta_{\lambda\kappa}&\Delta_{\mu\nu}\Delta_{\lambda\kappa}-c_s^2\Delta_{\mu\lambda}\Delta_{\nu\kappa}\end{pmatrix}\frac{1}{2}y\cdot\partial u^\lambda\partial_\perp^{(y)\kappa}+\frac{1}{2c_s}y\cdot\partial c_s\mathbb{L}^{(y)}, \tag{2.71}$$

results from the y-dependence in $u(x^\pm)$ and $c_s(x^\pm)$. Note that in deriving Eq. (2.69), we neglected higher order terms in y, based on the scale separation between background wavenumber k and fluctuation wavenumber q: $(\partial u)y\sim(\partial c_s)y\sim k/q\ll 1$.

Although we obtained Eq. (2.69) directly from the linearized equations by a brute-forth calculation, it is somewhat ugly, since we are considering each fluctuation separately as if they didn't know each other. However, the fluctuations are evolving on top of the fluid, one might then ask, is it possible to manipulate the equation adjusted by the fluid, such that the equation has a more crispy formulation? The answer is yes, and the way of manipulating the dynamic equations for multi-point functions adjusted by the fluid is called *confluentization*. As we shall soon see in the next section, the process of confluentization is more subtle than it might appear at first sight. However, after such a sophisticated adjustment, we would finally be able to arrive at a beautiful result.

2.4 Confluentization in Relativistic Flow

In this section we introduce several ingredients needed to translate equation (2.69) into an equation for the appropriately defined Wigner function. In Eq. (2.56) we defined the equal-time correlator of hydrodynamic variables as a function of the mid-point x and the separation vector y as $G_{AB}(x, y) \equiv \langle \phi_A(x + y/2)\, \phi_B(x - y/2)\rangle$, where the domain of y is the three-dimensional plane orthogonal to $u(x)$, i.e., y is purely spatial in the local rest frame at x. We would like to define a partial derivative of this object with respect to x. When taking a partial derivative it is important to specify what quantities are held fixed and what quantities change with x and how. There are two elements of the correlator $G_{AB}(x, y)$ which make this a nontrivial question: the indices AB and the variable y.

First, we would like the derivative to express how components AB of G_{AB} are changing with respect to the local rest frame $u(x)$, rather than with respect to an arbitrary fixed laboratory frame. Since $u(x)$ itself changes from point to point with the flow of the fluid we shall introduce a derivative which accounts for that change.

Second, and this is crucial for *relativistic* hydrodynamics, we want an x-derivative which keeps y “fixed”. But in what frame should the components of y be fixed? If we keep components of y fixed in an arbitrary fixed laboratory frame, the variation of x will, in general, violate the condition $u(x) \cdot y = 0$, i.e., the correlator will not remain an *equal-time* correlator. Therefore, as we vary x, we need to keep components of y in the local rest frame fixed as the frame itself, $u(x)$, changes with x.

We shall consider the two above elements separately and then combine them in the derivative which takes into account the fluid flow as described above. We shall refer to such a derivative as *confluent* in order to distinguish it from an ordinary covariant derivative in differential geometry of which it is reminiscent. In particular, the confluent derivative is similar to covariant derivative in the sense that its action depends on the type of the object it acts upon.

The key to defining these new concepts is a parallel transport or, equivalently a connection, that takes care of the change of $u(x)$ between two points, say, x and $x + \Delta x$.

2.4.1 Confluent Derivative of One-point Function

Let us first consider the action of the confluent derivative on the hydrodynamic fluctuation field $\phi_A(x)$. These variables transform covariantly under Lorentz boosts (six components of ϕ_A contain two scalars and a four-vector according to Eq. (2.51)). It is natural to define a derivative which measures the changes of the hydrodynamic variables with respect to the local rest frame defined by flow velocity u. I.e., we are not interested in the changes between $\phi_A(x + \Delta x)$ and $\phi_A(x)$ which are simply due to the difference in the local velocity u, i.e., induced by boost transformation from frame $u(x)$ to $u(x + \Delta x)$. In other words, we are interested in the "internal" state of the variables, not affected by frame choice. Let us introduce the boost which maps $u(x + \Delta x)$ to $u(x)$ by $\Lambda(\Delta x)$: [6]

$$\Lambda(\Delta x) u(x + \Delta x) = u(x) \, . \tag{2.72}$$

In principle, this boost is not unique. Nonetheless, we propose to use the most natural choice – a pure boost without a spatial rotation in the local rest frame of $u(x)$. Note that the boost in Eq. (2.72) is defined for arbitrary Δx. The explicit form of the infinitesimal boost defined by Eq. (2.72) is given by

$$\Lambda_\mu^{\ \nu}(\Delta x) = \delta_\mu^{\ \nu} + \delta\Lambda_\mu^{\ \nu}(\Delta x) = \delta_\mu^{\ \nu} - u_\mu \Delta u^\nu + u^\nu \Delta u_\mu \, , \tag{2.73}$$

---

[6] Strictly speaking Λ is also a function of x and should be denoted by $\Lambda(\Delta x, x)$. For notational simplicity we drop the x argument.

where

$$\Delta u^{\mu} \equiv u^{\mu}(x+\Delta x) - u^{\mu}(x) = \Delta x^{\lambda}(\partial_{\lambda} u^{\mu})\,. \tag{2.74}$$

The confluent derivative (denoted by $^{-}$) we described could be constructed by boosting the variable $\phi(x+\Delta x)$ in the same way as u in Eq. (2.72) before comparing to $\phi(x)$, i.e.,[7]

$$\Delta x \cdot \bar{\nabla}\phi(x) = \Lambda(\Delta x)\phi(x+\Delta x) - \phi(x). \tag{2.75}$$

This boost is depicted by Fig. 2.2. With respect to such a derivative, by design, the flow vector field $u(x)$ is "constant":

$$\bar{\nabla}_{\mu} u_{\nu} = 0\,, \tag{2.76}$$

according to Eqs. (2.72) and (2.75).

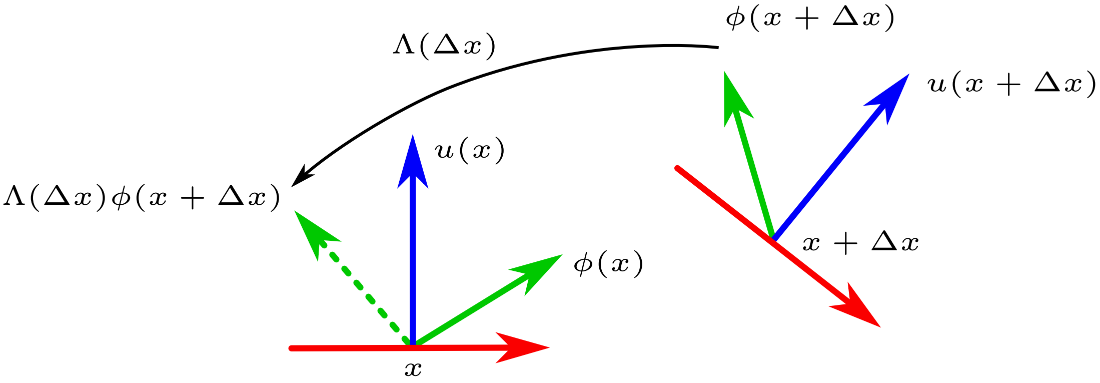

Figure 2.2: Schematic illustration of the confluent derivative for a Lorentz vector (one-point fluctuation ϕ_{μ}). In order to compare the "internal" difference of $\phi_{\mu}(x+\Delta x)$ and $\phi_{\mu}(x)$ at different spacetime points, we boost $\phi_{\mu}(x+\Delta x)$ (solid green arrow) from the local rest frame at $x+\Delta x$ to the local rest frame at x, the frame defines $\phi_{\mu}(x)$.

---

[7] Fermi-Walker transport along a world-line is constructed in a similar way, in which case Δx is displacement along the particle's trajectory. In our case Δx can point in any direction, not necessarily along u.

Eq. (2.75) defines the action of the confluent derivative on a Lorentz-covariant hydrodynamic field $\phi_A(x)$. Substitute Eq. (2.73) into Eq. (2.75), we obtain

$$(\Lambda(\Delta x)\phi)_\mu = \phi_\mu - u_\mu(\Delta u \cdot \phi) + \Delta u_\mu (u \cdot \phi)\,, \tag{2.77}$$

and the explicit expression for the derivative acting on a Lorentz vector reads

$$\bar{\nabla}_\lambda \phi_\mu = \partial_\lambda \phi_\mu - \bar{\omega}^{\nu}_{\lambda\mu}\phi_\nu\,, \tag{2.78}$$

where the connection associated with the boost created by flow gradients is given by

$$\bar{\omega}^{\nu}_{\lambda\mu} = u_\mu \partial_\lambda u^\nu - u^\nu \partial_\lambda u_\mu\,. \tag{2.79}$$

Note that this connection is antisymmetric with respect to $\mu\nu$, reminiscent of a spin connection. In a sense, it is a spin connection for the tangent space spanned by hydrodynamic variables ϕ_A at point x. In that sense confluent derivative is the covariant derivative for the connection given by flow gradients in Eq. (2.79). To unify equations we can extend the range of indices to accommodate the full six-dimensional space of variables and write

$$\bar{\nabla}_\lambda \phi_A = \partial_\lambda \phi_A - \bar{\omega}^{B}_{\lambda A}\phi_B\,, \tag{2.80}$$

including the case when A or B is m or p. The corresponding connection is, of course, zero, since $\phi_m = Tn\delta m$ and $\phi_p = \delta p/c_s$ are scalars.

2.4.2 Confluent Derivative of Equal-time Two-point Function

We now introduce the second element of the confluent derivative which comes into play when we consider its action on a *two-point* function. The most important issue for us here is the definition of the "equal time" in the equal-time correlator. To focus on it, we shall consider the action of the confluent derivative on a Lorentz scalar component of G (e.g, G_{mm} and G_{pp}). Since G is the same in any frame, the connection term in Eq. (2.78) vanishes, thus we can focus on understanding how to define a partial x derivative at "fixed" y. This is not straightforward, as the following expression illustrates:

$$\Delta x \cdot \partial G(x,y) = G(x+\Delta x, y) - G(x,y)\,. \tag{2.81}$$

In $G(x+\Delta x, y)$ the orthogonality condition $u(x+\Delta x)\cdot y = 0$ is, in general, false, given

$$u(x)\cdot y = 0 \tag{2.82}$$

is true: vector y spatial in the frame $u(x)$ is not spatial in $u(x+\Delta x)$ (see Fig. 2.3). To preserve the relationship between u and y we need to transform vector y by the same boost that takes $u(x)$ to $u(x+\Delta x)$, i.e., $\Lambda^{-1}(\Delta x)$, according to Eq. (2.72). We can then define a derivative at "fixed" y as

$$\Delta x\cdot\bar{\nabla}G(x,y) = G(x+\Delta x, \Lambda(\Delta x)^{-1}y) - G(x,y)\,. \tag{2.83}$$

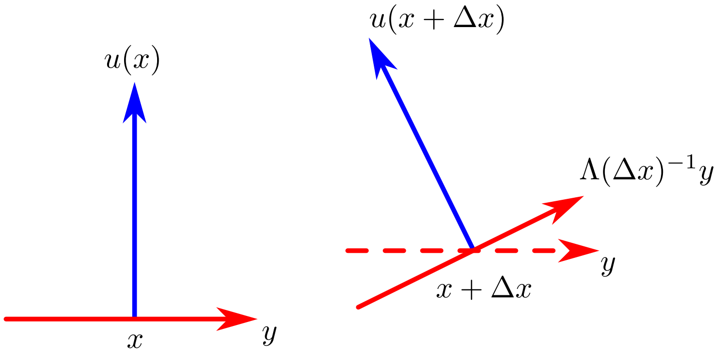

Figure 2.3: Schematic illustration of the Lorentz boost (represented here by an ordinary rotation) of point separation vector y needed to keep the point separation purely spatial in the local rest frame at a new point Δx, given $u(x+\Delta x) = \Lambda(\Delta x)^{-1}u(x)$.

In order to write confluent derivative in Eq. (2.83) in terms of partial derivatives with respect to x we must specify what variables are held fixed while we vary x. We cannot keep components of y^μ in a given laboratory frame fixed, since y must actually change (by boost, as in Fig. 2.3). We could keep components of y^a, $a = 1,2,3$, in the fluid's local rest frame fixed. To implement such a derivative we must introduce a basis triad $e_a(x)$ ($a = 1,2,3$) of four-vectors orthogonal to $u(x)$ at each point. The choice of the three fields $e_a(x)$ is arbitrary and different choices are related by local SO(3) rotations, subject to $e_a(x)\cdot u(x) = 0$. A convenient explicit example is given in Appendix C.1.

It is important to note that the vector $\Lambda^{-1}(\Delta)y$ in the definition of the confluent derivative in Eq. (2.83) is independent of the choice of the local triad e_a. This means that, in general, one should expect that the components of $\Lambda^{-1}(\Delta)y$ in local frame are different from those of y due to a possible rotation of the local basis triad between points x and $x+\Delta x$. In other words, not only $e_a(x+\Delta x) \neq e_a(x)$ but, in general, also $(\Lambda(\Delta x)e)_a(x+\Delta x) \neq e_a(x)$, in contrast to Eq. (2.72) (see Appendix C.1). Therefore, partial derivative with respect to x at y^a fixed will not alone capture the derivative defined in Eq. (2.83). We need to subtract the effect of the change of the basis triad $e_a(x)$. This can be achieved by introducing additional connection, $\mathring{\omega}^a_{\mu b}$, in the tangent space so that e^μ_a is "confluently constant":

$$\bar{\nabla}_\lambda e^\mu_a \equiv \partial_\lambda e^\mu_a + \bar{\omega}^\mu_{\lambda\nu} e^\nu_a - \mathring{\omega}^c_{\lambda a} e^\mu_c = 0\,, \tag{2.84}$$

The second term in Eq. (2.84) accounts for the boost of e_a as the one in Eq. (2.78) and illustrated in Fig. 2.3, while the last term accounts for the additional rotation in the tangent space.

Equation (2.84) can be solved for the connection $\mathring{\omega}^a_{\lambda b}$ by multiplying by dual basis vector e^b_μ such that $e_c \cdot e^b = \delta^b_c$:

$$\mathring{\omega}^b_{\lambda a} = e^b_\mu \partial_\lambda e^\mu_a\,, \tag{2.85}$$

where we used the definition of $\bar{\omega}$ connection in Eq. (2.79) and $u \cdot e^b = u \cdot e_a = 0$. In Appendix C.1 we provide a simple explicit example of the local triad e_a with the corresponding connection.

Now we can express the confluent derivative in Eq. (2.83) in terms of the partial x-derivative at y^a fixed:

$$\bar{\nabla}_\mu G = \partial_\mu G - \mathring{\omega}^b_{\mu a}\, y^a \frac{\partial}{\partial y^b} G\,. \tag{2.86}$$

In other words, and this is important for applications, the partial x-derivative $\partial_\mu G$ in Eq. (2.86) is taken at fixed y^a, i.e., $\partial_\mu y^a = 0$, and the boost needed to keep $y = e_a(x)y^a$ orthogonal to $u(x)$ is taken care of by e_a. The last term in Eq. (2.84) subtracts the effect of possible additional rotation of the arbitrarily chosen local triad e_a. [8]

2.4.3 Confluent Correlator and Wigner Function

In Sec. 2.4.2 we have defined the confluent derivative of a scaler two-point correlator. Now let's turn to a general case: define confluent derivative of a *tensor* so that the derivative obeys the Leibniz product rule. This is straightforward for a product like $\phi_A(x)\phi_B(x)$, but is not so for the correlator G_{AB}, because it contains a product of two fields in *different* spacetime points x^+ and x^-. More specifically, the "raw" definition of the two-point correlator G_{AB}, Eq. (2.56), satisfies the projection constraints Eq. (2.65). It prevents us from cleanly separating x and y dependence and performing Wigner transform. In order to address this issue we shall introduce confluent two-point correlator $\bar{G}_{AB}$ which will allow us to define a confluent derivative obeying the Leibniz rule in a straightforward way.

To achieve this we shall follow the same logic that led us to Eq. (2.75) and take into account the change of the flow velocity between the two points x^+ and x^-. Therefore, we shall define a "confluent correlator" by boosting both variables $\phi_A(x+y/2)$ and $\phi_B(x-y/2)$ into the rest frame at the midpoint, x, i.e,

$$\bar{G}_{AB}(x,y) = \Lambda_A{}^C(y/2)\,\Lambda_B{}^D(-y/2)\,G_{CD}(x,y)\,, \tag{2.87}$$

where $\Lambda_A{}^C(\Delta x) = \Lambda_\mu{}^\nu(\Delta x)$ when $AC = \mu\nu$, and an identity transformation otherwise. A schematic illustration of this quantity is provided by Fig. 2.4.

Substituting Eq. (2.73) and (2.74) into Eq. (2.87), we obtain a more specific expression

$$\bar{G}_{AB}(x,y) = G_{AB}(x,y) - \frac{1}{2}u_A y\cdot\partial u^C G_{CB}(x,y) + \frac{1}{2}u_B y\cdot\partial u^C G_{AC}(x,y)\,. \tag{2.88}$$

---

[8] The last term in Eq. (2.86) can be made more familiar if we Taylor expand $G = \sum_{n=0}^{\infty}\sum_{a_1,\dots,a_n} G_{a_1,\dots,a_n} y^{a_1}\dots y^{a_n}$ and consider each coefficient $G_{a_1,\dots,a_n}(x)$ as a rank-n tensor in the tangent space. Then the last term in Eq. (2.86) generates the appropriate connection terms, one for each index. To see also that the last term serves to eliminate the effect of the basis rotation, note that $\bar{\nabla}_\lambda y^a = \partial_\lambda y^a = 0$ because the connection term, which would arise because y^a is a vector, is canceled by the last term in Eq. (2.86).

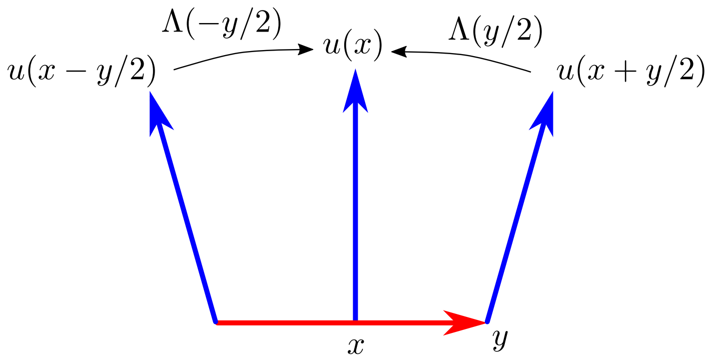

Figure 2.4: Schematic illustration of the confluent correlator.

As a result, the confluent correlator, in contrast to Eq. (2.65), satisfies a simpler orthogonality condition which involves $u(x)$ only (i.e., the constraints are independent of y):

$$u^A(x)\bar{G}_{AB}(x,y) = u^B(x)\bar{G}_{AB}(x,y) = 0\,. \tag{2.89}$$

As discussed later, this allows us to meaningfully perform the Wigner transformation of this object with respect to y coordinates without affecting the constraint.

Now combining all the ingredients given by Eqs. (2.75), (2.83) and (2.87) we define the action of the confluent derivative on a two-point equal-time correlator in the following way:

$$\Delta x \cdot \bar{\nabla}\bar{G}_{AB}(x,y) = \Lambda(\Delta x)_A{}^C \Lambda(\Delta x)_B{}^D \bar{G}_{CD}(x+\Delta x, \Lambda(\Delta x)^{-1}y) - \bar{G}_{AB}(x,y)\,. \tag{2.90}$$

This expression may be more useful for numerical integration of equations we derive, where derivatives need to be discretized. The expression which is used in analytical manipulations is obtained by Taylor expanding in Δx, and it combines Eqs. (2.78) and (2.86):

$$\bar{\nabla}_\mu \bar{G}_{AB} = \partial_\mu \bar{G}_{AB} - \bar{\omega}^C_{\mu A}\bar{G}_{CB} - \bar{\omega}^C_{\mu B}\bar{G}_{AC} - \mathring{\omega}^b_{\mu a}\, y^a \frac{\partial}{\partial y^b}\bar{G}_{AB}\,, \tag{2.91}$$

where the connection, $\bar{\omega}^\nu_{\lambda\mu}$, arises from the Lorentz boost acting on indices A and B, whereas the internal SO(3) connection, $\mathring{\omega}^b_{\lambda a}$, refers to an additional SO(3) rotation which is not captured by the pure boost.

We can now define the Wigner transform of the equal-time correlator $\bar{G}_{AB}(x,y)$ on the locally spatial hyper-surface $u(x)\cdot y = 0$, by integrating over the three-dimensional hyperplane normal to $u(x)$ at each point x. The integral can be expressed explicitly as the integral over coordinates y^a, in which form it can be practically evaluated in numerical applications, or, more formally, as an integral over y constrained to a plane by $u(x) \cdot y = 0$ condition, i.e.,

$$\int d^3y^a = \int d^4y \, \delta(u \cdot y) \, . \tag{2.92}$$

Thus we arrive at the definition of the confluent Wigner function:

$$W_{AB}(x, q) \equiv \int d^4y \, \delta(u(x) \cdot y) \, e^{-iq \cdot y} \, \bar{G}_{AB}(x, y) \, , \tag{2.93}$$

and obeys

$$u^A(x) W_{AB}(x, q) = W_{AB}(x, q) u^B(x) = 0 \, . \tag{2.94}$$

Note that, although the wave vector q is a four-vector, W_{AB} depends only on its projection on the hyper-plane defined by

$$u(x) \cdot q = 0 \, . \tag{2.95}$$

In other words, due to the delta-function constraint the Wigner function $W_{AB}(x, q)$ does not depend on the component of q along u (energy/frequency in local rest frame), and we only need three independent components for vector q. In order to eliminate the redundant component along $u(x)$ we can impose the constraint Eq. (2.95), similar to the gauge condition in gauge field theories. Using the triad basis we already introduced above for vector y (see also Appendix C.1), we could express four-vector q_μ in terms of its three independent components q_a as

$$q_\mu = e_\mu^a(x) q_a \, , \tag{2.96}$$

with an internal three-vector $\boldsymbol{q} = \{q^a\} \in \mathbb{R}^3$, and consider $W(x, q)$ as a function of $\boldsymbol{q}$:

$$W(x, \boldsymbol{q}) \equiv W(x, q = e_a(x) q^a) \, . \tag{2.97}$$

Because the constraint Eq. (2.95) depends on $u(x)$, a meaningful derivative of $W_{AB}(x, q)$ with respect to x should be then defined with a parallel transport of q by $\Lambda(\Delta x)$ from Eq. (2.72) to maintain the constraint. We shall also use the same transport to eliminate the purely kinematic effect of the boost on the vector components of variables ϕ_A. This leads to the notion of "confluent derivative", $\bar{\nabla}_\mu W_{AB}(x,q)$, which we define as

$$\Delta x^\mu \bar{\nabla}_\mu W_{AB}(x,q) \equiv \Lambda(\Delta x)_A{}^C \Lambda(\Delta x)_B{}^D W_{CD}(x+\Delta x, \Lambda(\Delta x)^{-1} q) - W_{AB}(x,q)\,. \tag{2.98}$$

It is straightforward to see that $\bar{\nabla}_\mu W_{AB}(x,q)$ is equal to the Wigner transformation of the confluent derivative $\bar{\nabla}_\mu \bar{G}_{AB}(x,y)$ similarly defined by Eq. (2.90). Thus, by using the rules of the Fourier transform to replace $y^a \to i\partial/\partial q_a$ and $\partial/\partial y^b \to iq_b$, from Eq. (2.91) we immediately obtain the expression for the confluent x derivative of the Wigner function at $q = e^a q_a$ fixed: [9]

$$\bar{\nabla}_\mu W_{AB}(x,q) = \partial_\mu W_{AB} - \bar{\omega}^C_{\mu A} W_{CB} - \bar{\omega}^C_{\mu B} W_{AC} + \mathring{\omega}^b_{\mu a}\, q_b \frac{\partial}{\partial q_a} W_{AB}\,, \tag{2.99}$$

where we also took into account $\mathring{\omega}^a_{\mu a} = 0$. The partial derivative ∂_μ in Eq. 2.99 is to be taken at fixed $\boldsymbol{q}$, *not* fixed q. To simplify notations below, we will use $W_{AB}(x,q)$ (instead of $W_{AB}(x,\boldsymbol{q})$), with understanding that it is a function of x and $\boldsymbol{q}$ given by Eq. (2.97). Furthermore, we shall also use the following expression involving derivatives with respect to components of q:

$$\frac{\partial}{\partial q_\lambda} \equiv e^\lambda_a(x)\, \frac{\partial}{\partial q_a}\,. \tag{2.100}$$

2.5 Relativistic Dynamics of Hydrodynamic Fluctuations

2.5.1 Fluctuation Evolution Equations

The two-point functions $W_{AB}(x,q)$ can be viewed as degrees of freedom additional to the hydrodynamic fields ψ_A (i.e., m, p and u) in ways similar to phase-space distribution functions in kinetic theory. This is not just a vague similarity. A certain linear combination of $W_{AB}(x,q)$ can be quantitatively interpreted as phonon distribution function satisfying Boltzmann equation for a particle with momentum $\boldsymbol{q}$ and energy $E = c_s|\boldsymbol{q}|$ as will be shown in Section 2.7. Regardless of this interpretation, these additional degrees of freedom satisfy a coupled differential (matrix) equation which we call somewhat loosely the "fluctuation kinetic equation" or simply "kinetic equation". The kinetic equations have to be supplemented by the usual hydrodynamic field equations of motion (with fluctuation feedback), $\partial_\mu \langle T^{\mu\nu} \rangle = 0$, to obtain a closed set of equations (somewhat similar to Vlasov equations) to be solved simultaneously. In this section we derive these fluctuation kinetic equations, i.e., equations for W_{AB}.

---

[9] One can introduce $W_{ab}(x,\boldsymbol{q})$ by $W_{AB} = e^a_A e^b_B W_{ab}$, so that the confluent derivative of W_{ab} involves only the SO(3) connection $\mathring{\omega}$. In other words, $\bar{\omega}$ reduces to a SO(3) connection when it acts on W_{AB}. It is a simple matter of choice to work with $W_{ab}(x,\boldsymbol{q})$ or with W_{AB}.

Having introduced the necessary mathematical tools, we return to Eq. (2.69) for G_{AB} and use it to derive the evolution equation for the Wigner function defined in the previous section. The crux of this derivation is expressing the equation for W_{AB} in terms of the confluent derivatives, which have a clear physical meaning as the derivatives in the co-moving frame. Both definitions of the Wigner functions and of the confluent derivative bring additional terms, but they also lead to many nontrivial cancellations.

Our goal is to express the evolution equation of Wigner function by Eq. (2.69). To proceed, we first project Eq. (2.99) onto the time-like direction $u(x)$:

$$u \cdot \bar{\nabla} W_{AB}(x,q) = u \cdot \partial\, W_{AB} - u_A (u \cdot \partial u^C) W_{CB} - u_B (u \cdot \partial u^C) W_{AC} + (e^b_\mu u \cdot \partial e^\mu_a) q_b \frac{\partial}{\partial q_a} W_{AB}\,, \tag{2.101}$$

where we have used the orthogonal condition Eq. (2.89). The tricky part arises from the first term on the RHS of Eq. (2.101), $u \cdot \partial W_{AB}(x,q)$, where W_{AB} is obtained by a Wigner transformation of $\bar{G}_{AB}(x,y)$, defined by Eq. (2.93) where the constraint $\delta(u(x)\cdot y)$ and transformation kernel $e^{-iq\cdot y} = e^{-ie^\mu_b(x) e^a_\mu(x) q^b y_a}$ as part of the integrand are not "constant" when $\partial^{(x)}$ applies, thus,

$$\begin{aligned}
u\cdot\partial\, W_{AB} &= u\cdot\partial\int d^4y\,\delta(u\cdot y)e^{-iq\cdot y}\bar{G}_{AB}(x,y)\\
&=\int d^4y\left(\delta(u\cdot y)e^{-iq\cdot y}u\cdot\partial+u\cdot\partial\left(\delta(u\cdot y)\right)e^{-iq\cdot y}+\delta(u\cdot y)u\cdot\partial\left(e^{-iq\cdot y}\right)\right)\bar{G}_{AB}(x,y)\\
&=\int d^4y\,\delta(u\cdot y)e^{-iq\cdot y}\left(u\cdot\partial+y^{\lambda}(u\cdot\partial u_{\lambda})u\cdot\partial^{(y)}+(e^{\mu}_{a}u\cdot\partial e^{b}_{\mu})q_b\frac{\partial}{\partial q_a}\right)\bar{G}_{AB}(x,y),
\end{aligned}\tag{2.102}$$

where we have used $u\cdot\partial^{(y)}e^{-iq\cdot y}=0$ due to Eq. (2.95). Substitute Eq. (2.102) back into Eq. (2.101), one immediately finds the last term in each equation cancels with the help of Eq. (2.93). Eq. (2.101) now reads

$$\begin{aligned}
&u\cdot\bar{\nabla}W_{AB}(x,q)\\
&=\int d^4y\,\delta(u\cdot y)e^{-iq\cdot y}\left\{\left(u\cdot\partial+y^{\lambda}(u\cdot\partial u_{\lambda})u\cdot\partial^{(y)}\right)\bar{G}_{AB}-u_A(u\cdot\partial u^C)\bar{G}_{CB}-u_B(u\cdot\partial u^C)\bar{G}_{AC}\right\}\\
&\approx\int d^4y\,\delta(u\cdot y)e^{-iq\cdot y}\left\{\left(u\cdot\partial+y^{\lambda}(u\cdot\partial u_{\lambda})u\cdot\partial^{(y)}\right)G_{AB}\right.\\
&\qquad\left.-u_A\left(u\cdot\partial u^C+\frac{1}{2}(y\cdot\partial u^C)u\cdot\partial\right)G_{CB}-u_B\left(u\cdot\partial u^C-\frac{1}{2}(y\cdot\partial u^C)u\cdot\partial\right)G_{AC}\right\}
\end{aligned}\tag{2.103}$$

where Eq. (2.88) is used and terms leading order in background gradients (in wave-vector k) are kept.

Given Eq. (2.103), from Eq. (2.69) and its partner equation

$$u\cdot\partial^{(y)}G_{AB}(x,y)\approx-\frac{1}{2}\mathbb{L}^{(y)}_{AC}\,G^{C}{}_{B}(x,y)-\frac{1}{2}\mathbb{L}^{(y)}_{BC}G_{A}{}^{C}(x,y)\tag{2.104}$$

whose leading order terms are sufficient for our calculation, one finds, after a rather lengthy and tedious algebraic manipulations, that

$$\begin{aligned}
u\cdot\bar{\nabla}W(x,q)=&-\left[i\mathbb{L}^{(q)},W\right]-\left[\frac{1}{2}\bar{\mathbb{L}}+\mathbb{D}^{(q)}+\mathbb{K}',W\right\}+2\mathbb{Q}^{(q)}+(\partial_{\perp\lambda}u_{\mu})q^{\mu}\frac{\partial W}{\partial q_{\lambda}}\\
&+\frac{1}{2}\left(a_{\lambda}+\frac{\partial_{\perp\lambda}c_s}{c_s}\right)\left\{\mathbb{L}^{(q)},\frac{\partial W}{\partial q_{\lambda}}\right\}+\frac{\partial}{\partial q_{\lambda}}\left([\mathbb{\Omega}_{\lambda},W\}-\frac{1}{4}[\mathbb{H}_{\lambda},[\mathbb{L}^{(q)},W]]\right),
\end{aligned}\tag{2.105}$$

where $[A, B] = AB - BA$ and $\{A, B\} = AB + BA$ are the usual matrix (anti-) commutators, while a new notation is introduced for the "quasi-commutator" which appears naturally in this context:

$$[A, B\} \equiv AB + BA^{\dagger}\,. \tag{2.106}$$

In the expression for the (anti-, quasi-) commutators, the usual matrix multiplication rules are assumed and the derivatives are assumed to act on W. The matrices that appear in Eq. (2.105) read

$$\begin{aligned}
&\mathbb{L}^{(q)} \equiv c_s \begin{pmatrix} 0 & 0 & 0 \\ 0 & 0 & q_\nu \\ 0 & q_\mu & 0 \end{pmatrix}, \quad \bar{\mathbb{L}} \equiv c_s \begin{pmatrix} 0 & 0 & 0 \\ 0 & 0 & \bar{\nabla}_{\perp\nu} \\ 0 & \bar{\nabla}_{\perp\mu} & 0 \end{pmatrix}, \\
&\mathbb{D}^{(q)} \equiv \begin{pmatrix} \gamma_\lambda q^2 & -(c_s T n \alpha_p)^{-1} \gamma_p q^2 & 0 \\ -c_s T n \alpha_p \gamma_\lambda q^2 & \gamma_p q^2 & 0 \\ 0 & 0 & \gamma_\eta \Delta_{\mu\nu} q^2 + \left(\gamma_\zeta + \frac{1}{3}\gamma_\eta\right) q_\mu q_\nu \end{pmatrix}, \\
&\mathbb{Q}^{(q)} \equiv T w \begin{pmatrix} -\alpha_m^{-1} \gamma_\lambda q^2 & -(c_s \alpha_p T n)^{-1} \gamma_p q^2 & 0 \\ -(c_s \alpha_p T n)^{-1} \gamma_p q^2 & \gamma_p q^2 & 0 \\ 0 & 0 & \left(\gamma_\eta \Delta_{\mu\nu} q^2 + \left(\gamma_\zeta + \frac{1}{3}\gamma_\eta\right) q_\mu q_\nu\right) \end{pmatrix}, \\
&\mathbb{K}' \equiv \mathbb{K} + \Delta\mathbb{K}, \quad \Delta\mathbb{K} \equiv -\frac{\theta}{2}\mathbb{1} - \frac{1}{2} \begin{pmatrix} 0 & 0 & 0 \\ 0 & 0 & c_s a_\nu + \partial_{\perp\nu} c_s \\ 0 & c_s a_\mu + \partial_{\perp\mu} c_s & -2 u_\mu a_\nu \end{pmatrix}, \\
&\mathbb{\Omega}_\lambda \equiv c_s^2 \begin{pmatrix} 0 & 0 & 0 \\ 0 & \omega_{\kappa\lambda} q^\kappa & 0 \\ 0 & 0 & \omega_{\mu\lambda} q_\nu \end{pmatrix}, \quad \mathbb{H}_\lambda \equiv c_s \begin{pmatrix} 0 & 0 & 0 \\ 0 & 0 & \partial_\nu u_\lambda \\ 0 & \partial_\mu u_\lambda & 0 \end{pmatrix},
\end{aligned} \tag{2.107}$$

where matrices $\mathbb{L}^{(q)}$ and $\bar{\mathbb{L}}$ are propagating operator linear in q and k respectively, $\mathbb{D}^{(q)}$ is the dissipative operator quadratic in q, $2\mathbb{Q}^{(q)}$ is the source for random noise, $\mathbb{K}'$ (with $\mathbb{K}$ defined in Eq. (2.55)), $\mathbb{\Omega}_\lambda$ and $\mathbb{H}_\lambda$ encode the terms proportional to the gradients of the background flow, including the fluid vorticity

$$\omega_{\mu\nu} \equiv \frac{1}{2}(\partial_{\perp\mu}u_\nu - \partial_{\perp\nu}u_\mu)\,. \tag{2.108}$$

and its symmetric partner $\theta_{\mu\nu}$ defined in Eq. (2.27).

Equation (2.105) is a linear equation in W but inhomogeneous due to the source term $2\mathbb{Q}^{(q)}$. In a static uniform background where gradient terms vanishes, the balance between terms involving $\mathbb{Q}^{(q)}$ and $\mathbb{D}^{(q)}$ gives the equation for the equilibrium value for the Wigner function:

$$-\left[i\mathbb{L}^{(q)}, W^{(0)}\right] - \left[\mathbb{D}^{(q)}, W^{(0)}\right\} + 2\mathbb{Q}^{(q)} = 0\,, \tag{2.109}$$

which is a fluctuation-dissipation relation discussed in Sec. 2.2.1. This equation is solved by

$$W^{(0)} = Tw\begin{pmatrix} c_pT/w & 0 & 0 \\ 0 & 1 & 0 \\ 0 & 0 & \Delta_{\mu\nu} \end{pmatrix}, \tag{2.110}$$

where we used Eq. (2.48): $\alpha_m^{-1} = -c_pT/w$. Eq. (2.110), taken together with Eq. (2.51), is in agreement with the well-known thermodynamic expectation values: $V\langle(\delta m)^2\rangle = c_p/n^2$, $V\langle(\delta p)^2\rangle = c_s^2Tw$, $V\langle(\delta u)^2\rangle = T/w$ and $\langle\delta m\delta p\rangle = \langle\delta m\delta u\rangle = \langle\delta p\delta u\rangle = 0$, where V is the volume of the system.

Note that, within the order of approximation we are working, we can further use the ideal hydrodynamic equation $wa_\mu = -\partial_{\perp\mu}p$ to eliminate the time-like derivatives of velocity, i.e., a_μ, on the right-hand side of Eq. (2.105). This may be useful for numerical solution of the equations which would require solving for time evolution of $u(x)$ simultaneously.

2.5.2 Hydro-kinetic Equations

The matrix $\mathbb{L}^{(q)}$ in the RHS of the kinetic equation Eq. (2.105) gives the dominant contribution since it is of order of q whereas the remaining terms are either order k or γq^2 both of which are assumed to be much smaller than q according to our hierarchy of scales in Eq. (2.29). Therefore, some of the components of $W_{AB}(x, q)$ oscillate fast with a characteristic frequency $\omega \sim \mathbb{L}^{(q)} \sim c_s q$. This separation of time scales leads to a new effective description of the system where the fast components of W_{AB} are eliminated by time averaging and only slow modes remain. We can use this separation of time scales to introduce (in addition to spatial coarse graining at scale b described in the Introduction) averaging over *time* intervals of order b_t such that[10]

$$c_s k \ll b_t^{-1} \ll c_s q\,. \tag{2.111}$$

The slow components of W_{AB} that survive time averaging correspond to effective distribution functions in a Boltzmann-like kinetic theory of fluctuations. Note that this is also similar to how we diagonalize a quantum density matrix to identify the particle distribution functions starting from quantum field theory.

To identify the fast components, we express the kinetic equation in the basis where $\mathbb{L}^{(q)}$ is diagonal. $\mathbb{L}^{(q)}$ has six eigenvalues:

$$\lambda_\pm = \pm c_s |q|\,, \quad \lambda_m = \lambda_{T_1,T_2} = \lambda_\| = 0\,, \tag{2.112}$$

corresponding to six eigenvectors $\psi_{\mathbf{A}}$ where $\mathbf{A} = m, +, -, T_1, T_2, \|$. We arrange the eigenvectors to form an orthogonal transformation matrix

$$\psi_A^{\mathbf{A}} = \begin{pmatrix} 1 & 0 & 0 & 0 & 0 & 0 \\ 0 & 1/\sqrt{2} & -1/\sqrt{2} & 0 & 0 & 0 \\ 0 & \hat{q}/\sqrt{2} & \hat{q}/\sqrt{2} & t^{(1)} & t^{(2)} & u \end{pmatrix}, \tag{2.113}$$

where $\hat{q} = q/|q|$ is the unit vector along q and $t^{(1)}$ and $t^{(2)}$ are two transverse unit vectors that satisfy

$$t^{(i)} \cdot t^{(j)} = \delta^{ij}\,, \quad t^{(i)} \cdot \hat{q} = 0\,, \quad t^{(i)} \cdot u = 0\,. \tag{2.114}$$

---

[10] Following our estimates for heavy-ion collisions in Footnote 3, a reasonable choice for b_t would lie between $\ell_{\rm eq}/c_s \sim 6$ fm/c and $\tau_{\rm ev} \sim 10$ fm/c.

In other words $t^{(1)}$, $t^{(2)}$ and $\hat{q}$ span the spatial hyperplane orthogonal to u,

$$t^{(1)}_\mu t^{(1)}_\nu + t^{(2)}_\mu t^{(2)}_\nu + \hat{q}_\mu \hat{q}_\nu = \Delta_{\mu\nu} \,. \tag{2.115}$$

The basis vectors in Eq. (2.113) correspond to the eigenmodes of ideal hydrodynamic equations. Their eigenvalues in Eq. (2.112) correspond to one diffusive mode, a pair of sound modes with positive and negative frequency, and two degenerate transverse momentum modes. The last zero mode, associated with the eigenvector $(0, 0, u)$, is a consequence of the orthogonality condition Eq. (2.89) and is not a physical fluctuation mode. The transverse dyad $t^{(i)}(x, q)$ are degenerate and the basis in this two-dimensional subspace is not unique, yet subject to a SO(2) rotations that are local in both x and q spaces. This local freedom will bring about additional connections in the confluent derivatives, after we project W_{AB} onto the slow components. A convenient explicit choice for $t^{(i)}$ is given in Appendix C.2.

We can now transform the kinetic equation (2.105) into the diagonal basis of $\mathbb{L}^{(q)}$ by the orthogonal transformation $M \to \psi^T M \psi$ [11] and express the equation in terms of new variables:

$$W_{\mathbf{AB}} = \psi^A_{\mathbf{A}} W_{AB} \psi^B_{\mathbf{B}} \,. \tag{2.116}$$

The spurious components $W_{\mathbf{A}\|}$, $W_{\|\mathbf{B}}$, and $W_{\|\|}$ vanish automatically due to the constraint, Eq. (2.94), and effectively we are left with 5×5 matrix $W_{\mathbf{AB}}$. In the diagonal basis, we have

$$[\mathbb{L}^{(q)}, W]_{\mathbf{AB}} = (\lambda_{\mathbf{A}} - \lambda_{\mathbf{B}}) W_{\mathbf{AB}} \,, \tag{2.117}$$

which means that the fourteen modes with $\lambda_{\mathbf{A}} \neq \lambda_{\mathbf{B}}$ are the fast modes. They average out on the coarse grained time scale b_t and thus can be neglected. The remaining eleven modes are not all independent. In particular,

$$W_{++}(x, q) = W_{--}(x, -q) \equiv W_L(x, q) \tag{2.118}$$

---

[11] Note that since there are derivatives with respect to x and q in Eq. (2.105), one needs to use $\psi^T dM\psi = d(\psi^T M \psi) + [\psi^T d\psi, \psi^T M \psi]$.

is the longitudinal mode associated with sound fluctuations. The remaining diffusive modes form a 3×3 matrix and obey $W_{\mathbf{AB}}(x, q) = W_{\mathbf{BA}}(x, -q)$, i.e., only six of these modes are independent. These seven independent components, W_L and $W_{\mathbf{AB}}$, $(\mathbf{A}, \mathbf{B} = m, T_1, T_2)$, constitute the degrees of freedom in the new effective kinetic description of fluctuations. Note that the 3×3 block of $W_{\mathbf{AB}} \equiv \widehat{W}$ $(\mathbf{A}, \mathbf{B} = m, T_1, T_2)$ still contains off-diagonal components, which reflects the fact that the three modes of $\mathbf{A} = m, T_1, T_2$ are degenerate and can mix with each other.

The kinetic equation for the surviving slow components follows straightforwardly from Eq. (2.105). The sound fluctuation mode completely decouples from other components and satisfies

$$(u + c_s\hat{q}) \cdot \bar{\nabla} W_L = -\gamma_L q^2 (W_L - Tw) + \left((c_s a_\mu + \partial_{\perp\mu} c_s) |q| + (\partial_{\perp\mu} u_\nu) q^\nu + 2c_s^2 q^\lambda \omega_{\lambda\mu} \right) \frac{\partial W_L}{\partial q_\mu}$$
$$- \left((1 + c_s^2 + \dot{c}_s)\theta + \theta_{\mu\nu}\hat{q}^\mu \hat{q}^\nu + \frac{1 + \left(2 - \frac{(\alpha_p T n)^2}{\alpha_m}\right) c_s^2}{c_s} \hat{q} \cdot a - \frac{c_s \alpha_p T^2 n^2}{\alpha_m w} \hat{q} \cdot \partial\alpha \right) W_L \,, \quad (2.119)$$

where the sound damping coefficient γ_L is given by

$$\gamma_L = \gamma_\zeta + \frac{4}{3}\gamma_\eta + \gamma_p \,, \quad (2.120)$$

and γ_ζ, γ_η and γ_p are defined by Eq. (2.42). Here, the confluent derivative of W_L is defined as

$$\bar{\nabla}_\mu W_L \equiv \partial_\mu W_L + \mathring{\omega}^a_{\mu b} q_a \frac{\partial W_L}{\partial q_b} \,, \quad (2.121)$$

consistent with the fact that W_L behaves as a Lorentz scalar. Defining

$$N_L \equiv \frac{W_L}{c_s |q| w} \,, \quad (2.122)$$

such that its equilibrium value, $N_L^{(0)} = T/c_s|q|$, is equal to what one would expect for the distribution function of "phonons" with the dispersion relation $\omega = c_s|q|$, Eq. (2.119) can be recast into the form that resembles a Boltzmann kinetic equation for phonons,

$$\begin{aligned}\mathcal{L}_L[N_L] &\equiv \left((u + c_s\hat{q})\cdot\bar{\nabla} - \big((c_s a_\mu + \partial_{\perp\mu}c_s)\,|q| + (\partial_{\perp\mu}u_\nu)q^\nu + 2c_s^2 q^\lambda \omega_{\lambda\mu}\big)\frac{\partial}{\partial q_\mu}\right)N_L \\ &= -\gamma_L q^2\left(N_L - \frac{T}{c_s|q|}\right). \qquad (2.123)\end{aligned}$$

Remarkably, the advection operator $\mathcal{L}_L[N_L]$ is precisely equal to the Liouville operator in the relativistic kinetic theory of massless (quasi-) particles which can be identified as phonons propagating in a flowing fluid. Their dispersion relation can be written as an on-shell condition $g^{\mu\nu}_{\text{eff}}(x)q_\mu q_\nu = 0$ in terms of an effective spacetime dependent inverse metric $g^{\mu\nu}_{\text{eff}}(x) = -u^\mu u^\nu + c_s^2\Delta^{\mu\nu}$ that gives the dispersion relation of sound waves $\omega = c_s(x)|\boldsymbol{q}|$ in the local rest frame of the fluid (see Sec. 2.7 for the derivation). It should be emphasized that the Liouville operator $\mathcal{L}_L[N_L]$ in Eq. (2.123) emerges after $\partial_\perp\alpha$ terms vanish due to rather nontrivial cancellations. Equally striking is the simplicity of the collision (relaxation) term in the RHS of Eq. (2.123), emerging after cancellation of all the background gradient terms in Eq. (2.119).

The diffusive and transverse shear modes, contained in 3×3 matrix $\widehat{W}$, satisfy the matrix equation

$$u\cdot\bar{\nabla}\widehat{W} = -\left\{\widehat{\mathbb{D}}, \widehat{W} - \widehat{W}^{(0)}\right\} + (\partial_{\perp\mu}u_\nu)q^\nu\nabla^\mu_{(q)}\widehat{W} - \left[\widehat{K}, \widehat{W}\right\}, \qquad (2.124)$$

where

$$\begin{aligned}&\widehat{\mathbb{D}} \equiv \begin{pmatrix}\gamma_\lambda & 0\\ 0 & \delta_{ij}\gamma_\eta\end{pmatrix}q^2, \quad \widehat{W}^{(0)} \equiv Tw\begin{pmatrix}\frac{c_pT}{w} & 0\\ 0 & \delta_{ij}\end{pmatrix}, \\ &\widehat{K} \equiv \begin{pmatrix}\frac{1}{2}(1+2\dot{T})\theta & \frac{Tn}{\alpha_m}\left(\alpha_p a\cdot t^{(j)} + \frac{1}{w}t^{(j)}\cdot\partial_\perp\alpha\right)\\ \alpha_p Tna\cdot t^{(i)} & \frac{1}{2}\theta\,\delta^{ij} + t^{(i)}_\mu t^{(j)}\cdot\partial u^\mu\end{pmatrix}, \quad i = 1,2\,.\end{aligned} \qquad (2.125)$$

Here we introduced a covariant q-derivative that takes into account the rotation of the basis $t^{(i)}(x,q)$ of the transverse modes in q space:

$$\nabla^\mu_{(q)}\widehat{W} \equiv \frac{\partial\widehat{W}}{\partial q_\mu} + \left[\widehat{\omega}^\mu, \widehat{W}\right], \quad \text{where} \quad \widehat{\omega}^{ij}_\mu \equiv t^{(i)}_\nu\frac{\partial}{\partial q^\mu}t^{(j)\nu}, \quad \widehat{\omega}^{mm}_\mu = \widehat{\omega}^{mi}_\mu = \widehat{\omega}^{im}_\mu = 0\,. \quad (2.126)$$

The confluent derivative in Eq. (2.124) also includes additional SO(2) connection $\widehat{\mathring{\omega}}^{ij}_{\mu} \equiv t^{(i)}_{\nu}\partial_{\mu}t^{(j)\nu}$, associated with the x-dependence of the basis vectors $t^{(i)}$:

$$\bar{\nabla}_{\mu}\widehat{W} \equiv \partial_{\mu}\widehat{W} + \mathring{\omega}^{a}_{\mu b}\, q_a \nabla^{b}_{(q)}\widehat{W} + \left[\widehat{\mathring{\omega}}_{\mu}, \widehat{W}\right]. \tag{2.127}$$

In Appendix C.2 we propose a simple and intuitive choice for the $t^{(i)}$ basis suitable for applications, and compute corresponding connections $\widehat{\omega}^{ij}_{\mu}$ and $\widehat{\mathring{\omega}}^{ij}_{\mu}$.

Introducing the rescaled variables

$$N_{mm} \equiv \frac{W_{mm}}{nT^2}\,, \qquad N_{m(i)} \equiv \frac{W_{m(i)}}{nT}\,, \qquad N_{(i)(j)} \equiv \frac{W_{(i)(j)}}{n}\,, \tag{2.128}$$

and also a Liouville-like operator,

$$\mathcal{L}[\widehat{W}] \equiv \Big(u\cdot\bar{\nabla} - (\partial_{\perp\mu}u_{\nu})q^{\nu}\nabla^{\mu}_{(q)}\Big)\,\widehat{W}\,, \tag{2.129}$$

we can simplify Eq. (2.124) substantially:

$$\mathcal{L}[N_{mm}] = -\,2\gamma_{\lambda}q^2\left(N_{mm} - \frac{c_p}{n}\right) - \frac{n}{w}t^{(i)}\cdot\partial m\left(N_{(i)m} + N_{m(i)}\right), \tag{2.130a}$$

$$\mathcal{L}[N_{m(i)}] = -\,(\gamma_{\eta}+\gamma_{\lambda})q^2 N_{m(i)} - \partial^{\nu}u^{\mu}t^{(i)}_{\mu}t^{(j)}_{\nu}N_{m(j)} - \frac{n}{w}t^{(j)}\cdot\partial m N_{(j)(i)} + \frac{\alpha_p T^2 n}{w}t^{(i)}\cdot\partial p N_{mm}\,, \tag{2.130b}$$

$$\begin{aligned}\mathcal{L}[N_{(i)(j)}] = &-\,2\gamma_{\eta}q^2\left(N_{(i)(j)} - \frac{Tw}{n}\delta_{ij}\right) - \partial^{\nu}u^{\mu}\left(t^{(i)}_{\mu}t^{(k)}_{\nu}N_{(k)(j)} + t^{(j)}_{\mu}t^{(k)}_{\nu}N_{(i)(k)}\right)\\ &+\frac{\alpha_p T^2 n}{w}\partial^{\mu}p\left(t^{(i)}_{\mu}N_{m(j)} + t^{(j)}_{\mu}N_{(i)m}\right),\end{aligned} \tag{2.130c}$$

where $\alpha_p = (1-\dot{T}/c_s^2)/Tn$, given by Eq. (2.48).

The kinetic equations for fluctuations, Eqs. (2.119) and (2.124), are the main results in this section. By considering these equations together with the conservation equation for the energy-momentum tensor, including nonlinear feedback from the fluctuations presented in Eq. (2.64), we obtain a closed system of equations that determines the dynamics of both the background flow and the fluctuation correlators self-consistently. These equations can be then applied to numerical studies of fluctuations in hydrodynamically evolving systems, such as heavy-ion collisions. In order for this program to work in practice, we need to deal with the singularity of $G^{\mu\nu}(x)$ which is manifested in the ultraviolet divergence of the the wave-vector integral relating W_{AB} to G_{AB}. To eliminate the resulting unphysical cutoff dependence we shall absorb ultraviolet divergent contributions of fluctuations into renormalization of a *finite* number of physical parameters that define first order viscous hydrodynamics, i.e. the equation of state and transport coefficients. The remaining part of fluctuation contributions is physical, well-defined and not suffer from short-distance ambiguity (i.e., insensitive to the cutoff). In Sec. 2.6, we describe in detail how this renormalization procedure is carried out analytically.

2.5.3 Hydro-kinetic Equations for Bjorken Flow

The purpose of this section is to compare our equations with the ones for a particular case of Bjorken flow derived in Ref. [49].

The first observation we need to make is that the definition of the equal-time correlator in Ref. [49] is subtly different. The Bjorken flow allows us to define a hypersurface globally which is orthogonal to the flow four-vector $u(x)$ at each point: the constant proper-time surface $\tau = \text{const}$. It is then natural to define "equal time" correlator in such a way that points $x^{\pm}$ lie on the same proper-time hypersurface as x. The difference with our definition is subtle because our equal-time hyperplane is tangential to the equal-τ hypersurface at point x and the difference is of order y^2, due to the curvature of the surface. This difference does lead to a subtle change in the last term in Eq. (2.105), which is necessary to make this equation agree with Ref. [49].

To describe this in more detail, let us consider a definition of the equal-time correlator which is slightly different from ours, but will coincide with $\tau = \text{const}$ for Bjorken flow. It is possible to define a hypersurface orthogonal to flow if the flow is conservative, i.e., $u^\mu = \partial^\mu \tau$ (as is the case for the Bjorken flow, for example). In general it is not possible, however, one can perform a Helmholtz decomposition into conservative (potential) and purely vortical flow: $u^\mu = \partial^\mu \tau + v^\mu$, where $\partial \cdot v = 0$ (see Fig. 2.5 for illustration). We will not be interested in doing this *globally* since we only need to describe the surface near a given point x to quadratic order in y. Thus we Taylor expand u to linear order in Δx:

$$u_\mu(x+\Delta x) = u_\mu(x) + \frac{1}{2}(\partial_\mu u_\nu + \partial_\nu u_\mu)\Delta x^\nu + \frac{1}{2}(\partial_\mu u_\nu - \partial_\nu u_\mu)\Delta x^\nu. \tag{2.131}$$

The last term is purely vortical, while the first two terms are potential, i.e.,

$$\tau(x+\Delta x) = \tau(x) + u\cdot\Delta x + \frac{1}{2}\partial_\mu u_\nu \Delta x^\mu \Delta x^\nu\,. \tag{2.132}$$

We can then define equal-time correlator in such a way that points x and $x^\pm = x \pm y/2$ lie on the same curved surface $\tau =$ const. Using 3-dimensional vector y in the tangent plane to $u(x)$ to parameterize points on such a surface, we can write explicitly

$$x^\pm_\lambda = x_\lambda \pm \frac{y_\lambda}{2} + \frac{1}{8}u_\lambda \theta_{\mu\nu} y^\mu y^\nu\,, \tag{2.133}$$

where $y \cdot u(x) = 0$ and the last term describes the curvature of the surface. Using this definition of $x^\pm$ instead of Eq. (2.57) will change the definition of the "equal-time" correlator and of the Wigner function.

In what follows in this section we shall use that modified definition, but retain the same notation for simplicity. Due to the modification described above, we must replace $\mathbb{L}^{(y)}$ defined in Eq. (2.70) by

$$\mathbb{L}^{(y)} \quad\to\quad \mathbb{L}^{(y)} - \frac{1}{4}y^\lambda \Theta_\lambda u\cdot\partial^{(x)}, \tag{2.134}$$

where

$$\Theta_\lambda \quad\equiv\quad \frac{c_s}{2}\begin{pmatrix} 0 & \theta_{\nu\lambda} \\ \theta_{\mu\lambda} & 0 \end{pmatrix}. \tag{2.135}$$

As a consequence, Eq. (2.69) and (2.105) are modified and take the form

$$\begin{aligned} u\cdot\partial G_{AB}(x,y) \;=\; & -\left(\mathbb{L}^{(y)}+\frac{1}{2}\mathbb{L}+\mathbb{Q}^{(y)}+\mathbb{K}+\mathbb{Y}\right)_{AC} G^{C}{}_{B}(x,y) \\ & -\left(-\mathbb{L}^{(y)}+\frac{1}{2}\mathbb{L}+\mathbb{Q}^{(y)}+\mathbb{K}+\mathbb{Y}\right)_{BC} G_{A}{}^{C}(x,y) \\ & +\frac{1}{4}\big((y^{\lambda}\mathbb{\Theta}_{\lambda})_{AC}\,u\cdot\partial G^{C}{}_{B}(x,y)-(y^{\lambda}\mathbb{\Theta}_{\lambda})_{BC}\,u\cdot\partial G_{A}{}^{C}(x,y)\big)+2Tw\mathbb{Q}^{(y)}_{AB}\delta^{3}(y_{\perp}) \end{aligned} \tag{2.136}$$

and

$$\begin{aligned} u\cdot\bar{\nabla}W(x,q) = & -\left[i\mathbb{L}^{(q)},W\right]-\left[\frac{1}{2}\bar{\mathbb{L}}+\mathbb{D}^{(q)}+\mathbb{K}',W\right\}+2\mathbb{Q}^{(q)}+(\partial_{\perp\lambda}u_{\mu})q^{\mu}\frac{\partial W}{\partial q_{\lambda}} \\ & +\frac{1}{2}\left(a_{\lambda}+\frac{\partial_{\perp\lambda}c_s}{c_s}\right)\left\{\mathbb{L}^{(q)},\frac{\partial W}{\partial q_{\lambda}}\right\}+\frac{\partial}{\partial q_{\lambda}}\left([\mathbb{\Omega}_{\lambda},W\}-\frac{1}{4}[\mathbb{\Omega}_{\lambda},[\mathbb{L}^{(q)},W]]\right), \end{aligned} \tag{2.137}$$

respectively, where

$$\mathbb{\Omega}_{\lambda}\equiv\mathbb{H}_{\lambda}-\mathbb{\Theta}_{\lambda}=c_s\begin{pmatrix}0 & \omega_{\nu\lambda}\\ \omega_{\mu\lambda} & 0\end{pmatrix}. \tag{2.138}$$

Note, that the only change compared to Eq. (2.105) is in the double commutator term.[12] For the Bjorken flow, $a_\mu=\omega_{\mu\nu}=\partial_\perp c_s=0$, and all the terms on the second line in Eq. (2.137) vanish.

To complete the comparison, for the boost-invariant flow, we perform the coordinate transformation from (t,x,y,z) to (τ,x,y,Y) given by $t=\tau\cosh Y$, $x=x$, $y=y$, $z=\tau\sinh Y$, where τ is the proper time and Y is the space-time rapidity. One can easily check that for the Bjorken flow $u\cdot\bar{\nabla}=\partial_\tau$, $\theta=1/\tau$, $a_\mu=\omega_{\mu\nu}=0$. Thus Eq. (2.137) is reduced to

$$\partial_\tau W(x;q)=-\left[i\mathbb{L}^{(q)},W\right]-\left\{\frac{1}{2}\bar{\mathbb{L}}+\mathbb{Q}^{(q)}+\mathbb{K}',W\right\}+2\mathbb{Q}^{(q)}+\frac{1}{\tau}W+\frac{q_z}{\tau}\frac{\partial W}{\partial q_z}. \tag{2.139}$$

---

[12] This is consistent with the fact that upon diagonalization and time-averaging over faster modes this term drops completely. Indeed, the scale of time-averaging, b_t is much longer than the typical time-like separation between the plane tangent to u and the $\tau=$ const defined by Eq. (2.133), which is of order $(\partial u)y^2\sim k/q^2\ll 1/q$, compared to $b_t\gg 1/q$ according to Eq. (2.111).

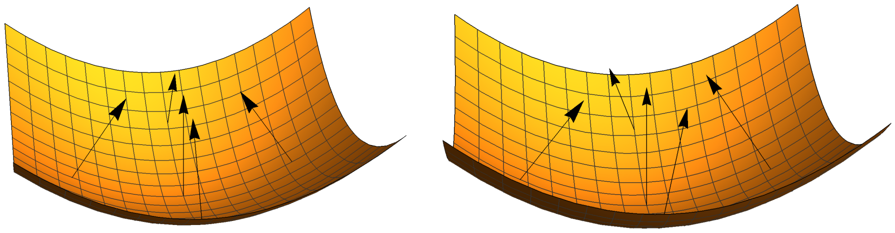

Figure 2.5: *Left:* Illustration of the surface orthogonal to the conservative flow u at each point. Boost is represented by ordinary rotation, preserving angles, for clarity. *Right:* The same is not possible for non-conservative flow, i.e., for nonzero vorticity. However, it is possible to make the normal vector to the surface (not shown) and the flow vector u (shown) at the same point be different by a purely vortical vector: $v^\mu = \partial^\mu \tau - u^\mu$, such that $\partial \cdot v = 0$.

Since $q_Y = \tau q_z$ where q_Y is the wave vector conjugate to Y, we define $W_B(x; q_Y) = W(x; q_z)/\tau$ to take into account the change in the measure of the momentum integration. Using

$$\partial_\tau W(x;q_z) = \partial_\tau W(x;q_z)\Big|_{q_Y} - \frac{\partial W(x;q_z)}{\partial q_z}(\partial_\tau q_z)\Big|_{q_Y} = \partial_\tau\left[\tau W_B(x;q_Y)\right] + \frac{q_z}{\tau}\frac{\partial W(x;q_z)}{\partial q_z}, \quad (2.140)$$

we obtain

$$\partial_\tau W_B(x;q_Y) \;=\; -\left[i\mathbb{L}^{(q)}, W_B\right] - \left\{\frac{1}{2}\bar{\mathbb{L}} + \mathbb{Q}^{(q)} + \mathbb{K}', W_B\right\} + \frac{2\mathbb{Q}^{(q)}}{\tau}, \quad (2.141)$$

where the last two terms in Eq. (2.139) were eliminated by the momentum rescaling. Similarly, one can check that our Eqs. (2.123) and (2.124), rewritten in terms of W_B, will reduce to Eq. (A7) in Ref. [49] exactly.

2.6 Renormalization of Hydrodynamics

In this section we discuss two aspects of the fluctuation feedback: (i) the renormalization of the variables, the equation of state and the transport coefficients as well as (ii) the time lagged hydrodynamic response, falling off as a power of time, known as “long-time tails”, or, equivalently, non-analytic frequency dependence of the response at low frequencies.

2.6.1 Renormalization of Hydrodynamic Variables

The locality of the noise in stochastic hydrodynamics is manifested by the delta functions in Eqs. (2.32). In the coarse-grained picture, this singularity is smeared out and the amplitude of the noise is proportional to $b^{-3/2}$ where b is the size of the fluid cell. That means taking $b \to 0$ requires infinitely large noise. The fluid cell must be larger than the microscopic correlation length, say T^{-1} or ξ whichever larger, for hydrodynamic description to be valid, but it is otherwise arbitrary. And because it is arbitrary, the physical results obtained from hydrodynamic equations cannot depend on the cutoff b.

The infinite (delta function) noise has its counterpart in our deterministic approach – the singularities appear as infinite contributions to $G_{AB}(x)$, which arise as ultraviolet divergences in the integrals over the fluctuation wave-vector q in Eq. (2.154). Introducing the UV cutoff $\Lambda = 1/b$, we expect that these Λ dependent terms must be separated *analytically* and absorbed into the renormalized variables, equation of state and transport coefficients in order for the physics to be cutoff independent.

This renormalization procedure has been by now well understood in both non-relativistic hydrodynamics [47] and relativistic hydrodynamics without conserved charge [49, 1] or in some special cases, such as, e.g., conformal fluids, [50]. In this section, we complete this line of developments by performing the renormalization of hydrodynamics of arbitrary fluid with conserved charge in arbitrary backgrounds.

It must be kept in mind that, while Λ is an ultraviolet cutoff from the perspective of the scale of fluctuations, q, it is still considered small compared to the microscopic scales, T or ξ^{-1} (see Eq. (2.29)). Taking the feedback term G_{AB}/w in Eq. (2.64) as an example, one finds even the most dominant ultraviolet divergent contribution to $G_{AB}/w \propto \Lambda^3 T$ is still a small correction to the average background variables that are of order T^4. However, in practical numerical simulations, where this separation of scales in not ideal, these corrections will introduce a noticeable cutoff dependence. Therefore, the elimination of the cutoff dependence via renormalization is not only a matter of principle, but also an issue of practical importance.

The first issue one need to address is, how to define the local rest frame in deterministic fluctuating hydrodynamics? This ambiguity of frame choices already emerges in ideal hydrodynamics (i.e., without turning on the gradient terms). Although this ambiguity is unlike the way we deal with the ambiguity of frame choices due to the non-equilibrium correction to ideal hydrodynamics in first-order gradients, which is discussed in Sec. 2.1, it share similar spirit: one needs to adjust the definition of physical variables observed in certain frames to preserve the Landau's matching conditions given by Eq. (2.22). It is obvious that according to Eq. (2.64), the matching conditions is no longer valid, i.e., $\langle \breve{T}^{\mu}_{\nu}\rangle u^{\nu} \neq \varepsilon u_{\mu}$, $\langle \breve{J}^{\mu}\rangle u_{\mu} \neq -n$, etc. Thus, we need to identify the physical, or "renormalized", fluid velocity u_R and the physical local energy and charge densities (ε_R, n_R) which are determined by the matching condition

$$-\langle \breve{T}^{\mu}_{\nu}\rangle u^{\nu}_{R} = \varepsilon_R u^{\mu}_{R}\,, \tag{2.142a}$$

$$-\langle \breve{J}^{\mu}\rangle u_{R\mu} = n_R\,. \tag{2.142b}$$

in terms of the "bare" variables u, ε and n. Another important issue one should notice is that, although the fluctuating fluid velocity is properly normalized (i.e. $\breve{u}\cdot\breve{u} = -1$), the average velocity, $u \equiv \langle \breve{u}\rangle$, is not since

$$u\cdot u = -1 - \langle \delta u\cdot\delta u\rangle = -1 - \frac{1}{w^2}G^{\mu}_{\mu}(x)\,. \tag{2.143}$$

In other word, we define u_R such that it is not only subject to the matching condition (2.142), but also normalized to unity, $u_R^2 = -1$. Taking these two issues into account and expanding

u_R to first order in G_{AB}, we obtain [13]

$$\begin{aligned} u^\mu_R \equiv u^\mu + \delta_R u^\mu &= \frac{u^\mu + \frac{\varepsilon_m}{w^2 T n} G^{m\mu}(x) + \frac{c_s(1+\varepsilon_p)}{w^2} G^{p\mu}(x)}{\sqrt{1 + G^\mu_\mu(x)/w^2}} \\ &\approx u^\mu + \frac{\varepsilon_m}{w^2 T n} G^{m\mu}(x) + \frac{1+c_s^2}{c_s w^2} G^{p\mu}(x) - \frac{u^\mu}{2w^2} G^\nu_\nu(x)\,. \end{aligned} \tag{2.144}$$

Once the local physical fluid velocity is properly defined, we can similarly introduce

$$\varepsilon_R \equiv \varepsilon + \delta_R \varepsilon\,, \quad n_R \equiv n + \delta_R n\,, \tag{2.145}$$

where the fluctuation corrections to local rest frame energy and charge densities are derived from Eqs. (2.142):

$$\delta_R \varepsilon = \frac{1}{w} G^\mu_\mu(x) + \frac{\varepsilon_{mm}}{2T^2 n^2} G_{mm}(x) + \frac{c_s^2 \varepsilon_{pp}}{2} G_{pp}(x)\,, \tag{2.146a}$$

$$\delta_R n = \frac{n}{2w^2} G^\mu_\mu(x) + \frac{n_{mm}}{2T^2 n^2} G_{mm}(x) + \frac{c_s^2 n_{pp}}{2} G_{pp}(x)\,. \tag{2.146b}$$

In terms of the ε_R, n_R and u_R, we have now the following expressions for $\langle \breve{T}^{\mu\nu} \rangle$ and $\langle \breve{J}^\mu \rangle$:

$$\langle \breve{T}^{\mu\nu}(x) \rangle = \varepsilon_R u^\mu_R u^\nu_R + p(\varepsilon, n) \Delta^{\mu\nu}_R + \Pi^{\mu\nu} + \frac{1}{w} G^{\mu\nu}(x)\,, \tag{2.147a}$$

$$\langle \breve{J}^\mu(x) \rangle = n_R u^\mu_R + \nu^\mu - \frac{n}{w^2} G^{m\mu}(x) - \frac{c_s n}{w^2} G^{p\mu}(x)\,. \tag{2.147b}$$

where $\Delta^{\mu\nu}_R \equiv g^{\mu\nu} + u^\mu_R u^\nu_R$. The transformation to physical variables is not yet complete in Eqs. (2.147a) and (2.147b) – the "bare" values ε and n still appear in, e.g., $p(\varepsilon, n)$, which will need to be expressed in terms of physical ε_R and n_R. We shall do this below.

After establishing the expressions for physical energy and charge densities, our next goal is to determine the physical values of pressure and transport coefficients. Their physical values differ from their "bare values" that appear in the constitutive relations Eq. (2.8) and Eq. (2.26) due to fluctuations. The fluctuations contain local terms that are zeroth order

---

[13] This expansion is based on the assumption that the two-point function contributions are parametrically smaller than the corresponding bare quantities, due to $\Lambda \ll \min(T, \xi^{-1})$, according to the scale hierarchy Eq. (2.29). Because of this separation of scales, bare quantities that multiply G_{AB} can be simply replaced by their renormalized values.

(nonvanishing for homogeneous backgrounds) and first order in gradients. We shall denote these as $G^{(0)}_{AB}(x)$ and $G^{(1)}_{AB}(x)$ respectively. The former contributes to the physical value of the pressure and the latter contributes to the physical values of the transport coefficients. The remaining parts of $G_{AB}(x)$, denoted by $\widetilde{G}(x)_{AB}$, are higher order in gradients (in fact, as we shall see, they are nonlocal functionals of hydrodynamic variables):

$$G_{AB}(x) = G^{(0)}_{AB}(x) + G^{(1)}_{AB}(x) + \widetilde{G}_{AB}(x)\,, \tag{2.148}$$

where the superscripts '(0)' and '(1)' denote the terms that are zeroth order and first order in gradient expansion[14]. Similarly since $\delta_R\varepsilon$ and $\delta_R n$ in Eq. (2.146) are linear combinations of $G_{AB}(x)$, these quantities can be also expanded:

$$\delta_R\varepsilon = \delta^{(0)}_R\varepsilon + \delta^{(1)}_R\varepsilon + \widetilde{\delta}_R\varepsilon\,, \quad \delta_R n = \delta^{(0)}_R n + \delta^{(1)}_R n + \widetilde{\delta}_R n\,, \tag{2.149}$$

where expressions for $\delta^{(0)}_R(\varepsilon, n)$, $\delta^{(1)}_R(\varepsilon, n)$ and $\widetilde{\delta}_R(\varepsilon, n)$ are the same as $\delta_R(\varepsilon, n)$ in Eq. (2.146) with G_{AB} replaced with $G^{(0)}_{AB}$, $G^{(1)}_{AB}$ and $\widetilde{G}_{AB}$ respectively.

By substituting this gradient expansion, Eqs. (2.148) and (2.149) into Eqs. (2.147a) and (2.147b) we can identify the physical values of pressure and transport coefficients by collecting terms zeroth order in gradients into physical (renormalized) pressure p_R and terms first order in gradients into physical (renormalized) values of kinetic coefficients:

$$\langle \breve{T}^{\mu\nu}(x)\rangle = \varepsilon_R u^\mu_R u^\nu_R + p_R\Delta^{\mu\nu}_R + \Pi^{\mu\nu}_R + \widetilde{T}^{\mu\nu}, \tag{2.150a}$$

$$\langle \breve{J}^{\mu}(x)\rangle = n_R u^\mu_R + \nu^\mu_R + \widetilde{J}^{\mu}. \tag{2.150b}$$

where the zeroth-order terms in gradient expansion transverse to u_R are given by

$$\begin{aligned} p_R(\varepsilon_R, n_R)\Delta^{\mu\nu}_R &= p(\varepsilon, n)\Delta^{\mu\nu}_R + \frac{1}{w}G^{\mu\nu(0)}(x) \\ &= \left(p(\varepsilon_R, n_R) - \left(\frac{\partial p}{\partial \varepsilon}\right)_n \delta^{(0)}_R\varepsilon - \left(\frac{\partial p}{\partial n}\right)_\varepsilon \delta^{(0)}_R n\right)\Delta^{\mu\nu}_R + \frac{1}{w}G^{\mu\nu(0)}(x)\,, \end{aligned} \tag{2.151}$$

---

[14] Note that $G^{(0)}_{AB}(x)$ still depends on x via terms such as $w(x)$ however it does not contain any gradient terms such as $\partial_\mu u$ or $\partial_\mu \alpha$ and it does not vanish in a homogeneous background. $G^{(1)}_{AB}(x)$ terms are explicitly linear in gradients and do vanish in a homogeneous background.

and the first-order terms are given by

$$\Pi^{\mu\nu}_R = \Pi^{\mu\nu} - \left(\left(\frac{\partial p}{\partial \varepsilon}\right)_n \delta^{(1)}_R \varepsilon + \left(\frac{\partial p}{\partial n}\right)_\varepsilon \delta^{(1)}_R n \right) \Delta^{\mu\nu} + \frac{1}{w} G^{\mu\nu\,(1)}(x)\,, \tag{2.152a}$$

$$\nu^\mu_R = \nu^\mu - \frac{n}{w^2} G^{m\mu\,(1)}(x) - \frac{c_s n}{w^2} G^{p\mu\,(1)}(x)\,. \tag{2.152b}$$

The remaining, i.e., higher-order in gradients (and nonlocal), contributions to constitutive equations are given by

$$\begin{aligned}\widetilde{T}^{\mu\nu} =& -\left(\left(\frac{\partial p}{\partial \varepsilon}\right)_n \widetilde{\delta}_R \varepsilon + \left(\frac{\partial p}{\partial n}\right)_\varepsilon \widetilde{\delta}_R n \right) \Delta^{\mu\nu} + \frac{1}{w} \widetilde{G}^{\mu\nu}(x) \\ =& \frac{1}{2w} \left((1-\dot{c}_p) \frac{w}{c_p T} \widetilde{G}_{mm}(x) + \left(c_s^2 - \dot{T} + 2\dot{c}_s\right) \widetilde{G}_{pp}(x) - \left(c_s^2 + \dot{T}\right) \widetilde{G}^{\lambda}_{\lambda}(x) \right) \Delta^{\mu\nu} \\ &+ \frac{1}{w} \widetilde{G}^{\mu\nu}(x)\,, \end{aligned} \tag{2.153a}$$

$$\widetilde{J}^\mu = -\frac{n}{w^2} \widetilde{G}^{m\mu}(x) - \frac{c_s n}{w^2} \widetilde{G}^{p\mu}(x)\,. \tag{2.153b}$$

Let us now work out the explicit expressions for the physical pressure and transport coefficients. As usual, due to contribution of short-wavelength fluctuations the coincident point correlators such as $G_{AB}(x) \equiv G_{AB}(x, 0)$ are divergent. These divergences fall into two classes which are leading and sub-leading respectively. The leading singularity is apparent even in static homogeneous equilibrium, since within our coarse-grained resolution $G^{(0)}_{AB}(x, y) \sim \delta^{(3)}(y)$ (i.e., correlation length is negligible) and thus $G^{(0)}_{AB}(x, 0)$ is undefined. Of course, this is an artifact of neglecting the finiteness of coarse-graining scale $b = 1/\Lambda$. The sub-leading singularity, though less obvious, reflects the feedback of non-equilibrium fluctuations at the short-wavelength scale. These two divergences are easier to disentangle using the Wigner transform of $G_{AB}(x, y)$, i.e., Fourier transform with respect to y: $W_{AB}(x, q)$ that we define in Eq. (2.93). With the help of Eq. (2.88), the inverse Wigner transformation from the q-space to y-space reads

$$G_{AB}(x) \equiv G_{AB}(x, y = 0) = \bar{G}_{AB}(x, y = 0) = \int \frac{d^3 q}{(2\pi)^3} W_{AB}(x, q)\,. \tag{2.154}$$

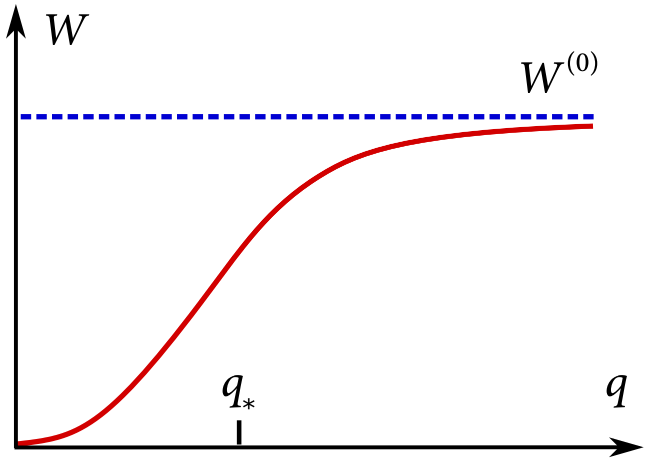

Figure 2.6: A schematic curve of $W(x,q)$ (in red color) that manifests the decomposition given by Eq. (2.155). $W^{(0)}$ is the equilibrium value (blue dashed line) achieved at large q. The gradient expansion at small $k/\gamma q^2$ gives rise to the part linear in gradient, $W^{(1)}$. The remaining part $\widetilde{W}$, in large part from the contributions of wavenumber modes around q_*, is the long-time tails discussed in Sec. 2.6.2. The feedback contributions from the small-q modes are suppressed by the phase space integration.

The corresponding decomposition of Eq. (2.148) in phase space is given by (see also Fig. 2.6)

$$W_{AB}(x,q) = W^{(0)}_{AB}(x,q) + W^{(1)}_{AB}(x,q) + \widetilde{W}_{AB}(x,q)\,. \tag{2.155}$$

The zeroth-order contribution $G^{(0)}_{AB}$ follows from the equilibrium solution to the fluctuation evolution equations given by Eq. (2.110)[15]. Since $W^{(0)}$ does not depend on q, the integration over q is divergent. We regularize this integral by the wavenumber cutoff $q < \Lambda$.

$$G^{(0)}_{AB}(x) = \int \frac{d^3q}{(2\pi)^3} W^{(0)}(x,q) = \frac{\Lambda^3}{6\pi^2}\mathrm{diag}\left(c_p T^2, Tw, Tw\Delta_{\mu\nu}\right)\,. \tag{2.156}$$

---

[15] The expression of $W^{(0)}_{AB}$ (and $G^{(0)}_{AB}$) depends on the frame choice. In the local rest frame defined by the renormalized velocity u_R, all relevant variables in Eq. (2.110) shall be renormalized accordingly to keep the form of $W^{(0)}_{AB}$ intact. However, as we shall see below, the non-renormalized expression of $W^{(0)}_{AB}$ is sufficient for our demand since it already appears as the correction to the bare quantities. Thus, the "correction of a correction" is in higher orders according to our scale hierarchy Eq. (2.29).

Though the tensor part of the two-point function, $G^{(0)\mu\nu}(x)$ appearing in Eq. (2.151) is cutoff-dependent, it is proportional to $\Delta_R^{\mu\nu}$, and thus is absorbed into the definition of the physical (renormalized) pressure. Combining this contribution with the contributions from the terms containing $\delta_R^{(0)}\varepsilon$ and $\delta_R^{(0)}n$ in Eq. (2.151) we find for the renormalized, i.e., physical, pressure (renormalized equation of state):

$$\begin{aligned}
p_R(\varepsilon_R, n_R) &= p(\varepsilon_R, n_R) + \frac{1-3\left(1-\frac{\varepsilon_m}{2Tn}\right)c_s^2}{3w}G^{(0)\mu}{}_{\mu} \\
&\quad + \frac{c_s^2 w}{2T^3n^4}\left(n_m\varepsilon_{mm} - \varepsilon_m n_{mm}\right)G^{(0)}_{mm} + \frac{c_s^4 w}{2Tn^2}\left(n_m\varepsilon_{pp} - \varepsilon_m n_{pp}\right)G^{(0)}_{pp} \\
&= p(\varepsilon_R, n_R) + \frac{2-3\left(c_s^2+\dot{T}\right)}{6w}G^{(0)\mu}{}_{\mu} + \frac{1-\dot{c}_p}{2c_pT}G^{(0)}_{mm} + \frac{c_s^2-\dot{T}+2\dot{c}_s}{2w}G^{(0)}_{pp} \\
&= p(\varepsilon_R, n_R) + \frac{T\Lambda^3}{6\pi^2}\left((1-c_s^2-2\dot{T}+\dot{c}_s) + \frac{1}{2}(1-\dot{c}_p)\right). \qquad (2.157)
\end{aligned}$$

where we used

$$n_m\varepsilon_{mm} - \varepsilon_m n_{mm} = \frac{T^2n^4}{c_s^2c_pw}(1-\dot{c}_p)\,, \quad n_m\varepsilon_{pp} - \varepsilon_m n_{pp} = \frac{Tn^2}{c_s^4w^2}(c_s^2-\dot{T}+2\dot{c}_s)\,, \qquad (2.158)$$

which can be derived by using Eq. (2.48) and (2.63). This procedure of defining the physical pressure that combines "bare" pressure with the effects of equilibrium fluctuations is similar to the standard renormalization procedure in quantum field theory. Having performed the renormalization of hydrodynamic variables and the equation of state, in what follows, for notational simplicity, we will drop the subscript R on hydrodynamic variables ε_R, n_R and u_R and thermodynamic functions such as p_R.

We now turn to the first-order terms in the gradient expansion given by Eq. (2.152). Since these terms are linear in gradients, they must be combined with the "bare" transport terms into the physical transport terms. It may seem that this procedure, similar to renormalization of pressure, is guaranteed to succeed. It indeed does, but this is not trivial because not all gradient (transport) terms are allowed by second law of thermodynamics. The fact that only those that are allowed arise from fluctuation emerges after delicate cancellations and is a nontrivial test of the conceptual validity of the framework we develop.

In the presence of background gradients, $W_{AB}(x,q)$ deviates from the equilibrium q-independent value given by Eq. (2.110). This Wigner function is a solution to Eq. (2.105) – a linear differential equation with coefficients linear in the gradients of velocity. As such, W_{AB} is a nonlocal functional of those gradients. The fact that allows us to remove divergences by redefining physical parameters (as in quantum field theories) is that the divergent contributions are simply *local* functions of the velocity gradients.

To derive the expressions for $W^{(1)}_{AB}(x,q)$, we begin with inserting the decomposition Eq. (2.155) into our main kinetic equation given in Eqs. (2.123) and (2.130). This substitution leads to an equation for $W^{(\text{neq})}_{\mathbf{AB}}(x,q)$ which we then expand to first order in gradients of the background flow. Because the kinetic equation already contains gradients of the leading term $W^{(0)}_{\mathbf{AB}}(x)$, we can use the ideal equations of motion to convert the time derivatives into spatial derivatives:

$$\begin{aligned}
u\cdot\partial(Tw) &= -\left(1+c_s^2+\dot{T}\right)Tw\theta\,, \quad u\cdot\partial(c_pT^2) = -c_pT^2(\dot{c}_p+2\dot{T})\theta\,,\\
\partial_{\perp\mu}(Tw) &= -Tw\left(\frac{1+2c_s^2}{c_s^2}+\left(1-\frac{\dot{T}}{c_s^2}\right)^2\frac{c_pT}{w}\right)a_\mu - T^2n\left(1+\left(1-\frac{\dot{T}}{c_s^2}\right)\frac{c_pT}{w}\right)\partial_{\perp\mu}\alpha\,.
\end{aligned} \tag{2.159}$$

In deriving these, we use thermodynamic relations given in Appendix B. Keeping only the terms that are linear in background gradients, the equations for $W^{(1)}_{\mathbf{AB}}$ can be solved as

$$\begin{gathered}
W^{(1)}_{L}(x,q) = \frac{Tw}{\gamma_L q^2}\left((\dot{T}-\dot{c}_s)\theta - \theta_{\mu\nu}\hat{q}^\mu\hat{q}^\nu + \frac{c_sTn}{w}\hat{q}\cdot\partial\alpha\right),\\
W^{(1)}_{mm}(x,q) = \frac{c_pT^2}{2\gamma_\lambda q^2}\left(\dot{c}_p-1\right)\theta\,, \quad W^{(1)}_{(i)m}(x,q) = W^{(1)}_{m(i)}(x,q) = \frac{c_pT^3n/w}{(\gamma_\eta+\gamma_\lambda)q^2}t^{(i)}\cdot\partial\alpha\,,\\
W^{(1)}_{(i)(j)}(x,q) = \frac{Tw}{2\gamma_\eta q^2}\left(\left(c_s^2+\dot{T}\right)\theta\,\delta^{ij} - 2\theta^{\mu\nu}t^{(i)}_\mu t^{(j)}_\nu\right).
\end{gathered} \tag{2.160}$$

Note that these expressions are given in the $(\mathbf{A},\mathbf{B})$ basis where $\mathbb{L}^{(q)}$ is diagonal and we need to convert them back into the (A,B) basis:

$$
\begin{aligned}
W_{AB} = \psi_A^{\mathbf{A}} W_{\mathbf{AB}} \psi_B^{\mathbf{B}} &= \begin{pmatrix} W_{mm} & W_{mp} & W_{m\nu} \\ W_{pm} & W_{pp} & W_{p\nu} \\ W_{\mu m} & W_{\mu p} & W_{\mu\nu} \end{pmatrix} \\
&= \begin{pmatrix} W_{mm} & 0 & W_{m(j)} t_\nu^{(j)} \\ 0 & \frac{1}{2}(W_{++} + W_{--}) & \frac{1}{2}(W_{++} - W_{--})\hat{q}_\nu \\ W_{(i)m} t_\mu^{(i)} & \frac{1}{2}(W_{++} - W_{--})\hat{q}_\mu & \frac{1}{2}(W_{++} + W_{--})\hat{q}_\mu \hat{q}_\nu + W_{(i)(j)} t_\mu^{(i)} t_\nu^{(j)} \end{pmatrix},
\end{aligned}
\tag{2.161}
$$

which finally gives $W_{AB}^{(1)}(x,q)$ in components,

$$
\begin{aligned}
&W_{mm}^{(1)}(x,q) = \frac{c_p T^2}{2\gamma_\lambda q^2}\left(\dot{c}_p - 1\right)\theta\,, \quad W_{pp}^{(1)}(x,q) = \frac{Tw}{\gamma_L q^2}\left((\dot{T} - \dot{c}_s)\theta - \theta_{\mu\nu}\hat{q}^\mu \hat{q}^\nu\right), \\
&W_{m\mu}^{(1)}(x,q) = W_{\mu m}^{(1)}(x,q) = \frac{c_p T^3 n/w}{(\gamma_\eta + \gamma_\lambda) q^2} t_\mu^{(i)} t^{(i)} \cdot \partial\alpha\,, \quad W_{p\mu}^{(1)}(x,q) = W_{\mu p}^{(1)}(x,q) = \frac{c_s T^2 n}{\gamma_L q^2}\hat{q}^\mu \hat{q} \cdot \partial\alpha\,, \\
&W_{\mu\nu}^{(1)}(x,q) = \frac{Tw}{\gamma_L q^2}\left((\dot{T} - \dot{c}_s)\theta - \theta_{\lambda\kappa}\hat{q}^\lambda \hat{q}^\kappa\right)\hat{q}_\mu \hat{q}_\nu + \frac{Tw}{2\gamma_\eta q^2}\left(\left(c_s^2 + \dot{T}\right)\theta\,\widehat{\Delta}_{\mu\nu} - 2\theta^{\lambda\kappa}\widehat{\Delta}_{\lambda\mu}\widehat{\Delta}_{\kappa\nu}\right),
\end{aligned}
\tag{2.162}
$$

where $\widehat{\Delta}_{\mu\nu} = \sum_{i=1}^{2} t_\mu^{(i)} t_\nu^{(i)} = \Delta_{\mu\nu} - \hat{q}_\mu \hat{q}_\nu$. With the help of the integrals

$$
\begin{gathered}
\int \frac{d^3q}{(2\pi)^3}\frac{1}{q^2} = \frac{\Lambda}{2\pi^2}, \quad \int \frac{d^3q}{(2\pi)^3}\frac{\hat{q}_\mu \hat{q}_\nu}{q^2} = \frac{\Lambda}{6\pi^2}\Delta_{\mu\nu}, \\
\int \frac{d^3q}{(2\pi)^3}\frac{\hat{q}_\lambda \hat{q}_\kappa \hat{q}_\mu \hat{q}_\nu}{q^2} = \frac{\Lambda}{30\pi^2}(\Delta_{\lambda\kappa}\Delta_{\mu\nu} + \Delta_{\lambda\mu}\Delta_{\kappa\nu} + \Delta_{\lambda\nu}\Delta_{\kappa\mu}),
\end{gathered}
\tag{2.163}
$$

the corresponding $G_{AB}^{(1)}(x)$ are given by

$$
G_{mm}^{(1)}(x) = \frac{c_p T^2 \Lambda}{4\pi^2 \gamma_\lambda}\left(\dot{c}_p - 1\right)\theta\,, \quad G_{pp}^{(1)}(x) = -\frac{Tw\Lambda}{6\pi^2\gamma_L}\left(1 - 3\dot{T} + 3\dot{c}_s\right)\theta\,, \tag{2.164a}
$$

$$
G_{m\mu}^{(1)}(x) = \frac{(c_p T^3 n/w)\Lambda}{3\pi^2(\gamma_\eta + \gamma_\lambda)}\partial_{\perp\mu}\alpha\,, \quad G_{p\mu}^{(1)}(x) = \frac{c_s T^2 n\Lambda}{6\pi^2\gamma_L}\partial_{\perp\mu}\alpha\,, \tag{2.164b}
$$

$$
G_{\mu\nu}^{(1)}(x) = -\frac{Tw\Lambda}{6\pi^2\gamma_L}\left(\left(\frac{1}{5} - \dot{T} + \dot{c}_s\right)\theta\Delta_{\mu\nu} + \frac{2}{5}\theta_{\mu\nu}\right) - \frac{Tw\Lambda}{60\pi^2\gamma_\eta}\left((2 - 10(c_s^2 + \dot{T}))\theta\Delta_{\mu\nu} + 14\theta_{\mu\nu}\right). \tag{2.164c}
$$

Finally we substitute the above expressions for $G^{(1)}$ into Eq. (2.152). The resulting contributions are linear in the gradients and have the same form as "bare" viscous terms in $\Pi^{\mu\nu}$

and diffusion term in ν^μ. Therefore they can be absorbed into the definitions of viscosities η, ζ and conductivity λ. After straightforward computation, we obtain the renormalized transport coefficients as

$$\eta_R = \eta + \frac{T\Lambda}{30\pi^2}\left(\frac{1}{\gamma_L} + \frac{7}{2\gamma_\eta}\right), \tag{2.165a}$$

$$\zeta_R = \zeta + \frac{T\Lambda}{18\pi^2}\left(\frac{1}{\gamma_L}(1 - 3\dot{T} + 3\dot{c}_s)^2 + \frac{2}{\gamma_\eta}\left(1 - \frac{3}{2}(\dot{T} + c_s^2)\right)^2 + \frac{9}{4\gamma_\lambda}(1 - \dot{c}_p)^2\right), \tag{2.165b}$$

$$\lambda_R = \lambda + \frac{T^2 n^2 \Lambda}{3\pi^2 w^2}\left(\frac{c_p T}{(\gamma_\eta + \gamma_\lambda)w} + \frac{c_s^2}{2\gamma_L}\right). \tag{2.165c}$$

A couple of comments are in order. First, all the gradients appearing in the expansion of $G^{(1)}$ are matched by the gradients appearing in the first-order terms in the constitutive equations, $\Pi^{\mu\nu}$ and ν^μ. For $\Pi^{\mu\nu}$, this is a simple consequence of the fact that, by construction, $\Pi^{\mu\nu}$ involves all gradients allowed by Lorentz symmetry, so nothing else could have appeared in Eqs. (2.164a) or (2.164c). However, this is less trivial in the case of the corrections to ν^μ. This is because there are *two* linearly independent gradient terms allowed by Lorentz symmetry alone, e.g., $\partial_\mu\alpha$ and $\partial_\mu p$, and, naively, any their linear combination could have appeared in the expression for $G^{(1)}$ in Eqs. (2.164b). However, precisely $\partial_\mu\alpha$ appears in Eqs. (2.164b), which allows us to absorb the fluctuation contribution into λ_R. Any other linear combination would require additional kinetic coefficient to absorb it. However, according to Eq. (2.26b) and discussions thereby, the second law of thermodynamics only allows the gradient $\partial_\mu\alpha$ to appear in ν^μ in order to guarantee the semi-positivity of entropy production rate. The way this constraint is respected by fluctuation contributions appears to be highly nontrivial, relying on delicate cancellations that result in rather elegant thermodynamic identities given by Eq. (2.158). Of course, we can view this as one of the many nontrivial checks of the consistency of this approach and the validity of the calculations.

Second, in a similarly remarkable deference to the second law of thermodynamics manifested in delicate cancellations, the correction to the bulk viscosity given in Eq. (2.165b) is nonnegative, consistent with Eq. (2.28). Also, as expected, but similarly achieved through nontrivial cancellations, the fluctuation corrections vanish in the conformal limit, where $c_s^2 = 1/3$ and $\varepsilon = 3p$, when bulk viscosity must vanish.

2.6.2 Long-time Tails

After all constitutive equations are expressed in terms of the physical, i.e., renormalized, variables, pressure and transport coefficients, the remaining contributions, denoted by $\widetilde{T}^{\mu\nu}$ are cutoff independent. This is very similar to renormalization in quantum field theory, and it works for a similar reason – the locality of the first-order hydrodynamics (similar to the locality of quantum field theory Lagrangian). On a more technical level, the gradient expansion in W_{AB} is accompanied by the expansion in $1/q^2$. This can be traced back to the power-counting scheme in which $k \sim q^2$. The terms of order k^2 are accompanied by $1/q^4$ leading to convergent integrals in $\widetilde{G}_{AB}$.

Thus, expressed in terms of physical quantities, the constitutive equations (2.150) do not contain UV divergences which could lead to cutoff dependence. Together with the conservation equations

$$\partial_\mu \langle \breve{T}^{\mu\nu}(x) \rangle = 0\,, \tag{2.166a}$$

$$\partial_\mu \langle \breve{J}^{\mu}(x) \rangle = 0\,, \tag{2.166b}$$

and the fluctuation evolution equations (2.123) and (2.124), they now form a closed set of cutoff-independent, deterministic equations that describe the evolution of the background flow, including the feedback of the fluctuating modes $\widetilde{W}$.

In principle this coupled system of equations can be solved numerically and nonlocal effects of long-time tails in an arbitrary background can be studied. We leave such a numerical study for future work. Instead, for the remainder of this section we will describe important analytical properties of the long-time tails in simple backgrounds by solving the fluctuation evolution equations (2.123).

A quick look at the evolution equations, (2.124) and (2.123) leads to the following "impressionistic" expression for the non-equilibrium part of the Wigner function:

$$W^{(\mathrm{neq})} \equiv W - W^{(0)} \sim \frac{\partial f}{\gamma q^2 + i(u+v)\cdot k + \partial f} \tag{2.167}$$

where $v = \pm c_s \hat{q}$ or 0 depending on which mode we are considering and γ and ∂f are schematic notations for the relaxation rate coefficients and terms linear in background gradients respectively. Note that $k \sim \partial$ and $u \cdot k = \omega$ is the frequency. After subtracting the term linear in the background gradients, which is absorbed into the definitions of renormalized transport coefficients, we obtain a schematic expression for the finite part of the Wigner function:

$$\widetilde{W} \sim \frac{\partial f}{\gamma q^2 + i(u+v)\cdot k + \partial f} - \frac{\partial f}{\gamma q^2} \sim \frac{(u+v)\cdot k}{\gamma q^2 + i(u+v)\cdot k + \partial f}\,\frac{\partial f}{\gamma q^2}\,. \tag{2.168}$$

This procedure could be viewed a a subtraction scheme that regulates the phase-space integral of the fluctuation modes where the local (and instantaneous) short distance term is subtracted. The integration over q leads to $\widetilde{G} \sim k^{1/2}\partial f/\gamma^{3/2} \sim k^{3/2}$ which is a nonlocal functional of the gradients [47]. Notice that $k^{3/2}$ in terms of gradient expansion lies in between k (first order, viscous terms) and k^2 (second order terms) After Fourier transformation these terms lead to power-law corrections which correspond to the long-time tails.

To be more quantitative, let us consider a special case and focus on the non-analytic ω dependence, by taking spatial k to zero for simplicity. This means that we only keep the k dependence for the background gradient term ∂f that is in the numerator of Eq. (2.167) which is consistent with the order of gradient expansion that we are working with. In other words we are looking at the frequency dependence of the transport coefficients. From Eq. (2.168) we see that the frequency dependence can be expressed as

$$\widetilde{W}(x,q) = W^{(1)}(x,q)\Big|_{\gamma q^2 \to \gamma q^2 - i\omega} - W^{(1)}(x,q)\,. \tag{2.169}$$

The contribution of the two-point functions to the constitutive relation for the charge current is given in Eq. (2.153b). We can calculate the relevant $\widetilde{W}(x,q)$ by using the substitution, Eq. (2.169), in Eq. (2.162). By plugging the resulting expression into Eq. (2.153b), we obtain

$$\begin{aligned}
\lambda(\omega)\partial_\perp^\mu\alpha &\equiv \lambda\partial_\perp^\mu\alpha + \frac{n}{w^2}\widetilde{G}^{m\mu}(x) + \frac{c_s n}{w^2}\widetilde{G}^{p\mu}(x)\\
&= \lambda\partial_\perp^\mu\alpha + i\omega\frac{c_pT^3n^2}{w^3}\partial_\perp^\nu\alpha\int_q \frac{\Delta_{\mu\nu}-\hat{q}_\mu\hat{q}_\nu}{((\gamma_\eta+\gamma_\lambda)q^2-i\omega)(\gamma_\eta+\gamma_\lambda)q^2}\\
&\quad + i\omega\frac{c_s^2T^2n^2}{w^2}\partial_\perp^\nu\alpha\int_q\frac{\hat{q}_\mu\hat{q}_\nu}{(\gamma_Lq^2-i\omega)\gamma_Lq^2}\,,
\end{aligned}$$

from which we find the frequency dependent conductivity, $\lambda(\omega)$, to be

$$\lambda(\omega) = \lambda - \omega^{1/2}\frac{T^2n^2}{w^2}\frac{(1-i)}{6\sqrt{2}\pi}\left(\frac{c_pT}{(\gamma_\eta+\gamma_\lambda)^{3/2}w} + \frac{c_s^2}{2\gamma_L^{3/2}}\right). \tag{2.170}$$

Here, λ denotes the *renormalized* value of the zero frequency conductivity. This result is consistent with the already known result for the special case of a conformal, boost invariant plasma with conserved charge given in Eq. (50b) in Ref. [50].

The frequency dependent viscosities can be computed in the same way. The fluctuation contributions to the viscous tensor is:

$$\begin{aligned}
\Pi^{\mu\nu}(\omega) &\equiv -2\eta(\omega)\left(\theta^{\mu\nu}-\frac{1}{3}\Delta^{\mu\nu}\theta\right) - \zeta(\omega)\theta\Delta^{\mu\nu}\\
&\equiv \Pi^{\mu\nu} + \frac{1}{w}\widetilde{G}^{\mu\nu}(x)\\
&+\frac{1}{2w}\left(\frac{(1-\dot{c}_p)w}{c_pT}\widetilde{G}_{mm}(x) + \left(c_s^2-\dot{T}+2\dot{c}_s\right)\widetilde{G}_{pp}(x) - \left(c_s^2+\dot{T}\right)\widetilde{G}^{\lambda}_{\lambda}(x)\right)\Delta^{\mu\nu},
\end{aligned} \tag{2.171}$$

where $\Pi^{\mu\nu}$ stands for $\Pi^{\mu\nu}(\omega=0)$. After substituting the ω dependence in Eq. (2.169) in Eq. (2.171) we obtain

$$\begin{aligned}
\Pi^{\mu\nu}(\omega) = \Pi^{\mu\nu} &+ i\omega T\int_q\left\{\frac{\left((\dot{T}-\dot{c}_s)\theta-\theta_{\lambda\kappa}\hat{q}^\lambda\hat{q}^\kappa\right)\hat{q}^\mu\hat{q}^\nu}{(\gamma_Lq^2-i\omega)\gamma_Lq^2} + \frac{\left(c_s^2+\dot{T}\right)\theta\,\widehat{\Delta}^{\mu\nu}-2\theta^{\lambda\kappa}\widehat{\Delta}^\mu_\lambda\widehat{\Delta}^\nu_\kappa}{(2\gamma_\eta q^2-i\omega)2\gamma_\eta q^2}\right\}\\
&+\frac{i\omega T}{2}\Delta^{\mu\nu}\int_q\left\{-\frac{(1-\dot{c}_p)^2\theta}{(2\gamma_\lambda q^2-i\omega)2\gamma_\lambda q^2} + \frac{\left(c_s^2-\dot{T}+2\dot{c}_s\right)\left((\dot{T}-\dot{c}_s)\theta-\theta_{\mu\nu}\hat{q}^\mu\hat{q}^\nu\right)}{(\gamma_Lq^2-i\omega)\gamma_Lq^2}\right.\\
&\qquad\left.-\left(c_s^2+\dot{T}\right)\left[\frac{(\dot{T}-\dot{c}_s)\theta-\theta_{\lambda\kappa}\hat{q}^\lambda\hat{q}^\kappa}{(\gamma_Lq^2-i\omega)\gamma_Lq^2} + \frac{2\left(c_s^2+\dot{T}\right)\theta-2\theta_{\lambda\kappa}\widehat{\Delta}_{\lambda\kappa}}{(2\gamma_\eta q^2-i\omega)2\gamma_\eta q^2}\right]\right\}
\end{aligned} \tag{2.172}$$

from which find the frequency dependent viscosities,

$$\begin{aligned}\eta(\omega) &= \eta - \omega^{1/2}T\frac{(1-i)}{60\sqrt{2}\pi}\left(\frac{1}{\gamma_L^{3/2}}+\frac{7}{(2\gamma_\eta)^{3/2}}\right),\\ \zeta(\omega) &= \zeta - \omega^{1/2}T\frac{(1-i)}{36\sqrt{2}\pi}\left[\frac{1}{\gamma_L^{3/2}}\left(1-3\dot{T}+3\dot{c}_s\right)^2+\frac{4}{(2\gamma_\eta)^{3/2}}\left(1-\frac{3}{2}(\dot{T}+c_s^2)\right)^2\right.\\ &\qquad\left.+\frac{9}{2(2\gamma_\lambda)^{3/2}}\left(1-\dot{c}_p\right)^2\right].\end{aligned} \tag{2.173}$$

Here, η and ζ denote the *renormalized* values of the zero frequency viscosities.

The experimental observation of long-time tails can be found in Ref. [105, 106].

2.7 Phonon Interpretation of the Hydro-kinetic Equation

2.7.1 Phonon Kinetic Equation

Consider a classical particle whose motion is described in terms of the space-time vector x^μ and 4-momentum p^μ with dispersion relation given by some condition $F(p) = 0$. For example, for a massive particle in vacuum $F = p^2 - m^2$. A phonon dispersion relation is given by $p^0 = E(\boldsymbol{p}) \equiv c_s|\boldsymbol{p}|$ in the rest frame of the fluid. This can be represented by

$$F_+(p) = p\cdot u + E(p_\perp), \tag{2.174}$$

where u is the the 4-velocity of the fluid rest frame $E = c_s|p_\perp|$ and

$$p_\perp^\mu = p^\mu + (p\cdot u)u^\mu. \tag{2.175}$$

The classical action can be then written as

$$S = \int (\, p\cdot dx - \lambda F_+\, d\tau\,) \tag{2.176}$$

where λ is a Lagrange multiplier. Variation of the action is given by:

$$\delta S = \int\left[\delta p_\mu\left(dx^\mu - \lambda\frac{\partial F_+}{\partial p_\mu}d\tau\right) + \delta x^\mu\left(-dp^\mu - \lambda\frac{\partial F_+}{\partial x^\mu}d\tau\right) - \delta\lambda F_+ d\tau\right] \tag{2.177}$$

Classical trajectory is then given by equations of motion

$$\dot{x}^\mu = \frac{\partial F_+}{\partial p_\mu} = u^\mu + v^\mu \tag{2.178}$$

where dot denotes $d/(\lambda d\tau)$ (or one can use reparametrization invariance to set $\lambda\tau$ to equal coordinate time x^0 in frame u) and

$$v^\mu = \frac{\partial E}{\partial p_\mu} = \Delta^\mu_\nu \frac{\partial E}{\partial p_{\perp\nu}} = c_s \hat{p}^\mu_\perp\,, \tag{2.179}$$

(where we used $\partial p_{\perp\nu}/\partial p_\mu = \Delta^\mu_\nu$) as well as

$$\dot{p}_\mu = -\frac{\partial F_+}{\partial x^\mu} = -p_\nu \partial_\mu u^\nu - \partial_\mu E \tag{2.180}$$

together with the condition $F_+ = 0$. We consider local properties of the fluid to be varying (sufficiently slowly) in space and time. I.e., $u^\mu = u^\mu(x)$, as well as $E = E(x, p_\perp)$, which in the case of a phonon means $c_s = c_s(x)$.

The corresponding Liouville operator acting on a function $\mathcal{N}(x,p)$ is given by

$$\mathcal{L}[\mathcal{N}] \equiv \dot{x}^\mu \frac{\partial \mathcal{N}}{\partial x^\mu} + \dot{p}^\mu \frac{\partial \mathcal{N}}{\partial p_\mu}\,. \tag{2.181}$$

Note that $\mathcal{L}[F_+] = 0$. This property is important because it allows us to restrict the 8-dimensional phase space to the 7-dimensional subspace defined by $F_+ = 0$, i.e., to consider functions of the form

$$\mathcal{N} = \delta(F_+) N(x, p_\perp)\,, \tag{2.182}$$

where N is the usual phase-space distribution function (of 7 variables only). In other words $\mathcal{L}[\delta(F_+)N] = \delta(F_+)\mathcal{L}[N]$.

In order to write the kinetic equation in terms of the distribution function $N(x, p_\perp)$ we need to express x derivatives in $\mathcal{L}[N]$ at fixed p ($\partial/\partial x^\mu$ in Eq. (2.181)) in terms of x derivatives at fixed $p_\perp$. These derivatives are not the same because the relationship between p and $p_\perp$ depends on x (via $u(x)$ in Eq. (2.175)). One finds

$$\frac{\partial N}{\partial x^\mu} = \bar{\nabla}_\mu N + (\partial_\mu p_{\perp\nu}) \frac{\partial N}{\partial p_{\perp\nu}}\,, \tag{2.183}$$

where we denoted by $\bar{\nabla}_\mu$ the x derivative at $p_\perp$ fixed [16]. Correspondingly, the last term in Eq. (2.180) should be written as

$$\partial_\mu E = \bar{\nabla}_\mu E + (\partial_\mu p_{\perp\nu}) v^\nu . \tag{2.184}$$

Similarly, the p derivatives at fixed x should be expressed as $p_\perp$ derivatives

$$\frac{\partial N}{\partial p_\mu} = \Delta^\mu_\nu \frac{\partial N}{\partial p_{\perp\nu}} . \tag{2.185}$$

Substituting Eqs. (2.178), (2.180), (2.184), (2.183) and (2.185) into Eq. (2.181) we find

$$\mathcal{L}[N] = (u+v)\cdot\bar{\nabla}N - \left[p_{\perp\nu}\partial_{\perp\mu}u^\nu + \bar{\nabla}_{\perp\mu}E + v^\nu(\partial_{\perp\mu}p_{\perp\nu} - \partial_{\perp\nu}p_{\perp\mu}) - (u\cdot\partial)p_{\perp\mu}\right]\frac{\partial N}{\partial p_{\perp\mu}} . \tag{2.186}$$

Finally, using $\partial_\mu p_{\perp\nu} = -E\partial_\mu u_\nu + u_\nu\partial_\mu(p\cdot u)$, we can write the Liouville operator as

$$\mathcal{L}[N] = (u+v)\cdot\bar{\nabla}N - \left[E(a_\mu + 2v^\nu\omega_{\nu\mu}) + p_{\perp\nu}\partial_{\perp\mu}u^\nu + \bar{\nabla}_{\perp\mu}E\right]\frac{\partial N}{\partial p_{\perp\mu}} \tag{2.187}$$

The expression in the square brackets is (the negative of) the force acting on the phonon. [17] The two terms in parentheses multiplied by E are easily recognized as the inertial force due to acceleration a and the Coriolis force due to rotation $\omega_{\mu\nu}$, respectively. The force $-p_{\perp\nu}\partial_{\perp\mu}u^\nu$ is easier to understand by considering isotropic Hubble-like expansion, i.e., such that $\partial_{\perp\mu}u^\nu = H\Delta^\nu_\mu$, where H is the rate of expansion (Hubble constant). This term then describes the rescaling of the momentum $p_\perp$ (stretching of the sound wave) due to expansion of the background medium, leading to the "red shift" of the phonon spectrum, similar to the photon red shift in the expanding universe. The last term is the force due to the dependence of energy on the location of the phonon via the coefficient c_s in its dispersion relation:

$$-\bar{\nabla}_{\perp\mu}E = \partial_{\perp\mu}c_s|p_\perp| . \tag{2.188}$$

---

[16] A more explicit definition involves projections p_a of $p_\perp$ on the local triad $p_{\perp\mu} = e^a_\mu p_a$, in terms of which $\bar{\nabla}_\mu N = \partial_\mu N + \mathring{\omega}^a_{\mu b} p_a \partial N/\partial p_b$ (cf. Eqs. (2.84), (2.85) and (2.99)). The projections p^a are kept fixed while taking x derivative, and connection term accounts for the rotation of the basis triad $e^a(x)$ which changes $p_\perp$ while p_a is fixed. Similarly, $p_\perp$ derivatives at fixed x are more explicitly written as $\partial/\partial p_{\perp\mu} = e^\mu_a\,\partial/\partial p_a$ (cf. Eq. (2.100)).

[17] One can also obtain this expression by taking the spatial projection of the rate of change of $p_\perp$, i.e., the force is $\Delta^\nu_\mu \dot{p}_{\perp\nu}$, and using equations of motion (2.178) and (2.180) together with Eq. (2.175).

Remarkably, upon changing the notation for the phonon momentum

$$p_\perp \to q\,, \tag{2.189}$$

the Liouville operator in Eq. (2.187) with $E = c_s|p_\perp|$ is identical to the one in Eq. (2.123) obtained using completely different (but apparently complementary) considerations. The two signs in front of c_s in Eq. (2.123) correspond to positive and negative frequency sound waves, or positive/negative energy solutions of the condition

$$F_+F_- \equiv (p\cdot u)^2 - E^2 = 0, \tag{2.190}$$

where $F_\pm = (p\cdot u) \pm E$ and the positive energy solution is given by $F_+ = 0$ in Eq. (2.174).

Curiously, for linear dispersion, $E = c_s|p_\perp|$, the condition in Eq. (2.190) can be written as $g^{\mu\nu}p_\mu p_\nu = 0$ using flow induced effective "metric tensor" $g^{\mu\nu} = -u^\mu u^\nu + c_s^2\Delta^{\mu\nu}$. Since $d(F_+F_-) = F_-dF_+ + F_+dF_-$ and $\delta(F) = \delta(F_+)/F_- + \delta(F_-)/F_+$, we see that the equations of motion localized on the $F_+ = 0$ surface are given by Eqs. (2.178) and (2.180) up to rescaling of proper time. On the other hand, the equations of motion with the constraint $F_+F_- = 0$ are given by

$$\dot{x}^\mu = \frac{1}{2}\frac{\partial(F_+F_-)}{\partial p_\mu} = g^{\mu\nu}p_\nu \quad , \quad \dot{p}_\mu = -\frac{1}{2}\frac{\partial(F_+F_-)}{\partial x^\mu} = -\frac{1}{2}(\partial_\mu g^{\alpha\beta})p_\alpha p_\beta\,, \tag{2.191}$$

from which one can derive the "geodesic" equation of motion by taking additional time derivative to the first equation and using these equations once more. From this point of view the forces in Eq. (2.187) can be viewed as "gravitational" forces.

Perhaps even more remarkably than the matching of the Liouville operators in Eqs. (2.187) and (2.123), the identification

$$W_\pm(x,q) = c_s|q|wN_\pm(x,q) \tag{2.192}$$

leads to nontrivial cancellation of the whole second line in Eq. (2.123) (i.e., of all terms proportional to the background gradients $\theta_{\mu\nu}$ and a^μ times $W_\pm$) leaving simply the relaxation term in Eq. (2.123):

$$\mathcal{L}_\pm[N_\pm] = -\gamma_L q^2(N_\pm - T/E)\,, \tag{2.193}$$

where $\mathcal{L}_\pm$ are different by the sign in front of c_s in Eq. (2.123). Note that the equilibrium value of $N_\pm$, $N_\pm^{(0)} = W_\pm^{(0)}/(c_s|p_\perp|w)$, equals T/E as expected for the low-energy limit of the phonon Bose-Einstein distribution function.

In contrast to Eqs. (2.123) for longitudinal modes which reduces to a simple form Eq. (2.193) upon rescaling given by Eq. (2.192), Eq. (2.124) for transverse modes cannot be simplified in this way. This may be related to the fact that there is no quasiparticle interpretation for these non-propagating, diffusive modes.

2.7.2 Phonon Contributions to Stress-Energy Tensor

It is also remarkable that certain contributions of the fluctuations to stress-energy tensor can be related directly to the stress-energy tensor of the phonon gas via Eq. (2.192). This provides a justification to the two-fluid picture (hydrodynamic fluid plus gas of phonons) which guided the original approach by Andreev [97].

Let us start with the expression for the stress tensor for one particle moving along a trajectory specified by $x(\tau)$:

$$T^{\mu\nu}_{(1)}(x) = \int d\tau \frac{1}{2}(p^\mu \dot{x}^\nu + p^\nu \dot{x}^\mu)\delta^4(x - x(\tau)). \tag{2.194}$$

This means for a gas of such particles with distribution functions $N_+(x, p_\perp)$ we have ('s' for 'sound'):

$$T^{\mu\nu}_{(s)}(x) = \int_{p_\perp} \frac{1}{2}(p^\mu \dot{x}^\nu + p^\nu \dot{x}^\mu)\, N_+(x, p_\perp). \tag{2.195}$$

Using equation of motion $\dot{x} = u + v$ (Eq. (2.178)) we obtain:

$$T^{\mu\nu}_{(s)} = \int_{p_\perp} \Big[E u^\mu u^\nu + \frac{1}{2}\left((p^\mu_\perp + E v^\mu)u^\nu + (\mu \leftrightarrow \nu)\right) + \frac{1}{2}(p^\mu_\perp v^\nu + (\mu \leftrightarrow \nu))\Big]\, N_+\,. \tag{2.196}$$

Using now $E = c_s|p_\perp|$ and $v^\mu = c_s \hat{p}^\mu_\perp$ for the phonon, we find:

$$T^{\mu\nu}_{(s)} = \int_{p_\perp} \left[c_s|p_\perp| u^\mu u^\nu + \frac{1 + c_s^2}{2}\left(p^\mu_\perp u^\nu + (\mu \leftrightarrow \nu)\right) + c_s|p_\perp|\, \hat{p}^\mu_\perp \hat{p}^\nu_\perp \right] N_+\,. \tag{2.197}$$

The first term gives the contribution of the phonon gas to the energy density:

$$\varepsilon_{(s)} = -T^{\mu\nu}_{(s)} u_\mu u_\nu = \int_p c_s|p_\perp| N_+\,. \tag{2.198}$$

This matches exactly the contribution of the sound mode fluctuations, i.e., $W_\pm$ terms in Eq. (2.161), to the energy density in Eq. (2.146) when we identify (as in Eq. (2.192)) $c_s|p_\perp|N_+ = W_+/w$ and use the relation $W_-(x,q) = W_+(x,-q)$.

Similarly, the last term in Eq. (2.197) gives the contribution of the phonon gas to the pressure:

$$p_{(s)} = \frac{1}{3}T^{\mu\nu}\Delta_{\mu\nu} = \frac{1}{3}\int_{p_\perp} c_s|p_\perp|N_+\,. \tag{2.199}$$

This matches exactly the contribution of the sound mode fluctuations ($W_\pm$ terms in Eq. (2.161)) to the pressure given by the last term in Eq. (2.151).

2.8 Discussion

In this chapter, we present the deterministic approach to fluctuation hydrodynamics for an arbitrary relativistic fluid carrying conserved U(1) charge. In QCD the relevant charge is the baryon number. Our ultimate goal is practical – a formalism which would allow to simulate heavy-ion collisions with dynamical effects of fluctuations, especially relevant for the QCD critical point search. We would like to emphasize that, despite its practical aim, this formalism is based on a systematic and *controllable* expansion, similar to the effective field theory formalism in quantum field theory. The expansion parameter in hydrodynamics is the ratio of the wavenumber $k = 1/L$ associated with background flow and density gradients to a microscopic scale which sets the scale of hydrodynamic coefficients and which we denote $1/\ell_{\text{mic}}$. This allows us to view hydrodynamics as an effective theory.

Instead of directly solving stochastic hydrodynamic equations, we convert them into a hierarchy of equations for equal-time correlation functions, which we truncate at two-point correlators. This truncation is controlled by the same expansion parameter as the gradient expansion in hydrodynamics. One can see how the relevant power counting emerges by considering the effects of fluctuations on the constitutive equations for stress tensor (or conserved current). In stochastic hydrodynamics the noise is local, i.e., it is only correlated inside a hydrodynamic cell, as reflected in the delta function value of the two-point noise correlator in Eq. (2.32). This locality is the source of short-distance singularities, similar to ultraviolet singularities in quantum field theories. Hydrodynamics is regulated by finiteness of the cell size, which we denote by $b \gg \ell_{\text{mic}}$, equivalent to wavenumber cutoff $\Lambda = 1/b$. As a function of this regulator, the square variance of the noise in each cell is proportional to Λ^3 – the regulated value of the delta function. This is, of course, the source of the cutoff dependent contribution to renormalized pressure in Eq. (2.157) and, as such, is not of physical relevance.

The physically consequential contribution comes from the fluctuations whose relaxation time is comparable to the evolution time of the background. Correspondingly, this scale, characterized by wavenumber q_*, can be estimated by the condition $\gamma q_*^2 \sim c_s k$. The effect of these fluctuations is the delayed or nonlocal response to perturbations of the background (such as long-time tails) and cannot be simply absorbed by renormalization of the local hydrodynamic parameters such as pressure or transport coefficients. Since $q_* \ll \Lambda$, the noise on these longer distance scales, $\ell_* = 1/q_*$, averages out and the magnitude of the fluctuations is effectively reduced by a factor $(b^3/\ell_*^3)^{1/2} = (q_*/\Lambda)^{3/2}$ – the inverse of the square root of the number of uncorrelated cells in a region of linear size ℓ_* – the familiar random walk factor. Therefore the physically relevant magnitude of the fluctuations, obtained by averaging over scales ℓ_* is given by $\Lambda^{3/2} \times (q_*/\Lambda)^{3/2} \sim q_*^{3/2} \sim k^{3/4}$. It is cutoff independent, of course. Therefore, the two-point correlator of these fluctuations contributes at order $k^{3/2}$, suppressed compared to first-order gradients, but more important than second order gradients. Similarly, the contribution of n-point functions, due to higher order nonlinearities in the constitutive equations, would come at order $k^{3n/4}$ One can see that the hierarchy of higher-point contributions is controlled by a power of k, or more precisely, a power of dimensionless parameter $k\ell_{\text{mic}} = \ell_{\text{mic}}/L \ll 1$.

The equations we derive form a closed set of deterministic equations which can be solved numerically. The one-point functions (averaged values of hydrodynamic variables) obey conservation equations (2.166). The constitutive equations (2.150) contain contributions $\widetilde{T}^{\mu\nu}$

and $\widetilde{J}^{\mu}$ which are given in terms of the subtracted two-point functions $\widetilde{G}$ in Eqs. (2.153). The unsubtracted two-point functions G are evaluated at coinciding points and therefore contain short-range singularities. When unsubtracted G are expressed in terms of the wavenumber integrals of the Wigner functions Eq. (2.154), these singularities appear as ultraviolet divergences which need to be subtracted. The unsubtracted Wigner functions are obtained by solving equations (2.123) and (2.130), rescaling according to Eqs. (2.122) and (2.128) and substituting into the matrix in Eq. (2.161). The subtraction of terms of zero and first order in gradients, $W^{(0)}$ and $W^{(1)}$, given by Eqs. (2.110) and (2.162) respectively, can be done analytically, and either before or after solving equations (2.123) and (2.130), depending on numerical efficiency. The resulting solutions to one-point and two-point equations will describe evolution of the average hydrodynamic variables, their fluctuations, as well as the feedback of the fluctuations on the evolution of average quantities.

As usual, numerical implementation of *relativistic* hydrodynamic equations is hindered by well-known causality and stability issues which, in ordinary hydrodynamics *without fluctuations*, can be addressed by adding non-hydrodynamic degrees of freedom with relaxation dynamics, as reviewed in Ref. [101] (see also interesting recent developments in Refs. [107, 108, 109]). In a nutshell, the approach amounts to modification of the equations in the domain (characterized by large gradients) where hydrodynamic description is not applicable. As such these modifications are inconsequential from the point of view of physics, but make the equations mathematically well-posed and suitable for numerical implementation [110]. The hydrodynamic equations we obtained in this work will require a similar treatment before they can be implemented numerically. It is reasonable to expect that the approaches which work for non-fluctuating hydrodynamics will also work in this case. The additional equations for the Wigner functions introduced in our formalism describe *relaxation* (as opposed to relativistically problematic diffusion) and, as such, should not lead to causality/stability problems. Moreover, it is also reasonable to expect that the relaxation dynamics of fluctuations could improve (if not solve) the stability problems, similar to the way relaxational dynamics of fluxes in Israel-Stewart approach achieve this. We expect that these issues will be addressed by future research.

Chapter 3

Dynamics of Critical Fluctuations

This chapter contains materials published in

- X. An, G. Basar, M. Stephanov and H.-U. Yee, *Relativistic Hydrodynamic Fluctuations*, Phys. Rev. C **100** no. 2, (2019) 024910, arXiv:1902.09517 [hep-th] [1]. Copyright (2019) by the American Physical Society (APS).
- X. An, G. Basar, M. Stephanov and H.-U. Yee, *Fluctuation dynamics in a relativistic fluid with a critical point*, accepted by Phys. Rev. C, arXiv:1912.13456 [hep-th] [2]. Copyright (2020) by the American Physical Society (APS).
- X. An, *Fluctuation dynamics in a relativistic fluid with a critical point*, accepted by Nucl. Phys. A, arXiv:2003.02828 [hep-th] [3]. Copyright (2020) by authors.

In the preceding chapter we saw that kinetic coefficients, ζ, η and λ receive contributions from fluctuations. These contributions are dominated by the fluctuations at the cutoff scale Λ and therefore depend on the cutoff.

In this chapter we consider the physics of fluctuations at the critical point. The main feature of the critical point is that the equilibrium correlation length of the fluctuations, ξ, becomes infinite. To maintain the separation between the hydrodynamic scales $L \sim k^{-1}$ and microscopic scales, such as ξ, we must limit the domain of applicability of hydrodynamic description to wave-vectors $k \ll \xi^{-1}$. However, as emphasized in Ref. [39], this does not mean that hydrodynamics applies until $k \sim \xi^{-1}$. Instead, hydrodynamics breaks down before k reaches that limitation. Hydrodynamics breaks down when the frequency of the fastest hydrodynamic mode (the sound, with $\omega \sim c_s k$) reaches the rate of the relaxation of the slowest non-hydrodynamic mode. Near the critical point this rate vanishes much faster than ξ^{-1}.

The slowest non-hydrodynamic variable at the critical point is the fluctuation of the slowest hydrodynamic mode (diffusive mode m), given by N_{mm}. The relaxation rate depends on q and equals $2\gamma_\lambda q^2$ for $q \ll \xi^{-1}$. Because the contribution of the fluctuations to pressure and kinetic coefficient is UV divergent, it is dominated by the modes near the cutoff, which in the case of the critical point is effectively $\Lambda \sim \xi^{-1}$. Thus the characteristic rate of non-hydrodynamic relaxation, Γ_ξ, is of order $\gamma_\lambda \xi^{-2}$. Together with the fact that γ_λ vanishes as a power of ξ, i.e., to a good approximation $\gamma_\lambda \sim \xi^{-1}$, [1] we find that the hydrodynamic breaks down already when the frequency reaches $\omega \sim \xi^{-3}$. For the sound modes this corresponds to $k \sim \xi^{-3}$, much earlier than ξ^{-1}.

To extend hydrodynamics past $k \sim \xi^{-3}$ we need to include the slowest non-hydrodynamic mode, which is the idea behind Hydro+ [39]. In our notations this mode (or modes, labeled by index q) is N_{mm}. In this section we intend to show that in the regime $k > \xi^{-3}$ our formalism reproduces Hydro+. This is a nontrivial check because Hydro+ formalism was derived in Ref. [39] using a completely different approach by considering a generalized entropy which depends on the non-hydrodynamic variables (2PI entropy).

The formalism of Hydro+, while extending ordinary hydrodynamics beyond the scales $k \sim \xi^{-3}$, in turn, also breaks down well before k reaches $k \sim \xi^{-1}$. The breakdown occurs when the frequency reaches the relaxation rate Γ'_ξ of the next-to-slowest nonhydrodynamic mode. This mode (or modes) are the fluctuations of velocity transverse to the wave-vector. This relaxation rate is of order $\gamma_\eta q^2$ at $q \ll \xi^{-1}$. Again, the dominant contribution comes from modes at $q \sim \xi^{-1}$ and, since γ_η to a good approximation can be treated as finite at the critical point [66], Hydro+ breaks down when frequency reaches $\omega \sim \Gamma'_\xi \sim \xi^{-2}$, which for the sound modes corresponds to $k \sim \xi^{-2}$. Near the critical point this scale is still much lower than ξ^{-1}.

---

[1] This can be easily estimated from Eq. (2.165c). The contribution of fluctuations which dominates at the critical point is in the term proportional to c_p, i.e., $\lambda_R \sim \Lambda c_p$. Given that $c_p \sim \xi^2$ and $\Lambda \sim \xi^{-1}$, we find $\lambda \sim \xi^1$ and $\gamma_\lambda \sim \lambda / c_p \sim \xi^{-1}$. We neglected the critical exponent η_x ($c_p \sim \xi^{2-\eta_x}$) and the divergence of the shear viscosity $\eta \sim \xi^{x_\eta}$ (an error of less than 10%). Taking those into account, we would obtain the exact relation for the exponent x_λ, defined by $\lambda \sim \xi^{x_\lambda}$: $x_\lambda = d - 2 - x_\eta - \eta_x$ (cf. Ref. [66]). Since $\Gamma_\xi \sim \gamma_\lambda \xi^{-2}$, the standard dynamical critical exponent z defined as $\Gamma_\xi \sim \xi^{-z}$ is related to x_λ as $z = 4 - \eta_x - x_\lambda$.

In our formalism the next-to-slowest modes responsible for the breakdown of Hydro+ are $N_{m(i)}$ and $N_{(i)(j)}$ (normalized Wigner functions obeying Eqs. (2.130b) and (2.130c)). Therefore, within our formalism we can extend Hydro+ beyond its limit at $k \sim \xi^{-2}$. In Section 3.2 we shall describe how to do that. Prior to that, in Section 3.1, we shall verify that in the regime where Hydro+ is applicable, it is in agreement with our more general formalism.

3.1 Hydro+

While the framework of hydrodynamics for describing an ideal (non-dissipative) system is well known, the presence of the gradients brings the system out of equilibrium, or more precisely, the non-equilibrium hydrodynamic variables shall be approximated by the gradient expansion series, with an expansion parameter characterized by Knudsen number which satisfies $K_n \sim \ell_{\text{mic}}/L \leq 1$ [2], a constraint for near-equilibrium hydrodynamics (cf. Sec. 2.1). Such constraint manifested in the ordinary hydrodynamics is not always applicable in a realistic system, one such case is what we are considering here: a fluid with a critical point. Let's consider the bulk viscous term in Eq. (2.26a), where the non-equilibrium correction to pressure is proportional to the bulk viscosity ζ. Away from the critical point, $\zeta \sim \ell_{\text{mic}}$ is much smaller than L, however, due to the critical slowing down, ζ diverges near the critical point as ξ^3, manifesting the breakdown of gradient expansion since $K_n \gg 1$. The non-equilibrium corrections of fluctuations to the background quantities (such as pressure) also demand a dynamic description for their relaxation processes responsible for the critical slowing-down. Such corrections should be considered as an consequence of adding an additional mode (or modes labeled by q) of an extended hydrodynamic framework called *Hydro+*.

---

[2] Recently a frame work of far from equilibrium hydrodynamics is established.

The main ingredient of Hydro+ is the entropy density $s_{(+)}$ of the system in partial equilibrium state where a non-hydrodynamically slow variable φ, or more generally, a set of variables φ_q indexed by a discrete or continuous index q is not equal to the equilibrium value $\varphi_q^{(0)}(\varepsilon, n)$ for given ε and n. For brevity of notations we shall denote such a set of variables by a bold letter, similar to a vector with components φ_q:

$$\boldsymbol{\varphi} \equiv \{\varphi_q\}\,. \tag{3.1}$$

The equations of motion for $\boldsymbol{\varphi}$ describe relaxation to equilibrium (maximum of $s_{(+)}$) accompanied, in general, by dilution due to expansion:

$$u \cdot \partial \boldsymbol{\varphi} = -\boldsymbol{F}_\varphi - \boldsymbol{A}_\varphi \theta\,. \tag{3.2}$$

Second law of thermodynamics requires $(F_\varphi)_q = \sum_{q'} \gamma_{qq'} \pi_{q'}$ with semi-positive-definite γ where π_q is the thermodynamic “force” defined, as usual, via

$$ds_{(+)} = \beta_{(+)} d\varepsilon - \alpha_{(+)} dn - \boldsymbol{\pi} \cdot d\boldsymbol{\varphi}\,, \tag{3.3}$$

where $\boldsymbol{\pi} \cdot \boldsymbol{\varphi} = \sum_q \pi_q \varphi_q$. The coefficient A_φ in Eq. (3.2) describes the response of the variable φ to the expansion or compression of the fluid (since $\theta = \partial \cdot u$ is the expansion rate). [3]

The hydrodynamic variables ε and u obey, as usual, equations of the energy-momentum conservation. The equation of state enters into constitutive equations

$$T^{\mu\nu} = \varepsilon u^\mu u^\nu + p_{(+)} \Delta^{\mu\nu} + \Pi^{\mu\nu} \tag{3.4}$$

---

[3] For comparison, we can also cast evolution of hydrodynamic variables or, in general, any function of ε and n, in the form of Eq. (3.2). In this case $F_\varphi = 0$ and $A_\varphi = \varphi\dot{\varphi}$. For example, for charge density n: $A_n = n$, since $\dot{n} = 1$, – the density changes proportionally with inverse volume, while for the ratio $m = s/n$, $A_m = 0$, since $\dot{m} = 0$.

via pressure $p_{(+)}$ which, as a function of ε, n, and φ, is given by the Legendre transform of $s_{(+)}$:

$$\beta_{(+)}p_{(+)} = s_{(+)} - \beta_{(+)}\varepsilon + \alpha_{(+)}n + \boldsymbol{\pi}\cdot\boldsymbol{A}_{\varphi}\,. \tag{3.5}$$

This relationship between pressure and entropy is dictated by the second law of thermodynamics [39].

Near equilibrium, the deviation of the entropy $s_{(+)}(\varepsilon, n, \varphi)$ from the equilibrium value $s(\varepsilon, n)$ is quadratic in $\boldsymbol{\pi}$, since entropy is maximized in equilibrium. The deviation of pressure $p_{(+)}$ from equilibrium p is linear in π,

$$p_{(+)} = p + \boldsymbol{p}_{\pi}\cdot\boldsymbol{\pi} + \mathcal{O}(\pi^2)\,. \tag{3.6}$$

The coefficient p_π can be expressed (see Appendix B in Ref. [39]) using Eqs. (3.3) and (3.5), in terms of the equilibrium value of φ at given ε and n, which we denote by $\varphi^{(0)}(\varepsilon, n)$, as

$$\beta\boldsymbol{p}_{\pi} = -w\left(\frac{\partial\boldsymbol{\varphi}^{(0)}}{\partial\varepsilon}\right)_n - n\left(\frac{\partial\boldsymbol{\varphi}^{(0)}}{\partial n}\right)_\varepsilon + \boldsymbol{A}_{\varphi} = -s\left(\frac{\partial\boldsymbol{\varphi}^{(0)}}{\partial s}\right)_m + \boldsymbol{A}_{\varphi} = -\boldsymbol{\varphi}^{(0)}(\boldsymbol{\varphi}^{(0)})^{\boldsymbol{\cdot}} + \boldsymbol{A}_{\varphi}\,. \tag{3.7}$$

We wish to show that the constitutive equations in Hydro+ with generalized pressure $p_{(+)}$ are in agreement with the equations we derived by expanding to quadratic order in fluctuations, such as Eq. (2.150).

Application of the Hydro+ approach near the critical point consists of considering the two-point correlation function of the slowest mode ($m \equiv s/n$): $\varphi \sim \langle\delta m\delta m\rangle$. Essentially, using our notations

$$\varphi_q(x) = N_{mm}(x, q)\,. \tag{3.8}$$

Due to the reparametrization invariance of Hydro+ (see Appendix C in Ref. [39]), either choice, N_{mm} or W_{mm}, different by a normalization factor in Eq.(2.128), will lead to the same result. The choice of N_{mm} is convenient because in this case the compression coefficient vanishes: $A_\varphi = 0$ (see Eq. (2.130a)).

In order to find non-equilibrium correction to Hydro+ pressure in Eq. (3.6) we need to use the expression for the non-equilibrium contribution to entropy, Eq. (1.79), rewritten here as

$$s^{(\mathrm{neq})} \equiv s_{(+)} - s = \frac{1}{2}\int_q \left(\log \frac{N_{mm}}{N^{(0)}_{mm}} - \frac{N_{mm}}{N^{(0)}_{mm}} + 1\right) \tag{3.9}$$

to determine π:

$$\pi_q \equiv -\frac{\partial s_{(+)}}{\partial \varphi_q} = \frac{1}{2}\left(\frac{1}{N^{(0)}_{mm}} - \frac{1}{N_{mm}}\right) = \frac{1}{2}\big(N^{(0)}_{mm}\big)^{-2} N^{(\mathrm{neq})}_{mm} + \mathcal{O}(N^{(\mathrm{neq})}_{mm})^2\,, \tag{3.10}$$

where

$$N^{(\mathrm{neq})}_{mm} \equiv N_{mm} - N^{(0)}_{mm}\,. \tag{3.11}$$

The equilibrium value $N^{(0)}_{mm}$ of N_{mm} also determines the value of p_π via equation (3.7) with $\varphi^{(0)}$ replaced by $N^{(0)}_{mm}$ and $A_\varphi = 0$. Putting this together we find, to linear order in $N^{(\mathrm{neq})}_{mm}$,

$$p^{(\mathrm{neq})} \equiv p_{(+)} - p = -\frac{T}{2}\int_q \big(N^{(0)}_{mm}\big)^{-1} \dot{N}^{(0)}_{mm} N^{(\mathrm{neq})}_{mm} = \frac{nT}{2c_p}(1-\dot{c}_p)\int_q N^{(\mathrm{neq})}_{mm} = \frac{1-\dot{c}_p}{2c_pT} G^{(\mathrm{neq})}_{mm} \tag{3.12}$$

where we used $N^{(0)}_{mm} = c_p/n$, which follows from Eq. (2.110) and (2.128) (and can be seen in Eq. (2.130a)) together with the property of the log-derivative, Eq. (2.46).

We should compare this to the non-equilibrium contribution to pressure from N_{mm} (which is dominant near critical point due to being proportional to c_p) in Section 2.6:

$$p^{(\mathrm{neq})} = \left(\frac{\partial p}{\partial \varepsilon}\right)_n (\delta_R\varepsilon - \delta^{(0)}_R\varepsilon) + \left(\frac{\partial p}{\partial n}\right)_\varepsilon (\delta_R n - \delta^{(0)}_R n) = \frac{1-\dot{c}_p}{2c_pT} G^{(\mathrm{neq})}_{mm}\,, \tag{3.13}$$

which is similar to equilibrium contribution (renormalization of static pressure) found in Eq. (2.157) with index '(0)' replaced by '(neq)'. One can see that Hydro+ reproduces these non-equilibrium contributions exactly. We emphasize that this is a very nontrivial cross-check, involving an elaborate thermodynamic identity for third derivatives of entropy in Eq. (2.158). This is in contrast to Ref. [39], where Hydro+ formalism emerged via a very different route, starting from the derivation of the non-equilibrium entropy functional $s^{(+)}$ in Eq. (3.9).

3.2 Hydro++

3.2.1 Equations for Hydro++

Since, as we already discussed above, the fluctuation contributions are dominated by the modes near the cutoff Λ, and for critical fluctuations the role of this cutoff is played by ξ^{-1}, the contributions responsible for the breakdown of ordinary hydrodynamics and of Hydro+ are dominated by fluctuations at scale $q \sim \xi^{-1}$. These modes themselves cannot be described by ordinary hydrodynamics. The dynamics of these modes is essentially nonlinear and nonlocal (often referred to as mode-coupling phenomenon). However, this dynamics is universal in the sense of universality of dynamical critical phenomena and is described by model H in the classification of Ref. [66]. We shall, therefore, use the known results from this universality class to describe the dynamics of these fluctuation modes.

Near the critical point, where the correlation length ξ greatly exceeds all other *microscopic* scales, the description simplifies due to (static and dynamic) scaling. That means the relaxation rates, even though no longer polynomial in q, as in the hydrodynamic regime where gradient expansion applies, depend on the q and ξ via functions of only the dimensionless combination $q\xi$ (times a power of ξ). Furthermore, these functions (and the powers of ξ) are universal, i.e., independent of the microscopic composition or properties of the system close to the critical point in a given universality class. The universality class relevant for our discussion is that of model H, defined in Ref. [66] as *dynamic* universality class of liquid-gas phase transitions.

As we already said, the fluctuation kinetic equations, such as (2.130), do not apply in the regime $q\xi \sim 1$ as they are. However, a modification of these equations, to match the known results from model H is possible and shall be described below. We must emphasize, that unlike the formalism derived in the preceding sections, which was exact to a certain order in a systematic expansion, here our out goal is to provide the formalism which reproduces the physics of critical point fluctuations correctly, but not necessarily exactly. For once, the exact description would at a minimum require exact solution to model H, which is not available. Our approximation is essentially equivalent to a one-loop approximation introduced by Kawasaki in Ref. [111], which is known to be in good quantitative agreement with experimental data [66]. Similarly to Hydro+ formalism, the purpose of the new extended formalism, which we shall refer to as Hydro++ in this thesis, is to provide a practical way of simulating the dynamics near the critical point, e.g., in heavy-ion collisions.

There are two main modifications required. First of all, we need to modify equation for N_{mm} to make sure that the equilibrium correlation function has finite correlation length ξ. Thus, the delta-function approximation in Eq. (1.96) at $\xi \ll L$ is no longer valid, and one has to use the Yukawa form given by Eq. (1.97), i.e., $N^{(0)}_{mm}(x, q)$ must depend on momentum q. We shall express this as

$$N^{(0)}_{mm} = \frac{c_p(q)}{n} \tag{3.14}$$

where we defined function $c_p(q)$ in such a way that $c_p(0) = c_p$ is the usual thermodynamic quantity (heat capacity at constant pressure). In this work we adopt the simple approximation for the momentum dependence provided by Eq. (1.97):

$$c_p \to c_p(q) = \frac{c_p}{1 + (q\xi)^2}\,. \tag{3.15}$$

This is known as Ornstein-Zernike form and is consistent with other approximations we are making.[4] A more sophisticated form and a better approximation to the exact correlation function (which is not known exactly as of this writing[5]) can be used if necessary, see Ref. [39].

The second essential modification is required to correctly describe relaxation rate of the slowest non-hydrodynamic mode, N_{mm}. The critical contribution, $\sim \xi^{-1}$ dominates near the critical point. It is given in terms of the Kawasaki function

$$K(x) = \frac{3}{4x^2}\left[1 + x^2 + \left(x^3 - x^{-1}\right)\arctan x\right] = 1 + \mathcal{O}(x^2)\,. \tag{3.16}$$

---

[4] Such as $c_p \sim \xi^2$ instead of $c_p \sim \xi^{2-\eta_x}$.

[5] It is the correlation function of the 3d Ising model.

Such modification results from the nonlocal contribution of the gradient $\partial_\perp\alpha$ to the conductivity λ, i.e.,

$$\partial_\perp^\mu \alpha(x) \to \partial_\perp^\mu \alpha(x,q) = \int d^3y e^{-iq\cdot y}\frac{e^{-|y|/\xi}}{4\pi|y|\xi^2}\partial_\perp^\mu\alpha(x+y), \tag{3.17}$$

which reduces to $\partial_\perp^\mu\alpha$ by replacing the Yukawa kernel by the delta function. In other words, the feedback of the charge conduction due to the perturbative source $\partial_\perp\alpha$ is no longer local, instead, it is a superposition of all contributions of such sources from the correlated volume ξ^3 around x. As a consequence, the expression $W^{(1)}_{m(i)}$ and $W^{(1)}_{m\mu}$ given by Eq. (2.160) and (2.162) shall be modified accordingly and finally (cf. Eq (2.164))

$$\begin{aligned}
G^{(1)}_{m\mu}(x) &= \frac{(c_pT^3n/w)\Lambda}{3\pi^2(\gamma_\eta+\gamma_\lambda)}\partial_{\perp\mu}\alpha\,, \\
G^{(1)}_{m\mu}(x) &= \int\frac{d^3q}{(2\pi)^3}W^{(1)}_{m\mu}(x,q) = \int\frac{d^3q}{(2\pi)^3}W^{(1)}_{m(i)}t^{(i)}_\mu \\
&= \int\frac{d^3q}{(2\pi)^3}\frac{c_pT^3n/w}{\gamma_\eta q^2}t^{(i)}_\mu\int d^3y e^{-iq\cdot y}\frac{e^{-|y|/\xi}}{4\pi|y|\xi^2}t^{(i)}\cdot\partial\alpha(x+y) \\
&= \frac{c_pT^3n}{\gamma_\eta w}\int\frac{d^3qd^3p}{(2\pi)^6}\frac{\Delta_{\mu\nu}-\hat q_\mu\hat q_\nu}{q^2(1+(p\xi)^2)}\int d^3y e^{i(p-q)\cdot y}\partial^\nu_\perp\alpha(x+y) \\
&= \frac{c_pT^3n}{\gamma_\eta w}\int\frac{d^3qd^3p}{(2\pi)^6}e^{i(q-p)\cdot x}\frac{i(q-p)^\nu(\Delta_{\mu\nu}-\hat q_\mu\hat q_\nu)}{q^2(1+(p\xi)^2)}\widetilde\alpha(q-p) \\
&= \frac{c_pT^3n}{\gamma_\eta w}\int\frac{d^3pd^3q}{(2\pi)^6}e^{ip\cdot x}\frac{i(p_\mu-\hat q\cdot p\hat q_\mu)}{(1+((p+q)\xi)^2)q^2}\widetilde\alpha(p) \\
&= \frac{c_pT^3n}{\gamma_\eta w}\int\frac{d^3p}{(2\pi)^3}e^{ip\cdot x}\int\frac{d^3q}{(2\pi)^3}\frac{q^2-(q\cdot\hat p)^2}{(1+((p+q)\xi)^2)q^4}ip_\mu\widetilde\alpha(p) \\
&= \frac{c_pT^3n}{\gamma_\eta w}\int\frac{d^3p}{(2\pi)^3}e^{ip\cdot x}ip_\mu\widetilde\alpha(p)\int\frac{dq}{(2\pi)^3}\frac{q^2}{1+(q\xi)^2}\int d\Omega\frac{|q\times\hat p|^2}{(q-p)^4} \\
&= \frac{c_pT^3n}{\gamma_\eta w}\int\frac{d^3p}{(2\pi)^3}e^{ip\cdot x}ip_\mu\widetilde\alpha(p)\int_0^\infty\frac{dq}{(2\pi)^3}\frac{q^2}{1+(q\xi)^2}\frac{\pi}{p^2}\left[\frac{q^2+p^2}{2qp}\ln\left(\frac{q+p}{q-p}\right)^2-2\right] \\
&= \frac{c_pT^3n}{6\pi\gamma_\eta w\xi}\int\frac{d^3p}{(2\pi)^3}e^{ip\cdot x}\frac{K(p\xi)}{1+(p\xi)^2}ip_\mu\widetilde\alpha(p) = \frac{c_pT^3n}{6\pi\gamma_\eta w\xi}\int\frac{d^3p}{(2\pi)^3}e^{ip\cdot x}K_\lambda(p\xi)ip_\mu\widetilde\alpha(p) \\
&= \frac{c_pT^3n}{6\pi\gamma_\eta w\xi}\int d^3\left(\frac{x'}{\xi}\right)\widetilde K_\lambda\left(\frac{x-x'}{\xi}\right)\partial_{\perp\mu}\alpha(x'),
\end{aligned} \tag{3.18}$$

where we have introduced

$$K_\lambda(x) = \frac{K(x)}{1+x^2} \tag{3.19}$$

identified as the weight kernel of the nonlocal contribution to $G^{(1)}_{m\mu}(x)$ and hence λ:

$$\lambda(q) \approx \lambda_0 + \frac{n}{w^2}\frac{c_p T^3 n}{6\pi\eta\xi}K_\lambda(q\xi) \tag{3.20}$$

where we have neglected the contribution from $G^{(1)}_{p\mu}(x)$, which is less dominant compare to the contribution from $G^{(1)}_{m\mu}(x)$ near the critical point. Meanwhile, we also keep the noncritical contribution λ_0. Using $\gamma_\lambda = \kappa/c_p$, we also have similar expression for the heat conductivity:

$$\kappa(q) \approx \kappa_0 + \frac{c_p T}{6\pi\eta\xi}K_\lambda(q\xi)\,. \tag{3.21}$$

The latter increases with ξ as $\kappa \sim \xi$ (in Kawasaki approximation). Finally, we can write for the q-dependent rate

$$\Gamma(q) \equiv 2\gamma_\lambda(q)q^2 = 2\frac{\kappa(q)}{c_p(q)}q^2 = 2\left(\frac{\kappa_0}{c_p(q)} + \frac{T}{6\pi\eta\xi}K(q\xi)\right)q^2. \tag{3.22}$$

Note that at small q, i.e., $q\xi \ll 1$, the rate is given by twice the diffusion rate $\gamma_\lambda q^2$.

With these two modifications, the equations for Hydro++ we propose read:

$$\mathcal{L}[N_{mm}] = -\,2\gamma_\lambda(q)q^2\left(N_{mm} - \frac{c_p(q)}{n}\right) - \frac{n}{w}t^{(i)}\cdot\partial m\left(N_{(i)m} + N_{m(i)}\right), \tag{3.23a}$$

$$\begin{aligned}\mathcal{L}[N_{m(i)}] = &-\left(\gamma_\eta + \gamma_\lambda(q)\right)q^2 N_{m(i)} \\ &- \partial^\nu u^\mu t^{(i)}_\mu t^{(j)}_\nu N_{m(j)} - \frac{n}{w}t^{(j)}\cdot\partial m N_{(j)(i)} + Tn\left(\frac{1}{c_p(q)}t^{(i)}\cdot\partial m + \frac{T}{w}t^{(i)}\cdot\partial\alpha\right)N_{mm}\,,\end{aligned} \tag{3.23b}$$

$$\begin{aligned}\mathcal{L}[N_{(i)(j)}] = &-\,2\gamma_\eta q^2\left(N_{(i)(j)} - \frac{Tw}{n}\delta_{ij}\right) \\ &- \partial^\nu u^\mu\left(t^{(i)}_\mu t^{(k)}_\nu N_{(k)(j)} + t^{(j)}_\mu t^{(k)}_\nu N_{(i)(k)}\right) + \frac{\alpha_p T^2 n}{w}\partial^\mu p\left(t^{(i)}_\mu N_{m(j)} + t^{(j)}_\mu N_{(i)m}\right),\end{aligned} \tag{3.23c}$$

where again, $\alpha_p = (1 - \dot{T}/c_s^2)/Tn$. The function $\gamma_\lambda(q)$ is defined in Eq. (3.22). The presence of function $c_p(q)$, defined in Eq. (3.15), in Eq. (3.23b) ensures important property of $N_{m(i)}$ in equilibrium – proportionality to $\partial\alpha$, which follows from the second law of thermodynamics as we already discussed in connection with Eq. (2.130b). [6] Other terms may also contain "formfactors", i.e., functions of $q\xi$, which could be determined from a more detailed calculation of three-point functions in model-H. We leave such and similar refinements to future work. It is likely that given the general degree of applicability of hydrodynamics in heavy-ion collisions these will be beyond the experimentally relevant precision.

Eq. (3.23a) describes relaxation of the slowest non-hydrodynamic mode, N_{mm}, to equilibrium given by Eq. (3.14). Of course, the equilibrium value depends on how one defines N_{mm} (or normalize $\phi_m \sim \delta m$). Here we have chosen the most convenient rescaling to simplify our final equations (cf. (2.128)). The corresponding equation used in Ref. [39, 40, 42], are identical to ours except the difference of the definition (normalization factor) of N_{mm}. However, one can argue that, as long as the equation for N_{mm} is applied in the vicinity of a critical point, this difference is sub-leading compared to the blowing-up of the equilibrium values of N_{mm}. More specifically, since $N^{(0)}_{mm} \sim c_p \sim \xi^2$, the LHS of Eq. (3.23a) is dominated by a term like $u \cdot \partial c_p \sim c_p \dot{c}_p \theta$. It is much large than the gradient terms like $c_p\theta$ aroused from the different normalization of N_{mm}, and the enhancement factor is given by $\dot{c}_p \sim \xi^{3/2}$. The conclusion for a generic two-point functions N_{AB} is similar if $N^{(0)}_{AB}$ is singular near the critical point. Namely, the gradient terms in the equation for N_{AB} generated from rescaling are always less important by a factor of $\dot{N}^{(0)}_{AB}$ than the most singular terms, thus the normalization of N_{mm} does not matters near the critical point. Provided such fact, Eq. (3.23a) would be identical to the corresponding Hydro+ equation in Ref. [39], but for the last term describing the coupling to next-to-slowest mode, $N_{m(i)}$. Again, because $c_p \sim \xi^2$ diverges at the critical point, and furthermore, the relaxation rate for $N_{m(i)}$ is parametrically faster than N_{mm} by a factor of ξ, this term is indeed much smaller than the first term sufficiently close to the critical point. However, if we want to interpolate Hydro+ description close to the critical point with dynamics of fluctuations away from the critical point this term has to be kept.

---

[6] Heuristically, one can obtain Eq. (3.23b) from Eq. (2.130b) by preforming substitution of c_p according to Eq. (3.15)

In summary, the general hydro-kinetic formalism presented in Chap. 2 provides a systematic description of fluctuating hydrodynamics away from the critical point, as long as the scale hierarchy is hold. Near the critical point, the implementation of our general formalism is more subtle, however. The main feature in the critical region is that, the equilibrium correlation length ξ, which is microscopically small away from the critical point, becomes macroscopically large in the thermodynamic limit as the system approach the critical point. Thus, the scale hierarchy we have used in hydro-kinetic theory breaks down, and the nonlocal effect is significant at the fluctuation scale. Due to the critical slowing down illustrated below Eq. (1.112), we have $\Gamma_\lambda \sim \xi^{-3} \ll \Gamma_\eta \sim \xi^{-2}$, thus different modes in Eqs. (2.130) may relax with parametrically different rates, and compete with the background evolution rate ω in different scenarios. As depicted by Fig. 3.1, in the long wavelength limit $\omega \ll \Gamma_\lambda \lesssim \Gamma_\eta$, manifested away from the critical point, most wavenumber modes equilibrate rapidly compared to ω, therefore ordinary hydrodynamics (Hydro) is sufficient to describe the system. As the system approaches the critical point (ξ increases), ω will first fall into the window $\Gamma_\lambda \lesssim \omega \ll \Gamma_\eta$ where hydrodynamics breaks down and Hydro+ applies [39], thus the slowest mode N_{mm} associated with Γ_λ has to be taken into account (see Eq. (2.130a)). Hydro++, however, nontrivially extends the applicability of Hydro+ further to $\Gamma_\lambda \ll \Gamma_\eta \lesssim \omega$, i.e., closer to the critical point, such that the whole set of equations in (2.130) must be involved. Nonetheless, we shall emphasis that Hydro++ is limited by $\omega \ll \xi^{-1}$, since the nonlocality at scale $\omega \sim \xi^{-1}$ is not negligible and an extended formalism is still plausible.

3.2.2 Frequency Dependence of Transport Coefficients

Let us discuss physics described by Eqs. (3.23) which is pertinent to the breakdown of Hydro+ and its crossover to Hydro++.

We can use Eqs. (3.23) to determine the critical contribution λ_ξ to the conductivity λ and verify it diverges as $\xi \to \infty$. Following the procedure of renormalization described in

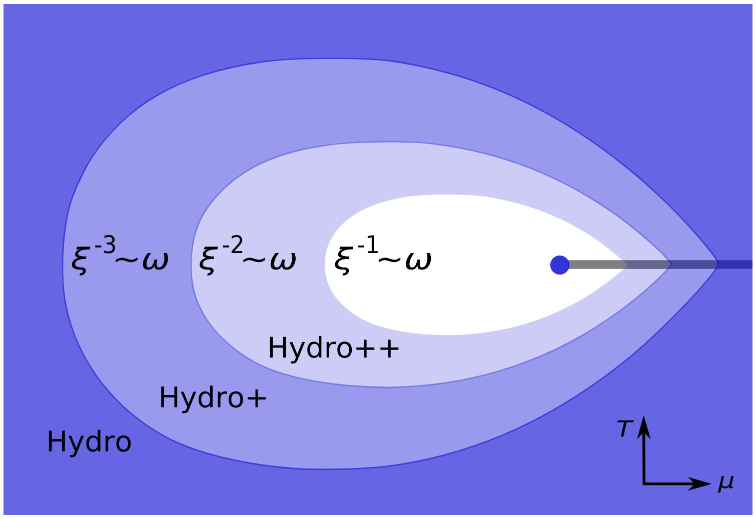

Figure 3.1: A schematic plot of the vicinity of the critical end point (blue point) in the $T-\mu$ plane of the QCD phase diagram. The contours of the equilibrium correlation length ξ separate several distinct regimes characterized by frequency ω. See text for detailed illustration.

Section 2.6 we now find that $W^{(1)}_{m\mu}$, i.e., the part of $W_{m\mu}$ linear in gradients, is given by Eq. (2.162) with a simple substitution $c_p \to c_p(q)$. This, in turn, makes the integral of $W^{(1)}_{m\mu}$, $G^{(1)}_{m\mu}(x)$, finite. The cutoff is now essentially given by $1/\xi$, instead of Λ. This means that instead of Eq. (2.164) we find, using $c_p(q)$ in Eq. (3.15), $\Lambda \to \pi/(2\xi)$. Substituting this result into equation (2.165c) for the renormalized conductivity we find a contribution to renormalized conductivity which diverges with ξ:

$$\lambda_\xi = \left(\frac{Tn}{w}\right)^2 \frac{c_p T}{6\pi\eta\xi} \sim \xi^1 \tag{3.24}$$

– a well-known result [66]. We used the fact that $c_p \sim \xi^2$. In particular, since $\gamma_\lambda \sim \lambda/c_p \sim \xi^{-1}$ we neglected γ_λ compared to $\gamma_\eta \sim \xi^0$. Denoting the noncritical contribution to conductivity by λ_0 we can write the total physical conductivity as

$$\lambda = \lambda_0 + \lambda_\xi = \lambda_0 + \left(\frac{Tn}{w}\right)^2 \frac{c_p T}{6\pi\eta\xi} = \left(\frac{Tn}{w}\right)^2 \left(\kappa_0 + \frac{c_p T}{6\pi\eta\xi}\right). \tag{3.25}$$

Note that the relaxation rate $\Gamma(q)$ in Eq. (3.22) at $q = 0$ matches twice the relaxation rate of the diffusive mode, $\gamma_\lambda = \kappa/c_p q^2$, as it should since this is the relaxation rate of the corresponding *two*-point function.

In the Hydro+ formulation in Ref. [39] the value of conductivity was given directly by Eq. (3.24). In our more general approach, which we refer to as Hydro++, the divergent value of the conductivity is generated "dynamically" via the contribution of the fluctuation mode $W_{m(i)}$ (via $G^{m\mu}(x)$) to the constitutive equation for the current in Eq. (2.147b). The value of $\lambda = \lambda_0$ in Eq. (2.26b) is finite as $\xi \to \infty$. This is similar to the way divergence of bulk viscosity with $\xi \to \infty$ is generated in Hydro+ (and, by extension, also in Hydro++), see Ref. [39]. Similarly to Hydro+, which describes frequency dependence of bulk viscosity (and sound speed) Hydro++ describes the frequency dependence of the kinetic coefficient λ. We shall consider it below.

Hydro++ allows us to see how Hydro+ breaks down when k (or, more precisely, the sound frequency $\omega = k/c_s$ at this wave number) exceeds a value of order ξ^{-2}. This happens because the characteristic relaxation rate of the mode $W_{mi}^{(1)}$ responsible for λ_ξ contribution also vanishes as $\xi \to \infty$:

$$\Gamma'_\xi \equiv \gamma_\eta q^2\Big|_{q\xi=1} \sim \xi^{-2}. \tag{3.26}$$

This is next-to-slowest relaxation rate, after the characteristic relaxation rate of W_{mm}, given by[7] [8]

$$\Gamma_\xi \equiv 2\gamma_\lambda q^2|_{q\xi=1} \sim \xi^{-3}\,. \tag{3.27}$$

As discussed in Ref. [39], when the evolution rate (or sound frequency) ω exceeds Γ_ξ the mode W_{mm} is no longer able to relax to its equilibrium value which is responsible for the divergence of the bulk viscosity. Therefore, the divergent contribution to the bulk viscosity is "switched off" for $\omega > \Gamma_\xi$. Similarly, when the evolution rate (or sound frequency) ω exceeds Γ'_ξ, the next to slowest mode, $W_{m\mu}$, is no longer able to relax to its zero-frequency value given in Eq. (2.162). As a result, the contribution of $W_{m\mu}$ to the current in Eq. (2.147b) "switches off". This behavior and corresponding scales are illustrated in Fig. 3.2.

---

[7] More precisely, $\Gamma_\xi \sim \xi^{x_\lambda - 4 + \eta_x} = \xi^{-z}$ and $\Gamma'_\xi \sim \xi^{x_\eta - 2} = \xi^{z+d-8}$ (see also footnote 1).

[8] Since the bulk viscosity is proportional to the longest microscopic relaxation time, vanishing Γ_ξ is responsible for the divergence of the the bulk viscosity $\zeta \sim c_s^2/\Gamma_\xi \sim \xi^{z-\alpha/\nu}$. In the Kawasaki approximation $\zeta \sim \xi^3$. Since ζ is the coefficient of the gradient expansion, the expansion breaks down at $k\xi^3 \sim 1$, which is an alternative way to see that ordinary hydrodynamics breaks down at this scale.

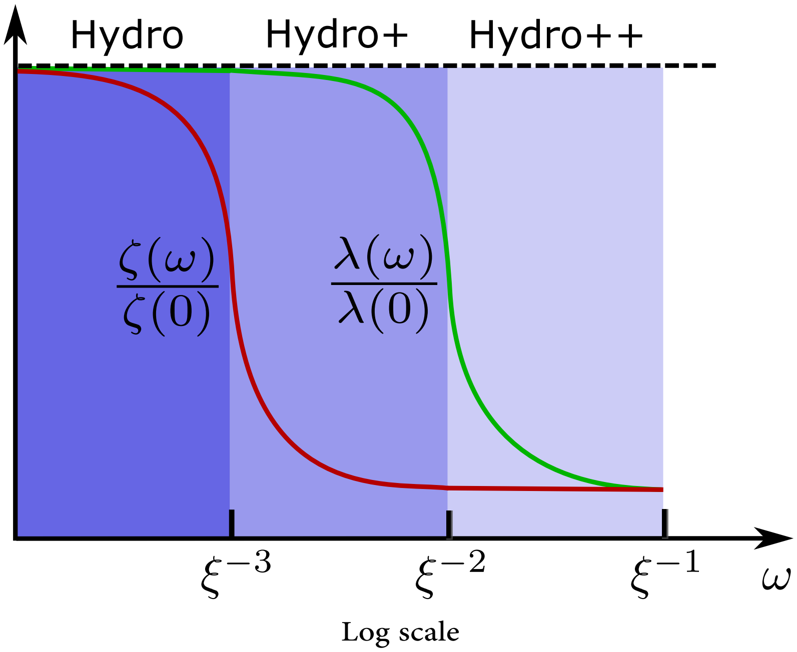

Figure 3.2: Frequency dependence of transport coefficients $\zeta(\omega)$ and $\lambda(\omega)$ in the vicinity of a critical point, where the divergence of ξ leads to several distinct regimes characterized by frequency ω (or corresponding wavenumber $k = \omega/c_s$). The crossover from ordinary hydrodynamics (Hydro) to Hydro+ is marked by the fall-off of $\zeta(\omega)$ at $\omega \sim \Gamma_\xi \sim \xi^{-3}$, while the Hydro+ itself breaks down at $\omega \sim \Gamma'_\xi \sim \xi^{-2}$ as signaled by the fall-off of $\lambda(\omega)$, when the crossover to Hydro++ regime occurs. Of course, in ordinary hydrodynamics both transport coefficients are constants independent of frequency (dashed line), while in Hydro+, which does describe the fall-off of $\zeta(\omega)$, the coefficient λ is still a constant. Hydro++ describes the fall-off of both $\zeta(\omega)$ and $\lambda(\omega)$.

We can further quantify this description by considering the dependence of $W^{(1)}_{m\mu}$ on frequency following the same procedure as in Sec. 2.6.2. Combining the substitution in Eq. (2.169) with the substitution (3.15) in Eqs. (2.153b) and (2.162) we find for frequency-dependent leading critical contribution to conductivity:

$$\lambda_\xi(\omega) = \lambda_\xi(0) F_\lambda \left(\omega/\Gamma'_\xi\right), \tag{3.28}$$

where

$$F_\lambda(y) = \frac{2}{\pi}\int_0^\infty \frac{dx x^2}{(x^2 - iy)(1+x^2)} = \frac{1}{1+\sqrt{y/i}}\,. \tag{3.29}$$

We do not need to regularize and subtract a divergence, as we did in Sec. 2.6.2, because the divergence is tamed by the fall-off of $c_p(q)$ at large q.

At small $\omega \ll \Gamma'_\xi$ Eq. (3.28) reproduces the power-law non-analytic dependence characteristic of the long-time tails in Eq. (2.170): $\lambda_\xi(\omega) - \lambda_\xi(0) \sim \lambda_\xi(0)\omega^{1/2}$. Not surprisingly, since, compared to Sec. 2.6.2, we only changed the nature of the cutoff Λ. At large ω we find $\lambda_\xi(\omega) \sim \omega^{-1/2}$ with no ξ dependence as expected from scaling behavior characterizing this regime. [9] The dependence of λ_ξ on ω described by Eqs. (3.28) and (3.29) corresponds to the physics we anticipated – the large critical contribution "switches off" when $\omega \gtrsim \Gamma'_\xi$.

It may also be helpful to note that while real part of $\lambda_\xi(\omega)$ corresponds to (frequency-dependent) conductivity, its imaginary part (divided by ω) is the electric permittivity.

One can also understand frequency dependence as a time-delayed medium response to gradient of density, i.e., $\partial\alpha$. The diffusive current induced by the gradient is given by

$$J_\xi(t) = \lambda_\xi \int_{-\infty}^t dt' \Gamma'_\xi \tilde{F}_\lambda\left(\Gamma'_\xi(t-t')\right)\partial\alpha(t')\,. \tag{3.30}$$

The delay is given by the Fourier transform of $F_\lambda(y)$:

$$\tilde{F}_\lambda(\tilde{y}) = \sqrt{\frac{1}{\pi\tilde{y}}} - e^{\tilde{y}}\mathrm{erfc}\left(\sqrt{\tilde{y}}\right). \tag{3.31}$$

As a function of $t - t'$ it has a characteristic width given by $1/\Gamma'_\xi \sim \xi^2$ and becomes delta function in the limit $\xi \to 0$ corresponding to instantaneous response. At large $t - t'$ it falls off as $(t-t')^{-3/2}$ typical of the long-time hydrodynamic tails.

The discussion of the frequency dependence of conductivity here carries many similarities to the discussion of the bulk viscosity in Ref. [39]. For completeness, let us present the calculation of the leading critical contribution to the bulk viscosity in Hydro++, which, of course, gives the same result as Hydro+. Near the critical point the leading contribution of fluctuations to the bulk viscosity comes from $G^{(1)}_{mm}$ in Eq. (3.13). In Hydro++ the corresponding $W^{(1)}_{mm}$ is given in Eq. (2.160), with the substitution of c_p with $c_p(q)$ as in Eq. (3.15), as well as γ_λ with $\gamma_\lambda(q)$ according to Eq. (3.22). As a result we obtain for the leading critical contribution to bulk viscosity:

---

[9] As before (see footnote 1), the exact value of the scaling exponent in $\lambda_\xi(\omega) \sim \omega^{-1/2}$ differs slightly from the rational value $-1/2$. The exact value in model H following from dynamic scaling $-x_\lambda/(2 - x_\eta) = -(4-\eta-z)/(d+2-z)$ is approximately $-1/2$ in the Kawasaki approximation we are using, which corresponds to $z \approx 3$ and $\eta_x \approx 0$.

$$\zeta_\xi(\omega) = \frac{3}{\pi}\eta\,\dot{\xi}^2 F_\zeta\left(\frac{\omega}{\Gamma_\xi}\right), \tag{3.32}$$

where we used $\dot{c}_p = 2\dot{\xi}$ (according to scaling $c_p \sim \xi^2$) and $\Gamma_\xi = T/(3\pi\eta\xi^3)$ (according to Eqs. (3.27) and (3.24)). We introduced

$$F_\zeta(y) = \int_0^\infty \frac{dx x^2}{(x^2K(x) - iy)(1+x^2)^2}\,. \tag{3.33}$$

This is a known result in Kawasaki approximation [111, 39].[10] At $\omega = 0$ Eq. (3.32) gives $\zeta_\xi(0) \sim \xi^3$ (according to the scaling of $\dot{\xi} \sim \xi^{3/2}$). This large critical contribution is "switched off" via function F_ζ when $\omega > \Gamma_\xi$.[11]

The resulting behavior is illustrated in Fig. 3.2 together with the behavior of $\lambda(\omega)$.

3.3 Discussion

With the hydro-kinetic equations we derived in Chap. 2, we can now describe the essential features of the hydrodynamic evolution near the QCD critical point. The critical phenomena are originating from the divergence of the correlation length ξ. The phenomenon of the most consequence for hydrodynamics is the critical slowing down. Since it is caused by the fluctuations of the slowest diffusive mode out of equilibrium, our formalism is ideally suited to accommodate and describe this phenomenon. The formalism of Hydro+ introduced earlier in Ref. [39] is based on the same observation and adds the two-point correlation function of the diffusive mode to hydrodynamics to describe critical slowing down. The approach in the present paper is very different from the derivation in Ref. [39], therefore, the exact agreement between the results is a nontrivial check on the validity of both derivations.

---

[10] As we already discussed, Kawasaki approximation only gives a good approximation to the correct scaling behavior. To match the exact scaling behavior on would need a more elaborate choice of the substitution in Eq. (3.15), see e.g., Refs.[111, 112, 39].

[11] The large ω asymptotics $\zeta_\xi(\omega) \sim \omega^{-1}$ in Kawasaki approximation is close to the exact asymptotics $\omega^{-1+\alpha/(z\nu)}$.

Since, our present approach is more general, we can now connect Hydro+ description of critical fluctuations to description of ordinary fluctuations away from the critical point. Because the validity of Hydro+ is limited by the relaxation rate of the next-to-slowest mode, and this mode, absent in Hydro+, is now a part of our description, we are able to extend the validity of hydrodynamic description closer to the critical point than Hydro+. We propose a set of equations, which we call Hydro++ which could accomplish this. It should be kept in mind that, unlike the systematic approach taken in the rest of the paper, the Hydro++ equations (3.23) are an attempt to interpolate between the description of fluctuations outside of the critical regime and the known properties of the fluctuations in the critical, scaling regime described by model H (in the standard classification of Ref. [66]). While the hydrodynamic description still works for the background gradients for which $k\ell_{\text{mic}} \sim k\xi \ll 1$, it breaks down for critical *fluctuations*, for which $q\xi \sim 1$. This means that the coefficients become non-polynomial in q and that the theory becomes fully nonlinear and the truncation to two-point functions is no longer, strictly speaking, controllable. However, it is known from the studies of model H that the results obtained in one-loop (Kawasaki) approximation are in good quantitative agreement with experiment [66]. Therefore we propose a set of equations (3.23) which incorporate the model H physics at the corresponding level of approximation. This approach is similar to the one taken in the derivation of Hydro+ and extends the region of applicability closer to the critical point. More precisely, while Hydro+ breaks down at $k \sim \xi^{-2}$, the validity of Hydro++ extends to $k \sim \xi^{-1}$. The physical phenomenon which leads to breakdown of Hydro+ is the frequency dependence of (i.e., time-lag of) conductivity, which is described by the next-to-slowest mode in Hydro++.

Once the fluctuation hydrodynamics in the deterministic approach is implemented in a fully functional hydrodynamic code, the extension to full Hydro++ approach should be straightforward and will allow eventual comparison with heavy-ion collision experiments not only near, but also away from the critical point. However, additional developments are needed to make this comparison more impactful. First of all, it should be straightforward to generalize this approach to multiple conserved charges. In the case of QCD, of course, fluctuations of isospin are a primary candidate. We have not included these fluctuations in our description because they are not exhibiting singularities near the critical point, unlike the baryon number fluctuations, which lead to signatures of the QCD critical point [113]. Furthermore, the approach must be extended to description of non-Gaussian fluctuations, which are related to most sensitive signatures of the critical point (Sec. 1.3 and 1.5.2). This means going beyond two-point correlators considered in this thesis. It would also be interesting and important for comparison with experiment to consider the extension of this approach to the fluctuations near the first-order phase transition, which is, of course, an inseparable part of the physics near a critical point. We defer these and other pertinent developments to future work.

Chapter 4

Fluctuations and Spinodal Points

This chapter contains materials published in

- X. An, Mesterhazy and M. Stephanov, *Functional renormalization group approach to the Yang-Lee edge singularity*, JHEP *07* (2016) 041, arXiv:1605.06039 [hep-th] [4]. Copyright (2016) by the International School for Advanced Studies (SISSA) and Springer.
- X. An, Mesterhazy and M. Stephanov, *On spinodal points and Lee-Yang edge singularities*, J. Stat. Mech. 033207 (2018), arXiv:1707.06447 [hep-th] [5]. Copyright (2017) by the International School for Advanced Studies (SISSA) and IOP Publishing (IOP).
- X. An, Mesterhazy and M. Stephanov, *Critical fluctuations and complex spinodal points*, PoS *CPOD2017* (2018) 040 [6]. Copyright (2018) by authors.

4.1 Non-perturbative Approach to Lee-Yang Edge Singularities

With the pioneering work of Lee and Yang a new perspective on the properties of statistical systems was established by pointing out the importance of the distribution of zeros of the partition function [51, 52]. Expressed in terms of an external parameter, which we shall denote by z, the partition function $\mathcal{Z} = \mathcal{Z}(z)$ of a finite system can in general be expressed in terms of its roots z_α in the complex plane, i.e., we may write $\mathcal{Z} = \prod_\alpha (z - z_\alpha)$. Their significance appears in the thermodynamic limit, $V \to \infty$, when they coalesce along one-dimensional curves that separate different infinite volume behaviors of the partition function.[1] These curves can be viewed as cuts that distinguish different branches of the free energy (or grand canonical potential)

$$\Omega = -\beta^{-1} \log \mathcal{Z} = -\beta^{-1} V \int \mathrm{d}\theta \, g(\theta) \log \left[z - z(\theta) \right] , \tag{4.1}$$

where $g(\theta)$ corresponds to the normalized density of zeros ($\int \mathrm{d}\theta \, g(\theta) = 1$) on a curve parametrized as $z(\theta)$ and $\beta = 1/T$ is the inverse temperature. Clearly, once the location of the zeros, or cuts they coalesce into, $z(\theta)$, and the distribution $g(\theta)$ is known, in principle, all thermodynamic properties of the system can be calculated. This has led to numerous efforts to determine $g(\theta)$ for a wide range of lattice models via numerical methods [114, 115, 116, 117] and also experimentally [118, 119, 120]. Besides providing a rigorous basis to study the thermodynamic properties of finite lattice systems, such attempts have also helped to elucidate features of fundamental theories. Drawing on the principle of universality they have led to important insights into the phase diagram of strongly-interacting matter at nonvanishing baryon densities [121, 122, 123].

Typically, for lattice spin models at temperature T and external field H the natural variable in terms of which the partition function is a polynomial is $z = \exp(-2\beta H)$. The zeros of $\mathcal{Z}(z)$ are commonly referred to as Lee-Yang or Yang-Lee zeros. In particular, for the ferromagnetic Ising model one finds these zeros distributed along the unit circle $z = \exp(i\theta)$, where $\theta = 2i\beta H$ and H is imaginary. This has been proven rigorously and is known as the Lee-Yang circle theorem [52, 124, 125, 126, 127, 128, 129, 130, 131]. Depending on the temperature one may distinguish different scenarios: In the low-temperature region of the Ising model ($T < T_c$), the set of zeros crosses the positive real z-axis at $z = 1$ ($\theta = 0$), which indicates the presence of a first-order phase transition as one traverses the $\mathrm{Re}\, H = 0$ axis from positive to negative real H (or vice versa). On the other hand, in the high-temperature region ($T > T_c$) one observes a finite gap in the distribution $g(\theta) = 0$ for $|\theta| < \theta_g$ that closes as $T \to T_c^+$ [114, 115]. Thus, for $T > T_c$ the free energy is analytic along the real H axis. However, at the edge of the gap $\theta = \pm\theta_g$, corresponding to *imaginary* values of the magnetic field $H = \pm i|H_c(T)|$, the distribution of zeros exhibits non-analytic behavior, i.e., $g(\theta) \simeq (|\theta| - \theta_g)^\sigma$, for $|\theta| \gtrsim \theta_g$, characterized by the exponent σ [116]. As pointed out by Fisher [132] this behavior can be identified with a thermodynamic singularity that yields a divergence in the isothermal susceptibility $\chi_T = (\partial M/\partial H)_T \sim |H - H_c(T)|^{\sigma-1}$, where M is the magnetization. Thus, the Lee-Yang edge singularity at nonvanishing imaginary values of the field is similar to a conventional second order phase transition [132, 133].

---

[1] In principle, the zeros may accumulate on a dense set in parameter space, which must not necessarily be one dimensional. However, such a scenario is not relevant to this work.

In contrast to the well-known ϕ^4 field theory that describes the critical point of the Ising model at $T = T_c$ and $H = 0$, the field theory at the Lee-Yang edge point, the ϕ^3 theory, admits no discrete reflection symmetry and is therefore characterized by only one independent (relevant) exponent. In two dimensions the corresponding universality class has been identified with that of the simplest nonunitary conformal field theory (CFT), the minimal model $M_{2,5}$, with central charge $c = -22/5$ [134]. This allowed to exploit conformal symmetry in two dimensions to calculate the scaling exponent $\sigma(d = 2) = -1/6$, which has been confirmed with remarkable accuracy by series expansions [135, 136], as well as by comparing with experimental high-field magnetization data [118, 119]. Furthermore, using integral kernel techniques it is possible to establish the exact result $\sigma(d = 1) = -1/2$ [132, 133]. On the other hand, most of our knowledge in the region $2 < d < 6$ relies on appropriately resummed results from the $\varepsilon = 6 - d$ expansion [137, 138, 139], strong-coupling expansions [140], Monte Carlo methods [141, 142], and conformal bootstrap [143]. Note that in contrast to the Ising critical point (described by ϕ^4 theory), the upper critical dimension of the Lee-Yang edge point (described by ϕ^3 theory) is $d_c = 6$ and therefore, fluctuations are important even above dimension $d = 4$.

Recently, there has been renewed interest in the Lee-Yang edge point for which the RG β functions to four-loop order in the ε expansion were determined in Ref. [139] and the corresponding critical exponents (obtained from constrained Padé approximants) were compared to estimates from other methods. In light of these developments, we examine the critical scaling properties of the Lee-Yang edge with the non-perturbative functional RG [144, 145] for dimensions $3 \leq d \leq 6$. In contrast to the ε expansion, the functional RG does not rely on the expansion in a small parameter and is therefore ideally suited to investigate the critical behavior of the Lee-Yang edge away from $d_c = 6$. However, care must be taken to address possible systematic errors that arise from the truncation of the infinite hierarchy of flow equations. We will address these issues in the following subsections and show that that these errors are under control and comment on the quality of different truncations.

The outline of this section is as follows: First, in Sec. 4.1.1, we give an overview of the non-perturbative functional RG and the truncations employed in this work. In Sec. 4.1.2 we discuss the scaling properties of the critical equation of state and the mean-field theory at the Lee-Yang edge singularity. In Sec. 4.1.3 we consider the general properties of RG flow trajectories and in particular their infrared behavior. In Secs. 4.1.5 – 4.1.6 we summarize our results for the critical exponents at the Lee-Yang edge singularity and analyze the expected systematic errors for the truncations employed in this work. Finally we compare our estimates for the critical exponents to recent data from Refs. [139] and [143].

4.1.1 Non-perturbative Functional Renormalization Group

In Chap. 1, we have summarized the main idea of the renormalization group theory, in the perturbative regime. The perturbative renormalization theory claims its validity in certain particular limit, for instance, ϕ^3 theory near $d = 6$, or ϕ^4 theory near $d = 4$, none of which manifests at $d = 3$ quantitatively. Thus we need to introduce alternatively the non-perturbative approach to resolve this problem, one of which is the non-perturbative functional renormalization group (FRG) theory [2], a renormalization group scheme that relies on a truncation of a hierarchy of flow equations derived from an exact flow equation for the scale-dependent effective action. As its name implies, this renormalization group theory is applies to the non-perturbative regime, and deals with the functional fields. It is worth to emphasize that there exist functional renormalization group which is perturbative, and non-perturbative renormalization which is not formulated in the functional path integral. Nevertheless, FRG is commonly specified to a non-perturbative theory.

Unlike Wilson's perturbative renormalization group theory where the short-distance fluctuations are integrate out either progressively or at once, FRG introduces a family of partition functions labeled by the renormalization group scale parameter k:

$$\mathcal{Z}_k(J) = e^{\mathcal{W}_k[J]} = \int \mathcal{D}\phi \exp\left\{-\mathcal{S}[\phi] - \Delta\mathcal{S}_k[\phi] + \int d^d x J(x) \cdot \phi(x)\right\}, \tag{4.2}$$

where the additional term (cf. Eq. (1.1)),

$$\Delta\mathcal{S}_k[\phi] = \frac{1}{2}\int \mathrm{d}^d x\, \mathrm{d}^d y\, \phi(x) R_k(x,y)\phi(y) = \frac{1}{2}\int \frac{\mathrm{d}^d q}{(2\pi)^d}\, \phi(-q) R_k(q)\phi(q), \tag{4.3}$$

is a quadratic functional where the regulator R_k plays the role of a scale-dependent mass in order to regularize the theory in the infrared (suppress the low-energy fluctuations), in the sense that $R_k(q)$ is suppressed for $|q| \gg k$ and is of order k^2 for $|q| \ll k$.[3] The generating functional of one-particle irreducible (1PI) diagrams (cf. Eq. (4.4))

$$\mathcal{W}_k[J] = \log \int \mathcal{D}\phi \, \exp\left\{ -\mathcal{S} - \Delta\mathcal{S}_k + \int \mathrm{d}^d x \, J(x) \cdot \phi(x)\right\}, \tag{4.4}$$

corresponds to the scale-dependent Gibbs free energy

$$G_k[J] = -\beta^{-1} \log \mathcal{Z}_k[J] \tag{4.5}$$

---

[2] Other non-perturbative approaches are also well studied, such as the Schwinger-Dyson equations approach.

[3] Here k and q are somewhat similar to the wavenumber scales introduced in Chap. 2, in a sense that k acts as a regularization (background homogeneity) scale for fluctuations such that fluctuations in larger distances ($q \lesssim k$) are suppressed, consequently only small-distances fluctuations ($q \gtrsim k$) contribute to the correlation functions obtained from the effective action Γ_k, which is precisely the region the fluctuating hydrodynamics is taking care of.

in statistic physics according to Tab. 1.1. It is more convenient to introduce the scale-dependent effective action [144, 145]

$$\Gamma_k[\varphi(x)] = \sup_J \left(\int \mathrm{d}^d x \, J(x)\varphi(x) - \mathcal{W}_k \right) - \Delta\mathcal{S}_k, \tag{4.6}$$

obtained from the functional Legendre transform of $\mathcal{W}_k[J]$ with respect to the external source $J = J(x)$, which is slightly modified to include the subtraction of $\Delta\mathcal{S}_k$, and

$$\varphi = \frac{\delta \mathcal{W}_k[J]}{\delta J} \tag{4.7}$$

is the scalar field expectation value (for reviews see, e.g., Refs. [146, 147, 148, 149, 150]).

As discussed in Sec. 1.2.3, the effective action is related to the n-point one-particle-irreducible correlators (cf. Eq. (1.58)),

$$\frac{\delta^n \Gamma_k[\varphi]}{\delta\varphi(x_1)\dots\delta\varphi(x_n)} = \langle \phi(x_1)\dots\phi(x_n)\rangle_{\mathrm{1PI}} = \Gamma_k^{(n)}, \tag{4.8}$$

while the generating function generates the n-point connected correlation functions by

$$\frac{\delta^n \mathcal{W}_k[J]}{\delta J(x_1)\dots\delta J(x_n)} = \langle \phi(x_1)\dots\phi(x_n)\rangle_{\mathrm{c}} = G_k^{(n)}. \tag{4.9}$$

One can express the connected correlation function by the effective vertex $\Gamma_k^{(n)}$. For instance, the two-point correlator can be expressed by

$$G_k^{(2)}[J] = \left(\Gamma_k^{(2)}[\varphi] + R_k \right)^{-1}. \tag{4.10}$$

In this thesis, we again consider a classical action $\mathcal{S}$ of a single-component scalar field

$$\mathcal{S}[\phi] = \int \mathrm{d}^d x \left\{ \frac{1}{2}(\partial\phi)^2 + U_\Lambda(\phi) \right\}, \tag{4.11}$$

and the explicit expression of classical potential U_Λ is specified in Sec. 4.1.2. In particular, the regulator function

$$R_k(x,y) = R_k(-\Box_x)\delta^{(d)}(x-y) \tag{4.12}$$

where $\Box \equiv \partial_\mu\partial_\mu$, is chosen in such a way that it leads to a decoupling of infrared modes. We require that

$$\lim_{k\to 0} R_k = 0 \quad \text{and} \quad \lim_{\Lambda\to\infty} R_{k=\Lambda} = \infty, \tag{4.13}$$

where Λ is a characteristic scale that regularizes the theory in the ultraviolet and can formally be sent to infinity. In effect, this defines a one-parameter family of theories ($0 \leq k \leq \Lambda$), which interpolates between the classical action, $\mathcal{S} = \lim_{k\to\Lambda} \Gamma_k$, and the full 1PI effective action, $\Gamma = \lim_{k\to 0} \Gamma_k$. Thus, the scale-dependent regulator function R_k induces a functional RG flow between these two limits, described by the flow equation, also known as the *Wetterich's equation*:

$$\frac{\partial}{\partial s}\Gamma_k = \frac{1}{2}\int \frac{\mathrm{d}^d q}{(2\pi)^d}\frac{\partial R_k(q)}{\partial s}\left[\Gamma_k^{(2)}(\varphi;q) + R_k(q)\right]^{-1}, \tag{4.14}$$

where $s = \log(k/\Lambda)$ is a dimensionless scale parameter, and

$$\delta^{(d)}\Big(\sum_{i=1}^{n} q_i\Big)\Gamma_k^{(n)}(\varphi;q_1,q_2,\ldots,q_{n-1}) \equiv (2\pi)^{(n-1)d}\frac{\delta^n\Gamma_k[\varphi]}{\delta\varphi(q_1)\delta\varphi(q_2)\cdots\delta\varphi(q_n)} \tag{4.15}$$

is obtained by the Fourier transform of Eq. (4.8). In principle, we may choose any (sufficiently smooth) regulator that satisfies the above limiting properties. For details of our implementation and necessary requirements imposed on the regulator function see Secs. 4.1.3 – 4.1.6.

Eq. (4.14) for the scale-dependent effective action Γ_k is exact, from which one can also obtain the flow equations for n-point scale-dependent vertices $\Gamma_k^{(n)}$ by using Eq. (4.8). All those flow equations can be presented in terms of Feynman diagrams, illustrated in Tab. 4.1. It is straightforward to see that the functional RG flow equations only involve one-loop diagrams, simplifying the calculation significantly.

Clearly, an exact solution for the full functional flow is not feasible in practice, so one has to rely on suitable approximations of Eq. (4.14). Here, we comment on the nature of our truncation and discuss its limitations. We use a truncated expansion in derivatives for the scale-dependent effective action [151, 152]

$$\begin{aligned}\Gamma_k[\varphi] \;\; = \;\; & \int \mathrm{d}^d x \bigg\{ U_k(\varphi) + \frac{1}{2}Z_k(\varphi)(\partial\varphi)^2 + \frac{1}{2}W_{1,k}(\varphi)(\Box\varphi)^2 \\ & + \frac{1}{2}W_{2,k}(\varphi)(\partial\varphi)^2\,\Box\varphi + \frac{1}{2}W_{3,k}(\varphi)\left[(\partial\varphi)^2\right]^2 \bigg\},\end{aligned} \tag{4.16}$$

Flow Equations	Diagrammatic Representation
$\frac{\partial}{\partial s}\Gamma_k$	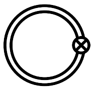
$\frac{\partial}{\partial s}\Gamma_k^{(1)}$	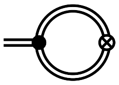
$\frac{\partial}{\partial s}\Gamma_k^{(2)}$	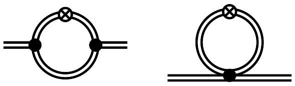
$\frac{\partial}{\partial s}\Gamma_k^{(3)}$	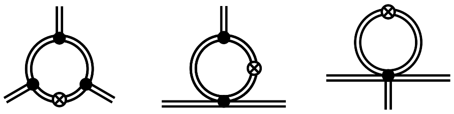
$\frac{\partial}{\partial s}\Gamma_k^{(4)}$	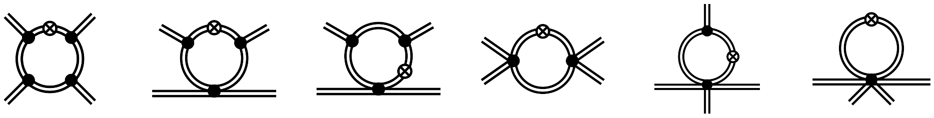

Table 4.1: Diagrammatic representation of the functional RG flow equations for the scale-dependent effective action Γ_k and the n-point 1PI vertices $\Gamma_k^{(n)}$ generated from the n-th order functional derivatives of Γ_k. The double line represents the regularized propagator $G^{(2)}$ defined in Eq. (4.10). The cross vertex stands for the insertion of $\partial_s R_k$, while the black verticies with n legs for $\Gamma^{(n)}$.

where U_k is the scale-dependent effective potential, and the scale-dependent functions Z_k and $W_{a,k}$, $a = 1, 2, 3$, parametrize the contributions to order ∂^4 (up to total derivative terms). Furthermore, for each of these functions, we employ a finite series expansion in the fluctuation $\delta\varphi_k = \varphi - \bar{\varphi}_k$ around a field configuration $\bar{\varphi}_k$, which is assumed to be homogeneous in space (cf. Sec. 4.1.3). In effect, this corresponds to an *ansatz* for Γ_k that includes only a finite set of independent operators, each of which is parametrized by a single parameter or coupling that is field independent, e.g., $Z_k(\varphi)(\partial\varphi)^2 = \big(\bar{Z}_k^{(0)} + \bar{Z}_k^{(1)}\delta\varphi_k + \dots\big)(\partial\varphi)^2$, and $\bar{Z}_k^{(n)} \equiv Z_k^{(n)}(\bar{\varphi}_k)$, $n \in \mathbb{N}$, and similar expansions apply to U_k and $W_{a,k}$. The canonical dimensions of these parameters are displayed in Tab. 4.2. Clearly, above dimension $d = 2$, $\bar{Z}_k^{(n)}$ and $\bar{W}_{a,k}^{(n)}$ are

Operator	Coupling	Canonical dimension
$\delta\varphi^n$	$\bar{U}^{(n)}$	$\dim \bar{U}^{(n)} = d - n(d-2)/2$
$\delta\varphi^n(\partial\varphi)^2$	$\bar{Z}^{(n)}$	$\dim \bar{Z}^{(n)} = -n(d-2)/2$
$\delta\varphi^n\,(\Box\varphi)^2$	$\bar{W}_1^{(n)}$	$\dim \bar{W}_1^{(n)} = -2 - n(d-2)/2$
$\delta\varphi^n(\partial\varphi)^2\,\Box\varphi$	$\bar{W}_2^{(n)}$	$\dim \bar{W}_2^{(n)} = -[d+2+n(d-2)]/2$
$\delta\varphi^n\left[(\partial\varphi)^2\right]^2$	$\bar{W}_3^{(n)}$	$\dim \bar{W}_3^{(n)} = -d - n(d-2)/2$

Table 4.2: Operators and canonical dimension of associated parameters and couplings that appear in the expansion of Γ_k (cf. Eq. (4.16)). Note that we drop the RG scale index k, since the canonical dimensions are defined at the Gaussian fixed point of the RG β functions.

irrelevant (cf. Eq. (1.31)) as far as a counting of canonical dimensions goes, but this is not sufficient to conclude that this is also the case at a nontrivial (i.e., non-Gaussian) fixed point of the RG β functions. Indeed, one of the objectives of this work is to investigate their effect at the Lee-Yang edge point as well as on RG trajectories that approach this scaling solution in the IR. We should point out that similar truncations of the scale-dependent effective action were considered also in Refs. [153, 154, 155, 156] to establish the critical exponents at the Ising critical point. Here, we study the scaling properties of Eq. (4.16) in the presence of a nonvanishing external field, when the discrete reflection symmetry $\varphi \leftrightarrow -\varphi$ of the Ising model is explicitly broken and the system is tuned to the Lee-Yang edge critical point.

The flow equations for U_k, Z_k, and $W_{a,k}$, $a = 1, 2, 3$, are derived from the exact functional flow equation for Γ_k (cf. Eq. (4.14)) by applying functional derivatives and projecting them onto the appropriate momentum contributions, i.e.,

$$\frac{\partial}{\partial s}U_k = \frac{\partial}{\partial s}\,\Gamma_k[\varphi]\big|_{\varphi=\text{const.}}\,, \tag{4.17a}$$

$$\frac{\partial}{\partial s}Z_k = \lim_{p\to 0}\frac{\partial}{\partial p^2}\frac{\partial}{\partial s}\Gamma_k^{(2)}(\varphi;p), \tag{4.17b}$$

$$\frac{\partial}{\partial s}W_{1,k} = \lim_{p\to 0}\frac{\partial}{\partial (p^2)^2}\frac{\partial}{\partial s}\Gamma_k^{(2)}(\varphi;p), \tag{4.17c}$$

$$\frac{\partial}{\partial s}W_{2,k} = \frac{1}{2}\lim_{p_i\to 0}\frac{\partial}{\partial (p_1\cdot p_2)^2}\frac{\partial}{\partial s}\Gamma_k^{(3)}(\varphi;p_1,p_2), \tag{4.17d}$$

$$\frac{\partial}{\partial s}W_{3,k} = -\frac{1}{4}\lim_{p_i\to 0}\left[\frac{\partial}{\partial (p_2\cdot p_3)} - \frac{1}{2}\frac{\partial}{\partial (p_1\cdot p_2)} - \frac{1}{2}\frac{\partial}{\partial (p_1\cdot p_3)}\right]\frac{\partial}{\partial p_1^2}\frac{\partial}{\partial s}\Gamma_k^{(4)}(\varphi;p_1,p_2,p_3), \tag{4.17e}$$

where $p{\cdot}q \equiv p_\mu q_\mu$. The corresponding RG flow equations for the field-independent parameters $\bar{Z}_k^{(n)}$ and $\bar{W}_{a,k}^{(n)}$ can be derived from Eqs. (4.17a) – (4.17e) by suitable differentiation and successive projection onto the reference field configuration $\bar{\varphi}_k$ that enters the series expansion.

The RG flow equations display the following chain of dependencies

$$U_k \leftarrow \{Z_k, W_{1,k}\} \leftarrow \{W_{2,k}, W_{3,k}\} \leftarrow \dots, \tag{4.18}$$

where the ellipsis denotes higher order contributions that we have chosen to neglect in our *ansatz*, Eq. (4.16). That is, the RG flow equation for the scale-dependent effective potential U_k depends on the quantities Z_k and $W_{1,k}$, but is independent of $W_{2,k}$ and $W_{3,k}$ etc. We exploit this structure explicitly by truncating the hierarchy Eq. (4.18) at the second level, i.e., we set $W_{2,k} = W_{3,k} = 0$ in Eq. (4.16), while U_k, Z_k, and $W_k \equiv W_{1,k}$ are expanded to some finite order in $\delta\varphi_k$. Note that the order of the employed expansion might be different for each of these coefficients. Similar approximations have led to reasonable estimates of the critical scaling exponents at the Ising critical point [155, 156] and we expect that this is also the case for the Lee-Yang edge critical point, which shall be manifested in the next section.

4.1.2 Critical Equation of State and Mean-field Scaling Prediction

Here, we consider a classical ϕ^4 potential of the following form

$$U_\Lambda = \frac{1}{2}t_\Lambda\phi^2 + \frac{1}{4!}\lambda_\Lambda\phi^4 + h_\Lambda\phi, \tag{4.19}$$

with a nonvanishing coupling to a symmetry-breaking field h_Λ, and $t_\Lambda \sim T - T_c$, with T_c the critical temperature at the Ising critical point. Upon integration of the RG flow equations (4.17a) – (4.17c) down from the cutoff scale Λ to the IR, the parameters and couplings of the classical potential acquire a scale dependence. In fact, the corresponding scale-dependent effective potential U_k for $0 \leq k < \Lambda$ will typically include a large number of fluctuation-induced interactions. The full effective potential is obtained only when the scale parameter k is sent to zero and all modes have been integrated out, i.e., $U = \lim_{k\to 0} U_k$.

In order to arrive at a critical point in the IR the relevant parameters of the classical action need to be tuned to their respective critical values, while all other parameters or couplings are kept constant. That is, in the case of the Lee-Yang edge critical point, we fix λ_Λ, $|h_\Lambda| > 0$, and tune t_Λ to its critical value $t_{\Lambda,c} = t_{\Lambda,c}(h_\Lambda) > 0$, for which $\bar{U}^{(1)} \equiv \lim_{k\to 0} \bar{U}_k^{(1)} = 0$ and $\bar{U}^{(2)} \equiv \lim_{k\to 0} \bar{U}_k^{(2)} = 0$ in the IR limit. At the Lee-Yang edge critical point, the first and second derivative are evaluated at a nonvanishing, *imaginary* field expectation value $\bar{\varphi}$. In the critical domain, the equation of state satisfies the scaling form

$$U'(\varphi) = \delta\varphi|\delta\varphi|^{\delta-1} f\left(\delta t_\Lambda |\delta\varphi|^{-1/\beta}\right), \tag{4.20}$$

where $\delta\varphi = \varphi - \bar{\varphi}$ and $f = f(x)$ is a universal, dimensionless scaling function, which is uniquely defined up to normalization. The critical exponents β and δ characterize the asymptotic scaling behavior of the magnetization φ for vanishing $U'(\varphi) = \delta h$ and $\delta t_\Lambda = t_\Lambda - t_{\Lambda,c}$, respectively. Here, the parameter $\delta h \sim H - H_c$, measures the deviation from the critical field strength $H_c = \pm i|H_c(T)|$, and $T > T_c$ for the range of values of δt_Λ studied in this work.

Before we go on to consider the solution of the RG flow equations (4.17a) – (4.17c), we discuss the mean-field scaling prediction. Since there is no scale dependence in this case, we simply drop the k (or Λ) index on all parameters. It is useful to express the potential in terms of an expansion in field differences $\delta\phi = \phi - \bar{\phi}$ around a reference field configuration $\bar{\phi}$, which is defined such that $U'(\bar{\phi}) = 0$. According to the strategy outlined above, we fix $|h| > 0$ and inquire about possible critical points, by imposing in addition the condition that $U''(\bar{\phi}) = 0$. Following Sec. 1.2 where we introduced ϕ^3 theory, we derive two independent scaling solutions for parameter t and h respectively, identify as

$$t_c = \frac{\lambda}{2}\left(\pm\frac{i3h}{\lambda}\right)^{2/3}, \quad h_c = \pm i\frac{\lambda}{3}\left(\frac{2t_c}{\lambda}\right)^{3/2}, \tag{4.21}$$

where we assume that $t_c > 0$, and the value of h_c is already derived as Eq. (1.40). Near the critical point $U'(\phi)$ satisfies the scaling form (4.20) with $\delta = 2$ and $\beta = 1$. Other critical exponents that characterize the power-law singularities of various thermodynamic quantities can be determined via scaling relations [157]. That is, in the absence of fluctuations the anomalous dimension vanishes, $\eta = 0$, and we obtain the following scaling exponents: $\alpha = -1$, $\gamma = 1$, $\nu = 1/2$, and $\nu_c = 1/4$. Note that the exponent α is negative and therefore, at the mean-field level, the specific heat does not diverge at the Lee-Yang edge point.

4.1.3 Solving the RG Flow Equations

To solve the RG equations we specify the classical action $\mathcal{S} = \int \mathrm{d}^d x \, \left\{\frac{1}{2}(\partial\phi)^2 + U_\Lambda(\phi)\right\}$, which is defined in terms of the short-distance potential U_Λ, and integrate the flow equations down to $s \to -\infty$. The classical potential is given in Eq. (4.19) and the coefficients that parametrize the kinetic contribution to the action are $Z_\Lambda = 1$ and $W_\Lambda = 0$.

We use a truncated series expansion for the scale-dependent effective potential U_k as well as for the field-dependent renormalization factors Z_k and W_k $(0 \leq k \leq \Lambda)$. Such a strategy is often sufficient to extract the leading or subleading critical scaling behavior [159, 160, 155, 161, 156]. The employed expansion is organized around a nonvanishing, imaginary, and

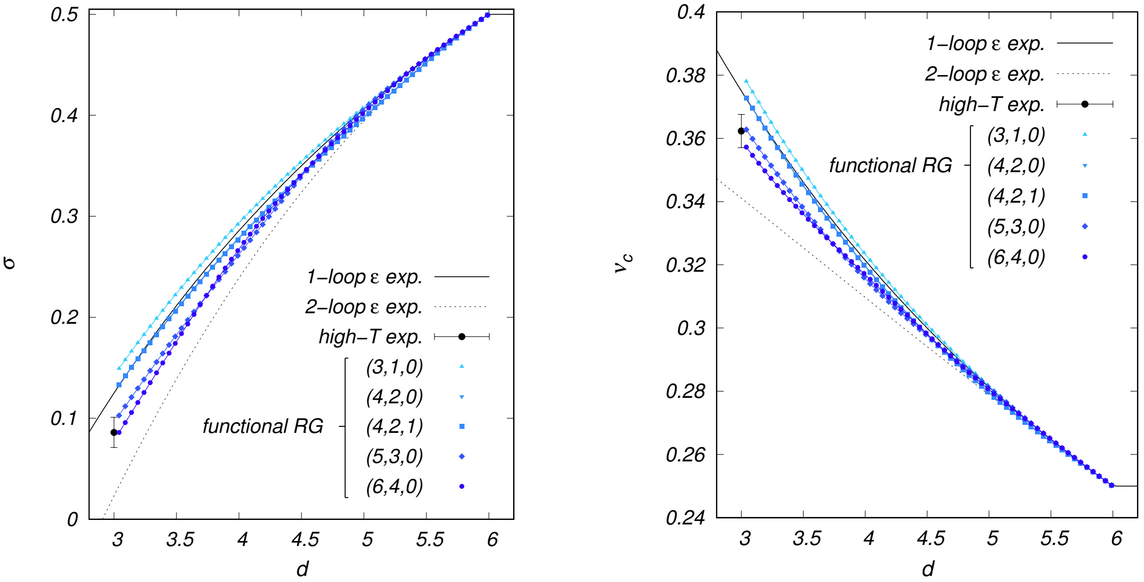

Figure 4.1: Critical exponents $\sigma = 1/\delta$ and ν_c as a function of Euclidean dimension d for different truncations of the scale-dependent effective action Γ_k, as specified by the set of integers (n_U, n_Z, n_W) (cf. Sec. 4.1.3). The data for the truncation $(4, 2, 1)$ lies almost exactly on top of that for $(4, 2, 0)$. Shown in comparison are results from the one- and two-loop ε expansion [158, 132] as well as high-temperature series expansion data ($d = 3$) [132, 133]. We observe that the numerical accuracy of the functional RG results improves significantly as one goes to higher orders in the derivative and field expansion, respectively.

homogeneous field configuration $\bar{\varphi}_k$, which depends on the scale parameter k, and is defined in the following way: 1) At the cutoff scale Λ, $\bar{\varphi}_{k=\Lambda} = \bar{\phi}_\Lambda$ is a solution to $U''_\Lambda(\bar{\phi}_\Lambda) = \tau$, and 2) the scale derivative of $\bar{U}^{(2)}_k \equiv U''_k(\bar{\varphi}_k)$, evaluated at $\bar{\varphi}_k = \bar{\varphi} + \bar{\chi}_k$, satisfies

$$\frac{\mathrm{d}}{\mathrm{d}s}\bar{U}^{(2)}_k = \frac{\partial}{\partial s}\bar{U}^{(2)}_k + \bar{U}^{(3)}_k \frac{\mathrm{d}\bar{\chi}_k}{\mathrm{d}s} = 0, \tag{4.22}$$

resulted from the fact that, although the imaginary field expectation value $\bar{\varphi}$ associated with the Lee-Yang edge point is scale independent, the RG flow changes the average configuration of $\bar{\varphi}_k$ at scale k (therefore $\mathrm{d}\bar{\varphi}_k/\mathrm{d}s = \mathrm{d}\bar{\chi}_k/\mathrm{d}s$), such that the condition $U^{(2)}_k(\bar{\varphi}_k) = \tau$ is maintained for any $0 \leq k \leq \Lambda$. Note that $\lim_{k\to 0} \bar{\chi}_k = 0$, i.e., $\lim_{k\to 0} \bar{\varphi}_k = \bar{\varphi}$, only when $\tau = 0$ and the system has been tuned to criticality. In other words, different initial values of τ may result in $\lim_{k\to 0} \bar{\varphi}_k \neq \bar{\varphi}$ after RG running. Clearly, conditions 1) and 2) fix one parameter of the model $\bar{U}^{(2)}_k = \tau$, at the expense of introducing another scale-dependent quantity, the field configuration $\bar{\chi}_k$, for which we obtain

$$\frac{\mathrm{d}\bar{\chi}_k}{\mathrm{d}s} = -\big(\bar{U}_k^{(3)}\big)^{-1}\frac{\partial}{\partial s}\bar{U}_k^{(2)}. \tag{4.23}$$

Note that the corresponding set of flow equations requires that $|\bar{U}_k^{(3)}| > 0$ for all $0 \leq k \leq \Lambda$. This does not hold true in the vicinity of the Ising critical point and therefore, the chosen expansion point is not adequate to investigate the scaling properties for critical points on the $\varphi \leftrightarrow -\varphi$ symmetry axis ($H = 0$).

Since Eq. (4.22) fixes the second derivative of the scale-dependent effective potential at all scales, the expansion of the scale-dependent effective potential reads

$$U_k = \bar{U}_k^{(0)} + \bar{U}_k^{(1)}\delta\varphi_k + \frac{1}{2}\tau\,\delta\varphi_k^2 + \sum_{n=3}^{n_U}\frac{1}{n!}\bar{U}_k^{(n)}\delta\varphi_k^n. \tag{4.24}$$

Here, the sum runs up to some finite integer value n_U, which defines our truncation for the scale-dependent effective potential with the prescribed expansion point. The coefficients $\bar{U}_k^{(n)}$, $n \in \mathbb{N}$, are related to the couplings and parameters of the classical potential at the short-distance cutoff Λ, i.e.,

$$\begin{gathered}\bar{U}_\Lambda^{(0)} = \bar{\phi}_\Lambda\left[h_\Lambda + \frac{1}{12}(5t_\Lambda + \tau)\bar{\phi}_\Lambda\right], \quad \bar{U}_\Lambda^{(1)} = h_\Lambda + \frac{1}{3}(2t_\Lambda + \tau)\bar{\phi}_\Lambda, \\ \bar{U}_\Lambda^{(2)} = \tau, \quad \bar{U}_\Lambda^{(3)} = \frac{1}{6}\lambda_\Lambda\bar{\phi}_\Lambda, \quad \bar{U}_\Lambda^{(4)} = \lambda_\Lambda, \quad \bar{U}_\Lambda^{(n>4)} = 0.\end{gathered} \tag{4.25}$$

Similarly, the expansions for Z_k and W_k read

$$Z_k = \sum_{n=0}^{n_Z-1}\frac{1}{n!}\bar{Z}_k^{(n)}\delta\varphi_k^n, \tag{4.26a}$$

$$W_k = \sum_{n=0}^{n_W-1}\frac{1}{n!}\bar{W}_k^{(n)}\delta\varphi_k^n, \tag{4.26b}$$

with $\bar{Z}_\Lambda^{(0)} = 1$, $\bar{Z}_\Lambda^{(n)} = 0$ for $n > 0$, and $\bar{W}_\Lambda^{(n)} = 0$ for $n \in \mathbb{N}$. We define $Z_k \equiv 0$ if $n_Z = 0$ and $W_k \equiv 0$ if $n_W = 0$. In the following, we denote these type of series truncations in short by the set of integers (n_U, n_Z, n_W). n_U is considered as a free parameter, while n_Z and n_W are chosen such that $\max_{n_Z} \dim \bar{Z}_k^{(n_Z)} \leq \dim \bar{U}_k^{(n_U)}$ and $\max_{n_W} \dim \bar{W}_k^{(n_W)} \leq \dim \bar{U}_k^{(n_U)}$ in

$d = 6$ dimensions. This choice defines what we consider to be consistent truncations (see Sec. 4.1.5).

Substituting Eqs. (4.24) – (4.26b) back into (4.17a) – (4.17c) we obtain a finite set of flow equations for the coefficients of the series expansion. In this work, we consider expansions of order up to $(n_U, n_Z, n_W) = (7, 5, 0)$ and $(5, 3, 2)$, which yields a coupled set of partial differential equations of up to 12 and 10 parameters, respectively. The Lee-Yang scaling solution is identified by inspecting the behavior of the first and second derivatives of the effective potential, which should satisfy $\bar{U}^{(1)} = \bar{U}^{(2)} = 0$, while $\operatorname{Im}\bar{U}^{(2n)} = \operatorname{Re}\bar{U}^{(2n+1)} = 0$, for $n \in \mathbb{N}$. Note that all of these coefficients are defined at a reference field configuration $\bar{\varphi}$ (where $\lim_{k\to 0}\bar{\chi}_k = 0$), which is imaginary, corresponding to the imaginary magnetic field $H_c = \pm i|H_c(T)|$, with $T > T_c$.

We introduce the following short-hand notation for the renormalization factor $\bar{Z}_k \equiv Z_k^{(0)}(\bar{\varphi}_k)$, which satisfies $\bar{Z}_k \sim (k/\Lambda)^{-\eta}$ at the critical point. Starting from a set of initial values for the parameters and coupling constants in the classical action, which are tuned to their critical values, we may therefore define the anomalous dimension by the corresponding value in the IR (cf. Eq. (1.29) and (1.83)):

$$\eta = -\lim_{k\to 0}\frac{\partial}{\partial s}\ln \bar{Z}_k. \tag{4.27}$$

Note that the anomalous dimension at the Lee-Yang edge critical point is negative for all values of $1 \leq d < 6$.

4.1.4 Critical Scaling Exponents and Hyperscaling Relations

The critical exponents at the Lee-Yang edge critical point are extracted by a stability analysis of the scaling solution with respect to perturbations with those operators included in our *ansatz* Eq. (4.16). That is, for any finite truncation of the scale-dependent effective action, we obtain a finite set critical exponents corresponding to the eigenvalues λ_n of the stability matrix,

$$\gamma_{mn} = \frac{\partial \beta_m\big(\{\bar{g}_{*,l}\}_{l\in I}\big)}{\partial \bar{g}_{n,k}}, \tag{4.28}$$

which is evaluated at the fixed point of the RG β functions, $\beta_m \equiv \partial \bar{g}_{m,k}/\partial s$, i.e.,

$$\beta_m\big(\{\bar{g}_{*,n}\}_{n\in I}\big) = 0. \tag{4.29}$$

The β functions are derived for the dimensionless, renormalized parameters and couplings of the model, $\bar{g}_{n,k}$, $n \in I = \{1, 2, \ldots, n_U + n_Z + n_W\}$, which are given by $\bar{g}_{1,k} = k^{-(d+2)/2}\bar{Z}_k^{-1/2}\bar{U}_k^{(1)}$, $\bar{g}_{2,k} = k^{(2-d)/2}\bar{Z}_k^{1/2}\bar{\chi}_k$, etc. We order the eigenvalues λ_n, $n = 1, 2, \ldots$, according to their values in $d = 6$ dimensions, where they are identical to the canonical dimension of the parameters and couplings associated with the operators that appear in Γ_k, e.g., $\lambda_1(d = 6) = \dim \bar{U}^{(1)} \geq \lambda_2(d = 6) = \dim \bar{\chi} \geq \ldots$. Of course, as the eigenvalues are analytically continued to dimensions below $d = 6$, this ordering might change.

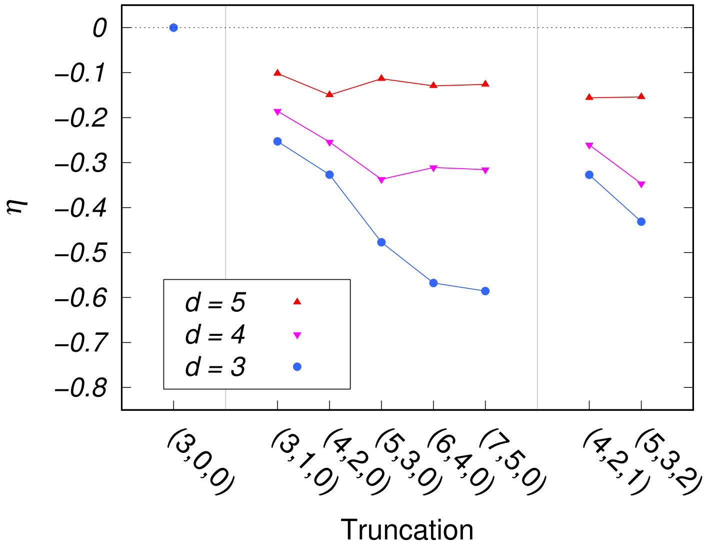

Figure 4.2: Anomalous dimension η for different truncations of the scale-dependent effective action in $d = 3$, 4, and 5 dimensions.

We observe that the largest eigenvalue $\lambda_1 \equiv 1/\nu_c$ satisfies the following scaling relation

$$1/\nu_c = (d + 2 - \eta)/2, \tag{4.30}$$

and therefore, the critical exponent ν_c is determined completely in terms of the anomalous dimension η. The Lee-Yang edge critical point is known to exhibit another hyperscaling relation, which follows from the equation of motion of the ϕ^3 theory [162] and can be written as

$$\lambda_1 + \lambda_2 = d, \tag{4.31}$$

with $\lambda_2 \equiv 1/\nu$, from which we obtain

$$1/\nu = (d - 2 + \eta)/2. \tag{4.32}$$

Furthermore, from scaling and hyperscaling relations, one can derive

$$\sigma = \frac{1}{\delta} = \frac{d - 2 + \eta}{d + 2 - \eta}, \tag{4.33}$$

and $\beta = 1$, independent of dimension [137]. Note, however, that for any finite truncation of Γ_k scaling relations between critical exponents need not necessarily be satisfied and therefore should be checked explicitly. This applies to both Eq. (4.32) and to Eq. (4.33). Taking Eq. (4.32) for example, one may define the relative difference $\Delta\lambda_2/[(d-2+\eta)/2] = 2\lambda_2/(d-2+\eta) - 1$ as an indicator for the quality of the employed truncation at the Lee-Yang edge fixed point. We observe that the relative error in the scaling relation (4.32) increases with smaller dimensions. For both the $(7, 5, 0)$ and $(5, 3, 2)$ truncations, we obtain a 15% error in $d = 5$ dimensions, a $60 - 70\%$ error in $d = 4$ dimensions etc. This is an indication that the considered series expansions are not fully converged yet. Nevertheless, since we expect these scaling relations to hold for high enough orders, we employ Eq. (4.32) in the following to determine the exponent ν, keeping in mind that the corresponding estimates will be associated with an error that is likely to decrease only when higher-order truncations are considered. In particular, the above numbers suggest that to reach a given precision, one will need to account for an increasing number of operators in Γ_k in lower dimensions.

The scaling properties of the Lee-Yang edge are completely determined by the anomalous dimension η. Therefore, we may use Eqs. (4.30) and (4.33) to calculate the critical exponents ν_c and σ. Our results are summarized in Fig. 4.1 where we show the overall performance

Critical exponent	$d = 3$	$d = 4$	$d = 5$
η	$-0.586(29)$	$-0.316(16)$	$-0.126(6)$
σ	$0.0742(56)$	$0.2667(32)$	$0.4033(12)$
ν_c	$0.3581(19)$	$0.3167(8)$	$0.2807(2)$

Table 4.3: Numerical values for the anomalous dimension η and critical exponents σ, ν_c in $d = 3$, 4, and 5 dimensions. Here, we show our best estimates with errors to account for possible systematic effects (see Sec. 4.1.6). These values were obtained with an exponential regulator ($\alpha = 1$) (cf. Eq. (4.36)) and the truncation of the type $(7, 5, 0)$.

of different truncations in the range $3 \leq d \leq 6$ at the example of σ and ν_c, contrasted against the one- and two-loop ε expansion. In Fig. 4.2 we show the values for η in $d = 3$, 4, and 5 dimensions for all truncations employed in this work, and our best estimates for the critical exponents η, ν_c, and σ are reported in Tab. 4.3. These values were obtained with the $(7, 5, 0)$ truncation for which, in contrast to the $(5, 3, 2)$ truncation, the values of η seem to be reasonably close to their asymptotic values that are reached in the infinite n_U and n_Z limit (cf. Fig. 4.2). That is, we observe that larger orders of the finite field expansion are necessary to reach the asymptotic scaling exponents and it seems that this order increases for dimensions well below the upper critical dimension $d_c = 6$, which is consistent with our previous observation on the validity of scaling relations.

In Tab. 4.3 and 4.4 we account for a systematic bias due to our choice of the IR regulator (see Sec. 4.1.6 for an in depth discussion of this issue). We remark that the difference in the values of the anomalous dimension between different high-order truncations is typically larger than that obtained for the critical exponents σ and ν_c, which is reflected in the errors for these quantities (cf. Tab. 4.3). This effect has also been observed with other methods and may be attributed to the scaling relations (4.30) and (4.33) that yield a smaller error for the exponents ν_c and σ (see, e.g., Ref. [139]).

Comparing our estimates for the critical exponent σ from FRG to available data on the Lee-Yang edge critical scaling exponents provided in Ref. [139], cf. Tab. 4.4, we find that our values lie within the error bounds provided by other methods, e.g., Refs. [140, 141, 142].

Dimension	functional RG	Ref. [139]		Ref. [140]	Ref. [141]	Ref. [142]	Ref. [143]
$d = 3$	0.0742(56)	0.0785	0.0747	0.076(2)	0.0877(25)	0.080(7)	0.085(1)
$d = 4$	0.2667(32)	0.2616	0.2584	0.258(5)	0.2648(15)	0.261(12)	0.2685(1)
$d = 5$	0.4033(12)	0.3989	0.3981	0.401(9)	0.402(5)	0.40(2)	0.4105(5)

Table 4.4: Different estimates for the critical exponent σ (as compiled in Ref. [139]) including results from the constrained three- and four-loop ε' expansion [139], strong-coupling expansion [140], Monte Carlo methods [141, 142], and conformal bootstrap [143]. The values obtained from the functional RG, with an exponential regulator ($\alpha = 1$) and truncation of the type $(7, 5, 0)$, lie within error bars of Refs. [140, 141, 142], and are slightly larger the values provided by constrained Padé approximants of three- and four-loop ε' expansion results [139], but are smaller than those obtained by conformal bootstrap methods [143].

They lie slightly above the values obtained from constrained Padé approximants of three- and four-loop ε expansion results [139], but are in general smaller than those values obtained from a recent conformal bootstrap analysis [143]. Considering the fact, that our numerical implementation of the RG flow equations is not overly sophisticated (limiting the truncations that can be considered to a relatively small number of operators) it is quite remarkable that our present results are competitive with other data in the literature.

4.1.5 Relevance of Composite Operators and Quality of Finite Truncations

We observe that certain truncations of the scale-dependent effective action, of the type $(n_U, 0, 0)$, $n_U > 3$, are inadequate to investigate the Lee-Yang scaling behavior. In fact, for these truncations, the Lee-Yang fixed point is unstable below $d \approx 5.6$.[4] This is certainly surprising and in conflict with other available data [140, 141, 142, 143, 139]. However, this behavior can be understood by examining the effect of operator insertions at the level of the one-loop $\varepsilon' = 6 - d$ expansion, as considered in Refs. [165, 53].

---

[4] We remark that this observation depends on the choice of the IR regulator. While the Lee-Yang edge fixed point is unstable for the smooth exponential regulator (4.36) ($\alpha = 1$), this is not the case for the optimized Litim regulator [163, 164]. However, the latter is not immediately applicable at higher orders in the derivative expansion.

In particular, we consider the renormalization of quartic operators at the Lee-Yang fixed point. This requires the simultaneous renormalization of all operators that carry the same canonical dimension as $\delta\varphi_k^4$, which mix under renormalization [166]. In $d = 6-\varepsilon'$ dimensions these operators can be listed as follows (up to total derivative contributions)

$$A_{1,k} = \delta\varphi_k^4/4!, \tag{4.34a}$$

$$A_{2,k} = k^{\varepsilon/2}\delta\varphi_k \left(\partial\delta\varphi_k\right)^2/2, \tag{4.34b}$$

$$A_{3,k} = k^{\varepsilon}\left(\Box\,\delta\varphi_k\right)^2/2. \tag{4.34c}$$

Note that they simply correspond to particular contributions in the finite series expansion of $U_k(\varphi)$, $Z_k(\varphi)(\partial\varphi)^2$, and $W_k(\varphi)\left(\Box\varphi\right)^2$, respectively, around the homogeneous field expectation value $\bar{\varphi}_k$. Different truncations of the scale-dependent effective action are distinguished by either including or neglecting some of these operators, (4.34a) – (4.34c). The $(n_U, 0, 0)$-type truncations, for instance do not include operators $A_{2,k}$ and $A_{3,k}$, while truncations of the type $(n_U, n_Z, 0)$ do not include $A_{3,k}$.

Treating the operators (4.34a) – (4.34c) on an equal footing, both $A_{2,k}$ and $A_{3,k}$ turn out to be more relevant in $d < 6$ dimensions than the quartic interaction $A_{1,k}$. Indeed, from a one-loop calculation [165, 53], we obtain the following eigenvalues of the stability matrix: $\lambda_4 = -2$, $\lambda_5 = -2-\varepsilon'/9$, and $\lambda_6 = -2-19\varepsilon'/9$. Each of them corresponds to a different linear combination of operators (4.34a) – (4.34c). One can show that the dominant contribution to λ_4 comes from $A_{3,k}$, for λ_5 it is the operator $A_{2,k}$, and for λ_6 it is $A_{1,k}$ that contributes the most. Thus, one might conclude that any truncation that includes only the quartic interaction $A_{1,k}$ is ill-defined, as it neglects the more relevant contributions, namely $A_{2,k}$ and $A_{3,k}$. Interestingly, it is sufficient to consider truncations of the type $(n_U, n_Z, 0)$ to stabilize the Lee-Yang edge fixed point. While $(n_U, 0, 0)$-type truncations, $n_U > 3$, fail to produce a Lee-Yang edge fixed point below $d \approx 5.6$, the $(n_U, n_Z, 0)$ truncations allow us to identify the corresponding scaling solution all the way down to $d = 3$ (cf. Fig. 4.1). In general, we expect that the scale-dependent effective action needs to respect the properties of the theory under simultaneous renormalization of operators with the same canonical dimension. This is important to define consistent truncations that are adequate to describe the Lee-Yang edge critical point.

4.1.6 Residual Regulator Dependence and Principle of Minimal Sensitivity

To determine the critical scaling properties of a given model, we may in principle choose any regulator function $R_k = R_k(q)$ as long as it satisfies the appropriate limiting behavior $\lim_{k\to 0} R_k = 0$ and $\lim_{\Lambda\to\infty} R_{k=\Lambda} = \infty$. Indeed, if an exact solution to the functional flow equation for Γ_k were available, the calculated observables should not depend on the way we choose to regularize the theory in the IR and therefore must be independent of the regulator. However, in practice, we are bound to consider truncations of the coupled infinite set of flow equations. This yields a finite set of RG equations for which one observes a residual regulator dependence [167]. To investigate this effect, we define a one-parameter family of functions

$$R_{\alpha,k} = \alpha R_k, \tag{4.35}$$

with $\alpha > 0$, and consider the α dependence of the critical exponents. We employ the following set of exponential regulators

$$R^{\mathrm{exp}}_{\alpha,k} = \frac{\alpha \bar{Z}_k q^2}{\exp(q^2/k^2) - 1}, \tag{4.36}$$

for this analysis.[5] One may identify an optimal value of α, which is determined by the principle of minimum sensitivity [155]. It states that the value of any given observable that is least sensitive to changes in α can be considered the best estimate for that quantity. Since by virtue of scaling relations all critical exponents at the Lee-Yang edge critical point can be

---

[5] Note that the regulator should be sufficiently smooth in momentum space if higher order approximations in the derivative expansion are considered (see, e.g., Ref. [155]).

	$d = 3$	$d = 4$	$d = 5$
$\eta(\alpha = 1)$	-0.3270	-0.2542	-0.1498
$\eta(\alpha = \alpha_{\text{opt}})$	-0.3340	-0.2587	-0.1500
Relative error	2.1%	1.7%	1.3%

Table 4.5: Anomalous dimension $\eta = \eta(\alpha)$ at the Lee-Yang point in d dimensions, evaluated for the (deformed) exponential regulator $R^{\text{exp}}_{\alpha,k}(q) = \alpha \bar{Z}_k q^2 \left[\exp(q^2/k^2) - 1\right]^{-1}$ with $\alpha > 0$. The optimal value of α depends on the dimension, i.e., $\alpha_{\text{opt}} = \alpha_{\text{opt}}(d)$ (cf. Fig. 4.3). The shown values were obtained using a truncation of the scale-dependent effective action Γ_k defined by the index set $(4, 2, 0)$.

expressed in terms of the anomalous dimension η, we apply this criterion to $\eta = \eta(\alpha)$, i.e., to find the optimal value, we require that

$$\eta'(\alpha = \alpha_{\text{opt}}) = 0. \tag{4.37}$$

In Tab. 4.5 we compare the values of $\eta(\alpha)$ evaluated for $\alpha = 1$ as well as $\alpha = \alpha_{\text{opt}}$ in different dimensions and determine the relative error $\Delta\eta/\eta(\alpha_{\text{opt}}) \equiv \left[\eta(1) - \eta(\alpha_{\text{opt}})\right]/\eta(\alpha_{\text{opt}})$. Largely independent of dimension, the anomalous dimension evaluated at $\alpha = 1$ seems to be slightly overestimated with a relative error of approximately 3%. From this comparison we conclude that $\eta(\alpha = 1)$ is typically already a good approximation to the optimal value $\eta(\alpha_{\text{opt}})$.

In principle, $\alpha_{\rm opt}$ might depend on the dimension. Indeed, as shown in Fig. 4.3, the optimal value of α shifts to larger values when the dimension d is lowered and eventually stabilizes around $\alpha \approx 1.7$. Although the value of $\alpha_{\rm opt}$ increases, the relative error in η remains roughly constant. At this point, we remark that below $d = 4$ an ambiguity appears: $\eta(\alpha)$ develops a second extremum, a local maximum, for $\alpha < 1$ (cf. Fig. 4.3). However, we do not consider this solution to be physical and define $\alpha_{\rm opt}(d)$ as the analytically continued local minimum from $d = 6 - \varepsilon'$.

Since the search for fixed points of the RG β functions becomes quite demanding numerically for higher-order truncations, we use this information to limit our calculations to the case $\alpha = 1$ and estimate the corresponding systematic error in $\eta(\alpha = 1)$ at the $3-5\%$ level (within the considered one-parameter family of regulators). This systematic effect in the estimation of the anomalous dimension has been accounted for and is indicated explicitly as a systematic error in the summary of our results in Tab. 4.3 and 4.4.

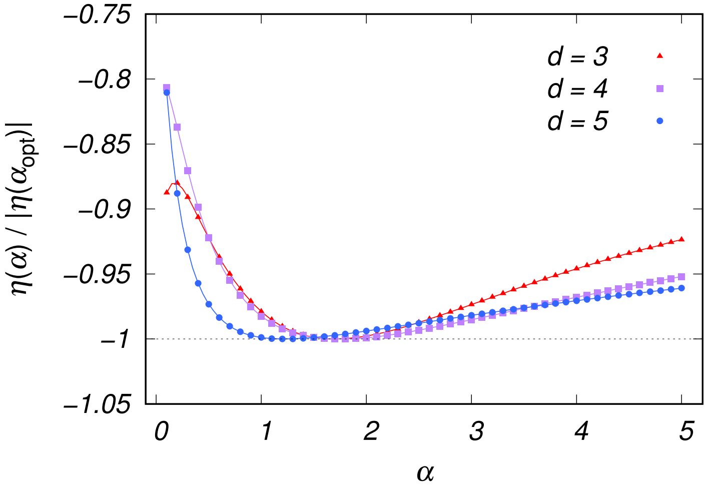

Figure 4.3: Rescaled anomalous dimension $\eta(\alpha)/|\eta(\alpha_{\rm opt})|$ shown as a function of α. Different curves correspond to data obtained in $d = 3$, 4, and 5 dimensions, respectively. The optimal value $\alpha_{\rm opt}$ for which the critical exponent i s least sensitive to changes in the deformation parameter, i.e., $\eta'(\alpha = \alpha_{\rm opt}) = 0$, shifts to larger values as the dimension d is lowered. The displayed values were obtained for a truncation of the scale-dependent effective action Γ_k of the type $(4, 2, 0)$.

4.2 Spinodal Points and Lee-Yang Edge Singularities

Owing to universality and scaling, the equation of state sufficiently close to the critical point, i.e., in the scaling region, can be characterized by a universal function of a single argument, a scale-invariant combination of two relevant variables – the magnetic field and the temperature. Determining this function is a well-posed mathematical problem which to this day, however, remains unsolved, at least in the analytically exact sense. Nevertheless, a lot is known about the equation of state [31]. This includes celebrated exact results, such as the Onsager solution of the two-dimensional Ising model in the absence of the magnetic field [25] or the Lee-Yang theorem regarding the distribution of zeros of the partition function in the complex plane of the magnetic field variable [51, 52]. The equation of state near the upper critical dimension, $d = 4$, is also understood in terms of the perturbative Wilson-Fisher fixed point using the $\varepsilon = 4 - d$ expansion [168, 169, 170, 171, 172]. Furthermore, there are numerous numerical studies based on the high-temperature series expansion [173, 174], perturbative field-theory expansions [73], Monte Carlo lattice simulations [175, 176, 177, 178, 179], the exact renormalization group [180], as well as the truncated free-fermion space approach [181].

In this thesis we focus on the analytic properties of the universal equation of state in the scaling regime near the Ising critical point as a function of a *complex* magnetic field H. Two notable facts will guide our discussion. The first is Lee and Yang's observation that the singularities in the complex magnetic field plane terminate two (complex conjugate) branch cuts, which according to the Lee-Yang theorem [52], must lie on the imaginary axis. These branch points, or Lee-Yang edge singularities, "pinch" the real axis as the temperature T approaches its critical value T_c from above, resulting in a singularity on the real axis at zero magnetic field – the Ising critical point. The second is the observation by Fisher that the thermodynamic singularity at the Lee-Yang edge point corresponds to the critical point in the ϕ^3 theory [132] (reviewed in Sec. 2.6). The upper critical dimension of this theory is six, which means that below this dimension the critical exponent σ that characterizes the vanishing of the discontinuity at the Lee-Yang branch point is not simply given by its mean-field value 1/2. This includes the case $d = 4 - \varepsilon$, where the Ising equation of state is believed to be described by mean-field theory with corrections suppressed by ε. Here, we address the apparent contradiction between the conclusions of Fisher's analysis and the ε expansion around $d = 4$.

Analyticity of the equation of state allows one to connect high- and low-temperature domains near the critical point [182, 183]. In particular, using the mean-field equation of state one can show that the Lee-Yang edge singularities, which reside on the imaginary magnetic field axis, are analytically connected to singularities that limit the domain of metastability – so-called spinodal singularities [184, 185, 186]. The latter reside on another Riemann sheet reachable by analytic continuation through the branch cut along the real magnetic field axis, describing the first-order phase transition at zero magnetic field. The position of these singularities on the real axis, however, is an artifact of the mean-field approximation. In fact, in $4 - \varepsilon$ dimensions the position of the spinodal point shifts into the complex plane by an amount of order ε^2. We analyze this phenomenon in the framework of the ε expansion employing parametric representations of the equation of state [71, 187, 188, 72]. Our goal is to confront the extended analyticity conjecture advanced by Fonseca and Zamolodchikov [181], which states that the complexified spinodal point is the nearest singularity to the real axis of the magnetic field.

The outline of this section is as follows: In Sec. 4.2.1 we review the properties of the mean-field equation of state of the scalar ϕ^4 theory, and introduce the Lee-Yang edge singularities with their low-temperature image – the spinodal points. Next, in Sec. 4.2.2, we discuss the limitations of the mean-field approximation. In particular, we derive the Ginzburg criterion which quantifies the breakdown of mean-field theory near the Lee-Yang edge singularities. Thereafter, in Sec. 4.2.3, we employ the $\varepsilon = 4 - d$ expansion and examine the nature of the complex-field singularities in the framework of parametric representations of the Ising equation of state. In Sec. 4.2.4 we consider the same problem from the point of view of the O(N)-symmetric ϕ^4 theory in the large-N limit. We argue that they are consistent with the extended analyticity conjecture put forward by Fonseca and Zamolodchikov and discuss the difficulty of establishing the latter rigorously in the ε expansion.

4.2.1 Critical Equation of State and the Mean-field Approximation

The scalar ϕ^4 theory in d dimensions can be defined by the Euclidean action in Eq. 1.2, which is rewritten here following the notation convention of Ref. [5] :

$$\mathcal{S} = \int d^d x \left[\frac{1}{2}(\partial_\mu \phi)^2 + \frac{r_0}{2}\phi^2 + \frac{u_0}{4!}\phi^4 - h_0\phi \right]. \tag{4.38}$$

The expectation value of the field ϕ, $\langle\phi\rangle = \varphi$, can be found by using Eq. (1.51) with the source replaced by h_0 here. The relation between the expectation value $\langle\phi\rangle$ and the bare parameters r_0 and h_0 (and, generally, also u_0 as well as the ultraviolet cutoff) defines the equation of state.

More specifically, we are interested in the critical point of this theory, i.e., the point in the parameter space where the correlation length ξ, measured in units of the cutoff scale, diverges. This point can be reached at $h_0 = 0$, by tuning $r_0 \to r_\text{c}$ for any given u_0. In fact, below the upper critical dimension, i.e., $d < 4$, the effective coupling runs into an infrared fixed point, the Wilson-Fisher fixed point and, as a result, the dependence on the coupling u_0 and the cutoff disappears – the equation of state becomes a relation between three variables: $\langle\phi\rangle$, h_0, and r_0.

The critical ϕ^4 theory provides a universal description of critical phenomena in many physically different systems such as liquid-gas or binary fluid mixtures or spin systems such as uniaxial ferromagnets. For the latter, the parameter h_0 can be mapped onto the applied external magnetic field, i.e., $h_0 \sim H$, while

$$t \equiv r_0 - r_\text{c}, \tag{4.39}$$

is proportional to the deviation of the temperature from the critical (Curie) point, i.e., $t \sim T - T_\text{c}$ (see also Sec. 1.3).

In terms of conveniently rescaled variables $\Phi = \sqrt{u_0/6}\,\phi$ and $H = \sqrt{u_0/6}\,h_0$, the action Eq. (4.38) takes the form

$$\mathcal{S} = \frac{6}{u_0}\int d^dx \left[\frac{1}{2}\left(\partial_\mu \Phi\right)^2 + V(\Phi)\right], \tag{4.40}$$

with the potential

$$V(\Phi) = \frac{r_0}{2}\Phi^2 + \frac{1}{4}\Phi^4 - H\Phi. \tag{4.41}$$

It is clear from Eq. (4.40) that for small u_0 fluctuations are suppressed and the path integral defining the partition function of the theory can be evaluated in the saddle-point, or mean-field, approximation. In this approximation the expectation value of the field, $\langle\Phi\rangle = M$, is a coordinate-independent constant that minimizes the potential (4.41), i.e.,

$$V'(M) = -H + r_0 M + M^3 = 0. \tag{4.42}$$

The correlation length ξ is defined in terms of the second derivative of the (effective) potential V at its minimum and, in the mean-field case, it is given by

$$\xi^{-2} = V''(M) = r_0 + 3M^2. \tag{4.43}$$

The Ising critical point, $\xi \to \infty$, is reached at $H = M = r_0 = 0$, and therefore

$$t = r_0. \tag{4.44}$$

The implicit (multivalued) function $M(t, H)$ defined by Eq. (4.42) represents the mean-field equation of state of the ϕ^4 theory (or Ising model).

It is clear from Eq. (4.43) that above the critical temperature of the Ising model, i.e., for $t = r_0 > 0$, the correlation length is finite for all *real* values of H. However, solving for $V'(M) = V''(M) = 0$, we find points on the *imaginary* axis, where $\xi \to \infty$ for $t > 0$:

$$M_{\mathrm{LY}} = \pm\frac{1}{\sqrt{3}}\,it^{1/2} \quad \text{and} \quad H_{\mathrm{LY}} = \pm\frac{2}{3\sqrt{3}}\,it^{3/2}. \tag{4.45}$$

For $t > 0$, these branch points of $M(H)$, known as Lee-Yang (LY) edge singularities, terminate cuts that lie on the imaginary H axis (according to the Lee-Yang theorem [51, 52]). They pinch the real H axis as the temperature T approaches its critical value T_c, i.e., $t \to 0$.

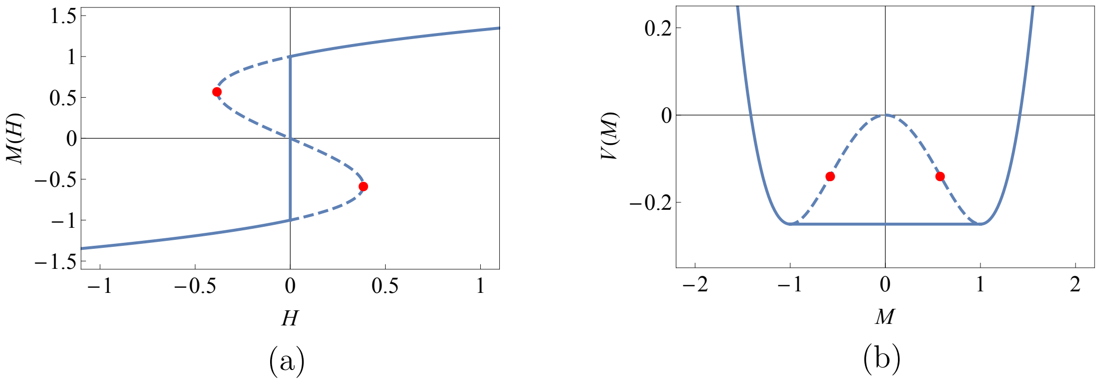

Figure 4.4: (a) The mean-field Ising equation of state $M(H)$ and (b) the corresponding effective potential $V(M)$ at $H = 0$ in the low-temperature phase ($T < T_c$). The analytic continuation of the stable branch (dashed curve) is bounded by the spinodal points (red). The straight line connecting the two minima of the effective potential is determined by the Maxwell construction.

On the other hand, below the critical temperature, $t < 0$, the mean-field approximation predicts that the correlation length, given by Eq. (4.43), diverges at *real* values of M and H. These so-called spinodal points are located on the metastable branch and limit the domain of metastability [184, 185, 186], as shown in Fig. 4.4 (and Fig. 1.4 as well).

An important property of the critical equation of state is scaling[6] [189, 184]: The relation between M, t, and H is invariant under simultaneous rescaling of these variables according to their scaling dimensions

$$t \to \lambda t, \quad H \to \lambda^{\beta\delta} H, \quad \text{and} \quad M \to \lambda^{\beta} M, \tag{4.46}$$

where β and δ are standard critical exponents. The mean-field equation of state in Eqs. (4.42), (4.44) scales with exponents

$$\beta = \frac{1}{2} \quad \text{and} \quad \delta = 3 \qquad \text{(mean field)}. \tag{4.47}$$

Scaling implies that the equation of state can be expressed as a relation between only two scaling-invariant variables. Depending on the choice of these variables it may be represented

---

[6] Generally, scaling is a consequence of the coupling u_0 running into an IR fixed point.

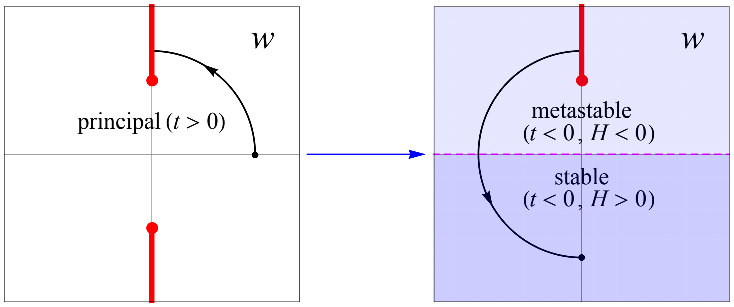

Figure 4.5: Analytic continuation $t \to -t$ from the principal, i.e., high-temperature sheet (left panel) to the low-temperature sheet (right panel) of the mean-field scaling function $z(w)$ in Eq. (4.52) with $w \sim Ht^{-3/2}$. Starting from $H > 0$ and $t > 0$, keeping $H > 0$ and $|t|$ fixed we rotate the phase $\arg t$ from 0 to $-\pi$ and trace the corresponding movement of the variable w along the shown circular path. The principal sheet features a pair of Lee-Yang branch cuts along the imaginary w axis, which terminate in the Lee-Yang edge singularities. Going through the cut we enter the metastable low-temperature branch ($H < 0$, $t < 0$). One reaches the stable branch ($H > 0$, $t < 0$) when $\arg t = -\pi$. From there one can also reach metastable branch $H < 0$ by rotating $\arg H$ from 0 to $\pm\pi$, which changes $\arg w$ by $\pm\pi$.

in several different ways. For example, we may express the equation of state in the Widom scaling form [189]

$$y = f(x), \quad \text{with} \quad x \sim tM^{-1/\beta} \quad \text{and} \quad y \sim HM^{-\delta}, \tag{4.48}$$

where symbols '$\sim$' reflect arbitrary normalization constants which can be chosen to bring the function $f(x)$ into canonical form. Here, we express the mean-field scaling function $f(x)$ as

$$f(x) = 1 + x, \tag{4.49}$$

with the scaling-invariant variables defined as

$$x = tM^{-1/\beta} \quad \text{and} \quad y = HM^{-\delta}. \tag{4.50}$$

However, the analytic properties as a function of H at fixed t are more manifest in another representation of the scaling equation of state

$$w = F(z), \quad \text{with} \quad w \sim Ht^{-\beta\delta} \quad \text{and} \quad z \sim Mt^{-\beta}. \tag{4.51}$$

Again, the normalization constants in Eqs. (4.51) can be chosen to achieve a conventional (canonical) form for the equation of state. We choose to express the mean-field scaling function $F(z)$ in the following form

$$F(z) = z(1 + z^2), \tag{4.52}$$

with the variables

$$w = Ht^{-\beta\delta} \quad \text{and} \quad z = Mt^{-\beta}. \tag{4.53}$$

The inverse of the (mean-field) function $F(z)$, i.e., $z(w)$, is multivalued and has three Riemann sheets associated with the high- and low-temperature regimes of the mean-field equation of state (Fig. 4.6). The principal sheet, which represents the equation of state $M(H)$ for $t > 0$, features two branch points. They are located on the imaginary axis in the complex w plane

$$w_{\text{LY}} = \pm \frac{2i}{3\sqrt{3}}, \tag{4.54}$$

and correspond to the Lee-Yang edge singularities at imaginary values of the magnetic field H, cf. Eqs. (4.45).

Going under either one of the associated branch cuts, e.g., by following the path shown in Fig. 4.5, one arrives on the secondary sheet, which corresponds to the metastable branch of the equation of state at $t < 0$. The same branch point in Eq. (4.54) viewed from this sheet represents the spinodal point located at real negative H. To arrive on the stable $t < 0$ branch, i.e., $H > 0$, one has to follow the circular path further in the anticlockwise direction, as shown in Fig. 4.5 (right). We conclude that, in the mean-field approximation, the spinodal points and the Lee-Yang edge singularities are manifestations of the *same* singularities of the scaling equation of state $z(w)$.

4.2.2 Beyond the Mean-field Approximation

The mean-field approximation relies on the smallness of the coupling u_0. As we discussed in Sec. 2.6, this is justifiable for $d \geq 4$, where the coupling runs into the Gaussian IR

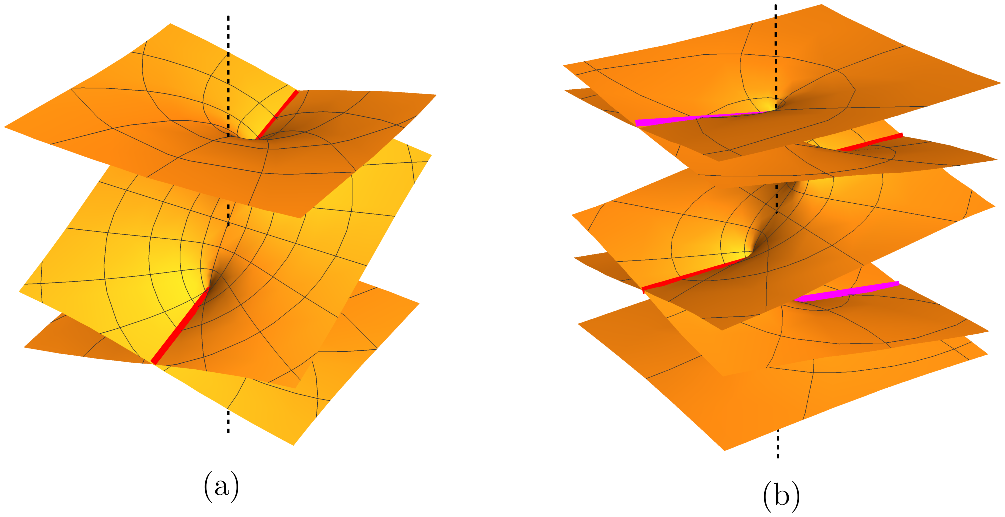

Figure 4.6: The Riemann sheet of $\operatorname{Im} z(w)$ in the complex w plane for the mean-field ϕ^4 theory subject to O(1) symmetry (a), and for the spherical model, i.e., the large-N limit of a O(N) theory (b). The red line stands for the Lee-Yang cut while the magenta line for the Goldstone cut.

fixed point and becomes arbitrary small as $\xi \to \infty$. For $d < 4$, according to Eq. (1.24), the Wilson-Fisher fixed-point value of the coupling, $u_0^{\mathrm{WF}} = \mathcal{O}(\varepsilon)$, is also small as long as $\varepsilon = 4 - d \ll 1$. However, for the most interesting case $d = 3$ the theory is non-perturbative and we cannot rely on the mean-field approximation. We would like to address the following question: What happens with the spinodal points and Lee-Yang edge singularities in this case? We shall begin with general considerations and later consider the case of small ε.

Langer cut and Fonseca-Zamolodchikov conjecture

According to the Lee-Yang theorem [51, 52] the singularities of the Ising model, and thus, by universality, of the ϕ^4 theory, must be located on the imaginary axis of H. Thus the result of the mean-field theory that the Lee-Yang edge singularities (and their associated cuts) are on the imaginary axis holds in general.[7]

---

[7] The theorem applies to singularities on physical stable branches of the function $M(H)$ (both below and above critical temperature) and thus cannot constrain the position of the spinodal singularities which are

What happens to the spinodal singularities away from mean-field? As we discussed, the scaling equation of state $z(w)$ describes both high- and low-temperature branches of $M(H)$, which correspond to primary and secondary Riemann sheets of the variable w. The Lee-Yang edge singularities are described by $w_{\rm LY}$, which lie on the imaginary w axis because $w \sim Ht^{-\beta\delta}$ and for $t > 0$ the value of H at the singularity, $H_{\rm LY}$, is imaginary. Thus analyticity and scaling imply that there must also be singularities on the low-temperature branch $t < 0$, at values of H given by:

$$H_{\rm sp} \sim w_{\rm LY}\, t^{\beta\delta} = \mp |w_{\rm LY}\, t^{\beta\delta}| e^{\pm i\pi(\beta\delta - 3/2)}, \quad t < 0, \tag{4.55}$$

where the different signs correspond to the two (complex conjugate) values of $w_{\rm LY}$ and to the two possible directions of rotation from t to $-t = e^{\pm i\pi}t$. Thus, in general, the spinodal points $H_{\rm sp}$ are displaced from the (negative) real H axis by a phase

$$\Delta\phi = \pi\left(\beta\delta - \frac{3}{2}\right), \tag{4.56}$$

where $\beta\delta > 3/2$ below the upper critical dimension, i.e., for $d < 4$ (cf. Eq. (4.67)), and $\beta\delta = 3/2$ for $d \geq 4$.

In order to understand the position of the points described by Eq. (4.55) it is important to take into account another property of the equation of state in the low-temperature domain – the Langer cut [190]. It is well-known that the Ising equation of state is weakly singular at $H = 0$ for $t < 0$, due to the presence of an essential singularity [191, 184, 192] associated with the decay of the metastable vacuum [193, 194, 195]. The rate of this decay gives the imaginary part of the free energy $\mathcal{F}(t, H)$ for H on the metastable branch at $t < 0$ and, since $M = \partial\mathcal{F}/\partial H$, also the imaginary part of the magnetization $M(t, H)$. Near $d = 4$, it takes the form (for $w \ll 1$)

$$\operatorname{Im} M(t, H) \sim \exp\left(-\frac{\text{const}}{u_0 |w|^3}\right), \tag{4.57}$$

---

located on the metastable branch.

demonstrating that there is an essential singularity, which is non-perturbative in u_0. Not only is this singularity absent in the mean-field equation of state, but it cannot be seen at any finite order of the ε expansion. The imaginary part of M is discontinuous (changes sign by Schwarz reflection principle) across the real axis of H on the metastable branch, which corresponds to a cut, known as the Langer cut [190].

This cut can be reached from the stable low-temperature branch ($H > 0$, $t < 0$) by rotating H along a semicircle in the complex H plane, such that $H \to -H$. Thus, its location in the complex w plane should be as shown in Fig. 4.7. If we translate Fig. 4.7 into the H plane, using $w \sim Ht^{-\beta\delta}$ (with $t < 0$), we find that the spinodal point can be found under the Langer cut as shown in Fig. 4.8, assuming, of course, that we start from the stable $H > 0$ branch. It is therefore natural to expect that the spinodal singularity (which is *also* the Lee-Yang edge singularity) is the closest singularity to the real axis (i.e., to the Langer cut). This is the essence of the "extended analyticity" conjecture put forward by Fonseca and Zamolodchikov [181]. Here, our goal is to see what one can say about the singularities of the equation of state and the validity of the conjecture using the ε expansion as well as large-N limit of the O(N)-symmetric ϕ^4 theory.

Lee-Yang edge singularities and Ginzburg criterion

As we discussed in Sec. 4.2.1, the mean-field (saddle-point) approximation is controlled by the quartic coupling u_0. For $d < 4$, in the scaling regime, the coupling is given by the IR (Wilson-Fisher) fixed-point value of order $\varepsilon = 4 - d$. This means that the true scaling equation of state should approach the mean-field one as $\varepsilon \to 0$. However, this approach is not uniform, especially, at the Lee-Yang edge singularities, which are the focus of this study.

The issue was first raised by Fisher, who observed that the singular behavior near the Lee-Yang point is described by a ϕ^3 theory [132]. This theory has an IR fixed point, albeit somewhat formally, since it occurs at *imaginary* values of the cubic coupling. The exponents (anomalous dimensions) can be calculated by an expansion around the upper critical dimen-

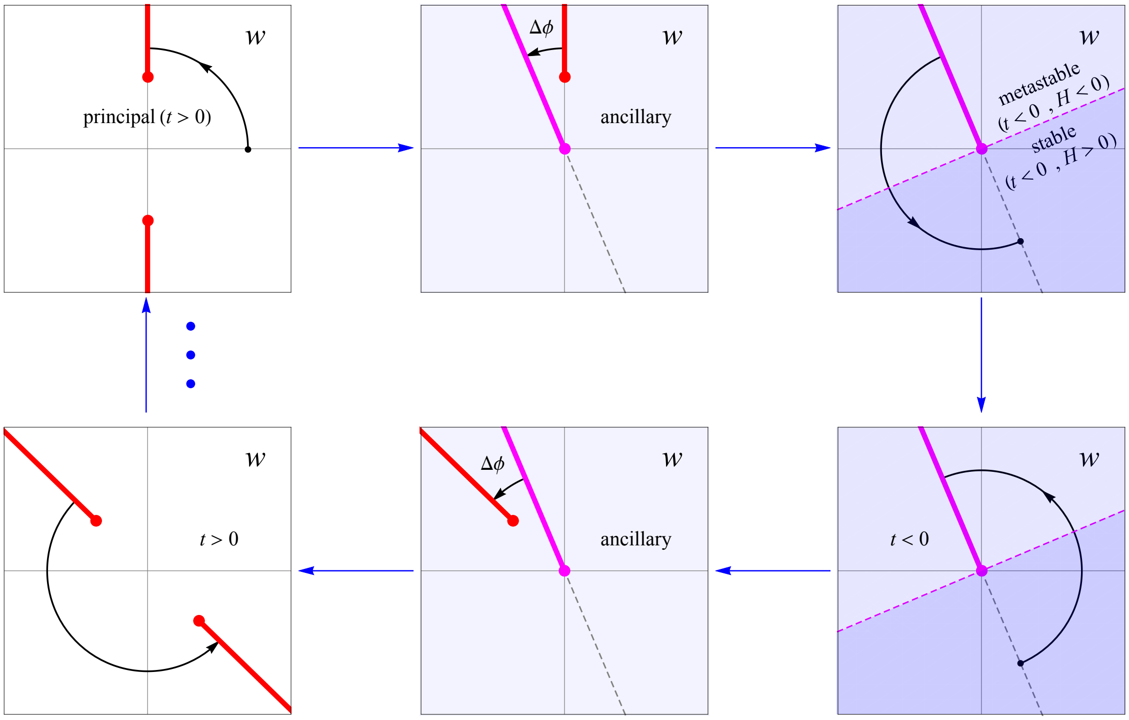

Figure 4.7: Analytic continuation $t \to -t$ from the principal, i.e., high-temperature sheet (top left panel) to the low-temperature sheet (top right panel) and the following successive processes (from bottom right panel to left) of the scaling function $z(w)$ of the Ising theory as conjectured by Fonseca and Zamolodchikov, where $w \sim Ht^{-\beta\delta}$, while keeping the magnetic field $H > 0$ fixed at $d = 4 - \varepsilon$. After analytic continuation the metastable branch $H < 0$ can be accessed by rotating H clockwise in the complex plane, while keeping $t < 0$ fixed. The line representing the Langer cut is rotated away from imaginary axis by an angle $\Delta\phi$, cf. Eq. (4.56).

sion $d = 6$ of the ϕ^3 theory where the theory becomes perturbative in terms of $\varepsilon' = 6 - d$. However, the ϕ^3 theory is *non-perturbative* in $d = 4$. In particular, the singular behavior in the vicinity of the Lee-Yang point

$$M - M_{\mathrm{LY}} \sim (H - H_{\mathrm{LY}})^{\sigma}, \tag{4.58}$$

is characterized by the exponent $\sigma \approx 0.26$ in $d = 4$ [143, 139, 4, 196], which differs significantly from the mean-field result $\sigma = 1/2$.

We appear to be facing a paradox. On the one hand, mean-field theory should become

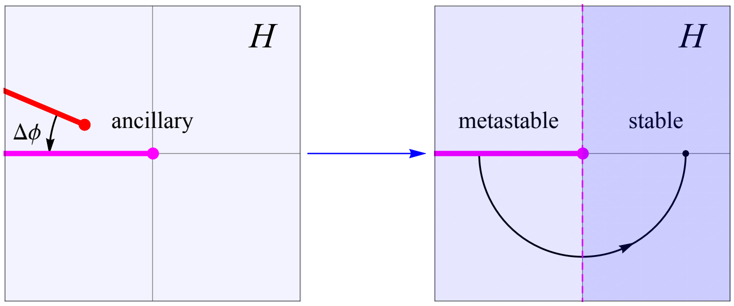

Figure 4.8: The Fonseca-Zamolodchikov conjecture for $t < 0$, illustrated in the complex H plane. The line along the negative real H axis represents the Langer cut. The second cut on the ancillary sheet is the Lee-Yang cut, which is associated with the Lee-Yang edge singularity. The latter is expected to be the nearest singularity under the Langer cut.

valid as $d \to 4$. On the other hand, this approximation fails to account for the correct exponent at the Lee-Yang point in the same limit. There is no contradiction, of course. The reason that mean-field theory becomes precise for $d \to 4$ is that the importance of fluctuations diminishes as the fixed-point value of the coupling vanishes at $d = 4$. However, at any given value of ε (and t), the magnitude of the fluctuations themselves increase as we approach the Lee-Yang points, since the correlation length ξ diverges at those points. In other words, the (squared) magnitude of fluctuations is proportional to the isothermal susceptibility $M'(H)$, which diverges as $H \to H_{\mathrm{LY}}$.

We are, therefore, led to seek a condition, similar to the Ginzburg criterion in the theory of superconductors [197], which determines how close the Lee-Yang edge singularity can be approached before mean-field theory breaks down. Even though the critical exponents, such as σ, cannot be determined reliably in the mean-field approximation, the domain of the validity of that approximation can be.

At the Lee-Yang point $H = H_{\mathrm{LY}}$ the mean-field potential Eq. (4.41) takes the following form (cf. Eq. (1.42))

$$V(\Phi)|_{H=H_{\mathrm{LY}}} = \frac{t^2}{12} + \frac{1}{\sqrt{3}}\, i t^{1/2} (\Phi - M_{\mathrm{LY}})^3 + \frac{1}{4} (\Phi - M_{\mathrm{LY}})^4. \tag{4.59}$$

It describes a *massless* ϕ^3 theory with imaginary cubic coupling ($t > 0$). When $H \neq H_{\rm LY}$ a quadratic (mass) term appears. Expanding in $H - H_{\rm LY}$ we find (cf. Eq. (1.44))

$$V(\Phi) = \frac{t^2}{12} + (-3t)^{1/4}(H - H_{\rm LY})^{1/2}(\Phi - M_{\rm LY})^2 + \frac{1}{\sqrt{3}}\, i t^{1/2}(\Phi - M_{\rm LY})^3 + \frac{1}{4}(\Phi - M_{\rm LY})^4 + \dots, \tag{4.60}$$

where we show only the leading-order contribution to each of the coefficients and the ellipsis denotes the subleading terms. From Eq. (4.60) we can determine the correlation length, given by Eq. (4.43), for small $H - H_{\rm LY}$. The result can be written in the following scaling form

$$\xi^{-2} = t\left[2(-3)^{1/4}(w - w_{\rm LY})^{1/2} + \dots\right], \tag{4.61}$$

where w and $w_{\rm LY}$ are given by (4.53) and (4.54), respectively. This analysis relies on the mean-field approximation and, therefore, assumes that fluctuations can be neglected.

The relative importance of fluctuations, is determined by the quartic coupling u_0, which is most evident in Eq. (4.40), where u_0 controls the applicability of the saddle-point approximation to the path integral. In $4 - \varepsilon$ dimensions, this coupling runs to the Wilson-Fisher fixed point in the IR, i.e., $u_0 \to u_0^{\rm WF} = \mathcal{O}(\varepsilon)$ and therefore a mean-field (saddle-point) analysis is justified for sufficiently small ε. How small ε, or u_0, should be, however, depends on the value of the scaling-invariant variable w. For a generic value away from $w_{\rm LY}$ the condition is simply $\varepsilon \ll 1$. However, as $w \to w_{\rm LY}$ the correlation length diverges, fluctuations are enhanced, and the condition on ε becomes more restrictive.

As $w \to w_{\rm LY}$, the relative importance of fluctuations is controlled by the most relevant coupling, the cubic coupling g_3, which can be read off as the coefficient of the $(\Phi - M)^3$ term in Eq. (4.60), i.e., $g_3 \sim i(u_0 t)^{1/2}$. Note that a factor $\sqrt{u_0}$ must be included in order to restore the canonical normalization of the field, $\Phi = \sqrt{u_0/6}\,\phi$. The mass dimension of the cubic coupling g_3 is $(6 - d)/2$ and thus its relative importance is determined by the dimensionless combination $\widetilde{g}_3 \equiv g_3 \xi^{(6-d)/2}$ which, according to Eq. (4.61), is given by

$$\widetilde{g}_3 \sim \widetilde{u}_0^{1/2} |w - w_{\rm LY}|^{-(6-d)/8} + \dots, \tag{4.62}$$

where $\widetilde{u}_0 \equiv u_0 t^{(d-4)/2} = u_0 t^{-\varepsilon/2}$. The mean-field analysis is applicable near the Lee-Yang edge singularity only as long as $\widetilde{g}_3 \ll 1$.[8] For $0 < \varepsilon \ll 1$, this yields the following requirement

$$|w - w_{\mathrm{LY}}| \gg \varepsilon^2, \tag{4.63}$$

where we replaced u_0 with its IR fixed-point value $u_0^{\mathrm{WF}} \sim \varepsilon$. Eq. (4.63) is the Ginzburg criterion that determines the size of the critical region around the Lee-Yang point. It is in a similar spirit of the criterion for the correlation size (cf. Eq. (1.34)) where the dimensionless mass term is of order 1. Inside this region the mean-field approximation breaks down and the correct scaling near that point is given by the fixed point of the ϕ^3 theory, which is non-perturbative in $d = 4$. One can also say that a typical condition for the mean-field approximation to apply, $\varepsilon \ll 1$, is not sufficient near the Lee-Yang points, where a stronger condition becomes necessary: Eq. (4.63).

It is instructive to consider also the case $4 < d < 6$. The critical behavior simplifies as the scaling is now controlled by the Gaussian IR fixed point. However, we cannot simply set the coupling u_0 to zero since the action becomes singular in this limit (cf. Eq. (4.40)). In other words, for $d > 4$, the coupling u_0 is a dangerously irrelevant variable [198]. In this case the equation of state depends on u_0 in addition to the variables t and H. Repeating the arguments leading to Eq. (4.62) we conclude that, for $4 < d < 6$, no matter how small the coupling u_0 is, the mean-field approximation will break down sufficiently close to the Lee-Yang point with the Ginzburg criterion given by

$$|w - w_{\mathrm{LY}}| \gg (\widetilde{u}_0)^{4/(6-d)}. \tag{4.64}$$

Finally, for $d \geq 6$ the variable w is not constrained by the Ginzburg criterion, and the condition $\widetilde{u}_0 \ll 1$ is sufficient for mean-field theory to apply for all w. This corresponds to the fact that $d = 6$ is the upper critical dimension of the ϕ^3 theory, and the exponent σ in Eq. (4.58) takes the mean-field value $1/2$ for $d \geq 6$ in accordance with [132].

---

[8] The basic idea of the Ginzburg criterion is to compare the tree-level amplitude, or coupling, g_3 in our case, to the one-loop contribution. The latter stems from a triangle diagram, which is IR divergent when $\xi \to \infty$. By counting dimensions (k^d from the loop integral and k^6 from the denominators) it is easy to see that the loop integral diverges as ξ^{6-d}. Thus, we need to compare g_3 to $(g_3)^3\xi^{6-d}$, or equivalently $g_3^2\xi^{6-d}$ to 1.

4.2.3 Singularities in the ε Expansion

Critical equation of state at $d = 4 - \varepsilon$

In this section we shall review the known results on the ε expansion of the equation of state relevant for our discussion.

Since the fixed-point value of the coupling u_0 is small near $d = 4$, the equation of state can be calculated perturbatively in $\varepsilon = 4 - d$ [168, 169, 170, 171, 172]. In terms of the rescaled variables t, M, and H, one finds to order ε^2 [170, 171][9]

$$\begin{aligned}\frac{H}{M} &= t + \frac{u}{8} r \left[1 + \ln(r) - \frac{\varepsilon}{4}\ln^2(r)\right] - \frac{u^2}{64} r \left[4 + \pi^2 - 8\lambda - \ln^2(r)\right] \\ &+ M^2 \left\{1 - \frac{3}{32}u^2 \left[6 + \frac{1}{2}\pi^2 - 4\lambda + 3\ln(r) + \frac{1}{2}\ln^2(r)\right]\right\}, \qquad (4.65)\end{aligned}$$

which reproduces the mean-field equation of state Eq. (4.42) with Eq. (4.44) when $u \to 0$. Here, the parameter u denotes the (Wilson-Fisher) fixed-point value of the conveniently normalized quartic coupling [10], i.e.,

$$u = u_0^{\mathrm{WF}} \frac{S_d}{(2\pi)^d} \frac{\pi\varepsilon}{\sin(\pi\varepsilon/2)} = \frac{4}{3}\varepsilon \left(1 + \frac{7}{54}\varepsilon\right) + \mathcal{O}(\varepsilon^3), \qquad (4.66)$$

where S_d is the area of the unit sphere in d dimensions introduced in Eq. (1.22) and $\lambda = (1/9)\left(3\Psi'(1/3) - 2\pi^2\right)$ involves the first derivative of the digamma function $\Psi(z) = d/dz \ln\Gamma(z)$. The inverse isothermal susceptibility $r = (\partial H/\partial M)_t$ is a function of the variables t and M, i.e., $r = r(t, M)$, and therefore Eq. (4.65) constitutes a relation between t, M, and H.

---

[9] While the equation of state is known to order ε^3 [170, 171, 172], for our purposes it is sufficient to consider only contributions up to order ε^2. We comment on some features specific to the ε^3 result (in particular related to parametric representation of the equation of state) in Appendix E.2.

[10] Note that the Wilson-Fisher fixed-point value for the quartic coupling here is different from the one given by Eq. (1.24), a consequence of different definition after the loop factor is absorbed. Our final results and conclusions shall be independent of the normalization or definition used, thus we follow the convention of Ref. [5].

As mentioned at the beginning of this section, in the scaling region, Eq. (4.65) can be written in a scaling form, in terms of scale-invariant combinations of two relevant variables. Among various choices it is more convenient for our work to write Eq. (4.65) in terms of the scaling variables $w \sim Ht^{-\beta\delta}$ and $z \sim Mt^{-\beta}$, i.e., $w = F(z)$. Expressing the critical exponents β and δ to order ε^2, the "gap" exponent is given by

$$\beta\delta = \frac{3}{2} + \frac{1}{12}\varepsilon^2 + \mathcal{O}(\varepsilon^3), \tag{4.67}$$

and the series expansion in ε of the scaling function $F(z)$ reads

$$F(z) = F_0(z) + F_1(z)\varepsilon + F_2(z)\varepsilon^2 + \mathcal{O}(\varepsilon^3), \tag{4.68}$$

with

$$F_0(z) = z + z^3, \tag{4.69a}$$

$$F_1(z) = \frac{1}{6}\left[-3z^3 + \left(z + 3z^3\right) L(z)\right], \tag{4.69b}$$

$$F_2(z) = \frac{1}{648}\left[-150z^3 + 2(25z - 6z^3)L(z) + 9(z + 9z^3)L^2(z)\right], \tag{4.69c}$$

and $L(z) = \ln\left[1 + 3z^2\right]$.[11] Note that the mean-field equation of state (4.52) is recovered in the limit $\varepsilon \to 0$. Here, the normalization of the scaling variables w and z in Eq. (4.51) is chosen in such a way that the two lowest order terms in the Taylor expansion

$$F(z) = z + z^3 + \sum_{n=2}^{\infty} \mathcal{F}_{2n+1} z^{2n+1}, \tag{4.70}$$

are fixed and coefficients $\mathcal{F}_{2n+1} = \mathcal{O}(\varepsilon)$, for all $n \geq 2$.

---

[11] Note at the Lee-Yang point, the argument of the logarithmic function vanishes. An imaginary part, which is analyzed by Weinberg and Wu [56], develops when the argument is negative and is associated with the cut terminating at the Lee-Yang edge singularity.

Since the singularities of the equation of state are associated with a diverging correlation length, the equation of state must be analytic away from the Ising critical point located at $t = M = H = 0$. Thus, if any one of these parameters is set to a nonzero value, the relation between the other two must be analytic. This translates into the following two properties of $F(z)$ often referred to as Griffiths' analyticity [199]. First, for fixed $t > 0$, we find that $F(z) \sim H$ is an analytic function of $z \sim M$ in the vicinity of $z = 0$, which should also be odd under reflection $H \to -H$ and $M \to -M$. This is easily seen in the explicit expressions for $F(z)$ in Eqs. (4.69). Second, for fixed $M > 0$ we find that the function $z^{-\delta}F(z) \sim H$ must be an analytic function of the variable $z^{-1/\beta} \sim t$ in the vicinity of $t = 0$ ($z = \infty$). The behavior of $F(z)$ at large z is not manifest in Eqs. (4.69) since the ε expansion of this function does not converge uniformly, due to the presence of large logarithms.

In this case, it is better to introduce the scaling variables $x \sim tM^{-1/\beta}$ and $y \sim HM^{-\delta}$ (as in Eq. (4.48)), and express the equation of state Eq. (4.65) as the Widom scaling function $y = f(x)$ [73], whose ε expansion is convergent when $x \to 0$ (corresponding to $z \sim x^{-\beta} \to \infty$). However, in this representation the analyticity at large x (corresponding to small z) is obscured, again due to lack of convergence of the ε expansion.

Thus it would be useful to have a representation of the equation of state where the analyticity is manifest in both regimes, i.e., a representation for which the ε expansion converges uniformly. The so-called parametric representations [71, 187], reviewed below, are designed to fulfill this requirement.

Parametric equation of state

As we discussed in the previous section and also in Sec. 1.4.3, the problem with representations using the pairs of scaling variables such as w and z, or y and x, is that the two points $z = 0$ and $x \sim z^{-1/\beta} \to 0$, where each of them is analytic, correspond to infinitely separated points $z = 0$ and $z = \infty$ (and similarly for x). This problem can be addressed by introducing a new scaling variable, θ, by means of a nonlinear variable transformation

$(t, M) \to (R, \theta)$:

$$t = Rk(\theta), \tag{4.71}$$

$$M = R^{\beta} m(\theta), \tag{4.72}$$

with *analytic* functions $k(\theta)$ and $m(\theta)$, chosen such that the two points $x \sim tM^{-1/\beta} = 0$ and $z \sim Mt^{-\beta} = 0$ are placed at positions $\theta = 1$ and $\theta = 0$, respectively. The simplest choice satisfying these conditions is

$$k(\theta) = 1 - \theta^2 \quad \text{and} \quad m(\theta) = \bar{m}\theta, \tag{4.73}$$

also known as the linear parametric model (LPM) [71, 188]. Here, $\bar{m}$ is a normalization constant, which can be chosen to bring the equation of state into canonical form (e.g., see Eq. (4.70)).

In the parametric representation, the equation of state becomes a relationship between H and the parameters R and θ, i.e.,

$$H = R^{\beta\delta} h(\theta), \tag{4.74}$$

where $h(\theta)$ is an odd function of θ (since $\theta \sim M$ is an odd variable under reflection $M \to -M$, $H \to -H$).

While R scales as the reduced temperature t, the variable θ is invariant under rescaling in Eq. (4.46). Therefore, the scaling variables w and z can be expressed in terms of θ alone, i.e.,

$$z \sim Mt^{-\beta} \sim \theta(1-\theta^2)^{-\beta} \quad \text{and} \quad w \sim Ht^{-\beta\delta} \sim h(\theta)(1-\theta^2)^{-\beta\delta}. \tag{4.75}$$

Inserting these expressions into the equation of state $w = F(z)$ one can determine the function $h(\theta)$ (as well as the normalization constant $\bar{m}$) order by order in the ε expansion [73].[12]

---

[12] Similarly, one could also use the equation of state in the form $y = f(x)$ with the scaling variables $x \sim \theta^{-1/\beta}(1-\theta^2)$ and $y \sim \theta^{-\delta}h(\theta)$ to determine $h(\theta)$.

In this section, we shall carefully examine the parametric representation obtained by matching equation of state to order ε^2. Our goal is to determine the location of singularities and their uncertainty due to higher orders of ε expansion. To focus on relevant features we present the results in the minimal form necessary for the argument, and collect explicit expressions needed for the derivation in Appendix E.1 and E.2.

It is known that to order ε^2 the function $h(\theta)$ is given by a cubic polynomial [168, 170, 171]

$$h(\theta) = \bar{h}(\theta + h_3\theta^3), \tag{4.76}$$

where $\bar{h}$ is a normalization parameter. As we shall see, the number of singularities is determined by the order of this polynomial while their positions are related to the coefficient h_3 which can be determined by matching to equation of state (4.70). For $\varepsilon = 0$ (mean-field equation of state), $h_3 = -2/3$.

In order to study the dependence of our results on ε we shall expand h_3 in ε. To this end we adopt the historical notation of Refs. [71, 188, 170, 171] and express h_3 in terms of parameter b defined by $h(\theta = b) = 0$, i.e., the closest zero to $\theta = 0$. Obviously,

$$h_3 = -\frac{1}{b^2}. \tag{4.77}$$

The coefficients of the ε expansion of b^2

$$b^2 = \frac{3}{2} + b_1\varepsilon + b_2\varepsilon^2 + \mathcal{O}(\varepsilon^2). \tag{4.78}$$

cannot be determined by matching at order ε^2 (or ε^3 for that matter, cf. Appendix E.2). It is a common choice [170, 171] to set $b_1 = 0$, but it is not necessary and we shall allow this parameter to have an arbitrary real value. It will be helpful for understanding the ε dependence of our results.

We shall now study the singularities that arise in the linear parametric representation in order to infer the analytic properties of the scaling equation of state. Specifically, we examine the equation of state to order ε^2 in the form $w = F(z)$, represented parametrically using Eqs. (4.75). This allows us to directly access the singularities in the complex w plane by examining the rescaled inverse isothermal susceptibility, given by

$$rt^{-\gamma} \sim F'(z) = \frac{w'(\theta)}{z'(\theta)}, \tag{4.79}$$

whose zeros correspond to the branching points of the multivalued function $z(w)$.

In terms of the linear parametric representation, Eqs. (4.71) – (4.74) and Eq. (4.76), the scaling variables z and w are given by

$$z = \frac{\bar{z}\theta}{(1-\theta^2)^\beta} \quad \text{and} \quad w = \frac{\bar{w}\,(\theta + h_3\theta^3)}{(1-\theta^2)^{\beta\delta}}, \tag{4.80}$$

where the normalization parameters $\bar{z}$ and $\bar{w}$, determined by matching the parametric model to the canonical equation of state Eq. (4.70) to order ε^2, are needed below to find the position of singularities to that order and are given by Eqs. (E.2). Substituting into Eq. (4.79) we arrive at the following expression for the inverse susceptibility

$$F'(\theta) = \frac{\bar{w}}{\bar{z}}(1-\theta^2)^{-\gamma}\frac{1 + (2\beta\delta + 3h_3 - 1)\,\theta^2 + (2\beta\delta - 3)h_3\theta^4}{1 - (1-2\beta)\,\theta^2}, \tag{4.81}$$

where the scaling exponents β, γ, and δ, as well as the parameters h_3, $\bar{w}$ and $\bar{z}$ should be expanded to order ε^2.

If we set $\varepsilon = 0$ and use the mean-field critical exponents, $\beta = 1/2$, $\gamma = 1$, and $\beta\delta = 3/2$, we observe that the only zeros of $F'(\theta) = (1-\theta^2)^{-1}$ lie at complex infinity (in the θ plane). Of course, this is consistent with the mean-field result, which is easily confirmed by examining the limit $|\theta| \to \infty$ in Eqs. (4.80), i.e., $\lim_{|\theta|\to\infty} w(\theta) = \pm 2i/(3\sqrt{3})$, and comparing with Eq. (4.54).

At nonzero ε, however, the structure of the singularities of Eq. (4.81) becomes more complicated. Now, the polynomial in the numerator has four zeros. There are also two zeros in the denominator, giving rise to two poles. In addition, there are two branch-point singularities at $\theta = \pm 1$. Since $w(\theta = 1) = z(\theta = 1) = \infty$ the latter can be seen to correspond to the behavior $F(z) \sim z^\delta$ (and, therefore, $F'(z) \sim z^{\gamma/\beta}$) at large z, required by Griffiths' analyticity. The four zeros and two poles on the other hand, occur at finite, albeit large, values of $\theta^2 = \mathcal{O}(\varepsilon^{-1})$. We shall now focus on these finite w singularities.

Since $F'(\theta)$ is an even function of θ it is convenient to consider its singularities as a function of θ^2. The numerator of Eq. (4.81) vanishes at two distinct values θ_n^2, which we label by indices $n = 1, 2$. These solutions can be expanded in powers of ε where the leading contribution appears at order ε^{-1}, i.e.,

$$\theta_n^2 = \frac{c_n}{\varepsilon}\left[1 + \mathcal{O}(\varepsilon)\right]. \tag{4.82}$$

Substituting θ_n into Eq. (4.80), $w_n \equiv w(\theta_n)$, and expanding in ε we get

$$w_n = \pm\frac{2i\,(-\hat{c}_n)^{\frac{3}{2}-\beta\delta}}{3\sqrt{3}}\left\{1 + \left[\omega^{(2)}(c_n, b_1) + \frac{1}{12}\ln\varepsilon\right]\varepsilon^2 + \mathcal{O}(\varepsilon^3)\right\}, \tag{4.83}$$

where $\hat{c}_n \equiv c_n/|c_n|$. Remarkably, only the leading-order coefficient of θ_n^2, c_n, appears in this expression.[13] The coefficient c_n is a function of b_1 and for the two solutions θ_n^2, $n = 1, 2$, we obtain

$$c_n = 3\left(2b_1 + (-1)^n\sqrt{1 + 4b_1^2}\right), \quad n = 1, 2, \tag{4.84}$$

with $c_1 < 0$ and $c_2 > 0$ for all real values of b_1. Note that the absolute value of w_n is determined by $\omega^{(2)}(c_n(b_1), b_1)$ – a function of b_1 (see Eq. (E.3)) while the dependence on n appears only via c_n in Eq. (4.84). Nontrivially, there are no $\mathcal{O}(\varepsilon)$ terms in Eq. (4.83) (they cancel) and there is no dependence on b_2 to this order.

Inserting the coefficient c_1 into (4.83), we find

$$w_1 = \pm\frac{2i}{3\sqrt{3}}\left\{1 + \left[\omega^{(2)}(c_1, b_1) + \frac{1}{12}\ln\varepsilon\right]\varepsilon^2 + \mathcal{O}(\varepsilon^3)\right\}, \tag{4.85}$$

which corresponds to the pair of Lee-Yang edge singularities (cf. Eq. (4.54)). As in the mean-field case they are located on the imaginary axis in accordance with Lee-Yang theorem. However, comparing with the mean-field result, we observe that its absolute value receives corrections of order ε^2, which depend on the parameter b_1. Since b_1 cannot be determined at this order of the ε expansion, practically, the position of the singularity also cannot be

---

[13] This happens because the leading corrections to the mean-field value of w are $\varepsilon\theta^{-2}$ and θ^{-4}, while $\theta_n^{-2} \sim \varepsilon$.

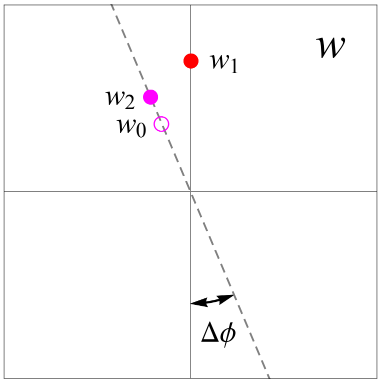

Figure 4.9: We show the position of the two zeros w_1 and w_2 (solid points) and single pole w_0 (open circle) of the parametrically represented inverse isothermal susceptibility $F'(z)$ at order $\mathcal{O}(\varepsilon^2)$ in the complex w plane ($b_1 \neq 0$). Note, only the singularities in the upper half of the complex w plane are shown.

established to precision of order ε^2. This agrees with our earlier observation in Sec. 4.2.2 that the non-perturbative domain around the Lee-Yang edge singularities has size $\mathcal{O}(\varepsilon^2)$, according to Ginzburg criterion Eq. (4.63).

The second pair of singularities, w_2, is located off the imaginary axis:

$$w_2 = \pm\frac{2i}{3\sqrt{3}}(-1)^{\frac{3}{2}-\beta\delta}\left\{1 + \left[\omega^{(2)}(c_2, b_1) + \frac{1}{12}\ln\varepsilon\right]\varepsilon^2 + \mathcal{O}(\varepsilon^3)\right\}. \tag{4.86}$$

One can easily see that they lie precisely where we expect the Langer cut (see Fig. 4.7). But what is their significance? Before answering this question, let us first consider the poles of $F'(z)$, which can be obtained by solving

$$1 - (1-2\beta)\,\theta^2 = 0. \tag{4.87}$$

The solution θ^2 to this equation, which we label by the index $n = 0$, can be also expanded in powers of ε. The corresponding leading coefficient c_0 (cf. Eq. (4.82)) is given by

$$c_0 = 3, \tag{4.88}$$

and according to Eq. (4.83), we find

$$w_0 = \pm\frac{2i}{3\sqrt{3}}(-1)^{\frac{3}{2}-\beta\delta}\left\{1 + \left[\omega^{(2)}(c_0, b_1) + \frac{1}{12}\ln\varepsilon\right]\varepsilon^2 + \mathcal{O}(\varepsilon^3)\right\}. \tag{4.89}$$

The position of the singularities w_0, w_1, and w_2, is shown schematically in Fig. 4.9 in the upper half of the complex w plane and for a generic value of b_1, according to Eq. (E.3). We observe that w_0 and w_2 lie on the same ray, which corresponds to the Langer cut of the *exact* equation of state. The distance between these points is given by

$$w_2 - w_0 = \mathcal{O}(\varepsilon^2), \tag{4.90}$$

and depends on the value of b_1. For the common and particular choice $b_1 = 0$, when $c_2 = c_0$, the two points coincide and the zero and the pole cancel each other to order ε^2.

It is also important to note that both w_0 and w_2 (on the Langer cut) are within distance $\mathcal{O}(\varepsilon^2)$ from the Lee-Yang edge singularity, since $\beta\delta - 3/2 = \mathcal{O}(\varepsilon^2)$. Therefore, according to the Ginzburg criterion in Eq. (4.63), these singularities and their position are non-perturbative. This is in agreement with the fact that we cannot determine the parameter b_1 within the ε expansion to establish their position. Furthermore, as we show in Appendix E.2, extending the linear parametric model to next order, ε^3, leads to terms in w_n that contribute at order ε^2 (in *addition* to the expected ε^3 contribution). Thus, the procedure based on matching to increasing orders of the ε expansion does not converge in the usual sense. In spite of this, it is still tempting to speculate that the sequence of (alternating) zeros and poles line up along the ray at angle $\Delta\phi$ relative to the imaginary axis and will eventually coalesce into the Langer cut – a purely non-perturbative feature, which cannot be reproduced at any finite order of ε expansion. In fact, such a scenario is common in rational-function (Padé) approximations of functions with branch cuts.[14]

Summarizing, we see that the Ginzburg criterion (4.63) sets the limit on the information that can be gained about the Lee-Yang edge singularities. The precision that we can reach, ε^2, is not sufficient to study the region between the Lee-Yang edge singularity and the

---

[14] The experience with Padé approximations suggests a guiding principle for constructing improved parametric representations: The choice of (polynomial) functions $h(\theta)$ and $m(\theta)$ should be such that the rank of polynomials in the numerator and the denominator in Eq. (4.81) increase at the same rate.

Langer cut, which is necessary to test the Fonseca-Zamolodchikov conjecture. Nevertheless, the results we find are nontrivially consistent with the conjecture.

4.2.4 Singularities in the $\mathrm{O}(N)$-symmetric ϕ^4 Theory

An alternative point of view on the question of extended analyticity and the nature of singularities in the complex H plane can be obtained by studying the generalization of the ϕ^4 theory to the N-component theory with $\mathrm{O}(N)$ global symmetry. This generalization is a well-known tool to study non-perturbative aspects of the theory. The finite-N cases describe the critical behavior of, e.g, the Heisenberg model ($N = 3$), the XY-model ($N = 2$), and, of course, the Ising model ($N = 1$). On the other hand, in the $N \to \infty$ limit the $\mathrm{O}(N)$ model describes the critical behavior of the exactly solvable spherical model [200, 201].

Similar to Eq. (4.38), the $\mathrm{O}(N)$ theory is defined by the Euclidean action

$$\mathcal{S} = \int d^d x \left[\frac{1}{2}(\partial_\mu \boldsymbol{\phi})^2 + \frac{r_0}{2}\boldsymbol{\phi}^2 + \frac{u_0}{4!}(\boldsymbol{\phi}^2)^2 - \boldsymbol{h_0} \cdot \boldsymbol{\phi}\right]. \tag{4.91}$$

Here, $\boldsymbol{\phi}$ is a (real) N-component vector field and the external magnetic field $\boldsymbol{h_0}$ has the same dimensionality. In the presence of a nonvanishing $\boldsymbol{h_0}$ the expectation value of $\boldsymbol{\phi}$, $\langle\boldsymbol{\phi}\rangle$, is directed along the former. Due to the $\mathrm{O}(N)$ invariance of the theory we may choose an axis along the vector $\boldsymbol{h}_0$ and define the equation of state as a relationship between the projections $\langle\phi\rangle$, h_0 of $\langle\boldsymbol{\phi}\rangle$ and $\boldsymbol{h}_0$ onto that direction, similar to the $N = 1$ case in Sec. 4.2.1.

We are interested in analytic properties of the universal equation of state, which describes the critical behavior of the ϕ^4 theory associated with the spontaneous breaking of the $\mathrm{O}(N)$ symmetry. However, since there can be no spontaneous symmetry breaking of continuous symmetries in $d \leq 2$ [202, 203], we shall limit our analysis to dimensions $d > 2$.

When $h_0 = 0$ the critical point is reached by tuning r_0 to its critical value, i.e., $t = r_0 - r_\mathrm{c} \to 0$. In this limit, and for $d < 4$ the quartic coupling u_0 runs into the $\mathrm{O}(N)$ Wilson-Fisher fixed point in the infrared, i.e., $u_0 \to u_0^{\mathrm{WF}}$ [204, 205] and therefore the critical equation of state becomes independent of the bare coupling u_0 as well as the ultraviolet cutoff. A systematic expansion in powers of $1/N$, yields a fixed-point value with $u_0^{\mathrm{WF}} \sim \mathcal{O}(1/N)$ [205, 206]. But this does not necessarily mean that the equation of state of the O(N) model reduces to the mean-field result in the limit $N \to \infty$. Indeed, the tree-level action for the longitudinal field ϕ receives a nontrivial contribution from integrating out the $N-1$ transverse-field degrees of freedom (which, for $t < 0$, correspond to the massless Goldstone modes associated with the spontaneous breaking of the O(N) symmetry) [205]. Both the tree-level action, proportional to $1/u_0 \sim \mathcal{O}(N)$ (as in Eq. (4.40)), as well as the one-loop contribution of the $N-1$ transverse-field modes are of order N. We may therefore apply the saddle-point approximation in the large-N limit.

We shall first consider the infinite-N case, or the spherical model, and then briefly comment on $1/N$ corrections below. As in Sec. 4.2.1 we introduce the rescaled field variables $M = \sqrt{u_0/6}\,\langle\phi\rangle$ and $H = \sqrt{u_0/6}\,h_0$ and employ the scaling variables $w = Ht^{-\beta\delta}$ and $z = Mt^{-\beta}$ etc.

In the $N \to \infty$ limit the critical exponents are known [205]

$$\beta = \frac{1}{2}, \quad \gamma = \frac{2}{d-2}, \quad \text{and} \quad \delta = \frac{d+2}{d-2}, \quad \text{for} \quad 2 < d < 4, \tag{4.92}$$

and take their mean-field values for $d \geq 4$. The scaling equation of state $w = F(z)$ is determined in terms of the scaling function

$$F(z) = z(1+z^2)^{\gamma}. \tag{4.93}$$

In $d \geq 4$ dimensions, where the critical exponent $\gamma = 1$, this agrees with the mean-field equation of state Eq. (4.52), as should be expected.

The imaginary part of the inverse function $z(w)$ is plotted in Fig. 4.6. The branching points of $z(w)$ correspond to solutions of $F'(z) = 0$. We find two (pairs of) such solutions

$$z^2 = -1 \quad \text{and} \quad z^2 = -\frac{1}{1+2\gamma}, \tag{4.94}$$

which map onto

$$w = 0 \quad \text{and} \quad w = \pm i(2\gamma)^{\gamma}(1+2\gamma)^{-\beta\delta}, \tag{4.95}$$

in the complex w plane.

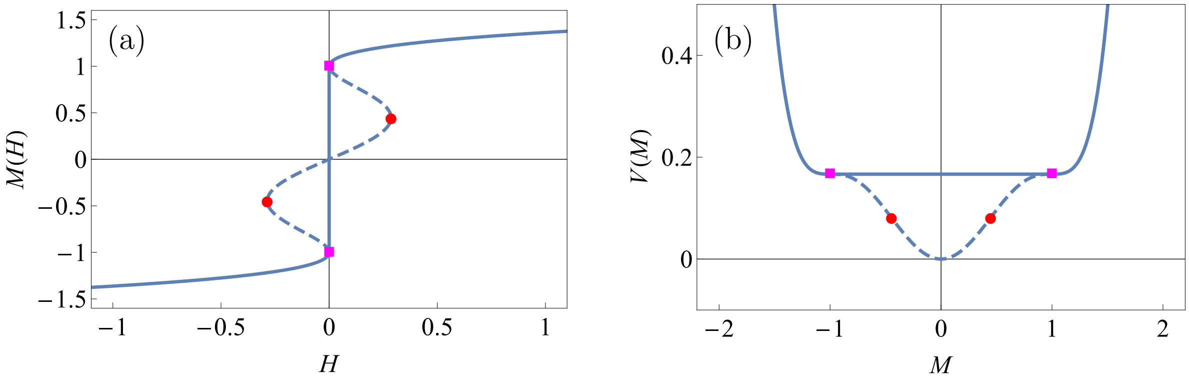

Figure 4.10: (a) Equation of state $M(H)$ of the three-dimensional $\mathrm{O}(N)$ model in the $N \to \infty$ limit and (b) the corresponding effective potential $V(M)$ at $H = 0$ in the low-temperature phase ($T < T_\mathrm{c}$). The dashed curve illustrates the analytic continuation of the stable branch (solid curve). In addition to the spinodal singularities at nonvanishing H, the presence of massless Goldstone modes induces singularities on the coexistence line ($T < T_\mathrm{c}$ and $H \to 0$).

The $w \neq 0$ solutions lie on the imaginary w axis. In fact, for $d = 4$ they are *identical* to the Lee-Yang edge singularities in Eq. (4.45). Thus, for $t > 0$, we can identify these solutions with the pair of Lee-Yang edge singularities at imaginary H. For $t < 0$, they lie on the real H axis for $d \geq 4$, while they are shifted off the real H axis by an angle[15]

$$\Delta\phi = \pi \frac{4-d}{d-2} > 0, \quad \text{for} \quad 2 < d < 4, \tag{4.96}$$

as expected, cf. Eq. (4.56).

But what is the meaning of the solution at $w = 0$ (i.e., $H = 0$) in Eq. (4.95)? Since $z^2 = -1$ and $M \sim z t^{1/2}$, this singularity corresponds to real M only for $t < 0$. It is located at the origin ($H = 0$) of the low-temperature sheet and is associated with a branch cut along the negative real H axis.

To understand the significance of this singularity and the associated branch cut, we illustrate the equation of state $M(H)$ in Fig. 4.10 for $t < 0$ and $d = 3$. Unlike the $N = 1$

---

[15] Note, the angular displacement $\Delta\phi$ is of order ε and *not* ε^2 as in the Ising-like ($N = 1$) case (cf. Sec. 4.2.2).

case there is no metastable regime (compare with Fig. 4.4). This can be understood as a consequence of the fact that, when H changes sign (relative to M), the effective potential as a function of $\boldsymbol{\phi}$ develops directions with negative curvature (i.e., the Goldstone bosons become tachyonic). This means that the false vacuum is classically unstable and, since there is no tunneling involved in the decay of the false vacuum, there is also no exponential suppression of the imaginary part, unlike the $N = 1$ case. That is, instead of the essential (and very weak) singularity (cf. Eq. (4.57)) the equation of state with $N > 1$ has a *power-law* singularity [204, 205, 207, 208] which comes from the IR-divergent contributions of the Goldstone bosons [207, 209]. Similar to the Langer cut in the Ising case, the $N > 1$ equation of state for $2 < d < 4$ has a "Goldstone cut" branching off from the origin and going along the real H axis on the unstable branch ($H < 0$ in our convention), with discontinuity given by[16]

$$\operatorname{Im} M \sim H^{(d-2)/2}, \quad \text{for } H \to 0, \quad t < 0. \tag{4.97}$$

Furthermore, from Fig. 4.10, we see that, for $T < T_{\rm c}$, the Lee-Yang edge singularities must lie on another (unphysical) branch of the equation of state $M(H)$. These singularities can be reached in the complex H plane by going under the Goldstone cut onto an ancillary Riemann sheet. In fact, the situation is very similar to the conjectured scenario shown in Fig. 4.8, where we observed a similar analytic structure of the equation of state.[17] The low-temperature singularities located off the Goldstone cut for $d < 4$ are very similar to the spinodal points. In fact, they become the spinodal points at $d = 4$ when the equation of state (4.93) takes the mean-field form (4.52).

Since there are no singularities in the equation of state Eq. (4.93) apart from the ones given by Eqs. (4.95), we conclude that the Fonseca-Zamolodchikov scenario is realized in the

---

[16] The coefficient of this singularity vanishes at $N = 1$ [207].

[17] Interestingly, the analytic structure of the scaling equation of state of the three-dimensional spherical model is also remarkably similar to that of the planar Ising model coupled to two-dimensional quantum gravity [210, 211, 212].

O(N) model in the $N \to \infty$ limit.

To complete our analysis, we finally comment on the $1/N$ corrections to the scaling function (4.93). Since the leading-order contribution to $\Delta\phi$ in Eq. (4.96) is already $\mathcal{O}(1/N^0)$, we observe that $1/N$ corrections cannot change the conclusion that there are no singularities at real (nonzero) H, provided that the only effect of these corrections is to shift the position of the singularities already present in the $N \to \infty$ limit.

The $1/N$ corrections can be expressed in terms of momentum integrals whose explicit form is not particularly illuminating (see Refs. [205, 206] for details). For simplicity we shall consider only $d = 3$, which is also the case that is most relevant for applications. In three dimensions, we find that the aforementioned momentum integrals yield only two branch points at $z^2 = -1$ and $z^2 = -1/5$, which coincide with the same singularities already found in the $N \to \infty$ limit, cf. Eq. (4.94), while the position of the corresponding points in the complex w plane is shifted by an amount of order $1/N$.[18] This is consistent with our expectation that the $1/N$ corrections only modify the position of the singularities (as determined in the $N \to \infty$ limit) and suggests that no new singularities appear at finite N.[19]

4.3 Discussion

In Chap. 4, we have examined the critical scaling properties of the Lee-Yang edge, or ϕ^3, theory in dimensions $3 \leq d \leq 6$. We find that the obtained values for the critical exponents are in good agreement with previous results obtained in $d = 3$ dimensions using high-temperature series expansions [133], the three- and four-loop ε expansion around $d = 6$ [137,

---

[18] At order $1/N$ the value of $\Delta\phi$, which controls the position of the spinodal points in the complex w (or H plane) is given by $\Delta\phi = \pi\left(\beta\delta - \frac{3}{2}\right) = \pi - 28/(\pi N) + \mathcal{O}(1/N^2)$ in $d = 3$ dimensions, where we have used Eq. (4.56) and critical exponents β and δ from Ref. [213, 205].

[19] Note that the position of the singularities in the complex w plane can be calculated reliably to order $1/N$, even though higher-order corrections become non-perturbative. Indeed, the Ginzburg criterion (see Eq. (4.62) or (4.64)) with $u_0 = \mathcal{O}(1/N)$ imposes a constraint on the applicability of the saddle-point approximation around the Lee-Yang point, which reads $|w - w_{\mathrm{LY}}| \gg N^{-4/(6-d)}$ (in agreement with Ref. [214]). This demonstrates that the non-perturbative region is *smaller* than $1/N$ for $d > 2$.

138] as well as other methods [140, 141, 142, 143]. Our estimates for the critical exponent σ are slightly larger than the values obtained from constrained Padé approximants for three- and four-loop ε expansion results [139], and generally lie below those from a conformal bootstrap analysis [143]. We expect that truncations at higher orders in the derivative and field expansion will improve our estimates for the critical exponents. However, more elaborate numerical treatment is necessary to study such truncations.

We observe that derivative interactions have an important effect on the stability of the scaling solution and need to be taken into account properly in the framework of the non-perturbative FRG. We have shown that the stability of nontrivial fixed point associated to the Lee-Yang edge singularity is sensitive to the insertion of operators that mix under renormalization. This might seem surprising since a similar behavior is not observed in applications of the functional RG to establish the scaling behavior at the Ising critical point. However, comparing our results with a stability analysis at the fixed point to one-loop order in the $\varepsilon' = 6 - d$ expansion provides a qualitative explanation for the observed lack of stability of the Lee-Yang edge fixed point for $(n_U, 0, 0)$-type truncations $(n_U > 3)$ of the scale-dependent effective action.

Based on mean-field arguments, one expects another thermodynamic singularity in the low-temperature phase of the Ising model $(T < T_c)$ with exactly the same critical exponents as those of the Lee-Yang edge point – the spinodal singularity. The corresponding critical point appears on the metastable branch of the free energy and is usually associated with the classical limit of metastability. However, its existence (beyond mean-field) as well as its scaling properties have been subject to some debate [215, 216, 217, 218]. The relation between the Lee-Yang edge point and the spinodal singularity [219, 181] are discussed in Sec. 4.2.

We firstly studied the relationship between singularities of the universal scaling equation of state of the ϕ^4 theory above and below the critical temperature. Above the critical temperature Lee-Yang edge singularities, by the Lee-Yang theorem, lie on the imaginary magnetic field axis and limit the domain of analyticity around the origin $H = 0$. On the other hand, below the critical temperature, there are singularities associated with the point where the metastable state becomes locally unstable and its decay occurs via spinodal decomposition.

In the mean-field approximation to the equation of state, $H = tM + M^3$, these spinodal points are related to the Lee-Yang edge singularities. In terms of the scaling variable $w = Ht^{-\beta\delta}$, they are essentially the same singularities. These singularities occur at imaginary w and, for $t > 0$, they correspond to imaginary H, i.e., the Lee-Yang points. For $t < 0$, however, they correspond to *real* H on the metastable branch (since in the mean-field approximation: $\beta\delta = 3/2$ and $i(-1)^{3/2} = -1$).

Since $\beta\delta \neq 3/2$ for $d < 4$, one naturally has to ask the question if the spinodal singularities on the real H axis exist at all. The analyticity of equation of state as a function of w would require the low-temperature manifestation of the Lee-Yang points to be points off the real axis by a phase $\Delta\phi = \pi(\beta\delta - 3/2)$. Fonseca and Zamolodchikov put forward a conjecture that these are the closest singularities to the real H axis. Our aim here was to test this conjecture in the small-ε and large-N regimes.

We have used a uniform approximation to the equation of state based on parametric representations, which are especially convenient to study the equation of state in the whole complex plane of w using the ε expansion. However, the vicinity of the Lee-Yang singularity is special in that the ε expansion must break down. In fact, there is an apparent paradox, identified first by Fisher [132], which is most acute in $4 < d < 6$. The equation of state is expected to be mean-field-like in this case, yet, near the Lee-Yang point the critical behavior must be given by nontrivial critical exponents of the ϕ^3 theory. For $d < 4$ the equation of state must approach the mean-field form as $\varepsilon \to 0$, yet this cannot be true near the Lee-Yang point because the ϕ^3 theory is non-perturbative at $d = 4$. We identify and quantify the solution to this apparent paradox. We show that the ε expansion must break down and the equation of state becomes non-perturbative in the (Ginzburg) region around the Lee-Yang point whose radius is proportional to ε^2 as $\varepsilon \to 0$.

We have considered the parametric representation to order ε^2 (and ε^3, see Appendix) and have shown that the singularities we find are consistent with the Fonseca-Zamolodchikov conjecture (for a range of parameters controlling the form of the parametric representation). However, we have also confirmed that the expansion breaks down near the Lee-Yang edge singularities in a way consistent with the derived Ginzburg criterion. In particular, the order ε^3 contribution modifies the results obtained at order ε^2 also at order ε^2! In other words, the behavior near the singularities (including their position) is non-perturbative at order ε^2. Since the distance between the Lee-Yang edge singularity at $t < 0$ (i.e., the spinodal point) from the real axis is itself of order $\beta\delta - 3/2 = \mathcal{O}(\varepsilon^2)$ we conclude that the ε expansion cannot be used to confirm or invalidate the Fonseca-Zamolodchikov conjecture.

We point out that the equation of state of the O(N)-symmetric ϕ^4 theory satisfies the Fonseca-Zamolodchikov conjecture in the large-N limit. In particular, for $d < 4$ there are no singularities on the metastable branch of the real H axis. Instead the singularities can be found off the real axis, and are, in fact, the Lee-Yang branching points, as predicted by extended analyticity. We have checked that (at least in $d = 3$) this result is not affected by the leading $1/N$ corrections. Although the Fonseca-Zamolodchikov conjecture for the Ising critical equation of state is difficult to prove using the analytic methods considered, we can conclude that it is nontrivially consistent with the various systematic approximations to the equation of state beyond the mean-field level.

The absence of singularities on the real H axis (except for the branch point at $H = 0$ associated with the Langer cut) could have implications for the behavior of systems undergoing cooling past the first-order phase transition (see, e.g., Refs. [220, 221, 222, 223]). In particular, it could prove important for the understanding of the experimental signatures of the first-order phase transition separating hadron gas and quark-gluon plasma phases of QCD associated with the QCD critical point, which is being searched for using the beam energy scan heavy-ion collision experiments.

It is important to realize that in the region of the parameter space where the spinodal singularities occur the equation of state is not, strictly speaking, defined in the usual sense as a property of the system *in thermal equilibrium*, due to the finite lifetime of the metastable state (Fig. 4.11). It is, however, defined mathematically by analytic continuation from the regime of thermodynamic stability. Many properties of the equation of state in the metastable region, such as the imaginary part and the discontinuity on the Langer cut are clearly reflecting dynamics of the system associated with the decay of the metastable state. Also the absence of the spinodal singularities at real H can be related to metastability: the presence of a thermodynamic singularity requires the correlation length to diverge and the equilibration to such a critical state requires infinite time, which is impossible due to the finite lifetime of the metastable state.

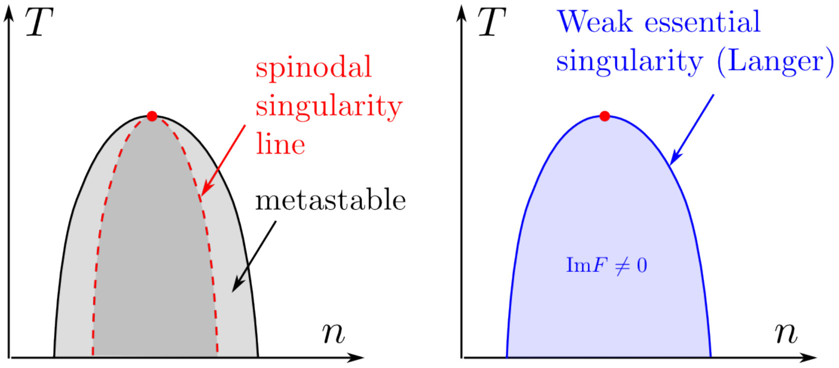
T
spinodal singularity line
metastable
n
T
Weak essential singularity (Langer)
$\mathrm{Im}F \neq 0$
n

Figure 4.11: The phase diagram of the ferromagnetic system in the $T - n$ plane. The left panel is phase diagram for a mean-field theory where there are distinct boundaries of the stable, metastable and unstable phase, separated by the coexistence curve (solid) and spinodal curve (dashed) respectively. However, such boundaries are dimmed beyond mean-field approximation when fluctuations are taken into account.

It is also interesting to note that the decay rate of the metastable state, which is controlled by the (small) coupling u_0 (see Eq. (4.57)) is no longer exponentially suppressed at the spinodal point. Moreover, for small $\widetilde{u}_0$, the nucleation rate near the spinodal point has the asymptotic form $\exp[-\mathrm{const}(w - w_{\mathrm{LY}})^{(6-d)/4}/\widetilde{u}_0]$ [224, 218]. Therefore exponential suppression disappears in the same region as defined by the Ginzburg criterion in Eq. (4.64). This is to be expected since the fluctuations leading to the decay become important in that region. The fact that the shift of the spinodal singularity into the complex H-plane is also due to fluctuation contribution to the "gap" exponent $\beta\delta$ suggests that the shift is related to metastability. It would be interesting to establish a more quantitative relation between this phenomenon and the Fonseca-Zamolodchikov conjecture.

We point out that our analysis is not complete, since the ε expansion fails to capture certain non-perturbative aspects of the universal Ising equation of state, most notably the Langer cut [190]. However, as we shall see, other important questions can nevertheless be addressed within such an approach. One has to bear in mind also that our results apply to the scaling region where the universal behavior is observed. However, many of the conclusions, such as those pertaining to the Langer cut, associated metastability and the shift of the spinodal point into the complex H-plane due to fluctuations should, arguably, remain true outside the scaling region.

We hope that the insights our study provides will contribute to a more complete picture of the ϕ^4 theory. In particular, our work could help develop better parametrizations of the equation of state by taking into account its correct analytic properties. The knowledge of the complex singularities of the equation of state is also important for determining the position of the QCD critical point using lattice Taylor expansion methods [123].

Chapter 5

Conclusion and Outlook

The aim of the thesis is trying to provide a self-contained materials for understanding the study of fluctuations in heavy-ion collision experiment, closely related to the QCD critical point. In this thesis, we attempt to combine and connect the work originally presented in Ref. [1, 2, 4, 5], under a macroscopic perspective as they are expected to be an integral part of the endeavor for discovering the QCD critical point. In addition, we provide more conceptual and technical details that are not presented in the original articles. We hope that what have been summarized and discussed in this thesis may be able to shed light on the future development of this subject.

In Chap. 1, we briefly reviewed the methodology and challenge of discovering the QCD critical point, with an emphasis on the theoretical tools which are necessary and sufficient for us to introduce the following-up discussion in this thesis. There are, however, many other studies on this subject, readers who are interested in may consult review articles and books such as Ref. [14, 33, 225, 59, 61, 64, 226, 227, 228, 229], to list just a few.

In Chap. 2, we present the state-of-the-art formalism describing dynamics of thermal fluctuations in an arbitrary relativistic hydrodynamic flow carrying baryon charge. We firstly introduce a concept of confluent connection which takes into account the relativity of “equal time” and the boost-related changes in the definition of the equal-time correlators and the covariant derivatives. Employing this concept, we derive a deterministic evolution equation for the fluctuation modes, among which the sound mode decouples and nontrivially matches the kinetic equation for phonons propagating on an arbitrary background including relativistic inertial and Coriolis forces due to acceleration and vorticity of the flow. We also describe the procedure of renormalization of short-distance singularities which eliminates cutoff dependence, allowing efficient numerical implementation of these equations [1]. The long-time tails resulted from the remaining finite parts are calculated in frequency space.

In Chap. 3, we discussed the implementation of the hydrodynamic framework introduced in Chap. 2 near the critical point. Focusing on the critical modes we show that this general formalism matches existing Hydro+ description of fluctuations near the QCD critical point [39] and nontrivially extends it inside and outside of the critical region [1]. As the fireball evolution approaches the critical point or variates toward smaller system, not only the slowest mode but also other modes relaxing parametrically slower than the bulk evolution rate, shall be taken into account as independent non-hydrodynamic variables giving feedback to the bulk evolution. The contexts presented in Chap. 2 and 3 are reviewed by Ref. [3].

Chap. 4 turns to the equilibrium aspect of the QCD phase diagram. Recently a family of lattice-QCD-based equation of state with an Ising-type critical point is established [74], yet very little is known about the critical equation of state itself. Following the fixed-point theory of a general $O(N)$ effective Lagrangian, the QCD critical point falls into the Ising (ϕ^4) universality class. We studied the analytic properties of the universal scaling equation of state of the ϕ^4 theory in both small $\varepsilon = 4 - d$ and large N limit. By using the *Josephson-Schofield representation* beyond mean-field approximation, we identified the Langer cut on the real axis associated with a weak essential singularity in the spirit of Padé approximation. We showed that the spinodal points, as the low-temperature images of the Lee-Yang edge singularities, are shifted from the real axis due to fluctuations, and are nevertheless the nearest singularities under the Langer cut, in agreement with the Fonseca-Zamolodchikov Conjecture. The vicinity of the Lee-Yang edge singularity is described by ϕ^3 theory, which is non-perturbative even for $d \gtrsim 4$. We derived the Ginzburg criterion that determines the size of the non-perturbative region where mean-field theory breaks down [5]. Furthermore, to determine the scaling properties of the Lee-Yang edge singularity, we applied the non-perturbative renormalization group approach by introduce a scale-dependent effective action in $3 \leq d \leq 6$. Keeping higher-order derivatives the results are in good agreement with other approaches in particular limits [4]. Our work implies that the dynamical description of the decay of metastable phase is underdeveloped. The major ideas and results of Chap. 4 are also reviewed by Ref. [6].

The work presented in this this paves the way for a comprehensive and quantitative understanding of the fluctuations in heavy-ion collisions, in particular those sensitive to the critical point. The studies could also be applied and extended to the subjects of cosmology, ultracold atomic Fermi gases and so on, in certain limits and scenarios. Focusing on the heavy-ion collision experiments, our results are an essential ingredient of the theoretical framework for interpreting the experimental results from the RHIC Beam Energy Scan Program. To accomplish such framework, among those possible developments pointed out in the discussion section of each chapters, we shall emphasize a few of them. For instance, it would be beneficial to extend our formalism by including higher-point functions that are more sensitive to the critical point, and connect it to the freezeout kinetics and observables. Moreover, it would be worthwhile to consider its accommodation to the first-order phase transition line and associated complex singularities, providing a more complete picture of fireball evolution in high baryon density region. These studies are deferred to future work.

Appendix A

Reduction to Non-relativistic Hydrodynamics

Although in this thesis we are mostly focusing on the *relativistic* hydrodynamic fluctuations, our results shall be readily reduced to the non-relativistic case. In the appendix, we offer a concise summary of the reduction of ideal relativistic hydrodynamics in the co-moving frame to its non-relativistic format in the laboratory frame.

The relativistic energy-momentum tensor is defined by Eq. (2.8), where all thermodynamic variables are *defined* in the local rest frame, except the velocity u^μ defining the frame itself. In the co-moving frame and laboratory frame, it reads respectively

$$u^\mu_{\mathrm{LRF}} = (1, \boldsymbol{0})\,, \quad u^\mu_{\mathrm{LF}} = \gamma(1, \boldsymbol{v})\,, \tag{A.1}$$

where $\boldsymbol{v}$ is the velocity measure in the laboratory frame, γ is the Lorentz factor. u^μ_{LF} is simply obtained from u^μ_{LRF} by a boost from the local rest frame. In the non-relativistic limit $v \ll 1$ where $v \equiv |\boldsymbol{v}|$ should be thought as v/c with $c = 1$,

$$\gamma \equiv \left(1 - v^2\right)^{-\frac{1}{2}} = 1 + \frac{1}{2}v^2 + \mathcal{O}(v^4). \tag{A.2}$$

Similarly, the thermodynamic variables in the laboratory frame are related to those in the co-moving frame by the Lorentz factor as

$$\bar{s} = \gamma s\,, \quad \bar{\varepsilon} = \gamma^2(\varepsilon + pv^2)\,, \quad \bar{w} = \gamma^2 w\,, \quad \bar{n} = \gamma n\,,$$
$$\bar{p} = p\,, \quad \bar{T} = T/\gamma\,, \quad \bar{\mu} = \mu/\gamma\,. \tag{A.3}$$

The constitutive relations in the laboratory frame are accordingly

$$\bar{T}^{00} \equiv \bar{\varepsilon} \equiv \gamma^2 w - p\,, \quad \bar{T}^{0i} \equiv \bar{\pi}^i \equiv \bar{w}v^i \equiv \gamma^2 w v^i\,, \quad \bar{T}^{ij} \equiv \bar{w}v^i v^j + p\delta^{ij} \equiv \gamma^2 w v^i v^j + p\delta^{ij}\,,$$
$$\bar{J}^0 \equiv \bar{n} \equiv \gamma n\,, \quad \bar{J}^i \equiv \bar{n}v^i \equiv \gamma n v^i\,. \tag{A.4}$$

In addition, we decompose the energy density as

$$\varepsilon = \rho(1+e) \tag{A.5}$$

where ρ is the proper mass (rest energy) density per unit volume measured in the co-moving (proper) frame and e is the (non-relativistic) internal energy density (per unit mass). The relativistic equation of continuity for ρ is

$$\partial_\mu(\rho u^\mu) = 0. \tag{A.6}$$

The proper mass density measured in the laboratory frame is

$$\bar{\rho} = \gamma^2 \rho, \tag{A.7}$$

satisfying the equation of continuity

$$\partial_t \bar{\rho} + \partial_i(\bar{\rho} v^i) = 0. \tag{A.8}$$

Correspondingly, we define

$$\bar{\varepsilon} = \bar{\rho}(1+\bar{e}), \quad \bar{w} = \bar{\varepsilon} + p = \bar{\rho}(1+\bar{e}) + p. \tag{A.9}$$

In the non-relativistic limit the rest energy is dominant, i.e.,

$$\rho \sim \bar{\rho} \sim \mathcal{O}(1), \quad p \sim e \sim \bar{e} \sim \mathcal{O}(v^2), \quad w \sim \bar{w} = \bar{\rho} + \mathcal{O}(v^2). \tag{A.10}$$

Therefore up to different truncation orders of v, we have

$$\begin{aligned}
\bar{T}^{ij} &= \bar{w}v^i v^j + p\delta^{ij} = \bar{\rho}v^i v^j + p\delta^{ij} + \mathcal{O}(v^4). \\
\bar{T}^{0i} &= \bar{w}v^i = \left(\bar{\rho} + \frac{1}{2}\bar{\rho}v^2 + p\right) v^i + \mathcal{O}(v^4) = \bar{\rho}v^i + \mathcal{O}(v^3). \\
\bar{T}^{00} &= \bar{w} - p = \left(\bar{\rho} + \frac{1}{2}\bar{\rho}v^2 + p\right) - p + \mathcal{O}(v^4) = \left(\bar{\varepsilon} + \frac{1}{2}\bar{\rho}v^2\right) + \mathcal{O}(v^4) = \bar{\rho} + \mathcal{O}(v^2).
\end{aligned} \tag{A.11}$$

To obtain the momentum density and energy flux density, we need to expand T^{0i} up to the first and third order respectively.

Expand $\partial_\mu T^{\mu 0} = 0$ up to second and fourth order, and $\partial_\mu T^{\mu j} = 0$ up to third order, we obtain the conservation of density, energy and momentum respectively, i.e.,

$$\partial_t T^{00} + \partial_i T^{i0} = 0 \implies \begin{cases} \partial_t \bar{\rho} + \partial_i(\bar{\rho}v^i) + \mathcal{O}(v^2) = 0, \\ \partial_t \left(\bar{\varepsilon} + \frac{1}{2}\bar{\rho}v^2\right) + \partial_i \left[\left(\bar{w} + \frac{1}{2}\bar{\rho}v^2\right) v^i\right] + \mathcal{O}(v^4) = 0. \end{cases} \tag{A.12}$$

$$\partial_t T^{0j} + \partial_i T^{ij} = 0 \quad \implies \quad \partial_t \left(\bar{\rho}v^j\right) + \partial_i \left(\bar{\rho}v^i v^j + p\delta^{ij}\right) + \mathcal{O}(v^3) = 0. \tag{A.13}$$

Note the equation of energy conservation expanded up to $\mathcal{O}(v)$ has the same form of

$$\partial_\mu j^\mu = 0 \quad \implies \quad \partial_t \bar{\rho} + \partial_i(\bar{\rho}v^i) = 0, \tag{A.14}$$

which is exact without expansion, so they are indeed independent equations.

The equations for non-relativistic hydrodynamics are boost invariant, i.e., under the boost $v^i \to v^i + u^i$ where u^i is a constant velocity, the equations are invariant if we identify $\partial_{t'} = \partial_t + u^i\partial_i$:

$$\begin{aligned}
&\partial_t \rho + \partial_i[\rho(v^i + u^i)] = \partial_{t'}\rho + \partial_i(\rho v^i) = 0, \\
&\partial_t \left(\rho v^j\right) + \partial_i \left[\rho(v^i + u^i)v^j + p\delta^{ij}\right] = \partial_{t'} \left(\rho v^j\right) + \partial_i \left[\rho v^i v^j + p\delta^{ij}\right] = 0, \\
&\partial_t \left(\varepsilon + \frac{1}{2}\rho(v+u)^2\right) + \partial_i \left[\left(w + \frac{1}{2}\rho(v+u)^2\right)(v^i + u^i)\right] \\
=\,&\partial_{t'} \left(\varepsilon + \frac{1}{2}\rho v^2\right) + \partial_i \left[\left(w + \frac{1}{2}\rho v^2\right) v^i\right] = 0,
\end{aligned} \tag{A.15}$$

where in the last equation we have used the first equation and the Euler's equation

$$\partial_i p + \rho \left[\partial_t + (v^j + u^j)\partial_j\right] v_i = 0. \tag{A.16}$$

Appendix B

Fundamental Thermodynamic Relations

The thermodynamic derivatives appearing in Eq. (2.38) and (2.39), i.e.,

$$d\varepsilon = \varepsilon_m dm + \varepsilon_p dp\,, \quad dn = n_m dm + n_p dp\,, \quad d\alpha = \alpha_m dm + \alpha_p dp\,, \tag{B.1}$$

are defined in the standard notation

$$\begin{aligned} \varepsilon_m \equiv \left(\frac{\partial \varepsilon}{\partial m}\right)_p, \quad \varepsilon_p \equiv \left(\frac{\partial \varepsilon}{\partial p}\right)_m, \quad n_m \equiv \left(\frac{\partial n}{\partial m}\right)_p, \\ n_p \equiv \left(\frac{\partial n}{\partial p}\right)_m, \quad \alpha_m \equiv \left(\frac{\partial \alpha}{\partial m}\right)_p, \quad \alpha_p \equiv \left(\frac{\partial \alpha}{\partial p}\right)_m. \end{aligned} \tag{B.2}$$

To obtain the relations of the second order thermodynamic coefficients, Eq. (2.48), we begin with the thermodynamic relations coming from the first law of thermodynamics (Eq. (2.10)):

$$d\varepsilon = Tndm + \frac{w}{n}dn\,, \quad dp = \frac{w}{T}dT + Tnd\alpha\,, \quad d\left(\frac{w}{n}\right) = Tdm + \frac{1}{n}dp\,, \tag{B.3}$$

from which we obtain

$$\begin{aligned} \left(\frac{\partial \varepsilon}{\partial m}\right)_n = \left(\frac{\partial p}{\partial \alpha}\right)_T = Tn\,, \quad \left(\frac{\partial \varepsilon}{\partial n}\right)_m = \frac{w}{n}\,, \quad \left(\frac{\partial n}{\partial m}\right)_\varepsilon = -\frac{Tn^2}{w}\,, \\ \left(\frac{\partial \alpha}{\partial T}\right)_p = -\frac{w}{T^2 n}\,, \quad \left(\frac{\partial T}{\partial p}\right)_m = -\frac{n_m}{n^2}\,. \end{aligned} \tag{B.4}$$

Therefore

$$\begin{aligned}\varepsilon_m &= \left(\frac{\partial\varepsilon}{\partial m}\right)_n + \left(\frac{\partial\varepsilon}{\partial n}\right)_m \left(\frac{\partial n}{\partial m}\right)_p = Tn\left(1+\frac{n_m w}{Tn^2}\right)\\ &= (Tn)^2\left(\left(\frac{\partial\alpha}{\partial p}\right)_T + \left(\frac{\partial\alpha}{\partial T}\right)_p\left(\frac{\partial T}{\partial p}\right)_m\right) = (Tn)^2\alpha_p\,.\end{aligned}\tag{B.5}$$

Noting that

$$\dot{T} = \frac{n}{T}\left(\frac{\partial T}{\partial n}\right)_m = \frac{n}{T}\left(\frac{\partial\varepsilon}{\partial n}\right)_m\left(\frac{\partial T}{\partial p}\right)_m\left(\frac{\partial p}{\partial\varepsilon}\right)_m = -\frac{c_s^2 n_m w}{Tn^2} = c_s^2\left(1-\frac{\varepsilon_m}{Tn}\right) = c_s^2\left(1-\alpha_p Tn\right),\tag{B.6}$$

we obtain

$$\varepsilon_m = Tn\left(1-\frac{\dot{T}}{c_s^2}\right),\quad \alpha_p = \frac{1}{Tn}\left(1-\frac{\dot{T}}{c_s^2}\right),\tag{B.7}$$

demonstrating the first identity in Eq. (2.48). Likewise, the remaining nontrivial identities in Eq. (2.48) are obtained by using Eq. (B.4) and turn out to be

$$\begin{aligned}n_m &= \left(\frac{\partial n}{\partial m}\right)_\varepsilon + \left(\frac{\partial n}{\partial\varepsilon}\right)_m\left(\frac{\partial\varepsilon}{\partial m}\right)_p = \frac{n}{w}\left(\varepsilon_m - Tn\right) = \frac{Tn^2}{w}\left(Tn\alpha_p - 1\right) = -\frac{\dot{T}Tn^2}{c_s^2 w}\,,\\ n_p &= \left(\frac{\partial n}{\partial\varepsilon}\right)_m\left(\frac{\partial\varepsilon}{\partial p}\right)_m = \frac{n}{c_s^2 w},\quad \alpha_m = \left(\frac{\partial\alpha}{\partial T}\right)_p\left(\frac{\partial T}{\partial m}\right)_p = -\frac{w}{nT^2}\left(\frac{\partial T}{\partial m}\right)_p = -\frac{w}{c_p T}\,.\end{aligned}\tag{B.8}$$

Throughout the above derivation, we have used the definition

$$c_s^2 \equiv \left(\frac{\partial p}{\partial\varepsilon}\right)_m,\quad c_p \equiv Tn\left(\frac{\partial m}{\partial T}\right)_p\,.\tag{B.9}$$

Similarly, the third order derivatives appearing in Eq. (2.62) are defined by

$$\varepsilon_{mm} \equiv \left(\frac{\partial^2\varepsilon}{\partial m^2}\right)_p,\quad \varepsilon_{pp} \equiv \left(\frac{\partial^2\varepsilon}{\partial p^2}\right)_m,\quad n_{mm} \equiv \left(\frac{\partial^2\varepsilon}{\partial m^2}\right)_p,\quad n_{pp} \equiv \left(\frac{\partial^2\varepsilon}{\partial p^2}\right)_m.\tag{B.10}$$

Note that the mixed third order derivatives are not presented here as they are not relevant in our calculation. The results presented in Eq. (2.63) can be derived straightforwardly from the known expression of second order thermodynamic derivatives given above. We leave this exercise to the reader.

Appendix C

Local Confluent Triad and Basis

C.1 A Local Confluent Triad

In order to describe the separation vector y (for example, to enable numerical solution of the equations for fluctuation correlators) we need to introduce a basis triad $e^a_\mu(x)$ for the tangent plane orthogonal to $u(x)$ at each point x. The basis is arbitrary and here we shall propose a simple and intuitive choice of $e_a(x)$. We choose a (lab) frame $\mathring{u}$ and a fixed triad ($a = 1, 2, 3$) satisfying $\mathring{e}_a \cdot \mathring{e}^b = \delta^b_a$ and $\mathring{e}_a \cdot \mathring{u} = \mathring{e}^b \cdot \mathring{u} = 0$. For simplicity we shall consider an orthogonal triad, equivalent to its dual, $e^a = e_a$.

We can then define $e^a(x)$ by a *finite* boost from $\mathring{u}$ to $u(x)$. The resulting triad vectors at point x are given by explicit algebraic formulas:

$$e_a = \mathring{e}_a + (u + \mathring{u})\frac{u \cdot \mathring{e}_a}{1 - u \cdot \mathring{u}}\,. \tag{C.1}$$

One can check that $e_a \cdot u = 0$ and $e^a \cdot e_b = \delta^a_b$.

Corresponding spin connection is given by Eq. (2.85)

$$\mathring{\omega}^b_{\mu a} \equiv e^b_\nu \partial_\mu e^\nu_a = e^b_\nu e^\lambda_a \left[\mathring{u}^\nu \partial_\mu u_\lambda - \mathring{u}_\lambda \partial_\mu u^\nu\right](1 - u \cdot \mathring{u})^{-1}\,. \tag{C.2}$$

In terms of the confluent connection defined in Eq. (2.79) one can express spin connection as

$$\mathring{\omega}^{b}_{\mu a} = \frac{\bar{\omega}^{\nu}_{\mu\lambda}\mathring{e}^{b}_{\nu}\mathring{e}^{\lambda}_{a}}{1 - u\cdot\mathring{u}}\,. \tag{C.3}$$

For certain flow configurations $u(x)$ it may be possible to find a choice of triad fields $e_a(x)$ which makes the spin connection $\mathring{\omega}$ vanish. This requires integrability of Eq. (2.84) with $\mathring{\omega} = 0$, which means that the change of vector e_a obtained by integrating Eq. (2.84) with $\mathring{\omega} = 0$ between two points should not depend on the path, i.e.,

$$\oint dx^{\lambda}\bar{\omega}^{\mu}_{\lambda\nu}e^{\nu}_{a} = 0. \tag{C.4}$$

Using Stokes theorem we see that this is possible if curvature associated with connection $\bar{\omega}^{\mu}_{\lambda\nu}$ vanishes. Using Eq. (2.79), we find:

$$\bar{R}_{\alpha\beta}{}^{\mu}{}_{\nu} = \partial_\alpha\bar{\omega}^{\mu}_{\beta\nu} + \bar{\omega}^{\mu}_{\alpha\lambda}\bar{\omega}^{\lambda}_{\beta\nu} - (\alpha\leftrightarrow\beta) = \partial_\alpha u_\nu\partial_\beta u^\mu - \partial_\beta u_\nu\partial_\alpha u^\mu\,. \tag{C.5}$$

One might say that $\bar{R}_{\alpha\beta}{}^{\mu}{}_{\nu} = 0$ means $\bar{\omega}^{\mu}_{\lambda\nu}$ is a “pure gauge” connection.

A nontrivial example of flow with $\bar{\omega}^{\mu}_{\lambda\nu} \neq 0$ but $\bar{R}_{\alpha\beta}{}^{\mu}{}_{\nu} = 0$ is the Bjorken flow. In this case our proposed choice of $e_a(x)$ in Eq. (C.1) provides a rotationless (i.e., $\mathring{\omega} = 0$) triad field.

C.2 A Basis in the Space Orthogonal to $\hat{q}$ and u and Monopole Connection

A basis in the space orthogonal to $\hat{q}$ and u (cf. Eq. (2.115)) can be obtained easily by rotating the local confluent basis e^a in such a way that one of the vectors, say e_3, lines up with $\hat{q}$. The result is given by

$$t^{(i)} = e^i - (e^3 + \hat{q})\,\frac{\hat{q}\cdot e^i}{1 + \hat{q}\cdot e_3}, \quad i = 1, 2, \tag{C.6}$$

satisfying $t^{(i)}\cdot t^{(j)} = \delta^{ij}$ and $t^{(i)}\cdot\hat{q}_\perp = t^{(i)}\cdot u = 0$.

Since $t^{(i)}$ depends on x (to maintain $u(x)\cdot t^{(i)} = 0$) as well as on q (to keep $\hat{q}\cdot t^{(i)} = 0$), there are two types of connections in Eq. (2.124) defined by Eqs. (2.127) and Eqs. (2.126).

Applying these definitions to our choice of $t^{(i)}$ in Eq. (C.6) we find for the x-derivative connection in Eq. (2.127)

$$\widehat{\mathring{\omega}}^{ij}_{\lambda} = \mathring{\omega}^{i}_{\lambda j} - (\mathring{\omega}^{i}_{\lambda 3}\hat{q}\cdot e_j + \mathring{\omega}^{3}_{\lambda j}\hat{q}\cdot e^i)(1+\hat{q}\cdot e_3)^{-1}\,, \tag{C.7}$$

where the connection $\mathring{\omega}^{a}_{\lambda b}$ is defined by Eq. (2.85).

For the q-derivative connection, using definition in Eq. (2.126), one obtains

$$\widehat{\omega}^{ij}_{\mu} = \frac{\hat{q}^{\lambda}(e^i_{\lambda}e^j_{\mu} - e^j_{\lambda}e^i_{\mu})}{|q|+q\cdot e_3} = \frac{e^{\lambda}_3(t^{(i)}_{\mu}t^{(j)}_{\lambda} - t^{(j)}_{\mu}t^{(i)}_{\lambda})}{|q|+q\cdot e_3} = \varepsilon^{ij}\,\frac{\varepsilon_{\mu\lambda\nu\sigma}e^{\lambda}_3u^{\nu}\hat{q}^{\sigma}}{|q|+q\cdot e_3}\,. \tag{C.8}$$

The last expression can be easily recognized as the connection describing a monopole at $q=0$ and Dirac string along $-e_3$. The corresponding curvature [1]

$$\widehat{R}^{ij}_{\mu\nu} = \partial^{(q)}_{\mu}\widehat{\omega}^{ij}_{\nu} - \partial^{(q)}_{\nu}\widehat{\omega}^{ij}_{\mu} = -\frac{(t^i_{\mu}t^j_{\nu} - t^j_{\mu}t^i_{\nu})}{|q|^2} = \varepsilon^{ij}\,\frac{\varepsilon_{\mu\nu\sigma\lambda}u^{\lambda}\hat{q}^{\sigma}}{|q|^2}\,. \tag{C.9}$$

is the field of a monopole with charge 1 (twice the amount of Berry curvature monopole charge for spin-1/2 fermion). The singularity at $q=0$ is associated with the ambiguity of $\hat{q}$ at $q=0$.

---

[1] Because the space spanned by $t^{(i)}$ is two-dimensional the connection is abelian, i.e., $[\widehat{\omega}_{\mu},\widehat{\omega}_{\nu}]=0$.

Appendix D

Comparison to Known Results

Our new results can be compared to some existing results in the literature for several special cases.

A charged fluid studied in Ref. [50] is (i) conformal and (ii) undergoes a boost-invariant (Bjorken) expansion. Thermodynamic functions of a conformal fluid satisfy $\dot{T} = c_s^2 = 1/3$, $\varepsilon_m = \alpha_p = \dot{c}_s = 0$, $\dot{c}_p = 1$ as summarized in Table D.1. The boost-invariant flow implies that $a_\mu = \omega_{\mu\nu} = 0$ and spatial gradients of background scalar fields vanish (e.g., $\partial_{\perp\mu}\alpha = 0$). Under these conditions our results are significantly simplified. Since in a boost-invariant Bjorken flow, the charge does not diffuse due to the absence of background gradients forbidden by boost-invariance, in order to generate the dissipative (ohmic) charge current, one needs to apply an external electric field to the system. Adding such a source term is indispensable for obtaining such important results as renormalized or frequency-dependent conductivity in Ref. [50]. We find that except for a few minor typos, our Eqs. (2.165a) and (2.165c) for renormalized transport coefficients, as well as Eq. (2.170) and (2.173) for frequency-dependent transport coefficients, reduce to Eq. (51) and (50) in Ref. [50] respectively. Notice that $\zeta = 0$ in conformal fluid.

Despite this agreement with Ref. [50], there are still some mismatches. For example, our Eq. (2.54) would have matched Eq. (62) in [50] in the absence of source term, if it wasn't for the last term $\sim 1/\tau$ in Eq. (64a), which should be $\sim (1+c_s^2)/\tau$ according to our results.

To compare one of the key results of our paper, Eqs. (2.130), to Ref. [50] we need to rescale our Wigner functions, somewhat similarly to Eq. (2.128),

$$N^{\rm B}_{mm} \equiv \frac{W_{mm}}{\tau}\,, \quad N^{\rm B}_{(i)(j)} \equiv \frac{W_{(i)(j)}}{\tau}\,, \tag{D.1}$$

where τ is the Bjorken proper time coordinate, and express the unit vectors in spherical coordinates

$$\hat{q} = (0, \sin\theta\cos\phi, \sin\theta\sin\phi, \cos\theta)\,, \tag{D.2}$$

$$t^{(1)} = (0, -\sin\phi, \cos\phi, 0)\,, \quad t^{(2)} = (0, \cos\theta\cos\phi, \cos\theta\sin\phi, -\sin\theta)\,. \tag{D.3}$$

Then, our equations read

$$\begin{aligned}
\partial_\tau N^{\rm B}_{mm} &= -2\gamma_\lambda q^2\left(N^{\rm B}_{mm} - \frac{c_p T^2}{\tau}\right) - \frac{2+2\dot{T}}{\tau}N^{\rm B}_{mm}\,,\\
\partial_\tau N^{\rm B}_{m(1)} &= -(\gamma_\eta+\gamma_\lambda)q^2 N^{\rm B}_{m(1)} - \frac{2+\dot{T}}{\tau}N^{\rm B}_{m(1)}\,,\\
\partial_\tau N^{\rm B}_{m(2)} &= -(\gamma_\eta+\gamma_\lambda)q^2 N^{\rm B}_{m(2)} - \frac{2+\dot{T}+\sin^2\theta}{\tau}N^{\rm B}_{m(2)}\,,\\
\partial_\tau N^{\rm B}_{(1)(1)} &= -2\gamma_\eta q^2\left(N^{\rm B}_{(1)(1)} - \frac{Tw}{\tau}\right) - \frac{2}{\tau}N^{\rm B}_{(1)(1)}\,,\\
\partial_\tau N^{\rm B}_{(2)(2)} &= -2\gamma_\eta q^2\left(N^{\rm B}_{(2)(2)} - \frac{Tw}{\tau}\right) - \frac{2(1+\sin^2\theta)}{\tau}N^{\rm B}_{(2)(2)}\,.
\end{aligned} \tag{D.4}$$

The equations for $N^{\rm B}_{(1)(1)}$ and $N^{\rm B}_{(2)(2)}$ match those in Ref. [50]. The remaining equations, although very similar, do not match completely. We believe our results are correct but do not have a definitive explanation for these disagreements.

Unlike the chargeless fluid in Ref. [1], the charged fluid in the present paper can be taken to non-relativistic limit, where it can be compared with Ref. [47, 230]. The most glaring omission in Ref. [47, 230] are the $G_{m(i)}$ components of the correlators. It appears they were omitted based on the observation that their equilibrium values vanish. They do, but they are not zero *out* of equilibrium and are essential, for example, for describing the dominant critical contribution to conductivity as discussed in Section 3.2.2.

To compare the equations for remaining components of W_{AB}, we need to rescale our variables as

$$N^{\rm A}_{mm} \equiv \frac{W_{mm}}{n^2T^2}\,, \quad N^{\rm A}_{(i)(j)} \equiv \frac{W_{(i)(j)}}{wn}\,. \tag{D.5}$$

Omitting $W_{m(i)}$ terms as in Ref. [47, 230] we find

$$\begin{aligned}\mathcal{L}[N^{\rm A}_{mm}] =& -2\gamma_\lambda q^2\left(N^{\rm A}_{mm}-\frac{c_p^{\rm A}}{n}\right)+\theta N^{\rm A}_{mm}\,,\\ \mathcal{L}[N^{\rm A}_{(i)(j)}] =& -2\gamma_\eta q^2\left(N^{\rm A}_{(i)(j)}-\frac{T}{n}\delta_{ij}\right)+(1+c_s^2)\theta N^{\rm A}_{(i)(j)}\\ &-(\theta^{\mu\nu}-\omega^{\mu\nu})\left(t^{(i)}_\mu t^{(k)}_\nu N^{\rm A}_{(k)(j)}+t^{(j)}_\mu t^{(k)}_\nu N^{\rm A}_{(i)(k)}\right)\,,\end{aligned}$$

where the specific heat per mass is $c_p^{\rm A} \equiv c_p/n$. This would agree nicely with Ref. [230] in the non-relativisitic limit ($c_s^2 \ll 1$) if we also follow Ref. [230] and impose $N^{\rm A}_{ij} \sim \delta_{ij}$ which will eliminate $\omega_{\mu\nu}$ term. Similar to the omission of $G_{m(i)}$, the assumption $G_{(i)(j)} \sim \delta_{ij}$ was apparently made by neglecting off-equilibrium contribution to this correlator.

Our equation (2.123) for sound fluctuations completely matches the Boltzmann equation given in Ref. [47] in the non-relativistic limit, where the $\gamma_p = \lambda c_s^2\alpha_p^2 Tw$, appearing in Eq. (2.120) is replaced by its non-relativistic limit

$$\gamma_p^{\rm NR} = \kappa\left(\frac{1}{c_v}-\frac{1}{c_p}\right)\,. \tag{D.6}$$

Indeed, since in our units the speed of light is 1, for a non-relativistic fluid $c_s^2 \ll 1$ (see also Table D.1),

$$(Tn)^2\alpha_p^2 = \left(1-\frac{\dot T}{c_s^2}\right)^2 \approx \frac{\dot T^2}{c_s^4} = \frac{w}{c_s^2 T}\left(\frac{1}{c_v}-\frac{1}{c_p}\right)\,, \tag{D.7}$$

where in writing '≈' we used $c_s^2 \ll \dot T$ (see Table D.1) and expressed $\dot T$ in terms of c_v, c_p and c_s:

$$\dot T^2 = \frac{c_s^2 w}{T}\left(\frac{1}{c_v}-\frac{1}{c_p}\right)\,, \quad c_v \equiv \left(\frac{\partial\varepsilon}{\partial T}\right)_n\,. \tag{D.8}$$

thermodynamic quantities	definition	conformal fluid	non-relativistic ideal gas ($T \ll M$)	scaling power of ξ at critical point
c_s^2	$\left(\frac{\partial p}{\partial \varepsilon}\right)_m$	$1/3$	$\gamma T/M$	$-\alpha/\nu$
c_p	$\left(\frac{Tn\partial m}{\partial T}\right)_p$	c_p	$\gamma n/(\gamma-1)$	$2-\eta$
$\dot{T}$	$\left(\frac{\partial \log T}{\partial \log s}\right)_m$	$1/3$	$\gamma - 1$	$-\alpha/\nu$
$\dot{c}_s$	$\left(\frac{\partial \log c_s}{\partial \log s}\right)_m$	0	$(\gamma-1)/2$	$(1-\alpha)/\nu$
$\dot{c}_p$	$\left(\frac{\partial \log c_p}{\partial \log s}\right)_m$	1	1	$(1-\alpha)/\nu$

Table D.1: The behavior of thermodynamic coefficients used in the paper in different limits. For non-relativistic ideal gas $\gamma = c_p/c_v > 1$ denotes adiabatic constant and M the molecule mass.

Appendix E

Details of the Parametric Equation of State

E.1 Parametric Equation of State at Order ε^2

For completeness, and for possible future use, in this Appendix we collect the results which are represented schematically in Sec. 4.2.3. In particular, they show explicit dependence (or independence) of expansion coefficients on (arbitrary at this order of ε) parameters b_1 and b_2. To obtain the complete expression for w_n in Eq. (4.83) up to $\mathcal{O}(\varepsilon^2)$ one needs to expand each quantity in Eq. (4.81) up to sufficient order. In particular, we need:

$$h_3 = -\frac{1}{b^2} = -\frac{2}{3} + \frac{4b_1}{9}\varepsilon + \frac{1}{9}\left(-\frac{8b_1^2}{3} + 4b_2\right)\varepsilon^2 + \mathcal{O}(\varepsilon^3), \tag{E.1}$$

and the normalization parameters in Eqs. (4.80):

$$\bar{z} = \frac{1}{\sqrt{3}}\left[1 + \frac{1}{6}\left(4b_1 - 1\right)\varepsilon + \frac{1}{648}\left(229 + 45\pi^2 - 360\lambda - 144b_1(2 + 3b_1) + 432b_2\right)\varepsilon^2 + \mathcal{O}(\varepsilon^3)\right], \tag{E.2a}$$

$$\bar{w} = \frac{1}{\sqrt{3}}\left[1 + \frac{2b_1}{3}\varepsilon + \frac{1}{24}\left(7 + \pi^2 - 8\lambda - 8b_1(1 + 2b_1) + 16b_2\right)\varepsilon^2 + \mathcal{O}(\varepsilon^3)\right]. \tag{E.2b}$$

Substituting Eqs. (E.1) and (E.2) into Eq. (4.80) and using the ansatz for θ_n, Eq. (4.82), we obtain Eq. (4.83), where $\mathcal{O}(\varepsilon)$ terms cancel and the $\mathcal{O}(\varepsilon^2)$ coefficient

$$\omega^{(2)}(c_n, b_1) = \frac{1}{24}\left(7 + \pi^2 - 8\lambda - \ln|c_n|^2 - 8b_1(1 + 2b_1)\right) - \frac{3}{8c_n^2} - \frac{b_1}{c_n}, \tag{E.3}$$

is independent of the parameter b_2.

E.2 Parametric Equation of State at Order ε^3

Here, we consider the *extended* linear parametric model, i.e., Eqs. (4.71) – (4.74), in order to examine the robustness of our conclusions at $\mathcal{O}(\varepsilon^2)$. In particular, we will show how the $\mathcal{O}(\varepsilon^2)$ terms in $|w_n|$ are modified by introducing the $\mathcal{O}(\varepsilon^3)$ contributions, which again demonstrates the non-perturbative nature of the problem.

In the extended model,

$$h(\theta) = \bar{h}(\theta + h_3\theta^3 + h_5\theta^5), \tag{E.4}$$

where $\bar{h}$ is an appropriate normalization constant. In contrast to the parametric model of Sec. 4.2.3, the inclusion of a fifth-order contribution in θ is necessary to match to the equation of state at order ε^3 [170, 171]. The coefficients h_3 and h_5 are given by

$$\begin{aligned} h_3 &= -\frac{1 - e\varepsilon^3}{b^2} \\ &= -\frac{2}{3} + \frac{4b_1}{9}\varepsilon + \frac{1}{9}\left(-\frac{8b_1^2}{3} + 4b_2\right)\varepsilon^2 + \frac{2}{81}\left(8b_1^3 - 24b_1b_2 + 18b_3 + 27e\right)\varepsilon^3 + \mathcal{O}(\varepsilon^4), && \text{(E.5)} \\ h_5 &= -\frac{e\varepsilon^3}{b^4} = -\frac{4}{9}e\varepsilon^3 + \mathcal{O}(\varepsilon^4), && \text{(E.6)} \end{aligned}$$

with the parameter

$$e = \frac{1}{48}\left(1 + 2\lambda - 4\zeta(3) - 16b_1^2\right), \tag{E.7}$$

which is negative for all real-valued b_1, and

$$b^2 = \frac{3}{2} + b_1\varepsilon + b_2\varepsilon^2 + b_3\varepsilon^3 + \mathcal{O}(\varepsilon^4), \tag{E.8}$$

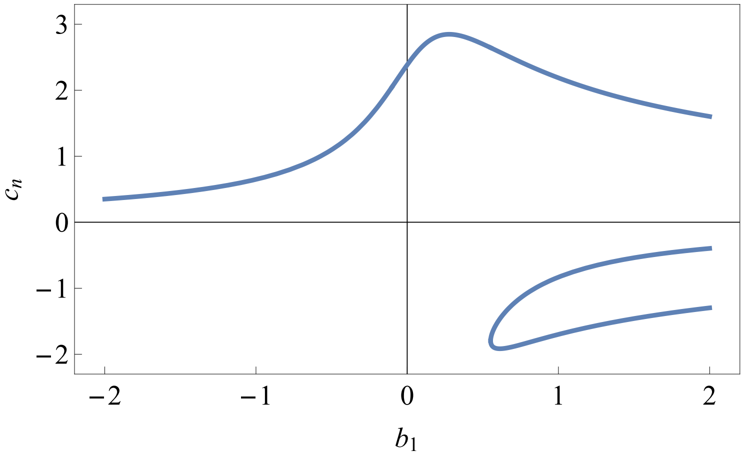

Figure E.1: The parameters c_n, $n = 1, 2, 3$ as a function of b_1. We observe a critical value $b_1 \approx 0.552$ above which all solutions θ_n^2, $n = 1, 2, 3$, are real.

expanded in powers of ε. The significance of these parameters becomes clear if we factor decompose Eq. (E.4) to the following form

$$h(\theta) = \bar{h}\theta\big[1 - (\theta/b)^2\big]\big[1 + e\varepsilon^3(\theta/b)^2\big]\,, \tag{E.9}$$

i.e., b and e are related to the zeros of h on the coexistence line ($t < 0$, $H \to 0$). Note, while $\theta = \pm b$ stays finite in the limit $\varepsilon \to 0$, $\theta = \pm b/\sqrt{-e\varepsilon^3}$ diverges in the same limit.

To order ε^3, the extended linear parametric representation depends on three real-valued parameters b_1, b_2, and b_3. These parameters cannot be fixed by matching to the equation of state alone [171], which parallels the behavior we have already observed with the order ε^2 parametric model (cf. Sec. 4.2.3). Essentially, we therefore obtain a three-parameter family of extended linear models that we employ in the following to study the complex-field singularities of the equation of state.

At order ε^3 we find that the (rescaled) inverse susceptibility is given by

$$F'(\theta) = \frac{\bar{w}}{\bar{z}}(1-\theta^2)^{-\gamma}\frac{1 + (2\beta\delta + 3h_3 - 1)\,\theta^2 + [(2\beta\delta - 3)h_3 + 5h_5]\,\theta^4 + (2\beta\delta - 5)h_5\theta^6}{1 - (1 - 2\beta)\,\theta^2}, \tag{E.10}$$

where the exponents β, γ, and δ, as well as the normalization constants $\bar{w}$ and $\bar{z}$, should be expanded to order ε^3 (for details we refer to [170, 171]). The zeros of this function, which

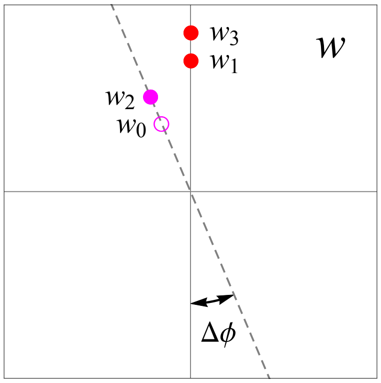

Figure E.2: We show the distribution of the zeros w_1, w_2, and w_3 (solid points) and pole w_0 (open circle) of the parametrized inverse isothermal susceptibility $F'(z)$ up to $\mathcal{O}(\varepsilon^3)$. Here, $b_1 \gtrsim 0.552$, such that all singular points align either along the Lee-Yang cut (situated on the imaginary w axis) or the Langer cut (along the dashed line). Note, only the singularities in the upper half of the complex w plane are shown.

we consider in terms of θ^2, can be found by solving for the roots of the numerator and can be determined in closed form.

We find three distinct (pairs of) zeros, θ_n^2, which we label by $n = 1, 2, 3$. It is sufficient to use the ansatz Eq. (4.82) with the leading-order coefficient given by

$$c_n = \frac{1}{24e}\left[1 + \zeta_n + (1 - 288b_1 e)\zeta_n^{-1}\right], \quad n = 1, 2, 3, \tag{E.11}$$

and

$$\zeta_n = (-1)^{(2/3)(n-1)}\left[1 - 432b_1 e - 7776e^2 + \sqrt{(1 - 432b_1 e - 7776e^2)^2 - (1 - 288b_1 e)^3}\right]^{1/3}, \tag{E.12}$$

a function of b_1 only. In Fig. E.1 we illustrate the real-valued coefficients c_n in the range of parameters $-2 \le b_1 \le 2$. Note that there is a "critical" value of $b_1 \approx 0.552$ above which all values of c_n are real – this has interesting implications as we show below.

As in Appendix. E.1, we finally obtain

$$\begin{aligned} w_n = \pm &\frac{2i\,(-\hat{c}_n)^{\frac{3}{2}-\beta\delta}}{3\sqrt{3}} \\ &\times \left\{1 + \left[\frac{1}{24}\left(7 + \pi^2 - 8\lambda + \ln\frac{\varepsilon^2}{c_n^2} - 8b_1(1 + 2b_1)\right) - \frac{3}{8c_n^2} - \frac{b_1}{c_n} + \frac{2ec_n}{3}\right]\varepsilon^2 + \mathcal{O}(\varepsilon^3)\right\}, \end{aligned} \tag{E.13}$$

where we keep terms up to $\mathcal{O}(\varepsilon^2)$ to compare with Eq. (4.83) and Eq. (E.3). It is clear that the $\mathcal{O}(\varepsilon^2)$ term of the absolute value is modified by the term with parameter e, which appears at $\mathcal{O}(\varepsilon^3)$ in the extended $h(\theta)$ (see Eq. (E.5)). However, the additional corrections to the absolute value do not affect the *phases* of the corresponding singularities in the complex w plane.

The above results lead to the following picture, which depends on the parameter b_1: If $b_1 \gtrsim 0.552$, two points w_1 and w_3 are imaginary and thus distribute along the Lee-Yang cut, while another point is located on the Langer cut, i.e., $\hat{w}_2 = \pm i(-1)^{3/2-\beta\delta}$. At $b_1 \approx 0.552$ the two zeros w_1 and w_3 collide and move off the imaginary axis, into the complex w plane, while w_2 remains on the Langer cut. On the other hand, from Eq. (E.10), we also obtain a pole, θ_0^2, determined by the same equation as Eq. (4.87), albeit with the critical exponent β expanded to order ε^3. Thus, this pole is displaced from the imaginary axis and located along the Langer cut, i.e., $\hat{w}_0 = \pm i(-1)^{3/2-\beta\delta}$ (see Fig. E.2).

Summarizing, it appears that the free parameters b_1, b_2, and b_3 can be chosen in such a way that the zeros and poles of the inverse isothermal susceptibility $F'(z)$ align either on the Lee-Yang and/or the Langer cut. If $b_1 \gtrsim 0.552$, there are always singular points located on the Lee-Yang cut, which we might identify with the Lee-Yang edge singularities. This observation supports our earlier suspicion on the nature of rational approximations of functions with a branch cut.

Appendix F

Copyright Statements

All reproduction of part of my previous publications in this dissertation is in accordance with the copyright policies of the corresponding publishers.

APS

Reuse and Permissions

It is not necessary to obtain permission to reuse this article or its components as it is available under the terms of the Creative Commons Attribution 4.0 International license. This license permits unrestricted use, distribution, and reproduction in any medium, provided attribution to the author(s) and the published article's title, journal citation, and DOI are maintained. Please note that some figures may have been included with permission from other third parties. It is your responsibility to obtain the proper permission from the rights holder directly for these figures.

Springer and SISSA

Open Access and Copyright Terms

Present-day scientific publishing operates with various legal and financial models. JHEP is presently an open access journal, fully sponsored by the consortium SCOAP3 and published by Springer. Articles are distributed under the creative commons license CC-BY 4.0 which permits any use, distribution, and reproduction in any medium, provided the original author(s) and source are credited. In this sense copyright is retained by the authors by default.

IOP and SISSA

Author Rights

1 IOP and SISSA Medialab Srl grant the Named Authors the rights specified in 2 and 3. All such rights must be exercised for non-commercial purposes, if possible should display citation information and IOP's copyright notice, and for electronic use best efforts must be made to include a link to the on-line abstract in the Journal. Exercise of the rights in 3 additionally must not use the final published IOP format but the Named Author's own format (which may include amendments made following peer review).

2 The rights are:

2.1 To make copies of the Article (all or part) for teaching purposes;

2.2 To include the Article (all or part) in a research thesis or dissertation;

2.3 To make oral presentation of the Article (all or part) and to include a summary and/or highlights of it in papers distributed at such presentations or in conference proceedings; and

2.4 All proprietary rights other than copyright.

3 The additional rights are to:

3.1 Use the Article (all or part) without modification in personal compilations or publications of a Named Author's own works (provided not created by third party publisher);

3.2 Include the Article (all or part) on a Named Author's own personal web site;

3.3 Include the Article (all or part) on web sites of the Institution (including its repository) where a Named Author worked when research for the Article was carried out; and

3.4 No sooner than 12 months after publication to include the Article (all or part) on third party web sites including e-print servers, but not on other publisher's web sites.

Bibliography

[1] Xin An et al. “Relativistic Hydrodynamic Fluctuations”. In: *Phys. Rev. C* 100.2 (2019), p. 024910. DOI: `10.1103/PhysRevC.100.024910`. arXiv: `1902.09517 [hep-th]`.

[2] Xin An et al. “Fluctuation dynamics in a relativistic fluid with a critical point”. In: (2019). arXiv: `1912.13456 [hep-th]`.

[3] Xin An. “Relativistic Dynamics of Fluctuations and QCD Critical Point”. In: *28th International Conference on Ultrarelativistic Nucleus-Nucleus Collisions*. Mar. 2020. arXiv: `2003.02828 [hep-th]`.

[4] X. An, D. Mesterházy, and M. A. Stephanov. “Functional renormalization group approach to the Yang-Lee edge singularity”. In: *JHEP* 07 (2016), p. 041. DOI: `10.1007/JHEP07(2016)041`. arXiv: `1605.06039 [hep-th]`.

[5] X An, D Mesterházy, and M A Stephanov. “On spinodal points and Lee-Yang edge singularities”. In: *Journal of Statistical Mechanics: Theory and Experiment* 2018.3 (2018), p. 033207. ISSN: 1742-5468. DOI: `10.1088/1742-5468/aaac4a`. arXiv: `1707.06447 [hep-th]`. URL: `http://dx.doi.org/10.1088/1742-5468/aaac4a`.

[6] X. An, D. Mesterházy, and M. A. Stephanov. “Critical fluctuations and complex spinodal points”. In: *PoS* CPOD2017 (2018), p. 040. DOI: `10.22323/1.311.0040`.

[7] David J. Gross and Frank Wilczek. “Ultraviolet Behavior of Non-Abelian Gauge Theories”. In: *Phys. Rev. Lett.* 30 (26 1973), pp. 1343–1346. DOI: `10.1103/PhysRevLett.30.1343`. URL: `https://link.aps.org/doi/10.1103/PhysRevLett.30.1343`.

[8] H. David Politzer. "Reliable Perturbative Results for Strong Interactions?" In: *Phys. Rev. Lett.* 30 (26 1973), pp. 1346–1349. DOI: 10.1103/PhysRevLett.30.1346. URL: https://link.aps.org/doi/10.1103/PhysRevLett.30.1346.

[9] H. Fritzsch, M. Gell-Mann, and H. Leutwyler. "Advantages of the color octet gluon picture". In: *Physics Letters B* 47.4 (1973), pp. 365 –368. ISSN: 0370-2693. DOI: https://doi.org/10.1016/0370-2693(73)90625-4. URL: http://www.sciencedirect.com/science/article/pii/0370269373906254.

[10] Misha A. Stephanov, K. Rajagopal, and Edward V. Shuryak. "Signatures of the tricritical point in QCD". In: *Phys. Rev. Lett.* 81 (1998), p. 4816. DOI: 10.1103/PhysRevLett.81.4816. arXiv: hep-ph/9806219.

[11] Mikhail A. Stephanov. "QCD phase diagram and the critical point". In: *Prog. Theor. Phys. Suppl.* 153 (2004). [*Int. J. Mod. Phys. A* **20** (2005) 4387], p. 139. DOI: 10.1142/S0217751X05027965. arXiv: hep-ph/0402115.

[12] Kenji Fukushima and Tetsuo Hatsuda. "The phase diagram of dense QCD". In: *Reports on Progress in Physics* 74.1 (2010), p. 014001. ISSN: 1361-6633. DOI: 10.1088/0034-4885/74/1/014001. URL: http://dx.doi.org/10.1088/0034-4885/74/1/014001.

[13] M. A. Stephanov and Y. Yin. "Chiral Kinetic Theory". In: *Physical Review Letters* 109.16 (2012). ISSN: 1079-7114. DOI: 10.1103/physrevlett.109.162001. URL: http://dx.doi.org/10.1103/PhysRevLett.109.162001.

[14] Allan Adams et al. "Strongly correlated quantum fluids: ultracold quantum gases, quantum chromodynamic plasmas and holographic duality". In: *New Journal of Physics* 14.11 (2012), p. 115009. ISSN: 1367-2630. DOI: 10.1088/1367-2630/14/11/115009. URL: http://dx.doi.org/10.1088/1367-2630/14/11/115009.

[15] Alberto Cortijo et al. "Strain-induced chiral magnetic effect in Weyl semimetals". In: *Physical Review B* 94.24 (2016). ISSN: 2469-9969. DOI: 10.1103/physrevb.94.241405. URL: http://dx.doi.org/10.1103/PhysRevB.94.241405.

[16] O. K. Baker and D. E. Kharzeev. "Thermal radiation and entanglement in proton-proton collisions at energies available at the CERN Large Hadron Collider". In: *Physical Review D* 98.5 (2018). ISSN: 2470-0029. DOI: 10.1103/physrevd.98.054007. URL: http://dx.doi.org/10.1103/PhysRevD.98.054007.

[17] Ofer Aharony et al. "Large N field theories, string theory and gravity". In: *Physics Reports* 323.3-4 (2000), 183–386. ISSN: 0370-1573. DOI: 10.1016/s0370-1573(99)00083-6. URL: http://dx.doi.org/10.1016/S0370-1573(99)00083-6.

[18] Dam T. Son and Andrei O. Starinets. "Viscosity, Black Holes, and Quantum Field Theory". In: *Annual Review of Nuclear and Particle Science* 57.1 (2007), 95–118. ISSN: 1545-4134. DOI: 10.1146/annurev.nucl.57.090506.123120. URL: http://dx.doi.org/10.1146/annurev.nucl.57.090506.123120.

[19] Makoto Natsuume. *String theory and quark-gluon plasma*. 2007. arXiv: hep-ph/0701201 [hep-ph].

[20] Steven S. Gubser. "Using string theory to study the quark-gluon plasma: progress and perils". In: *Nuclear Physics A* 830.1-4 (2009), 657c–664c. ISSN: 0375-9474. DOI: 10.1016/j.nuclphysa.2009.10.115. URL: http://dx.doi.org/10.1016/j.nuclphysa.2009.10.115.

[21] Michael Schirber. "Standard Bearer". In: *Physics* 11 (134 2018). URL: https://physics.aps.org/articles/v11/134.

[22] Charles Cagniard de la Tour. In: *Annales de chimie et de physique* 24 (1822), pp. 127–132.

[23] Van der Waals. "Over de Continuiteit van den Gas- en Vloeistoftoestand (on the continuity of the gas and liquid state)". PhD thesis. University of Leiden, 1873.

[24] E. Ising. “Beitrag zur Theorie des Ferromagnetismus (Contribution to the Theory of Ferromagnetism)”. In: *Z. Physik* 31 (253–258). DOI: `https://doi.org/10.1007/BF02980577`.

[25] L. Onsager. “Crystal statistics. I. A two-dimensional model with an order-disorder transition”. In: *Phys. Rev.* 65 (1944), p. 117. DOI: `10.1103/PhysRev.65.117`.

[26] L.D. Landau. “On the Theory of Phase Transitions”. In: *Zh. Eksp. Teor. Fiz.* 7 (1937), pp. 19–32.

[27] Leo P. Kadanoff. “Scaling laws for ising models near T_c”. In: *Physics Physique Fizika* 2 (6 1966), pp. 263–272. DOI: `10.1103/PhysicsPhysiqueFizika.2.263`. URL: `https://link.aps.org/doi/10.1103/PhysicsPhysiqueFizika.2.263`.

[28] Kenneth G. Wilson. “Renormalization Group and Critical Phenomena. I. Renormalization Group and the Kadanoff Scaling Picture”. In: *Phys. Rev. B* 4 (9 1971), pp. 3174–3183. DOI: `10.1103/PhysRevB.4.3174`. URL: `https://link.aps.org/doi/10.1103/PhysRevB.4.3174`.

[29] Kenneth G. Wilson. “Renormalization Group and Critical Phenomena. II. Phase-Space Cell Analysis of Critical Behavior”. In: *Phys. Rev. B* 4 (9 1971), pp. 3184–3205. DOI: `10.1103/PhysRevB.4.3184`. URL: `https://link.aps.org/doi/10.1103/PhysRevB.4.3184`.

[30] Kenneth G. Wilson and Michael E. Fisher. “Critical exponents in 3.99 dimensions”. In: *Phys. Rev. Lett.* 28 (1972), p. 240. DOI: `10.1103/PhysRevLett.28.240`.

[31] A. Pelissetto and E. Vicari. “Critical phenomena and renormalization group theory”. In: *Phys. Rep.* 368 (2002), p. 549. DOI: `10.1016/S0370-1573(02)00219-3`. arXiv: `cond-mat/0012164`.

[32] K. Rummukainen et al. “The universality class of the electroweak theory”. In: *Nucl. Phys. B* 532 (1998), p. 283. DOI: `10.1016/S0550-3213(98)00494-5`. arXiv: `hep-lat/9805013`.

[33] Edward Shuryak. “Strongly coupled quark-gluon plasma in heavy ion collisions”. In: *Reviews of Modern Physics* 89.3 (2017). ISSN: 1539-0756. DOI: `10.1103/revmodphys.89.035001`. URL: `http://dx.doi.org/10.1103/RevModPhys.89.035001`.

[34] Masayuki Asakawa and Masakiyo Kitazawa. “Fluctuations of conserved charges in relativistic heavy ion collisions: An introduction”. In: *Progress in Particle and Nuclear Physics* 90 (2016), 299–342. ISSN: 0146-6410. DOI: `10.1016/j.ppnp.2016.04.002`. URL: `http://dx.doi.org/10.1016/j.ppnp.2016.04.002`.

[35] Miki Sakaida et al. “Dynamical evolution of critical fluctuations and its observation in heavy ion collisions”. In: *Physical Review C* 95.6 (2017). ISSN: 2469-9993. DOI: `10.1103/physrevc.95.064905`. URL: `http://dx.doi.org/10.1103/PhysRevC.95.064905`.

[36] Marlene Nahrgang et al. “Diffusive dynamics of critical fluctuations near the QCD critical point”. In: *Physical Review D* 99.11 (2019). ISSN: 2470-0029. DOI: `10.1103/physrevd.99.116015`. URL: `http://dx.doi.org/10.1103/PhysRevD.99.116015`.

[37] Xinyi Chen-Lin, Luca V. Delacrétaz, and Sean A. Hartnoll. “Theory of Diffusive Fluctuations”. In: *Phys. Rev. Lett.* 122 (9 2019), p. 091602. DOI: `10.1103/PhysRevLett.122.091602`. URL: `https://link.aps.org/doi/10.1103/PhysRevLett.122.091602`.

[38] D. T. Son and M. A. Stephanov. “Dynamic universality class of the QCD critical point”. In: *Phys. Rev. D* 70 (2004), p. 056001. DOI: `10.1103/PhysRevD.70.056001`. arXiv: `hep-ph/0401052`.

[39] M. Stephanov and Y. Yin. “Hydrodynamics with parametric slowing down and fluctuations near the critical point”. In: *Phys. Rev. D* 98 (3 2018), p. 036006. DOI: `10.1103/PhysRevD.98.036006`.

[40] Yukinao Akamatsu et al. “Transits of the QCD critical point”. In: *Phys. Rev. C* 100.4 (2019), p. 044901. DOI: `10.1103/PhysRevC.100.044901`. arXiv: `1811.05081 [nucl-th]`.

[41] Krishna Rajagopal et al. “Hydro+ in Action: Understanding the Out-of-Equilibrium Dynamics Near a Critical Point in the QCD Phase Diagram”. In: (2019). arXiv: `1908.08539 [hep-ph]`.

[42] Lipei Du et al. “Fluctuation dynamics near the QCD critical point”. In: (Apr. 2020). arXiv: `2004.02719 [nucl-th]`.

[43] J. I. Kapusta, B. Muller, and M. Stephanov. “Relativistic Theory of Hydrodynamic Fluctuations with Applications to Heavy Ion Collisions”. In: *Phys. Rev. C* 85 (2012), p. 054906. DOI: `10.1103/PhysRevC.85.054906`. arXiv: `1112.6405 [nucl-th]`.

[44] Joseph I. Kapusta and Juan M. Torres-Rincon. “Thermal Conductivity and Chiral Critical Point in Heavy Ion Collisions”. In: *Phys. Rev. C* 86 (2012), p. 054911. DOI: `10.1103/PhysRevC.86.054911`. arXiv: `1209.0675 [nucl-th]`.

[45] C. Young et al. “Thermally Fluctuating Second-Order Viscous Hydrodynamics and Heavy-Ion Collisions”. In: *Phys. Rev. C* 91.4 (2015), p. 044901. DOI: `10.1103/PhysRevC.91.044901`. arXiv: `1407.1077 [nucl-th]`.

[46] Mayank Singh et al. “Hydrodynamic Fluctuations in Relativistic Heavy-Ion Collisions”. In: *Nucl. Phys. A* 982 (2019). Ed. by Federico Antinori et al., pp. 319–322. DOI: `10.1016/j.nuclphysa.2018.10.061`. arXiv: `1807.05451 [nucl-th]`.

[47] AF Andreev. “Corrections to the hydrodynamics of liquids”. In: *Zh. Ehksp. Teor. Fiz.* 75.3 (1978), pp. 1132–1139.

[48] Yukinao Akamatsu, Aleksas Mazeliauskas, and Derek Teaney. “Kinetic regime of hydrodynamic fluctuations and long time tails for a Bjorken expansion”. In: *Phys. Rev. C* 95 (1 2017), p. 014909. DOI: `10.1103/PhysRevC.95.014909`.

[49] Yukinao Akamatsu, Aleksas Mazeliauskas, and Derek Teaney. "Bulk viscosity from hydrodynamic fluctuations with relativistic hydrokinetic theory". In: *Phys. Rev. C* 97 (2 2018), p. 024902. DOI: `10.1103/PhysRevC.97.024902`.

[50] M. Martinez and Thomas Schäfer. "Stochastic hydrodynamics and long time tails of an expanding conformal charged fluid". In: *Phys. Rev. C* 99.5 (2019), p. 054902. DOI: `10.1103/PhysRevC.99.054902`. arXiv: `1812.05279 [hep-th]`.

[51] C.-N. Yang and T. D. Lee. "Statistical theory of equations of state and phase transitions. I. Theory of condensation". In: *Phys. Rev.* 87 (1952), p. 404. DOI: `10.1103/PhysRev.87.404`.

[52] T. D. Lee and C.-N. Yang. "Statistical theory of equations of state and phase transitions. II. Lattice gas and Ising model". In: *Phys. Rev.* 87 (1952), p. 410. DOI: `10.1103/PhysRev.87.410`.

[53] J. E. Kirkham and D. J. Wallace. "Comments on the field-theoretic formulation of the Yang-Lee edge singularity". In: *J. Phys. A: Math. Gen.* 12 (1979), p. L47. DOI: `10.1088/0305-4470/12/2/001`.

[54] Jeffrey Goldstone, Abdus Salam, and Steven Weinberg. "Broken Symmetries". In: *Phys. Rev.* 127 (3 1962), pp. 965–970. DOI: `10.1103/PhysRev.127.965`. URL: `https://link.aps.org/doi/10.1103/PhysRev.127.965`.

[55] Cecile DeWitt and Bryce DeWitt. *Relativity, Groups and Topology*. 1964.

[56] Erick J. Weinberg and Aiqun Wu. "Understanding complex perturbative effective potentials". In: *Phys. Rev. D* 36 (8 1987), p. 2474. DOI: `10.1103/PhysRevD.36.2474`.

[57] Sidney Coleman. *Aspects of Symmetry: Selected Erice Lectures*. Cambridge, U.K.: Cambridge University Press, 1985. ISBN: 978-0-521-31827-3. DOI: `10.1017/CBO9780511565045`.

[58] L.V. Keldysh. "Diagram technique for nonequilibrium processes". In: *Zh. Eksp. Teor. Fiz.* 47 (1964), pp. 1515–1527.

[59] Pavel Kovtun. "Lectures on hydrodynamic fluctuations in relativistic theories". In: *Journal of Physics A: Mathematical and Theoretical* 45.47 (2012), p. 473001. ISSN: 1751-8121. DOI: `10.1088/1751-8113/45/47/473001`. URL: `http://dx.doi.org/10.1088/1751-8113/45/47/473001`.

[60] Tomoya Hayata et al. "Relativistic hydrodynamics from quantum field theory on the basis of the generalized Gibbs ensemble method". In: *Phys. Rev. D* 92.6 (2015), p. 065008. DOI: `10.1103/PhysRevD.92.065008`. arXiv: `1503.04535 [hep-ph]`.

[61] Paolo Glorioso and Hong Liu. *Lectures on non-equilibrium effective field theories and fluctuating hydrodynamics*. 2018. arXiv: `1805.09331 [hep-th]`.

[62] M. Combescot, M. Droz, and J. M. Kosterlitz. "Two point correlation function for general fields and temperatures in the critical region". In: *Phys. Rev. B* 11 (11 1975), pp. 4661–4673. DOI: `10.1103/PhysRevB.11.4661`. URL: `https://link.aps.org/doi/10.1103/PhysRevB.11.4661`.

[63] M. A. Stephanov. "Non-Gaussian fluctuations near the QCD critical point". In: *Phys. Rev. Lett.* 102 (2009), p. 032301. DOI: `10.1103/PhysRevLett.102.032301`. arXiv: `0809.3450 [hep-ph]`.

[64] Adam Bzdak et al. "Mapping the Phases of Quantum Chromodynamics with Beam Energy Scan". In: (2019). arXiv: `1906.00936 [nucl-th]`.

[65] Xin An et al. "Working in progress". In: (2020).

[66] P. C. Hohenberg and B. I. Halperin. "Theory of dynamic critical phenomena". In: *Rev. Mod. Phys.* 49 (3 1977), pp. 435–479. DOI: `10.1103/RevModPhys.49.435`.

[67] P. C. Hohenberg and B. I. Halperin. "Theory of Dynamic Critical Phenomena". In: *Rev. Mod. Phys.* 49 (1977), p. 435.

[68] Ani Aprahamian et al. "Reaching for the horizon: The 2015 long range plan for nuclear science". In: (Oct. 2015).

[69] Frank R. Brown et al. “On the existence of a phase transition for QCD with three light quarks”. In: *Phys. Rev. Lett.* 65 (20 1990), pp. 2491–2494. DOI: `10.1103/PhysRevLett.65.2491`. URL: `https://link.aps.org/doi/10.1103/PhysRevLett.65.2491`.

[70] Robert D. Pisarski and Frank Wilczek. “Remarks on the Chiral Phase Transition in Chromodynamics”. In: *Phys. Rev. D* 29 (1984), p. 338. DOI: `10.1103/PhysRevD.29.338`.

[71] P. Schofield. “Parametric representation of the equation of state near a critical point”. In: *Phys. Rev. Lett.* 22 (1969), p. 606. DOI: `10.1103/PhysRevLett.22.606`.

[72] P. Schofield. “ε-expansion of the parametric equation of state near the critical point”. In: *Phys. Lett. A* 46 (1973), p. 197. DOI: `10.1016/0375-9601(73)90132-1`.

[73] R. Guida and J. Zinn-Justin. “3D Ising model: The scaling equation of state”. In: *Nucl. Phys. B* 489 (1997), p. 626. DOI: `10.1016/S0550-3213(96)00704-3`. arXiv: `hep-th/9610223`.

[74] Paolo Parotto et al. “QCD equation of state matched to lattice data and exhibiting a critical point singularity”. In: *Physical Review C* 101.3 (2020). ISSN: 2469-9993. DOI: `10.1103/physrevc.101.034901`. URL: `http://dx.doi.org/10.1103/PhysRevC.101.034901`.

[75] Maneesha Sushama Pradeep and Mikhail Stephanov. “Universality of the critical point mapping between Ising model and QCD at small quark mass”. In: *Phys. Rev. D* 100.5 (2019), p. 056003. DOI: `10.1103/PhysRevD.100.056003`. arXiv: `1905.13247 [hep-ph]`.

[76] Swagato Mukherjee, Raju Venugopalan, and Yi Yin. “Real-time evolution of non-Gaussian cumulants in the QCD critical regime”. In: *Phys. Rev. C* 92 (3 2015), p. 034912. DOI: `10.1103/PhysRevC.92.034912`. URL: `https://link.aps.org/doi/10.1103/PhysRevC.92.034912`.

[77] M. Stephanov. “Thermal fluctuations in the interacting pion gas”. In: *Physical Review D* 65.9 (2002). ISSN: 1089-4918. DOI: 10.1103/physrevd.65.096008. URL: http://dx.doi.org/10.1103/PhysRevD.65.096008.

[78] Bo Ling and Mikhail A. Stephanov. “Acceptance dependence of fluctuation measures near the QCD critical point”. In: *Phys. Rev. C* 93.3 (2016), p. 034915. DOI: 10.1103/PhysRevC.93.034915. arXiv: 1512.09125 [nucl-th].

[79] Raimond Snellings. “Collective expansion at the LHC: selected ALICE anisotropic flow measurements”. In: *Journal of Physics G: Nuclear and Particle Physics* 41.12 (2014), p. 124007. ISSN: 1361-6471. DOI: 10.1088/0954-3899/41/12/124007. URL: http://dx.doi.org/10.1088/0954-3899/41/12/124007.

[80] L. Adamczyk et al. “Beam-Energy Dependence of the Directed Flow of Protons, Antiprotons, and Pions in Au+Au Collisions”. In: *Physical Review Letters* 112.16 (2014). ISSN: 1079-7114. DOI: 10.1103/physrevlett.112.162301. arXiv: 1401.3043 [nucl-ex]. URL: http://dx.doi.org/10.1103/PhysRevLett.112.162301.

[81] Leszek Adamczyk et al. “Beam-Energy Dependence of Directed Flow of Λ, $\bar{\Lambda}$, $K^{\pm}$, K_s^0 and ϕ in Au+Au Collisions”. In: *Phys. Rev. Lett.* 120.6 (2018), p. 062301. DOI: 10.1103/PhysRevLett.120.062301. arXiv: 1708.07132 [hep-ex].

[82] Jochen Thäder. “Higher Moments of Net-Particle Multiplicity Distributions”. In: *Nucl. Phys. A* 956 (2016). Ed. by Y. Akiba et al., pp. 320–323. DOI: 10.1016/j.nuclphysa.2016.02.047. arXiv: 1601.00951 [nucl-ex].

[83] M. M. Aggarwal et al. “Higher Moments of Net Proton Multiplicity Distributions at RHIC”. In: *Physical Review Letters* 105.2 (2010). ISSN: 1079-7114. DOI: 10.1103/physrevlett.105.022302. URL: http://dx.doi.org/10.1103/PhysRevLett.105.022302.

[84] Xiaofeng Luo. *Energy Dependence of Moments of Net-Proton and Net-Charge Multiplicity Distributions at STAR*. 2015. arXiv: 1503.02558 [nucl-ex].

[85] J. Cleymans et al. "Comparison of chemical freeze-out criteria in heavy-ion collisions". In: *Physical Review C* 73.3 (2006). ISSN: 1089-490X. DOI: `10.1103/physrevc.73.034905`. URL: `http://dx.doi.org/10.1103/PhysRevC.73.034905`.

[86] M A Stephanov. "QCD critical point and event-by-event fluctuations". In: *Journal of Physics G: Nuclear and Particle Physics* 38.12 (2011), p. 124147. DOI: `10.1088/0954-3899/38/12/124147`. URL: `https://doi.org/10.1088%2F0954-3899%2F38%2F12%2F124147`.

[87] T. Csorgo et al. "Bose-Einstein or HBT correlation signature of a second order QCD phase transition". In: *AIP Conf. Proc.* 828.1 (2006). Ed. by Vladislav Simak et al., pp. 525–532. DOI: `10.1063/1.2197465`. arXiv: `nucl-th/0512060`.

[88] N. G. Antoniou et al. "Critical Opalescence in Baryonic QCD Matter". In: *Physical Review Letters* 97.3 (2006). ISSN: 1079-7114. DOI: `10.1103/physrevlett.97.032002`. URL: `http://dx.doi.org/10.1103/PhysRevLett.97.032002`.

[89] Kai-Jia Sun et al. "Probing QCD critical fluctuations from light nuclei production in relativistic heavy-ion collisions". In: *Phys. Lett. B* 774 (2017), pp. 103–107. DOI: `10.1016/j.physletb.2017.09.056`. arXiv: `1702.07620 [nucl-th]`.

[90] Edward Shuryak and Juan M. Torres-Rincon. *Light-nuclei production and search for the QCD critical point.* 2020. arXiv: `2005.14216 [nucl-th]`.

[91] Jasmine Brewer et al. "Searching for the QCD critical point via the rapidity dependence of cumulants". In: *Physical Review C* 98.6 (2018). ISSN: 2469-9993. DOI: `10.1103/physrevc.98.061901`. URL: `http://dx.doi.org/10.1103/PhysRevC.98.061901`.

[92] B. Alver and G. Roland. "Collision-geometry fluctuations and triangular flow in heavy-ion collisions". In: *Phys. Rev. C* 81 (5 2010), p. 054905. DOI: `10.1103/PhysRevC.81.054905`. URL: `https://link.aps.org/doi/10.1103/PhysRevC.81.054905`.

[93] Larry McLerran and Raju Venugopalan. “Gluon distribution functions for very large nuclei at small transverse momentum”. In: *Physical Review D* 49.7 (1994), 3352–3355. ISSN: 0556-2821. DOI: `10.1103/physrevd.49.3352`. URL: `http://dx.doi.org/10.1103/PhysRevD.49.3352`.

[94] M. M. Aggarwal et al. “An Experimental Exploration of the QCD Phase Diagram: The Search for the Critical Point and the Onset of De-confinement”. In: (2010). arXiv: `1007.2613 [nucl-ex]`.

[95] Misha A. Stephanov, K. Rajagopal, and Edward V. Shuryak. “Event-by-event fluctuations in heavy ion collisions and the QCD critical point”. In: *Phys. Rev. D* 60 (1999), p. 114028. DOI: `10.1103/PhysRevD.60.114028`. arXiv: `hep-ph/9903292`.

[96] Boris Berdnikov and Krishna Rajagopal. “Slowing out-of-equilibrium near the QCD critical point”. In: *Phys. Rev. D* 61 (2000), p. 105017. DOI: `10.1103/PhysRevD.61.105017`. arXiv: `hep-ph/9912274 [hep-ph]`.

[97] AF Andreev. “Two-liquid effects in a normal liquid”. In: *Zh. Ehksp. Teor. Fiz.* 59 (1970), pp. 1819–1827.

[98] L.D. Landau and E.M. Lifshitz. *Statistical Physics, Part 2*. Vol. 9. Course of Theoretical Physics. Elsevier Science, 2013.

[99] L.D. Landau and E.M. Lifshitz. *Fluid Mechanics*. Vol. 6. Course of Theoretical Physics. Elsevier Science, 2013. ISBN: 9781483161044.

[100] Sangyong Jeon and Ulrich Heinz. “Introduction to Hydrodynamics”. In: *Int. J. Mod. Phys. E* 24.10 (2015), p. 1530010. DOI: `10.1142/S0218301315300106`. arXiv: `1503.03931 [hep-ph]`.

[101] Paul Romatschke and Ulrike Romatschke. “Relativistic Fluid Dynamics In and Out of Equilibrium – Ten Years of Progress in Theory and Numerical Simulations of Nuclear Collisions”. In: (2017). arXiv: `1712.05815 [nucl-th]`.

[102] W. Israel and J .M. Stewart. "Transient relativistic thermodynamics and kinetic theory". In: *Annals Phys.* 118 (1979), pp. 341–372.

[103] R. Kubo. "The fluctuation-dissipation theorem". In: *Rep. Prog. Phys.* 29 (1966), p. 255. DOI: `10.1088/0034-4885/29/1/306`.

[104] Leo P Kadanoff and Paul C Martin. "Hydrodynamic equations and correlation functions". In: *Annals of Physics* 24 (1963), pp. 419 –469. ISSN: 0003-4916. DOI: `https://doi.org/10.1016/0003-4916(63)90078-2`. URL: `http://www.sciencedirect.com/science/article/pii/0003491663900782`.

[105] G L Paul and P N Pusey. "Observation of a long-time tail in Brownian motion". In: *Journal of Physics A: Mathematical and General* 14.12 (1981), pp. 3301–3327. DOI: `10.1088/0305-4470/14/12/025`. URL: `https://doi.org/10.1088%2F0305-4470%2F14%2F12%2F025`.

[106] Y Pomeau and P Résibois. "Time dependent correlation functions and mode-mode coupling theories". In: *Physics Reports* 19.2 (1975), pp. 63 –139. ISSN: 0370-1573. DOI: `https://doi.org/10.1016/0370-1573(75)90019-8`. URL: `http://www.sciencedirect.com/science/article/pii/0370157375900198`.

[107] Fábio S. Bemfica, Marcelo M. Disconzi, and Jorge Noronha. "Causality and existence of solutions of relativistic viscous fluid dynamics with gravity". In: *Phys. Rev. D* 98.10 (2018), p. 104064. DOI: `10.1103/PhysRevD.98.104064`. arXiv: `1708.06255 [gr-qc]`.

[108] Fábio S. Bemfica, Marcelo M. Disconzi, and Jorge Noronha. "Nonlinear Causality of General First-Order Relativistic Viscous Hydrodynamics". In: *Phys. Rev. D* 100.10 (2019), p. 104020. DOI: `10.1103/PhysRevD.100.104020`. arXiv: `1907.12695 [gr-qc]`.

[109] Pavel Kovtun. "First-order relativistic hydrodynamics is stable". In: *JHEP* 10 (2019), p. 034. DOI: `10.1007/JHEP10(2019)034`. arXiv: `1907.08191 [hep-th]`.

[110] Robert P. Geroch. “Relativistic theories of dissipative fluids”. In: *J. Math. Phys.* 36 (1995), p. 4226. DOI: 10.1063/1.530958.

[111] Kyozi Kawasaki. “Sound Attenuation and Dispersion near the Liquid-Gas Critical Point”. In: *Phys. Rev. A* 1 (6 1970), pp. 1750–1757. DOI: 10.1103/PhysRevA.1.1750. URL: http://link.aps.org/doi/10.1103/PhysRevA.1.1750.

[112] Akira Onuki. “Dynamic equations and bulk viscosity near the gas-liquid critical point”. In: *Phys. Rev. E* 55 (1 1997), pp. 403–420. DOI: 10.1103/PhysRevE.55.403. URL: http://link.aps.org/doi/10.1103/PhysRevE.55.403.

[113] Y. Hatta and M. A. Stephanov. “Proton number fluctuation as a signal of the QCD critical endpoint”. In: *Phys. Rev. Lett.* 91 (2003). [Erratum: Phys. Rev. Lett.91,129901(2003)], p. 102003. DOI: 10.1103/PhysRevLett.91.102003, 10.1103/PhysRevLett.91.129901. arXiv: hep-ph/0302002 [hep-ph].

[114] R. Abe. “Note on the Critical Behavior of Ising Ferromagnets”. In: *Prog. Theor. Phys.* 38 (1967), p. 72. DOI: 10.1143/PTP.38.72.

[115] M. Suzuki. “A Theory of the Second Order Phase Transitions in Spin Systems. II: Complex Magnetic Field”. In: *Prog. Theor. Phys.* 38 (1967), p. 1225. DOI: 10.1143/PTP.38.1225.

[116] P. J. Kortman and R. B. Griffiths. “Density of Zeros on the Lee-Yang Circle for Two Ising Ferromagnets”. In: *Phys. Rev. Lett.* 27 (1971), p. 1439. DOI: 10.1103/PhysRevLett.27.1439.

[117] C. Itzykson, R. B. Pearson, and J. B. Zuber. “Distribution of zeros in Ising and gauge models”. In: *Nucl. Phys. B* 220 (1983), p. 415. DOI: 10.1016/0550-3213(83)90499-6.

[118] Ch. Binek. “Density of Zeros on the Lee-Yang Circle Obtained from Magnetization Data of a Two-Dimensional Ising Ferromagnet”. In: *Phys. Rev. Lett.* 81 (1998),

p. 5644. DOI: 10.1103/PhysRevLett.81.5644. URL: http://link.aps.org/doi/10.1103/PhysRevLett.81.5644.

[119] Ch. Binek, W. Kleemann, and H. Aruga Katori. "Yang-Lee edge singularities determined from experimental high-field magnetization data". In: *J. Phys.: Condens. Matter* 13 (2001), p. L811. URL: http://stacks.iop.org/0953-8984/13/i=35/a=103.

[120] X. Peng et al. "Experimental Observation of Lee-Yang Zeros". In: *Phys. Rev. Lett.* 114 (2015), p. 010601. DOI: 10.1103/PhysRevLett.114.010601.

[121] A. M. Halász, A. D. Jackson, and J. J. M. Verbaarschot. "Yang-Lee zeros of a random matrix model for QCD at finite density". In: *Phys. Lett. B* 395 (1997), p. 293. DOI: 10.1016/S0370-2693(97)00015-4. arXiv: hep-lat/9611008.

[122] S. Ejiri. "Lee-Yang zero analysis for the study of QCD phase structure". In: *Phys. Rev. D* 73 (2006), p. 054502. DOI: 10.1103/PhysRevD.73.054502. arXiv: hep-lat/0506023.

[123] M. A. Stephanov. "QCD critical point and complex chemical potential singularities". In: *Phys. Rev. D* 73 (2006), p. 094508. DOI: 10.1103/PhysRevD.73.094508. arXiv: hep-lat/0603014.

[124] T. Asano. "Generalized Lee-Yang's Theorem". In: *J. Phys. Soc. Jpn.* 25 (1968), p. 1220. DOI: 10.1143/JPSJ.25.1220.

[125] T. Asano. "Generalization of the Lee-Yang Theorem". In: *Prog. Theor. Phys.* 40 (1968), p. 1328. DOI: 10.1143/PTP.40.1328.

[126] C. Kawabata et al. "Zeros of the partition function for the Ising model with higher spin". In: *Phys. Lett. A* 28 (1968), p. 113. DOI: 10.1016/0375-9601(68)90418-0.

[127] M. Suzuki. "Theorems on the Ising Model with General Spin and Phase Transition". In: *J. Math. Phys.* 9 (1968), p. 2064. DOI: 10.1063/1.1664546.

[128] R. B. Griffiths. "Rigorous Results for Ising Ferromagnets of Arbitrary Spin". In: *J. Math. Phys.* 10 (1969), p. 1559. DOI: 10.1063/1.1665005.

[129] M. Suzuki and M.E. Fisher. “Zeros of the Partition Function for the Heisenberg, Ferroelectric, and General Ising Models”. In: *J. Math. Phys.* 12 (1971), p. 235. DOI: 10.1063/1.1665583.

[130] D. Ruelle. “Some remarks on the location of zeroes of the partition function for lattice systems”. In: *Comm. Math. Phys.* 31 (1973), p. 265. DOI: 10.1007/BF01646488.

[131] J. L. Lebowitz, D. Ruelle, and E. R. Speer. “Location of the Lee-Yang zeros and absence of phase transitions in some Ising spin systems”. In: *J. Math. Phys.* 53, 095211 (2012), p. 095211. DOI: 10.1063/1.4738622.

[132] M.E. Fisher. “Yang-Lee edge singularity and ϕ^3 field theory”. In: *Phys. Rev. Lett.* 40 (1978), p. 1610. DOI: 10.1103/PhysRevLett.40.1610.

[133] D.A. Kurtze and M.E. Fisher. “Yang-Lee edge singularities at high temperatures”. In: *Phys. Rev. B* 20 (1979), p. 2785. DOI: 10.1103/PhysRevB.20.2785.

[134] John L. Cardy. “Conformal invariance and the Yang-Lee edge singularity in two dimensions”. In: *Phys. Rev. Lett.* 54 (1985), p. 1354. DOI: 10.1103/PhysRevLett.54.1354.

[135] G. A. Baker et al. “Yang-Lee edge for the two-dimensional Ising model”. In: *Phys. Rev. B* 33 (1986), p. 3187. DOI: 10.1103/PhysRevB.33.3187.

[136] S.-Y. Kim. “Density of Yang-Lee zeros for the Ising ferromagnet”. In: *Phys. Rev. E* 74 (2006), p. 011119. DOI: 10.1103/PhysRevE.74.011119. arXiv: cond-mat/0607257.

[137] O. F. de Alcantara Bonfim, J. E. Kirkham, and A. J. McKane. “Critical exponents to order ε^3 for ϕ^3 models of critical phenomena in $6-\varepsilon$-dimensions”. In: *J. Phys. A* 13 (1980). [Erratum: *J. Phys. A* **13** (1980) 3785], p. L247. DOI: 10.1088/0305-4470/13/7/006.

[138] O. F. de Alcantara Bonfim, J. E. Kirkham, and A. J. McKane. “Critical exponents for the percolation problem and the Yang-lee edge singularity”. In: *J. Phys. A* 14 (1981), p. 2391. DOI: 10.1088/0305-4470/14/9/034.

[139] J. A. Gracey. “Four loop renormalization of ϕ^3 theory in six dimensions”. In: *Phys. Rev. D* 92 (2015), p. 025012. DOI: `10.1103/PhysRevD.92.025012`. arXiv: `1506.03357 [hep-th]`.

[140] P. Butera and M. Pernici. “Yang-Lee edge singularities from extended activity expansions of the dimer density for bipartite lattices of dimensionality $2 \leq d \leq 7$”. In: *Phys. Rev. E* 86 (2012), p. 011104. DOI: `10.1103/PhysRevE.86.011104`. arXiv: `1206.0872 [cond-mat.stat-mech]`.

[141] S.N. Lai and M.E. Fisher. “The universal repulsive-core singularity and Yang-Lee edge criticality”. In: *J. Chem. Phys.* 103 (1995), p. 8144. DOI: `10.1063/1.470178`.

[142] H. P. Hsu, W. Nadler, and P. Grassberger. “Simulations of lattice animals and trees”. In: *J. Phys. A: Math. Gen.* 38 (2005), p. 775. DOI: `10.1088/0305-4470/38/4/001`. arXiv: `cond-mat/0408061`.

[143] Ferdinando Gliozzi and Antonio Rago. “Critical exponents of the 3d Ising and related models from conformal bootstrap”. In: *JHEP* 10 (2014), p. 042. DOI: `10.1007/JHEP10(2014)042`. arXiv: `1403.6003 [hep-th]`.

[144] C. Wetterich. “Average action and the renormalization group equations”. In: *Nucl. Phys. B* 352 (1991), p. 529. DOI: `10.1016/0550-3213(91)90099-J`.

[145] C. Wetterich. “Exact evolution equation for the effective potential”. In: *Phys. Lett. B* 301 (1993), p. 90. DOI: `10.1016/0370-2693(93)90726-X`.

[146] C. Bagnuls and C. Bervillier. “Exact renormalization group equations. An Introductory review”. In: *Phys. Rep.* 348 (2001), p. 91. DOI: `10.1016/S0370-1573(00)00137-X`. arXiv: `hep-th/0002034`.

[147] J. Berges, N. Tetradis, and C. Wetterich. “Nonperturbative renormalization flow in quantum field theory and statistical physics”. In: *Phys. Rep.* 363 (2002), p. 223. DOI: `10.1016/S0370-1573(01)00098-9`. arXiv: `hep-ph/0005122`.

[148] J. Polonyi. “Lectures on the functional renormalization group method”. In: *Central Eur. J. Phys.* 1 (2003), p. 1. DOI: `10.2478/BF02475552`. arXiv: `hep-th/0110026`.

[149] J. M. Pawlowski. “Aspects of the functional renormalisation group”. In: *Annals Phys.* 322 (2007), p. 2831. DOI: `10.1016/j.aop.2007.01.007`. arXiv: `hep-th/0512261`.

[150] B. Delamotte. “An Introduction to the nonperturbative renormalization group”. In: *Lect. Notes Phys.* 852 (2012), p. 49. DOI: `10.1007/978-3-642-27320-9_2`. arXiv: `cond-mat/0702365`.

[151] T. R. Morris. “The Exact renormalization group and approximate solutions”. In: *Int. J. Mod. Phys. A* 9 (1994), p. 2411. DOI: `10.1142/S0217751X94000972`. arXiv: `hep-ph/9308265`.

[152] T. R. Morris. “Derivative expansion of the exact renormalization group”. In: *Phys. Lett. B* 329 (1994), p. 241. DOI: `10.1016/0370-2693(94)90767-6`. arXiv: `hep-ph/9403340`.

[153] C. Wetterich. “The average action for scalar fields near phase transitions”. In: *Z. Phys. C* 57 (1993), p. 451. DOI: `10.1007/BF01474340`.

[154] S. Seide and C. Wetterich. “Equation of state near the endpoint of the critical line”. In: *Nucl. Phys. B* 562 (1999), p. 524. DOI: `10.1016/S0550-3213(99)00545-3`. arXiv: `cond-mat/9806372`.

[155] L. Canet et al. “Nonperturbative renormalization group approach to the Ising model: A Derivative expansion at order ∂^4”. In: *Phys. Rev. B* 68 (2003), p. 064421. DOI: `10.1103/PhysRevB.68.064421`. arXiv: `hep-th/0302227`.

[156] D. F. Litim and D. Zappala. “Ising exponents from the functional renormalisation group”. In: *Phys. Rev. D* 83 (2011), p. 085009. DOI: `10.1103/PhysRevD.83.085009`. arXiv: `1009.1948 [hep-th]`.

[157] A. Pelissetto and E. Vicari. “Critical phenomena and renormalization-group theory”. In: *Phys. Rep.* 368 (2002), p. 549. DOI: `10.1016/S0370-1573(02)00219-3`. arXiv: `cond-mat/0012164`.

[158] A. J. Macfarlane and G. Woo. “Φ^3 Theory in Six-Dimensions and the Renormalization Group”. In: *Nucl. Phys. B* 77 (1974), p. 91. DOI: 10.1016/0550-3213(74)90306-X.

[159] D. F. Litim. “Critical exponents from optimized renormalization group flows”. In: *Nucl. Phys. B* 631 (2002), p. 128. DOI: 10.1016/S0550-3213(02)00186-4. arXiv: hep-th/0203006.

[160] D. F. Litim and L. Vergara. “Subleading critical exponents from the renormalization group”. In: *Phys. Lett. B* 581 (2004), p. 263. DOI: 10.1016/j.physletb.2003.11.047. arXiv: hep-th/0310101.

[161] C. Bervillier, A. Jüttner, and D. F. Litim. “High-accuracy scaling exponents in the local potential approximation”. In: *Nucl. Phys. B* 783 (2007), p. 213. DOI: 10.1016/j.nuclphysb.2007.03.036. arXiv: hep-th/0701172.

[162] D. J. Amit. *Field Theory, the Renormalization Group, and Critical Phenomena.* Singapore: World Scientific, 1984.

[163] D. F. Litim. “Optimization of the exact renormalization group”. In: *Phys. Lett. B* 486 (2000), p. 92. arXiv: hep-th/0005245.

[164] D. F. Litim. “Optimized renormalization group flows”. In: *Phys. Rev. D* 64 (2001), p. 105007. DOI: 10.1103/PhysRevD.64.105007. arXiv: hep-th/0103195.

[165] D. J. Amit, D. J. Wallace, and R. K. P. Zia. “Universality in the percolation problem-Anomalous dimensions of ϕ^4 operators”. In: *Phys. Rev. B* 15 (1977), p. 4657. DOI: 10.1103/PhysRevB.15.4657.

[166] E. Brézin, J. C. Le Guillou, and J. Zinn-Justin. “Field Theoretic Approach to Critical Phenomena”. In: *Phase Transitions and Critical Phenomena. Vol. 6.* Ed. by C. Domb and M. S. Green. London: Academic Press, 1976, pp. 127–244.

[167] Jan M. Pawlowski et al. “Physics and the choice of regulators in functional renormalisation group flows”. In: *Annals Phys.* 384 (2017), pp. 165–197. DOI: 10.1016/j.aop.2017.06.017. arXiv: 1512.03598 [hep-th].

[168] E. Brézin, D. J. Wallace, and K. G. Wilson. “Feynman graph expansion for the equation of state near the critical point (Ising-like case)”. In: *Phys. Rev. Lett.* 29 (1972), p. 591. DOI: `10.1103/PhysRevLett.29.591`.

[169] G. M. Avdeeva and A. A. Migdal. “Equation of state in $(4 - \varepsilon)$-dimensional Ising model”. In: *JETP Lett.* 16 (1972), p. 178.

[170] D. J. Wallace and R. K. P. Zia. “The ε-expansion and parametric models for the Ising equation of state in the critical region”. In: *Phys. Lett. A* 46 (1973), p. 261. DOI: `10.1016/0375-9601(73)90212-0`.

[171] D. J. Wallace and R. K. P. Zia. “Parametric models and the Ising equation of state at order ε^3”. In: *J. Phys. C* 7 (1974), p. 3480. DOI: `10.1088/0022-3719/7/19/008`.

[172] J. F. Nicoll and P. C. Albright. “Crossover functions by renormalization-group matching: Three-loop results”. In: *Phys. Rev. B* 31 (1985), p. 4576. DOI: `10.1103/PhysRevB.31.4576`.

[173] M. Campostrini et al. “Improved high-temperature expansion and critical equation of state of three-dimensional Ising-like systems”. In: *Phys. Rev. E* 60 (1999), p. 3526. DOI: `10.1103/PhysRevE.60.3526`. arXiv: `cond-mat/9905078`.

[174] M. Campostrini et al. “25th-order high-temperature expansion results for three-dimensional Ising-like systems on the simple-cubic lattice”. In: *Phys. Rev. E* 65 (2002), p. 066127. DOI: `10.1103/PhysRevE.65.066127`. arXiv: `cond-mat/0201180`.

[175] M. M. Tsypin. “The universal effective potential for three-dimensional massive scalar field theory from the Monte Carlo study of the Ising model”. In: (1994). arXiv: `hep-lat/9401034`.

[176] M. M. Tsypin. “Universal effective potential for scalar field theory in three-dimensions by Monte Carlo computation”. In: *Phys. Rev. Lett.* 73 (1994), p. 2015. DOI: `10.1103/PhysRevLett.73.2015`.

[177] M. M. Tsypin. “Effective potential for a scalar field in three dimensions: Ising model in the ferromagnetic phase”. In: *Phys. Rev. B* 55 (1997), p. 8911. DOI: `10.1103/PhysRevB.55.8911`. arXiv: `hep-lat/9601021`.

[178] M. Caselle and M. Hasenbusch. “Universal amplitude ratios in the 3D Ising model”. In: *J. Phys. A* 30 (1997), p. 4963. DOI: `10.1088/0305-4470/30/14/010`. arXiv: `hep-lat/9701007`.

[179] M. Hasenbusch, K. Pinn, and S. Vinti. “Critical exponents of the three-dimensional Ising universality class from finite-size scaling with standard and improved actions”. In: *Phys. Rev. B* 59 (1999), p. 11471. DOI: `10.1103/PhysRevB.59.11471`. arXiv: `hep-lat/9806012`.

[180] J. Berges, N. Tetradis, and C. Wetterich. “Critical equation of state from the average action”. In: *Phys. Rev. Lett.* 77 (1996), p. 873. DOI: `10.1103/PhysRevLett.77.873`. arXiv: `hep-th/9507159`.

[181] P. Fonseca and A. Zamolodchikov. “Ising field theory in a magnetic field: Analytic properties of the free energy”. In: *J. Stat. Phys.* 110 (2003), p. 527. arXiv: `hep-th/0112167`.

[182] V. Privman and L.S. Schulman. “Analytic properties of thermodynamic functions at first-order phase transitions”. In: *J. Phys. A* 15 (1982), p. L231. DOI: `10.1088/0305-4470/15/5/004`.

[183] O. Penrose. “Metastable decay rates, asymptotic expansions, and analytic continuation of thermodynamic functions”. In: *J. Stat. Phys.* 78 (1993), p. 267. DOI: `10.1007/BF02183348`.

[184] M.E. Fisher. “The theory of condensation and the critical point”. In: *Physics* 3 (1967), p. 255.

[185] K. Binder and H. Müller-Krumbhaar. "Investigation of metastable states and nucleation in the kinetic Ising model". In: *Phys. Rev. B* 9 (1974), p. 2328. DOI: `10.1103/PhysRevB.9.2328`.

[186] K. Binder. "Theory of first-order phase transitions". In: *Rep. Prog. Phys.* 50 (1987), p. 783. DOI: `10.1088/0034-4885/50/7/001`.

[187] B. D. Josephson. "Equation of state near the critical point". In: *J. Phys. C* 2 (1969), p. 1113. DOI: `10.1088/0022-3719/2/7/302`.

[188] P. Schofield, J. D. Litster, and J. T. Ho. "Correlation between critical coefficients and critical exponents". In: *Phys. Rev. Lett.* 23 (1969), p. 1098. DOI: `10.1103/PhysRevLett.23.1098`.

[189] B. Widom. "Equation of state in the neighborhood of the critical point". In: *J. Chem. Phys.* 43 (1965), p. 3898. DOI: `10.1063/1.1696618`.

[190] J. S. Langer. "Theory of the condensation point". In: *Annals Phys.* 41 (1967). [*Annals Phys.* **281** (2000) 941], p. 108. DOI: `10.1016/0003-4916(67)90200-X`.

[191] A. F. Andreev. "Singularity of Thermodynamic Quantities at a First Order Phase Transition Point". In: *Sov. Phys. JETP* 18 (1964), p. 1415.

[192] S. N. Isakov. "Nonanalytic features of the first order phase transition in the Ising model". In: *Commun. Math. Phys.* 95 (1984), p. 427. DOI: `10.1007/BF01210832`.

[193] I. Yu. Kobzarev, L. B. Okun, and M. B. Voloshin. "Bubbles in metastable vacuum". In: *Sov. J. Nucl. Phys.* 20 (1975). [*Yad. Fiz.* **20** (1974) 1229], p. 644.

[194] S. Coleman. "Fate of the false vacuum: Semiclassical theory". In: *Phys. Rev. D* 15 (1977). [Erratum: *Phys. Rev. D* **16** (1977) 1248], p. 2929. DOI: `10.1103/PhysRevD.15.2929`.

[195] Curtis G. Callan Jr. and Sidney Coleman. "The fate of the false vacuum. II. First quantum corrections". In: *Phys. Rev. D* 16 (1977), p. 1762. DOI: `10.1103/PhysRevD.16.1762`.

[196] Luca Zambelli and Omar Zanusso. "Lee-Yang model from the functional renormalization group". In: *Phys. Rev. D* 95 (2017), p. 085001. DOI: 10.1103/PhysRevD.95.085001. arXiv: 1612.08739 [hep-th].

[197] V. L. Ginzburg. "Some remarks on phase transitions of the 2nd kind and the microscopic theory of ferroelectric materials". In: *Fiz. Tverd. Tela* 2 (1960). [*Sov. Phys. Solid State* **2** (1961) 1824], p. 2031.

[198] Daniel J. Amit and Luca Peliti. "On dangerous irrelevant operators". In: *Annals Phys.* 140 (1982), p. 207. DOI: 10.1016/0003-4916(82)90159-2.

[199] R. B. Griffiths. "Thermodynamic functions for fluids and ferromagnets near the critical point". In: *Phys. Rev.* 158 (1967), p. 176. DOI: 10.1103/PhysRev.158.176.

[200] T. H. Berlin and M. Kac. "The Spherical Model of a Ferromagnet". In: *Phys. Rev.* 86 (1952), p. 821. DOI: 10.1103/PhysRev.86.821.

[201] H. E. Stanley. "Spherical model as the limit of infinite spin dimensionality". In: *Phys. Rev.* 176 (1968), p. 718. DOI: 10.1103/PhysRev.176.718.

[202] N. D. Mermin and H. Wagner. "Absence of ferromagnetism or antiferromagnetism in one-dimensional or two-dimensional isotropic Heisenberg models". In: *Phys. Rev. Lett.* 17 (1966), p. 1133. DOI: 10.1103/PhysRevLett.17.1133.

[203] Sidney R. Coleman. "There are no Goldstone bosons in two-dimensions". In: *Commun. Math. Phys.* 31 (1973), p. 259. DOI: 10.1007/BF01646487.

[204] E. Brézin, D. J. Wallace, and K. G. Wilson. "Feynman-graph expansion for the equation of state near the critical point". In: *Phys. Rev. B* 7 (1973), p. 232. DOI: 10.1103/PhysRevB.7.232.

[205] E. Brézin and D. J. Wallace. "Critical behavior of a classical Heisenberg ferromagnet with many degrees of freedom". In: *Phys. Rev. B* 7 (1973), p. 1967. DOI: 10.1103/PhysRevB.7.1967.

[206] Ryuzo Abe and Shinobu Hikami. “Equation of state in $1/n$ expansion: n-vector model in the presence of magnetic field”. In: *Prog. Theor. Phys.* 57 (1977), p. 1197. DOI: `10.1143/PTP.57.1197`.

[207] D. J. Wallace and R. K. P. Zia. “Singularities induced by Goldstone modes”. In: *Phys. Rev. B* 12 (11 1975), p. 5340. DOI: `10.1103/PhysRevB.12.5340`.

[208] N. J. Gunther, D. J. Wallace, and D. A. Nicole. “Goldstone modes in vacuum decay and first-order phase transitions”. In: *J. Phys. A* 13 (1980), p. 1755. DOI: `10.1088/0305-4470/13/5/034`.

[209] I. D. Lawrie. “Goldstone modes and coexistence in isotropic N-vector models”. In: *J. Phys. A* 14 (1981), p. 2489. DOI: `doi.org/10.1088/0305-4470/14/9/041`.

[210] V. A. Kazakov. “Ising model on a dynamical planar random lattice: Exact solution”. In: *Phys. Lett. A* 119 (1986), p. 140. DOI: `10.1016/0375-9601(86)90433-0`.

[211] D. V. Boulatov and V. A. Kazakov. “The Ising Model on Random Planar Lattice: The Structure of Phase Transition and the Exact Critical Exponents”. In: *Phys. Lett. B* 186 (1987), p. 379. DOI: `10.1016/0370-2693(87)90312-1`.

[212] Jean-Emile Bourgine and Ivan Kostov. “On the Yang-Lee and Langer singularities in the $O(n)$ loop model”. In: *J. Stat. Mech.* 1201 (2012), P01024. DOI: `10.1088/1742-5468/2012/01/P01024`. arXiv: `1110.1108 [hep-th]`.

[213] R. Abe. “Expansion of a Critical Exponent in Inverse Powers of Spin Dimensionality”. In: *Prog. Theor. Phys.* 48 (1972), p. 1414. DOI: `10.1143/PTP.48.1414`.

[214] Myron Bander and Claude Itzykson. “Yang-Lee edge singularities in the large-N limit”. In: *Phys. Rev. B* 30 (11 1984), p. 6485. DOI: `10.1103/PhysRevB.30.6485`.

[215] Y. Saito. “Pseudocritical phenomena near the spinodal point”. In: *Prog. Theor. Phys.* 59 (1978), p. 375. DOI: `10.1143/PTP.59.375`.

[216] J. D. Gunton and M. C. Yalabik. “Renormalization-group analysis of the mean-field theory of metastability: A spinodal fixed point”. In: *Phys. Rev. B* 18 (1978), p. 6199. DOI: `10.1103/PhysRevB.18.6199`.

[217] W. Klein. “Percolation, Droplet Models, and Spinodal Points”. In: *Phys. Rev. Lett.* 47 (1981), p. 1569. DOI: `10.1103/PhysRevLett.47.1569`.

[218] C. Unger and W. Klein. “Nucleation theory near the classical spinodal”. In: *Phys. Rev. B* 29 (1984), p. 2698. DOI: `10.1103/PhysRevB.29.2698`.

[219] V. Privman and L.S. Schulman. “Analytic continuation at first-order phase transitions”. In: *J. Stat. Phys.* 29 (1982), p. 205. DOI: `10.1007/BF01020783`.

[220] Jorgen Randrup. “Spinodal decomposition during the hadronization stage at RHIC?” In: *Phys. Rev. Lett.* 92 (2004), p. 122301. DOI: `10.1103/PhysRevLett.92.122301`. arXiv: `hep-ph/0308271`.

[221] Volker Koch, Abhijit Majumder, and Jorgen Randrup. “Signals of spinodal hadronization: Strangeness trapping”. In: *Phys. Rev. C* 72 (2005), p. 064903. DOI: `10.1103/PhysRevC.72.064903`. arXiv: `nucl-th/0509030`.

[222] C. Sasaki, B. Friman, and K. Redlich. “Density fluctuations in the presence of spinodal instabilities”. In: *Phys. Rev. Lett.* 99 (2007), p. 232301. DOI: `10.1103/PhysRevLett.99.232301`. arXiv: `hep-ph/0702254`.

[223] C. Sasaki, B. Friman, and K. Redlich. “Chiral phase transition in the presence of spinodal decomposition”. In: *Phys. Rev. D* 77 (2008), p. 034024. DOI: `10.1103/PhysRevD.77.034024`. arXiv: `0712.2761 [hep-ph]`.

[224] A. Z. Patashinskii and B. I. Shumilo. “Metastable systems near the instability region”. In: *Sov. Phys. Solid State* 22 (1980), p. 655.

[225] M. Bluhm et al. *Dynamics of critical fluctuations: Theory – phenomenology – heavy-ion collisions*. 2020. arXiv: `2001.08831 [nucl-th]`.

[226] Jürgen Berges et al. “Thermalization in QCD: theoretical approaches, phenomenological applications, and interdisciplinary connections”. In: (May 2020). arXiv: `2005.12299 [hep-th]`.

[227] J.B. Kogut and M.A. Stephanov. *The phases of quantum chromodynamics: From confinement to extreme environments*. Vol. 21. Cambridge University Press, Dec. 2004. ISBN: 978-0-511-05738-0, 978-0-521-80450-9, 978-0-521-14338-7.

[228] K. Yagi, T. Hatsuda, and Y. Miake. *Quark-gluon plasma: From big bang to little bang*. Vol. 23. 2005.

[229] Sourav Sarkar, Helmut Satz, and Bikash Sinha, eds. *The physics of the quark-gluon plasma*. Vol. 785. 2010. DOI: `10.1007/978-3-642-02286-9`.

[230] AF Andreev. “The hydrodynamics of two- and one-dimensional liquids”. In: *Zh. Ehksp. Teor. Fiz.* 78.5 (1980), p. 2064.

Curriculum Vitae

Contact Information

Department of Physics, University of Illinois at Chicago
845 W Taylor St MC 273, Chicago, IL 60607
xan2@uic.edu (312) 996-0105

Education

University of Illinois, Chicago, IL, United States 2012 – 2020

Ph.D. in Physics

Advisor: Prof. M. Stephanov

Thesis: *Fluctuations and Criticality in Heavy-Ion Collisions.*

Nankai University, Tianjin, China 2008 – 2012

B.S. in Physics

Advisor: Prof. X. Zhang

Thesis: *Non-Abelian Vortices in the CFL Color Superconducting Quark Matter.*

Professional Experience

Teaching/Research Assistant 2012 – 2020

Department of Physics, University of Illinois, Chicago, IL, United States

Summer School Student 2016

Department of Physics, Massachusetts Institute of Technology, Boston, MA, United States

Exchange Student 2015

Department of Physics, University of Chicago, Chicago, IL, United States

Project Investigator 2009 – 2012

School of Physics/TEDA Applied Physics Institute, Nankai University, Tianjin, China

Awards and Honors

University of Illinois at Chicago

James Kouvel Fellowship (2019), Paul M. Raccah Award for Doctoral Studies (2013)

Nankai University

University Merit Student (2012), Excellent Innovation Research Award (2012), Excellent Undergraduate Scholarship (2009 – 2011), Champion of China Undergraduate Physics Tournament (2010), First Prize of Specialized Scholarship (2010)

Publications

X. An, *Relativistic dynamics of fluctuations and QCD critical point*, arXiv:2003.02828.

X. An, G. Basar, M. Stephanov and H.-U. Yee, *Fluctuation dynamics in a relativistic fluid with a critical point*, arXiv:1912.13456.

X. An, G. Basar, M. Stephanov and H.-U. Yee, *Relativistic hydrodynamic fluctuations*, Phys. Rev. C **100**, 024910, arXiv:1902.09517.

X. An, D. Mesterhazy abd M. Stephanov, *Critical fluctuations and complex spinodal points*, PoS CPOD2017 (2018) 040.

X. An, D. Mesterhazy abd M. Stephanov, *On spinodal points and Lee-Yang edge singularities*, J. Stat. Mech. (2018) 033207, arXiv:1707.06447.

X. An, D. Mesterhazy abd M. Stephanov, *Functional renormalization group approach to the Yang-Lee edge singularity*, JHEP **1607** (2016) 041, arXiv:1605.06039.